Technische Universität München

Max-Planck-Institut für Physik
(Werner-Heisenberg-Institut)

Two-Loop Corrections to the Higgs-Boson Masses in the Minimal Supersymmetric Standard Model with *CP*-Violation

Sebastian Paßehr

Vollständiger Abdruck der
von der Fakultät für Physik
der Technischen Universität München
zur Erlangung des akademischen Grades eines
Doktors der Naturwissenschaften (Dr. rer. nat.)
genehmigten Dissertation.

Vorsitzender:		apl. Prof. Dr. rer. nat., Dr. rer. nat. habil. N. Kaiser
Prüfer der Dissertation:	1.	Hon.-Prof. Dr. rer. nat. W. F. L. Hollik
	2.	Univ.-Prof. Dr. N. Brambilla

Die Dissertation wurde am 7. Juli 2014
bei der Technischen Universität München eingereicht und
durch die Fakultät für Physik am 1. September 2014 angenommen.

This thesis is based on the author's work conducted at the Max Planck Institute for Physics (Werner-Heisenberg-Institut) in Munich from February 2011 until Juli 2014. Parts of this work have already been published or are in preparation for publication:

[HP14a] Wolfgang Hollik and Sebastian Paßehr,
Two-loop top-Yukawa-coupling corrections to the Higgs boson masses in the complex MSSM,
in: Phys.Lett. **B733** (2014), pp. 144–150,
DOI: `10.1016/j.physletb.2014.04.026`,
arXiv: `1401.8275`.

[HP14b] Wolfgang Hollik and Sebastian Paßehr,
Full results of the two-loop top-Yukawa-coupling corrections to the Higgs boson masses in the complex MSSM,
in preparation.

Abstract

In this thesis, the top-Yukawa-coupling (h_t) enhanced two-loop corrections of the order h_t^4 ($\equiv \mathcal{O}(\alpha_t^2)$) to the neutral and charged Higgs-boson masses of the Minimal Supersymmetric Standard Model (MSSM) with charge–parity (CP) violation are calculated and analyzed. These corrections are required for an accurate theoretical prediction of the Higgs-Boson masses, in view of the experimental precision of the mass measurement for a Higgs-like particle which has been discovered at the Large Hadron Collider (LHC).

The $\mathcal{O}(\alpha_t^2)$ contributions to the Higgs-boson masses are calculated in the Feynman-diagrammatic approach. The approximation of the gauge-less limit with the external momentum and the bottom mass set to zero is applied yielding the dominant $\mathcal{O}(\alpha_t^2)$ terms. Two-loop renormalization of the tadpoles and self-energies is performed and all required renormalization constants are derived. The analytical results of the full computation are documented in this thesis.

For the numerical evaluation, the $\mathcal{O}(\alpha_t^2)$ contributions are combined with the previously known corrections with the help of the public code `FeynHiggs`. For the special case of the MSSM with real parameters agreement of our new results with an earlier computation of the $\mathcal{O}(\alpha_t^2)$ corrections in the effective potential approach is found. The treatment of complex parameters, however, is new and allows especially to study the dependence of the Higgs-boson masses on the phases of the parameters A_t and μ, which induce a shift of 2 GeV on top of a 5 GeV shift for real parameters. Furthermore, large CP-mixing of the neutral Higgs bosons can be induced by the complex parameters. The $\mathcal{O}(\alpha_t^2)$ contribution to the self-energy of the charged Higgs bosons required for renormalization in the complex MSSM and calculated here for the first time, is exploited for the real MSSM with the A-boson mass as an input parameter to predict an improved charged Higgs-boson mass, inducing a shift of -1 GeV.

Kurzdarstellung

In dieser Doktorarbeit werden die durch die Top-Yukawa-Kopplung h_t verstärkten Zweischleifenkorrekturen der Ordnung h_t^4 ($\equiv \mathcal{O}(\alpha_t^2)$) zu den neutralen und geladenen Higgs-Boson-Massen des Minimalen Supersymmetrischen Standard Modells (MSSM) mit CP-Verletzung berechnet und ausgewertet. Diese Korrekturen werden für eine genaue theoretische Vorhersage der Higgs-Boson-Massen benötigt, angesichts der experimentellen Präzision der Massenbestimmung des Higgs-artigen am Large Hadron Collider (LHC) entdeckten Teilchens.

Die $\mathcal{O}(\alpha_t^2)$-Korrekturen der Higgs-Boson-Massen werden Feynman-diagrammatisch berechnet. Die Anwendung der eichfreien Näherung mit verschwindendem äußeren Impuls und verschwindender Bottom-Masse liefert die dominanten $\mathcal{O}(\alpha_t^2)$-Beiträge. Die Zweischleifenrenormierung der Tadpole und Selbstenergien wird durchgeführt und alle benötigten Renormierungskonstanten werden bestimmt. Die analytischen Ergebnisse der kompletten Rechnung sind in dieser Arbeit dokumentiert.

Für die numerische Auswertung werden die $\mathcal{O}(\alpha_t^2)$-Beiträge und die zuvor bekannten Korrekturen mit Hilfe des öffentlichen Programms `FeynHiggs` kombiniert. Für den Spezialfall des MSSM mit reellen Parametern stimmen unsere neuen Ergebnisse mit denen einer vorhergehenden Berechnung der $\mathcal{O}(\alpha_t^2)$-Korrekturen im Zugang des effektiven Potentials überein. Die Berücksichtigung komplexer Parameter ist jedoch neu und erlaubt insbesondere die Abhängigkeit der Higgs-Boson-Massen von den Phasen der Parameter A_t und μ zu untersuchen, welche eine Verschiebung um 2 GeV zusätzlich zu den 5 GeV im reellen MSSM bewirken. Außerdem kann durch die komplexen Parameter starke CP-Mischung der neutralen Higgs-Bosonen erzeugt werden. Die für die Renormierung im komplexen MSSM notwendigen und hier erstmals berechneten $\mathcal{O}(\alpha_t^2)$-Beiträge zur Selbstenergie der geladenen Higgs-Bosonen werden im reellen MSSM mit der A-Boson-Masse als Eingabewert für eine verbesserte Vorhersage der geladenen Higgs-Boson-Masse benutzt, wo sie einen Beitrag von -1 GeV bewirken.

Contents

1. Introduction

What is a particle's mass?—this is a very short and clear, but fundamental question in the past, present and future research of elementary particle physics. Although the electroweak and strong interactions of the known matter particles are satisfactorily explained [LEP+04] by the long-time established Standard Model (SM) of particle physics [Gla61; Wei67; Sal68], the problem of explaining the origin of the mass of elementary particles persists. Through the recent discovery of a Higgs-like particle with the Large Hadron Collider (LHC) at the European Organization for Nuclear Research (CERN) by the experiments ATLAS [Aad+12] and CMS [Cha+12a], a big step towards understanding the mechanism for generating masses becomes accessible.

However, it is clear that the SM has unacceptable deficiencies because of the absence of a consistent explanation for other fundamental physical concepts like gravity, the strong CP-problem [Wei75; t H76a; t H76b], neutrino oscillations [Pon57; Pon68; GM08], baryon asymmetry, and the existence of dark matter [Zwi33; Zwi37; Tri87] and dark energy [PR03]. Furthermore, in comparisons of high-precision measurements and calculations differences of the order of three standard deviations are found for a few observables, providing hints to possible existence of physics beyond the Standard Model. The largest deviation is found for the anomalous magnetic moment of the muon [Ben+06; JN09; Mil+12], followed by the bottom-quark forward-backward asymmetry [GM13], and the top-quark forward-backward asymmetry [Aal+08; Aba+08; Pec12].

For many of these problems various solutions have been proposed. A concept which has become increasingly popular for the recent decades is supersymmetry (SUSY). A famous application of SUSY as an extension of the SM is given by the Minimal Supersymmetric Standard Model (MSSM) [HK85]. Its merits are a dark matter candidate, the stabilization of the electroweak scale, as well as a symmetry between fermions and bosons. Moreover, the MSSM has a very high predictive power. Thus, measurements of current experiments have the ability to check aspects of this model.

An immediate theoretical consequence of this minimal supersymmetric extension of the SM is the presence of a larger Higgs-boson sector consisting of two complex scalar doublets. Besides the Higgs boson of the SM four additional physical scalar bosons occur; the remaining three degrees of freedom are used by the (would-be) Goldstone bosons [Nam60; Gol61; GSW62]. Thus, at lowest order in perturbation theory there are two neutral CP-even bosons h and H (one of them being the SM-like Higgs boson), one neutral CP-odd boson A, two charged bosons $H^{\pm}$, one neutral unphysical Goldstone bosons G, and two charged unphysical Goldstone bosons $G^{\pm}$. The study of the masses and mixing properties of the physical Higgs bosons with particular emphasis on higher-order corrections in perturbation theory is the main subject of this thesis.

The discovery of a new bosonic particle with a mass around 125.5 GeV [Cha+14; Aad+14] by the experiments ATLAS [Aad+12] and CMS [Cha+12a] at CERN has triggered an intensive investigation to reveal the nature of this particle as a Higgs boson from the mechanism of electroweak symmetry breaking. Within the present experimental uncertainties, which are still considerably large, the measured properties of the new boson are consistent with the corresponding theoretical predictions for the SM Higgs boson [Lan13]. On the other hand, still a large variety of other interpretations which are connected to physics beyond the SM is possible. The MSSM is a promising and experimentally accessible candidate.

At lowest order, the masses of the five physical Higgs bosons of the MSSM only depend on two free parameters, commonly chosen as the A-boson mass m_A and the ratio of the two vacuum expectation values $\tan\beta = v_2/v_1$. At this order, the lightest Higgs-boson mass is constrained from above by the Z-boson mass. Furthermore, CP-invariance is preserved in the Higgs sector.

However, the masses and mixings in the neutral Higgs-boson sector are sizeably influenced by higher-order contributions. Moreover, in the MSSM with complex parameters, the cMSSM, CP-violation is induced in the Higgs sector by loop contributions with complex parameters from other SUSY sectors, leading to mixing between all three neutral Higgs bosons h, H and A [Pil98]. Accordingly, intensive work has been invested into higher-order calculations of the mass spectrum from the SUSY parameters, in the case of the real MSSM [HHW98; HHW99b; HHW99a; Hei+05; Zha99; Bri+02; Cas+95; Deg+03; HHW06; All+04; Mar02] as well as the complex MSSM [Dem99; PW99; Car+00; Hei+07].

The largest loop contributions arise from the Yukawa sector with the large top-Yukawa coupling h_t, or $\alpha_t = h_t^2/(4\pi)$, respectively. The full one-loop result [Fra+07] and the leading $\mathcal{O}(\alpha_t\alpha_s)$ terms [Hei+07], both accomplished in the Feynman-diagrammatic approach including complex parameters, have been implemented in the public program `FeynHiggs` [HHW99b; Deg+03; Fra+07; HHW00c; Hah+09]. The class of leading two-loop Yukawa-type corrections of $\mathcal{O}(\alpha_t^2)$ has been calculated so far only in the case of real parameters [Bri+02], applying the effective-potential method. It is also contained in `FeynHiggs`, but an evaluation of the $\mathcal{O}(\alpha_t^2)$ terms for the cMSSM has been missing until now. The Feynman-diagrammatic calculation of the leading $\mathcal{O}(\alpha_t^2)$ contributions to the Higgs-boson masses and mixings in the cMSSM is carried out in this thesis for the first time.

A brief introduction to SUSY is given in Chapter 2, supplemented by some remarks on the used notation in Appendix A. The particle content of the MSSM as an extension of those of the SM is illustrated in Chapter 3. Technical issues of loop calculations are outlined in Chapter 4, where a brief summary of the appearing divergences and their treatment is given. The used conventions for the arising mathematical expressions are defined herein, and solutions for the required integrals are given in Appendix B. Closely entangled with higher-order calculations is the framework of renormalization, which makes sure that physically meaningful quantities are free of divergences. An overview on that topic is reported in Chapter 5.

In Chapter 6 the Higgs potential and the lowest-order relations of the mass spectrum are introduced. On the side, a set of on-shell parameters is introduced. Subsequently, one-loop and two-loop renormalization of the tadpoles and mass matrices of the Higgs potential are carried out; various steps are described for the evaluation of the higher-order Higgs-boson masses. Some of the longer results are listed in Appendix C.

The class of $\mathcal{O}(\alpha_t^2)$ contributions extended to the case of complex parameters is presented in Chapter 7. The detailed expressions in Chapter 6 form the basis for the evaluation of these corrections. The computation has been carried out in the Feynman-diagrammatic approach [HP14a; HP14b]. Thereby the gauge-less limit is introduced and the bottom mass is set equal to zero. Moreover, the external momentum is set equal to zero in the two-loop self-energies. The application of these approximations provides the dominant terms of the $\mathcal{O}(\alpha_t^2)$ contributions; they also have been utilized for the evaluation of the $\mathcal{O}(\alpha_t\alpha_s)$ corrections before [Hei+07]. The partially vast mathematical expressions are put together in Appendix D for a better lucidity.

For the special case of real parameters an equivalent result to the one in Ref. [Bri+02] is obtained in an independent way, thus serving as a cross check and as a consolidation of former spectrum calculations and associated tools. The results for the $\mathcal{O}(\alpha_t^2)$ contributions which are derived in this thesis will be included in a public version of the code `FeynHiggs`.

Finally, the numerical evaluation of the full spectrum of the MSSM Higgs-boson masses is carried out in Chapter 8. Therefore, the newly derived $\mathcal{O}(\alpha_t^2)$ contributions are combined with the full one-loop result and the $\mathcal{O}(\alpha_t\alpha_s)$ corrections with the help of `FeynHiggs`. At first, the results in the real MSSM are investigated and compared with the previous result of the $\mathcal{O}(\alpha_t^2)$ terms. At second, the influence of the phases ϕ_{A_t} and ϕ_μ of the complex trilinear soft-breaking parameter A_t and the complex bilinear superpotential parameter μ, respectively, on the Higgs-boson masses is examined. Large deviations between the previously existing approximation based on a conjectured interpolation in `FeynHiggs` and the exact Feynman-diagrammatic calculation of the $\mathcal{O}(\alpha_t^2)$ contributions for the mass prediction of the heavy Higgs bosons are found. Furthermore, CP-mixing at higher orders is investigated. At third, the $\mathcal{O}(\alpha_t^2)$ corrections to the correlation between the A-boson mass and the charged Higgs-boson masses are analyzed in the real MSSM. In the cMSSM the charged Higgs-boson mass $m_{H^\pm}$ has to be chosen as an input parameter, and in higher-order corrections it is renormalized on-shell. Thus, the computation of the charged Higgs-boson self-energy is necessary for renormalization of the Higgs potential with complex parameters. The corresponding $\mathcal{O}(\alpha_t^2)$ contributions to the self-energy of the charged Higgs bosons are derived in this thesis for the first time. As a side-effect, in the real MSSM with m_A being an input parameter and renormalized on-shell at higher orders, the correlation between m_A and $m_{H^\pm}$ is obtained and used to determine the shift in the charged Higgs-boson mass resulting from the $\mathcal{O}(\alpha_t^2)$ contributions.

For convenience of the reader a List of Symbols which is subdivided into different sections corresponding to the chapters of this thesis is appended; its first section declares symbols that are frequently used throughout this thesis. Thereafter, a List of Tables and a List of Figures can be found. At the end, a bibliographical section is attached, with the citations primarily ordered by chapter, and secondarily in an alphabetical way.

2. Supersymmetry

The idea of a symmetry relation between fermionic and bosonic degrees of freedom has appeared first in string theory [Ram71]. The earliest application as a graded Lie algebra is found in Ref. [GL71] and a non-linear realization and the idea of spontaneous breakdown is described in Ref. [VA73]. The first supersymmetric (SUSY) field theories appeared in Refs. [WZ74b; WZ74c; SS74] and drew much attention in both theoretical and experimental physics.

2.1. Motivation

Despite the great success of the Standard Model (SM) of particle physics in predicting physical observables, it has several drawbacks. Supersymmetric theories can solve some of these issues straightaway:

- New particles, including the possibility of weakly interacting massive states, are predicted, thus providing cosmologically stable candidates for dark matter.
- Radiative corrections to the Higgs-boson mass in the Standard Model lead to quadratic divergences. The Higgs-boson mass m_h can only be restored at the electroweak scale by fine tuning. In contrast, supersymmetry introduces new contributions that automatically cancel quadratic divergences. Moreover, in exact supersymmetry radiative corrections by fermions and their corresponding superpartners cancel each other.
- It is mathematically proven that a quantum field theory may have internal symmetries and supersymmetry [HŁS75]. While the former are realized by the gauge symmetries, only the Poincaré part of the latter is contained in the SM. An extension to full supersymmetry, including a symmetry between bosons and fermions, seems to be natural.

- The supersymmetric particles enter the energy-scale dependence of the gauge couplings and alter them in a way that leads to a much better consolidation at the grand unification scale.

2.2. Super-Poincaré group

As described by Coleman and Mandula in Ref. [CM67] physical symmetry groups can be represented by the direct product of the Poincaré group and additional internal symmetries. The Standard Model accommodates

- the Lie algebra of the Poincaré group

$$[P^\mu,\, P^\nu] = 0 \ , \tag{2.1a}$$

$$[P^\mu,\, J^{\rho\sigma}] = \boldsymbol{i}\,(g^{\mu\rho}P^\sigma - g^{\mu\sigma}P^\rho) \ , \tag{2.1b}$$

$$[J^{\mu\nu},\, J^{\rho\sigma}] = \boldsymbol{i}\,(-g^{\mu\rho}J^{\nu\sigma} + g^{\nu\rho}J^{\mu\sigma} + g^{\mu\sigma}J^{\nu\rho} - g^{\nu\sigma}J^{\mu\rho}) \tag{2.1c}$$

  with the energy–momentum and angular momentum operators P^μ, $J^{\mu\nu}$ and the metric tensor $g^{\mu\nu}$, and

- the $SU(3)_\mathrm{c} \times SU(2)_\mathrm{L} \times U(1)_Y$ algebras

$$\left[G^a,\, G^b\right] = \boldsymbol{i}\, f^{abc}G^c \tag{2.2}$$

  with the corresponding structure constants f and generators G which fulfill the following relations:

$$[G^a,\, P^\mu] = 0 \ , \tag{2.3a}$$

$$[G^a,\, J^{\mu\nu}] = 0 \ . \tag{2.3b}$$

A natural, non-trivial extension of this algebra is described by the Haag–Łopuszański–Sohnius theorem in Ref. [HŁS75]. It introduces fermionic, anti-commuting generators Q_i, $i \in \{1, \ldots, N\}$ which extend the Lie algebra in the following way (cf. Refs. [Soh85; MW87; DGR04], the notation is introduced in Appendix A):

$$\left\{Q_{i,A},\, \bar{Q}_{j,\dot{B}}\right\} = 2\,\delta_{ij}\,\sigma^\mu_{A\dot{B}}\,P_\mu \ , \tag{2.4a}$$

$$\{Q_{i,A},\, Q_{i,B}\} = 0 \ , \qquad \left\{\bar{Q}_{i,\dot{A}},\, \bar{Q}_{i,\dot{B}}\right\} = 0 \ , \tag{2.4b}$$

$$[Q_{i,A},\, P_\mu] = 0 \; , \qquad \left[\bar{Q}_{i,\dot{A}},\, P_\mu\right] = 0 \; , \tag{2.4c}$$

$$[Q_{i,A},\, J_{\mu\nu}] = (\sigma_{\mu\nu})_A^{\;\;B}\, Q_{i,B} \; , \qquad \left[\bar{Q}_{i,\dot{A}},\, J_{\mu\nu}\right] = -\bar{Q}_{i,\dot{B}}\, (\bar{\sigma}_{\mu\nu})^{\dot{B}}_{\;\;\dot{A}} \; . \tag{2.4d}$$

The Minimal Supersymmetric Standard Model (MSSM) is described by the special case $N = 1$ where only one pair of supersymmetry generators Q_A and $\bar{Q}_{\dot{A}}$ exists. In the following, only this special case is investigated and the index i of the supersymmetry generators is suppressed.

A close relation between supersymmetry and spacetime symmetry is expressed by Eq. (2.4a): the non-trivial application of two supersymmetry operations yields the energy–momentum operator.

The Casimir operators of the Poincaré group are the mass-square operator $P^\mu P_\mu$ and the Pauli–Lubański pseudo-vector $W^\mu = \frac{1}{2}\,\epsilon_{\mu\nu\rho\sigma}\, J^{\nu\rho}\, P^\sigma$ squared which is related to the spin of a particle.[1] The Super-Poincaré algebra in Eqs. (2.4) yields the following relations:

$$[Q,\, P^\mu P_\mu] = 0 \; , \tag{2.5a}$$

$$[Q,\, W^\mu W_\mu] \neq 0 \; . \tag{2.5b}$$

As can be seen immediately, the operation of Q preserves a particle's mass, but changes its spin. Eqs. (2.4d) tell us that the change of the spin is equal to $\pm\frac{1}{2}$ at any time, which is why supersymmetry relates fermions and bosons to each other. The number of fermionic and bosonic degrees of freedom in one-particle representations of supersymmetry are identical [Soh85].

So far no supersymmetric particles have been found, especially not with the same mass of the Standard Model particles; for this reason an additional mechanism is necessary to break SUSY. A short description is found in Section 2.6.

In the case $N = 1$ exactly one additional internal $U(1)$ symmetry group which does not commute with Q exists; it is called R-symmetry and with its generator R the following chiral relations hold [Fay75]:

$$[Q_A, R] = Q_A \; , \quad \left[\bar{Q}^{\dot{B}}, R\right] = -\bar{Q}^{\dot{B}} \; , \quad [P_\mu, R] = 0 \; , \quad [J_{\mu\nu}, R] = 0 \; . \tag{2.6}$$

The R-symmetry is used to define the R-parity in Section 2.4.

[1] $\epsilon_{\mu\nu\rho\sigma}$ is the four-dimensional totally antisymmetric Levi-Civita symbol and $\epsilon_{1234} = +1$.

2.3. Superfields

Superfields are a convenient way of representing SUSY on the superspace, which is constructed from the direct product of the Minkowski space with the real-valued coordinates x_μ and two two-component spinor spaces with the Grassmann-valued coordinates θ_A and $\bar{\theta}_{\dot{A}}$.

2.3.1. General superfields

A general superfield $F(x^\mu,\, \theta^A,\, \bar{\theta}_{\dot{A}})$ can be expressed as

$$\begin{aligned} F(x^\mu,\, \theta^A,\, \bar{\theta}_{\dot{A}}) = f(x^\mu) & \\ & + \sqrt{2}\,\theta^A \xi_A(x^\mu) + \sqrt{2}\,\bar{\theta}_{\dot{A}}\bar{\chi}^{\dot{A}}(x^\mu) \\ & + \theta^A\theta_A\, M(x^\mu) + \bar{\theta}_{\dot{A}}\bar{\theta}^{\dot{A}}\, N(x^\mu) + \theta^A\bar{\theta}^{\dot{B}}\, A_{A\dot{B}}(x^\mu) \\ & + \theta^A\theta_A\, \bar{\theta}_{\dot{B}}\bar{\lambda}^{\dot{B}}(x^\mu) + \bar{\theta}_{\dot{A}}\bar{\theta}^{\dot{A}}\, \theta^B\zeta_B(x^\mu) \\ & + \frac{1}{2}\,\theta^A\theta_A\, \bar{\theta}_{\dot{B}}\bar{\theta}^{\dot{B}}\, D(x^\mu) \end{aligned} \tag{2.7}$$

with the scalar fields f, M, N, D, the vector field $A_{A\dot{B}} = \sigma^\mu_{A\dot{B}} A_\mu$ and the left/right-chiral Weyl-spinor fields ξ_A, ζ_A, $\bar{\chi}^{\dot{A}}$ and $\bar{\lambda}^{\dot{A}}$. Sums and products of superfields are again superfields (cf. Ref. [DGR04]).

The infinitesimal transformation

$$T\left(a^\mu,\, \tau^A,\, \bar{\tau}^{\dot{A}}\right) = \exp\left(\boldsymbol{i}\, a^\mu P_\mu + \boldsymbol{i}\, \tau^A Q_A + \boldsymbol{i}\, \bar{\tau}^{\dot{A}} \bar{Q}_{\dot{A}}\right) \tag{2.8}$$

translates a superspace element $\left(x^\mu,\, \theta^A,\, \bar{\theta}_{\dot{A}}\right)^T$ into

$$\begin{pmatrix} x'^\mu \\ \theta'^A \\ \bar{\theta}'_{\dot{A}} \end{pmatrix} = \begin{pmatrix} x^\mu + a^\mu + \boldsymbol{i}\, \tau^A \sigma^\mu_{A\dot{B}} \bar{\theta}^{\dot{B}} + \boldsymbol{i}\, \bar{\tau}_{\dot{A}} \bar{\sigma}^{\mu\dot{A}B}\theta_B \\ \theta^A + \tau^A \\ \bar{\theta}_{\dot{A}} + \bar{\tau}_{\dot{A}} \end{pmatrix}, \tag{2.9}$$

which leads to the following infinitesimal representation of the supersymmetry generators:

$$Q_A = -\boldsymbol{i}\, \left(\partial_A + \boldsymbol{i}\, \sigma^\mu_{A\dot{B}} \bar{\theta}^{\dot{B}} \partial_\mu\right)\,, \tag{2.10a}$$

$$\bar{Q}^{\dot{A}} = -\boldsymbol{i}\, \left(\bar{\partial}^{\dot{A}} + \boldsymbol{i}\, \bar{\sigma}^{\mu\dot{A}B}\theta_B \partial_\mu\right)\,. \tag{2.10b}$$

Consistently, a superfield F is transformed by

$$\begin{aligned} \delta F &\equiv F\left(x'^{\mu},\, \theta'^{A},\, \bar{\theta}'_{\dot{A}}\right) - F\left(x^{\mu},\, \theta^{A},\, \bar{\theta}_{\dot{A}}\right) \\ &= \boldsymbol{i}\left(\tau^{A} Q_{A} + \bar{\tau}_{\dot{A}} \bar{Q}^{\dot{A}}\right) F\left(x^{\mu},\, \theta^{A},\, \bar{\theta}_{\dot{A}}\right) \end{aligned} \tag{2.11}$$

where each component is transformed independently (cf. Ref. [DGR04]). Since the derivatives $\partial_A \equiv \partial \big/ \partial\theta^A$ and $\bar{\partial}^{\dot{A}} \equiv \partial \big/ \partial\bar{\theta}_{\dot{A}}$ do not commute with Q_A and $\bar{Q}^{\dot{A}}$, the chiral covariant derivatives

$$D_A = \partial_A - \boldsymbol{i}\, \sigma^{\mu}_{A\dot{B}} \bar{\theta}^{\dot{B}} \partial_{\mu}\ , \tag{2.12a}$$

$$\bar{D}^{\dot{A}} = \bar{\partial}^{\dot{A}} - \boldsymbol{i}\, \bar{\sigma}^{\mu \dot{A} B} \theta_B \partial_{\mu} \tag{2.12b}$$

are introduced.

In total a general superfield contains 32 parameters. However not all of them are independent from each other; the representation comprises auxiliary fields which can be reduced.

2.3.2. Chiral superfields

A first irreducible representation of supersymmetry are chiral superfields which are defined by

$$\bar{D}^{\dot{A}} \Phi = 0 \qquad \text{for left-chiral superfields,} \tag{2.13a}$$

$$D_A \Phi^{\dagger} = 0 \qquad \text{for right-chiral superfields.} \tag{2.13b}$$

A solution for the left-chiral superfield is given by (and analogously for the right-chiral superfield)

$$\Phi\left(x^{\mu},\, \theta^{A},\, \bar{\theta}_{\dot{A}}\right) = \exp\left(-\boldsymbol{i}\, \theta^{A} \sigma^{\mu}_{A\dot{B}} \bar{\theta}^{\dot{B}} \partial_{\mu}\right) \phi\left(x^{\mu},\, \theta^{A}\right)\ , \tag{2.14a}$$

$$\phi\left(x^{\mu},\, \theta^{A}\right) = A(x^{\mu}) + \sqrt{2}\, \theta^{A} \xi_{A} + \theta^{A} \theta_{A}\, F(x^{\mu})\ , \tag{2.14b}$$

with the scalar fields A, F and the spinor field ξ; only eight degrees of freedom remain. Herein F is an auxiliary field, which is necessary to describe supersymmetry off-shell. Sums and products of pure chiral superfields result in pure chiral superfields of the same kind. The complex conjugate of a left-chiral superfield yields a right-chiral superfield.

2.3.3. Vector superfields

A vector superfield $V = V^\dagger$ is another irreducible representation of supersymmetry. It can be created by the sum (or the product) of one left- and one right-chiral superfield. From Eq. (2.7) the conditions

$$f = f^* \ , \quad D = D^* \ , \quad \bar{\chi}^{\dot{A}} = \bar{\xi}^{\dot{A}} \ , \quad \zeta_A = \lambda_A \ , \quad N = M^* \ , \quad A^\mu = A^{\mu *} \tag{2.15}$$

are derived. In addition the replacements

$$\lambda_A \to \lambda_A - \frac{\boldsymbol{i}}{\sqrt{2}} \sigma^\mu_{A\dot{B}} \partial_\mu \bar{\xi}^{\dot{B}} \ , \tag{2.16a}$$

$$\bar{\lambda}^{\dot{A}} \to \bar{\lambda}^{\dot{A}} - \frac{\boldsymbol{i}}{\sqrt{2}} \bar{\sigma}^{\mu \dot{A} B} \partial_\mu \xi_B \ , \tag{2.16b}$$

$$D \to D - \frac{1}{2} \partial^\mu \partial_\mu f \tag{2.16c}$$

are conducted, yielding the expression of a general vector superfield

$$\begin{aligned} V\left(x^\mu, \theta^A, \bar{\theta}_{\dot{A}}\right) = {} & f(x^\mu) \\ & + \sqrt{2}\, \theta^A \xi_A(x^\mu) + \sqrt{2}\, \bar{\theta}_{\dot{A}} \bar{\xi}^{\dot{A}}(x^\mu) \\ & + \theta^A \theta_A\, M(x^\mu) + \bar{\theta}_{\dot{A}} \bar{\theta}^{\dot{A}}\, M^*(x^\mu) + \theta^A \bar{\theta}^{\dot{B}} A_{A\dot{B}}(x^\mu) \\ & + \theta^A \theta_A\, \bar{\theta}_{\dot{B}} \left(\bar{\lambda}^{\dot{B}}(x^\mu) - \frac{\boldsymbol{i}}{\sqrt{2}}\, \bar{\sigma}^{\mu \dot{B} C} \partial_\mu \xi_C(x^\mu) \right) \\ & + \bar{\theta}_{\dot{A}} \bar{\theta}^{\dot{A}}\, \theta^B \left(\lambda_B(x^\mu) - \frac{\boldsymbol{i}}{\sqrt{2}}\, \sigma^\mu_{B\dot{C}} \partial_\mu \bar{\xi}^{\dot{C}}(x^\mu) \right) \\ & + \frac{1}{2}\, \theta^A \theta_A\, \bar{\theta}_{\dot{B}} \bar{\theta}^{\dot{B}} \left(D(x^\mu) - \frac{1}{2}\, \partial^\mu \partial_\mu f(x^\mu) \right) \ . \end{aligned} \tag{2.17}$$

Furthermore, this superfield is invariant under a super-gauge transformation

$$V \to V + \boldsymbol{i}\, \Lambda + (\boldsymbol{i}\, \Lambda)^\dagger \tag{2.18}$$

with a chiral superfield Λ. A special gauge-fixing has been presented by Wess and Zumino in Ref. [WZ74b]; as a consequence f, ξ^A and M disappear and just

$$\begin{aligned} V_{\mathrm{WZ}}\left(x^\mu, \theta^A, \bar{\theta}_{\dot{A}}\right) = {} & \theta^A \bar{\theta}^{\dot{B}} A_{A\dot{B}}(x^\mu) \\ & + \theta^A \theta_A\, \bar{\theta}_{\dot{B}} \bar{\lambda}^{\dot{B}}(x^\mu) + \bar{\theta}_{\dot{A}} \bar{\theta}^{\dot{A}}\, \theta^B \lambda_B(x^\mu) \\ & + \frac{1}{2}\, \theta^A \theta_A\, \bar{\theta}_{\dot{B}} \bar{\theta}^{\dot{B}}\, D(x^\mu) \end{aligned} \tag{2.19}$$

remains. The corresponding super-gauge field strength for a general vector superfield V is given by

$$W_A = -\frac{1}{4}\bar{D}_{\dot{B}}\bar{D}^{\dot{B}}D_A V \qquad \text{(left-chiral field strength)}, \tag{2.20a}$$

$$\bar{W}^{\dot{A}} = -\frac{1}{4}D^B D_B \bar{D}^{\dot{A}} V \qquad \text{(right-chiral field strength)}. \tag{2.20b}$$

Applying the following super-gauge transformation to chiral superfields leaves the interaction term $\Phi^\dagger e^{2\,g\,V}\Phi$ invariant:

$$\Phi \to e^{-i\,2\,g\,\Lambda}\Phi \;, \tag{2.21a}$$

$$\Phi^\dagger \to \Phi^\dagger e^{i\,2\,g\,\Lambda^\dagger} \;, \tag{2.21b}$$

$$e^{2gV} \to e^{-i\,2\,g\,\Lambda^\dagger} e^{2\,g\,V} e^{i\,2\,g\,\Lambda} \;. \tag{2.21c}$$

2.4. *R*-parity

The already introduced R-symmetry can be easily applied to superfields:

$$\Phi\left(x^\mu,\, \theta^A,\, \bar{\theta}_{\dot{A}}\right) \to \Phi'\left(x^\mu,\, e^{i\,\alpha}\theta^A,\, e^{-i\,\alpha}\bar{\theta}_{\dot{A}}\right) = e^{i\,\alpha\,R_\Phi}\Phi\left(x^\mu,\, \theta^A,\, \bar{\theta}_{\dot{A}}\right) \;. \tag{2.22}$$

The components of the superfields have to be charged under R-symmetry in the following way to keep Eq. (2.14) consistent:

$$R(A) = R_\Phi \;, \quad R(\xi^A) = -R(\bar{\xi}_{\dot{A}}) = R_\Phi - 1 \;, \quad R(F) = R_\Phi - 2 \;. \tag{2.23}$$

The so called R-charges of products of multiple chiral superfields are summed up. Therefore, the R-charge of any vector superfield V is equal to zero and from Eq. (2.17) it follows

$$\begin{aligned} R(A^\mu) = 0 \;, \quad R(\lambda^A) = -R(\bar{\lambda}_{\dot{A}}) = 1 \;, \qquad R(M) = -R(M^*) = -2 \;, \\ R(f) = 0 \;, \quad R(\xi^A) = -R(\bar{\xi}_{\dot{A}}) \;= -1 \;, \qquad\qquad R(D) = 0 \;. \end{aligned} \tag{2.24}$$

However, because of the anomalies explained in Ref. [FW83] and required mass terms for the superpartners of the gauge bosons, R-symmetry cannot be realized globally, but only for the discret value $\alpha = \pi$. The numbers $e^{i\,\pi\,R}$ for the R-charges of the component fields within this subgroup are called R-parity R_{P} [Fay77]. Consistently, the R-parity of a product of several superfields is evaluated from the product of the corresponding R-parities of each field. Thereby SM particles acquire $R_\mathrm{P} = +1$, while their corresponding superpartners (from the same superfield) acquire $R_\mathrm{P} = -1$.

If the R-parity is preserved, only an even number of superparticles is allowed at each vertex. Since this condition is not necessary, intensive studies on R-parity violation are performed [Bar+05]. The corresponding couplings are however constrained by existing bounds on baryon- and lepton-number conservation [Wei82].

2.5. Supersymmetric Lagrangian

Chiral superfields Φ_i, vector superfields V and field-strength spinors W^a are used to construct supersymmetric Langrangians. As shown in Appendix A.4 only D terms of general superfields and F terms of chiral superfields are invariant under supersymmetry transformations. Thus, the most general supersymmetric, renormalizable [Col88] Lagrangian is given by

$$\begin{aligned}\mathcal{L}_\mathrm{SUSY} &= \mathcal{L}_\mathrm{gauge} + \mathcal{L}_\mathcal{W} + \mathcal{L}_\mathrm{matter} \\ &= \left[\int \mathrm{d}^2\theta \left(\frac{1}{4}\left(W^{aA}W^a_A\right) + \mathcal{W}(\Phi_i)\right) + \mathrm{h.\,c.}\right] + \int \mathrm{d}^4\theta\, \Phi_i^\dagger e^{2\,g\,V}\Phi_i \ ,\end{aligned} \tag{2.25}$$

with the chiral holomorphic superpotential

$$\mathcal{W}(\Phi_i) = c_i\,\Phi_i + \frac{1}{2}\,m_{ij}\,\Phi_i\,\Phi_j + \frac{1}{6}\,h_{ijk}\,\Phi_i\,\Phi_j\,\Phi_k \ . \tag{2.26}$$

The holomorphy of $\mathcal{W}$ becomes manifest by the fact that it contains only left-chiral fields; it is required to render the action invariant under supersymmetry transformations.

The Grassmann-variable integrals $\int \mathrm{d}^4\theta$, $\int \mathrm{d}^2\theta$ and $\int \mathrm{d}^2\bar\theta$ act as projectors on the integrands: their application yields the terms proportional to $\theta^A\theta_A\,\bar\theta_{\dot B}\bar\theta^{\dot B}$, $\theta^A\theta_A$ and $\bar\theta_{\dot A}\bar\theta^{\dot A}$, respectively (cf. Appendix A.2).

2.6. Supersymmetry breaking

As already mentioned before, each SM particle and its corresponding superpartner would have the same mass, if SUSY was realized in nature as an exact symmetry.

However this is excluded by experiment, requiring SUSY to be broken by some mechanism, which has to be gauge invariant and renormalizable.

Another desired feature is naturalness: in an exactly supersymmetric theory the renormalized scalar (Higgs) one-loop self-energy contributions by fermions and their corresponding superpartners cancel each other [DGR04]. As a consequence of the non-renormalization theorem this property is valid at all orders of perturbation theory [WZ74a]. If supersymmetry breaking is only allowed for certain parameters[2] of the MSSM, the results of the higher-order scalar self-energies yield just logarithmic divergences. These so-called soft-breaking parameters have to be of the order of a few TeV to preserve naturalness.

The possibility of using further scalar fields to perform spontaneous SUSY breaking is described in Ref. [KL04]. The general principle is the assumption that a field acquires a non-zero vacuum expectation value which breaks the vacuum of the supersymmetric theory. However, two conditions are imposed: the vacuum preserves Lorentz invariance and it cannot carry a four-momentum. Investigating the components of chiral superfields in Eq. (2.14) and vector superfields in Eq. (2.17) leaves only two possibilities: D-type supersymmetry breaking by an abelian auxiliary field D (Fayet–Iliopoulos mechanism [FI74; Fay76]) and F-type supersymmetry breaking by an auxiliary field F (O'Raifeartaigh mechanism [ORa75]).

A different option is given by the introduction of explicit supersymmetry breaking terms. The most general gauge invariant and renormalizable terms of mass dimension less than four are [GG82]

$$\mathcal{L}_{\text{breaking}} = -m_{ij}^2\, A_i^\dagger\, A_j - \left(a_i\, A_i + \frac{1}{2}\, b_{ij}\, A_i\, A_j + \frac{1}{6}\, c_{ijk}\, A_i\, A_j\, A_k - \frac{1}{2}\, M_\lambda\, \lambda^a\, \lambda^a + \text{h. c.} \right) , \tag{2.27}$$

with the conventions introduced by Eq. (2.14) and Eq. (2.17), i. e. A_i is the scalar component of a chiral superfield, and λ^a is a left-chiral Weyl spinor and the coefficient of $\bar{\theta}\bar{\theta}\,\theta$ inside of a vector superfield. A convenient explanation for generating these terms is provided by spontaneous symmetry breaking in a hidden sector (e. g. Ref. [Nil84]).

[2] All appearing field operators must have a mass dimension less than four, which is however just a necessary condition. Non-renormalization of the superpotential in the presence of certain soft-breaking operators has to be proven by an explicit calculation.

3. The Minimal Supersymmetric Standard Model

The Standard Model (SM) of particle physics is a Yang–Mills theory [YM54], i. e. a gauge theory whose interactions are described by (special) unitary groups, on top of a causal, relativistic, globally Poincaré-invariant (cf. Eq. (2.1)) quantum field theory [BDJ01; BS59]. The physical motivation is a common description of the electromagnetic, weak and strong interactions extended by the Higgs mechanism to arrange for the particles' masses [Gla61; EB64; Hig64; GHK64; Wei67; Sal68]. The SM incorporates the unitary group $U(1)_Y$ describing interactions via the hypercharge and the special unitary groups $SU(2)_\mathrm{L}$ representing the left-chiral weak interactions [LY56; Wu+57] and $SU(3)_\mathrm{c}$ explaining the strong interactions.

3.1. Fields and particles of the Standard Model

The gauge transformation of a SM matter field $f(x)$ can be described by

$$f(x) \to \exp\left(-\boldsymbol{i}\, g_Y\, \omega_Y(x)\, \frac{\hat{Y}}{2} - \boldsymbol{i}\, g_\mathrm{w}\, \omega_\mathrm{w}^a(x)\, \frac{\tau_a}{2} - \boldsymbol{i}\, g_\mathrm{s}\, \omega_\mathrm{s}^b(x)\, \frac{\lambda_b}{2}\right) f(x) \tag{3.1}$$

with the gauge couplings g_Y, g_w and g_s, the local gauge functions ω_Y, ω_w^a and ω_s^b and the generators of the gauge groups $\hat{Y}$, τ_a and λ_b. In the irreducible matrix representation of each group τ_a, $a \in \{1, 2, 3\}$ are the Pauli matrices and λ_b, $b \in \{1, \ldots, 8\}$ are the Gell-Mann matrices [Gel62]. The eigenvalues of the generators $\hat{Y}$, $\tau_3/2$ and λ_3, λ_8 are conventionally used as quantum numbers of the field f.[3] The electroweak quantum numbers are denoted as hypercharge Y_f and isospin T_f^3.

[3] The normalized Gell-Mann matrices λ_3 and λ_8 commute, thus they have common eigenvalues.

Furthermore, each generator receives a corresponding bosonic vector quantum field which acts as the messenger of the gauge interaction among the matter fields and, in the non-abelian case, also has self-interactions; the transformation of these fields is conducted in the adjoint representation of the corresponding group.

The Higgs boson H enters the SM as the neutral charge–parity (CP)-even component of a scalar complex $SU(2)_\mathrm{L}$ doublet. Via spontaneous electroweak symmetry breaking, three degrees of freedom, which would be the Goldstone bosons G, $G^\pm$ [Nam60; Gol61; GSW62], are used to achieve massive gauge bosons; the last remaining degree of freedom is interpreted as the physical Higgs boson. The latter acquires a non-vanishing vacuum expectation value and couples to the fermionic particles via Yukawa interactions [Yuk35]. The coefficients of these interactions are free parameters and thus allow for the assignment of the correct value of each particle's mass.

The particle spectrum of the SM is summarized in Tab. 3.1. The in principal possible right-handed neutrinos $\nu_{i,\mathrm{R}}$ which would not couple to any gauge particles are not accommodated by the minimal version of the SM. The generation index i runs from one to three, albeit a fourth generation cannot be excluded definitely [Ber+12]; though strong experimental bounds from the width of the Z boson and the mass of the Higgs boson on a fourth generation exist [Dec+89; Len13; BJN13]. The color index $j \in \{1, 2, 3\}$ is omitted in the following. The left-handed quarks and leptons can be combined to the depicted $SU(2)_\mathrm{L}$ doublets.

Table 3.1.: The particle content of the SM.

fermions	leptons		$l_{i,\mathrm{L}} = (\nu_{i,\mathrm{L}},\ e_{i,\mathrm{L}})^T, e_{i,\mathrm{R}}$
	quarks		$q_{i,\mathrm{L},j} = (u_{i,\mathrm{L},j},\ d_{i,\mathrm{L},j})^T, u_{i,\mathrm{R},j}, d_{i,\mathrm{R},j}$
bosons	gauge bosons	electromagnetic	B_μ
		weak	$W^a_\mu,\ a \in \{1, 2, 3\}$
		strong	$G^a_\mu,\ a \in \{1, \dots, 8\}$
	Higgs bosons	physical	H
		unphysical	$G, G^\pm$

3.2. Particle content of the MSSM

The Minimal Supersymmetric Standard Model (MSSM) [HK85] is an $N = 1$ supersymmetric extension of the SM, which contains exactly one pair of supersymmetry generators Q^A and $\bar{Q}_{\dot{A}}$. A Weyl spinor of a chiral superfield is assigned to each fermionic particle of the Standard Model while each SM gauge boson is described by the vector field inside of a vector superfield. The remaining components of the superfields are the superpartners of the Standard Model spectrum.

Similar to the Standard Model, electroweak symmetry breaking is carried out by a Higgs mechanism in the MSSM, too. Since the superpotential which contains the Yukawa couplings is required to be a holomorphic function to yield a supersymmetry-invariant action, two distinct scalar $SU(2)_\mathrm{L}$ doublets are necessary. At lowest order they can be decomposed to

$$\mathcal{H}_1 = \begin{pmatrix} v_1 + \frac{1}{\sqrt{2}}\,(\phi_1 - \boldsymbol{i}\,\chi_1) \\ -\phi_1^- \end{pmatrix}, \quad \mathcal{H}_2 = \begin{pmatrix} \phi_2^+ \\ v_2 + \frac{1}{\sqrt{2}}\,(\phi_2 + \boldsymbol{i}\,\chi_2) \end{pmatrix}, \tag{3.2}$$

with their vacuum expectation values v_1 and v_2, respectively; the ratio v_2/v_1 is commonly denoted as $\tan\beta \equiv t_\beta$.

Both scalar fields are accommodated by independent superfields H_1 and H_2, and receive corresponding fermionic $SU(2)_\mathrm{L}$ superpartners which are named higgsinos:

$$\tilde{\mathcal{H}}_1 = \begin{pmatrix} \tilde{h}_1^0 \\ \tilde{h}_1^- \end{pmatrix}, \quad \tilde{\mathcal{H}}_2 = \begin{pmatrix} \tilde{h}_2^+ \\ \tilde{h}_2^0 \end{pmatrix}. \tag{3.3}$$

The hypercharges of both doublets must be opposite to each other to cancel the anomalies which were otherwise introduced by these additional fermions.

The general supersymmetric Lagrangian of Eq. (2.25) can be specified for the MSSM. The part of the Higgs fields is given by

$$\mathcal{L}_\mathrm{Higgs} = \int \mathrm{d}^4\theta \sum_{j\,=\,1}^{2} H_j^\dagger \exp\left(g_Y\, Y\, V_Y + g_\mathrm{w}\,\tau_a\, V_\mathrm{w}^a\right) H_j + \left(\int \mathrm{d}^2\theta\, \mathcal{W}_\mathrm{MSSM} + \mathrm{h.\,c.}\right) \tag{3.4}$$

with the superpotential

$$\mathcal{W}_\mathrm{MSSM} = \mu\, H_1 \overset{SU}{\odot} H_2 - h_{e,\,ij}\, H_1 \overset{SU}{\odot} L_i\, E_j^C - h_{d,\,ij}\, H_1 \overset{SU}{\odot} Q_i\, D_j^C - h_{u,\,ij}\, Q_i \overset{SU}{\odot} H_2\, U_j^C\ . \tag{3.5}$$

Besides the Yukawa-coupling matrices $\mathbf{h}_f$, $f \in \{u,\, d,\, e\}$ with their corresponding elements $h_{f,\,ij}$, $i,\, j \in \{1,\, 2,\, 3\}$, also the bilinear μ term is part of the superpotential which is required to generate masses for $\tilde{\mathcal{H}}_1$ and $\tilde{\mathcal{H}}_2$.

The $SU(2)_\mathrm{L}$ product of two chiral superfield doublets Φ_1 and Φ_2 is defined by

$$\Phi_1 \overset{SU}{\odot} \Phi_2 = \epsilon_{\alpha\beta}\, \Phi_1^\alpha\, \Phi_2^\beta \tag{3.6}$$

with the doublet indices $\alpha,\ \beta \in \{1,\ 2\}$, the Levi–Civita symbol $\epsilon_{\alpha\beta}$ and the convention $\epsilon_{12} = -1$.

The vector superfields of the MSSM are listed in Tab. 3.2.1, and the left-chiral superfields in Tab. 3.2.2. The fields for the right-handed particles are displayed as charge-conjugate left-handed singlets in accordance with Eq. (3.5).

Table 3.2.: The particle content of the MSSM.

3.2.1: The gauge superfields of the MSSM.

Superfield	Components	Group	Index
V_Y	$B_\mu, \tilde{B}$	$U(1)_Y$	
V_w^a	$W_\mu^a, \tilde{W}^a$	$SU(2)_\mathrm{L}$	$a \in \{1, 2, 3\}$
V_c^a	$G_\mu^a, \tilde{G}^a$	$SU(3)_\mathrm{c}$	$a \in \{1, \ldots, 8\}$

3.2.2: The matter superfields of the MSSM with their corresponding quantum numbers; generation index $i \in \{1,\ 2,\ 3\}$.

Superfield	Components	Y_f	T_f^3	Isospin	Color
L_i	$l_{i,\mathrm{L}},\ \tilde{l}_{i,\mathrm{L}}$	-1	$\pm 1/2$	Doublet	Singlet
E_i^C	$(e_{i,\mathrm{R}})^C,\ (\tilde{e}_{i,\mathrm{R}})^C$	2	0	Singlet	Singlet
Q_i	$q_{i,\mathrm{L}},\ \tilde{q}_{i,\mathrm{L}}$	$1/3$	$\pm 1/2$	Doublet	Triplet
U_i^C	$(u_{i,\mathrm{R}})^C,\ (\tilde{u}_{i,\mathrm{R}})^C$	$-4/3$	0	Singlet	Triplet
D_i^C	$(d_{i,\mathrm{R}})^C,\ (\tilde{d}_{i,\mathrm{R}})^C$	$2/3$	0	Singlet	Triplet
H_1	$\mathcal{H}_1,\ \tilde{\mathcal{H}}_1$	-1	$\pm 1/2$	Doublet	Singlet
H_2	$\mathcal{H}_2,\ \tilde{\mathcal{H}}_2$	1	$\pm 1/2$	Doublet	Singlet

3.3. Supersymmetry breaking in the MSSM

The generally valid soft supersymmetry-breaking terms are listed in Eq. (2.27). Their specification for the MSSM yields

$$\begin{aligned}\mathcal{L}_\text{breaking} = &-\left(m_{\tilde{q}}^2\right)_{ij} \tilde{q}_{i,\mathrm{L}}^*\, \tilde{q}_{j,\mathrm{L}} - \left(m_{\tilde{u}}^2\right)_{ij} \tilde{u}_{i,\mathrm{R}}^*\, \tilde{u}_{j,\mathrm{R}} - \left(m_{\tilde{d}}^2\right)_{ij} \tilde{d}_{i,\mathrm{R}}^*\, \tilde{d}_{j,\mathrm{R}} \\ &- \left(m_{\tilde{l}}^2\right)_{ij} \tilde{l}_{i,\mathrm{L}}^*\, \tilde{l}_{j,\mathrm{L}} - \left(m_{\tilde{e}}^2\right)_{ij} \tilde{e}_{i,\mathrm{R}}^*\, \tilde{e}_{j,\mathrm{R}}\end{aligned}$$

$$
\begin{aligned}
&- \tilde{m}_1^2\, \mathcal{H}_1^\dagger\, \mathcal{H}_1 - \tilde{m}_2^2\, \mathcal{H}_2^\dagger\, \mathcal{H}_2 \\
&- \Big[(\mathbf{h}_u\, \mathbf{A}_u)_{ij}\, \tilde{q}_{i,\mathrm{L}} \overset{SU}{\odot} \mathcal{H}_2\, \tilde{u}^*_{j,\mathrm{R}} \\
&\quad + (\mathbf{h}_d\, \mathbf{A}_d)_{ij}\, \mathcal{H}_1 \overset{SU}{\odot} \tilde{q}_{i,\mathrm{L}}\, \tilde{d}^*_{j,\mathrm{R}} \\
&\quad + (\mathbf{h}_e\, \mathbf{A}_e)_{ij}\, \mathcal{H}_1 \overset{SU}{\odot} \tilde{l}_{i,\mathrm{L}}\, \tilde{e}^*_{j,\mathrm{R}} + \mathrm{h.\,c.} \Big] \\
&- \Big(b_{\mathcal{H}_1 \mathcal{H}_2}\, \mu\, \mathcal{H}_1 \overset{SU}{\odot} \mathcal{H}_2 + \mathrm{h.\,c.} \Big) \\
&- \frac{1}{2} \Big(M_1\, \tilde{B}\, \tilde{B} + M_2\, \tilde{W}^a\, \tilde{W}^a + \tilde{m}_{\tilde{g}}\, \tilde{G}^b\, \tilde{G}^b + \mathrm{h.\,c.} \Big) \ ,
\end{aligned}
\tag{3.7}
$$

with the generation indices i, $j \in \{1,\, 2,\, 3\}$ and the gauge-group indices $a \in \{1,\, 2,\, 3\}$ and $b \in \{1, \ldots, 8\}$.

It is noteworthy that no terms proportional to a single field remain in this expression. This is an immediate consequence of the absence of a $U(1)_Y$–$SU(2)_\mathrm{L}$–$SU(3)_\mathrm{c}$-invariant scalar field in the MSSM.

Neglecting all flavor-violating interactions[4] yields flavor-diagonal Yukawa coupling matrices $h_{f,\,ij}$ and mixing matrices $\mathbf{A}_f = A_{f,\,ij}$, $f \in \{u,\, d,\, e\}$. Furthermore, also the mass-breaking matrices $\left(m^2_{\tilde{f}}\right)_{ij}$, $\tilde{f} \in \{\tilde{q},\, \tilde{u},\, \tilde{d},\, \tilde{l},\, \tilde{e}\}$ are flavor-diagonal. In that case the matrix indices i and j are suppressed.

3.4. Mass eigenstates

Different particles with identical values for all their quantum numbers can build mixed states. In the MSSM this concerns the sfermion sector, the gaugino–higgsino sector, and the Higgs-boson sector. The former two are described in the following and the notation for the succeeding chapters is introduced. A detailed derivation of the Higgs- and Goldstone-boson masses is performed in Chapter 6.

3.4.1. Sfermions

In the following flavor-mixing is disregarded. Therefore the Yukawa couplings $h_{f,\,ij}$ and the soft-breaking mass and mixing parameters $\left(m^2_{\tilde{f}}\right)_{ij}$ and $A_{f,\,ij}$ are flavor-diagonal and denoted as h_f, $m^2_{\tilde{f}}$ and A_f, respectively.

[4]This implies the approximation of a diagonal CKM matrix [Cab63; KM73].

Each sfermion mass eigenstate is composed of the superpartners of its corresponding left- and right-chiral fermions:

$$\begin{pmatrix} \tilde{f}_1 \\ \tilde{f}_2 \end{pmatrix} = \mathbf{U}_{\tilde{f}} \begin{pmatrix} \tilde{f}_\mathrm{L} \\ \tilde{f}_\mathrm{R} \end{pmatrix} \tag{3.8}$$

with the unitary mixing matrix $\mathbf{U}_{\tilde{f}}$ ($\tilde{f} \in \{\tilde{u},\, \tilde{d},\, \tilde{e},\, \tilde{c},\, \tilde{s},\, \tilde{\mu},\, \tilde{t},\, \tilde{b},\, \tilde{\tau}\}$ if not stated otherwise). The transformation $\mathbf{U}_{\tilde{f}}\mathbf{M}_{\tilde{f}}\mathbf{U}^\dagger_{\tilde{f}}$ diagonalizes the mass matrix

$$\mathbf{M}_{\tilde{f}} = \begin{pmatrix} m^2_{\tilde{f}_\mathrm{L}} + m^2_f + M^2_Z\, c_{2\beta} \left(T^3_f - Q_f\, s^2_\mathrm{w}\right) & m_f\, X_f \\ m_f\, X^*_f & m^2_{\tilde{f}_\mathrm{R}} + m^2_f + M^2_Z\, c_{2\beta}\, Q_f\, s^2_\mathrm{w} \end{pmatrix}, \tag{3.9a}$$

$$X_f = A^*_f - \mu\, \kappa_f \;, \quad \kappa_{u,\,c,\,t} = \frac{1}{t_\beta} \;, \quad \kappa_{d,\,s,\,b,\,e,\,\mu,\,\tau} = t_\beta \;. \tag{3.9b}$$

which is composed of the bilinear field coefficients at the tree level comprising matter terms, soft breaking terms and gauge terms ($f \in \{u,\, d,\, e,\, c,\, s,\, \mu,\, t,\, b,\, \tau\}$ if not stated otherwise).[5] The eigenvalues are

$$\begin{aligned} m^2_{\tilde{f}_{1/2}} = \frac{1}{2} \Bigg[& m^2_{\tilde{f}_\mathrm{L}} + m^2_{\tilde{f}_\mathrm{R}} + 2\, m^2_f + M^2_Z\, c_{2\beta}\, T^3_f \\ & \mp \sqrt{\left(m^2_{\tilde{f}_\mathrm{L}} - m^2_{\tilde{f}_\mathrm{R}} + M^2_Z\, c_{2\beta} \left(T^3_f - 2\, Q_f\, s^2_\mathrm{w}\right)\right)^2 + 4\, m^2_f\, |X_f|^2}\, \Bigg] \;. \end{aligned} \tag{3.10}$$

3.4.2. Charginos and neutralinos

Furthermore, higgsinos and gauginos also mix among each other:

$$\begin{pmatrix} \chi^-_1 \\ \chi^-_2 \end{pmatrix} = \mathbf{U} \begin{pmatrix} \lambda^-_W \\ \tilde{h}^-_1 \end{pmatrix}, \quad \begin{pmatrix} \chi^+_1 \\ \chi^+_2 \end{pmatrix} = \mathbf{V} \begin{pmatrix} \lambda^+_W \\ \tilde{h}^+_2 \end{pmatrix}, \quad \begin{pmatrix} \chi^0_1 \\ \chi^0_2 \\ \chi^0_3 \\ \chi^0_4 \end{pmatrix} = \mathbf{N} \begin{pmatrix} \tilde{B} \\ \tilde{W}^3 \\ \tilde{h}^0_1 \\ \tilde{h}^0_2 \end{pmatrix} \tag{3.11}$$

with the unitary mixing matrices $\mathbf{N}$, $\mathbf{U}$, $\mathbf{V}$ and the gauginos after electroweak symmetry breaking

$$\begin{pmatrix} \lambda_A \\ \lambda_Z \end{pmatrix} = \begin{pmatrix} c_\mathrm{w} & s_\mathrm{w} \\ -s_\mathrm{w} & c_\mathrm{w} \end{pmatrix} \begin{pmatrix} \tilde{B} \\ \tilde{W}^3 \end{pmatrix}, \tag{3.12a}$$

[5] The symbols m_f, T^3_f and Q_f depict the mass, third component of the isospin and charge of the fermion f, respectively.

$$\begin{pmatrix} \lambda_W^- \\ \lambda_W^+ \end{pmatrix} = \frac{1}{\sqrt{2}} \begin{pmatrix} 1 & \boldsymbol{i} \\ 1 & -\boldsymbol{i} \end{pmatrix} \begin{pmatrix} \tilde{W}^1 \\ \tilde{W}^2 \end{pmatrix} . \tag{3.12b}$$

The Dirac spinors of the charginos $\tilde{\chi}_i^\pm$, $i \in \{1, 2\}$ and neutralinos $\tilde{\chi}_j^0$, $j \in \{1, 2, 3, 4\}$ are composed of these Weyl spinors $\chi_i^\pm$ and χ_i^0:

$$\tilde{\chi}_i^+ = \begin{pmatrix} \chi_i^+ \\ \left(\overline{\chi_i^-}\right)^T \end{pmatrix}, \quad \tilde{\chi}_i^- = \begin{pmatrix} \chi_i^- \\ \left(\overline{\chi_i^+}\right)^T \end{pmatrix}, \quad \tilde{\chi}_j^0 = \begin{pmatrix} \chi_j^0 \\ \left(\overline{\chi_j^0}\right)^T \end{pmatrix} . \tag{3.13}$$

Neutralinos are identically equal to their antiparticles, thus being Majorana particles.

The tree-level mass eigenstates of the charginos $\tilde{\chi}_i^\pm$ are acquired by the singular value decomposition $\mathbf{U}^*\mathbf{X}\mathbf{V}^\dagger$ of

$$\mathbf{X} = \begin{pmatrix} M_2 & \sqrt{2}\, M_W\, s_\beta \\ \sqrt{2}\, M_W\, c_\beta & \mu \end{pmatrix} \tag{3.14}$$

whose evaluation yields the positive real masses

$$m_{\tilde{\chi}_{1/2}^\pm} = \frac{\sqrt{2}}{2} \left[|M_2|^2 + |\mu|^2 + 2\, M_W^2 \mp \sqrt{\left(|M_2|^2 + |\mu|^2 + 2\, M_W^2\right)^2 - 4|X_{\tilde{\chi}^\pm}|^2} \right]^{\frac{1}{2}} \tag{3.15a}$$

with

$$X_{\tilde{\chi}^\pm} = M_2\, \mu - 2\, M_W^2\, c_\beta\, s_\beta \ . \tag{3.15b}$$

For the neutralinos $\tilde{\chi}_i^0$ just one unitary mixing matrix $\mathbf{N}$ is necessary due to their Majorana character. The mass eigenstates are calculated by applying Takagi's factorization [Tak27], i. e. the transformation $\mathbf{N}^*\mathbf{Y}\mathbf{N}^\dagger$, to the symmetric mass matrix

$$\mathbf{Y} = \begin{pmatrix} M_1 & 0 & -M_Z\, s_\mathrm{w}\, c_\beta & M_Z\, s_\mathrm{w}\, s_\beta \\ 0 & M_2 & M_Z\, c_\mathrm{w}\, c_\beta & M_Z\, c_\mathrm{w}\, s_\beta \\ -M_Z\, s_\mathrm{w}\, c_\beta & M_Z\, c_\mathrm{w}\, c_\beta & 0 & -\mu \\ M_Z\, s_\mathrm{w}\, s_\beta & M_Z\, c_\mathrm{w}\, s_\beta & -\mu & 0 \end{pmatrix} . \tag{3.16}$$

The four corresponding singular values are lengthy expressions in the most general case with the complex parameters μ, M_1 and M_2. They are given by the positive real square roots of the zeroes of the following fourth-order polynomial in x_0:

$$
\begin{aligned}
0 = \Bigg\{ & \left(\frac{1}{2}\, M_Z^2\, s_{2\beta}\, s_{2\mathrm{w}}\right)^4 + |\mu|^2 \left(|\mu|^2\, |M_1|^2\, |M_2|^2 + |M_1|^2\, M_Z^4\, c_\mathrm{w}^4 + |M_2|^2\, M_Z^4\, s_\mathrm{w}^4\right) \\
& + 2\, |\mu|^2\, M_Z^2 \left\{|M_1|^2\, c_\mathrm{w}^2\, \Re\mathfrak{e}[\mu\, M_2] + |M_2|^2\, s_\mathrm{w}^2\, \Re\mathfrak{e}[\mu\, M_1]\right\} + \frac{1}{2}\, |\mu|^2\, M_Z^4\, s_{2\mathrm{w}}^2\, \Re\mathfrak{e}[M_1\, M_2^*] \\
& + \frac{1}{2} \left(M_Z^2\, s_{2\beta}\, s_{2\mathrm{w}}\right)^2 \Re\mathfrak{e}\Big[\mu \left(\mu\, M_1\, M_2 + M_1\, M_Z^2\, c_\mathrm{w}^2 + M_2\, M_Z^2\, s_\mathrm{w}^2\right)\Big] \Bigg\} \\
& - x_0 \Bigg\{ |\mu|^2 \left(2\, |M_1|^2\, |M_2|^2 + M_Z^4\right) + \tfrac{1}{2} \left(M_Z^2\, s_{2\beta}\, s_{2\mathrm{w}}\right)^2 \left(|\mu|^2 - M_Z^2\right) \\
& \qquad + |M_1|^2 \left(|\mu|^2 + M_Z^2\, c_\mathrm{w}^2\right)^2 + |M_2|^2 \left(|\mu|^2 + M_Z^2\, s_\mathrm{w}^2\right)^2 \\
& \qquad + 2\, M_Z^2\, c_\mathrm{w}^2 \left(|M_1|^2 + |\mu|^2\right) \Re\mathfrak{e}[M_2\, \mu] + 2\, M_Z^2\, s_\mathrm{w}^2 \left(|M_2|^2 + |\mu|^2\right) \Re\mathfrak{e}[M_1\, \mu] \\
& \qquad + \left(M_Z^2\, s_{2\beta}\, s_{2\mathrm{w}}\right)^2 \Re\mathfrak{e}[\mu\, (M_1 + M_2)] + \tfrac{1}{2} \left(M_Z^2\, c_{2\beta}\, s_{2\mathrm{w}}\right)^2 \Re\mathfrak{e}[M_1\, M_2^*] \Bigg\} \\
& + x_0^2 \Big\{ \left(|M_1|^2 + M_Z^2 + |\mu|^2\right) \left(|M_2|^2 + M_Z^2 + |\mu|^2\right) + 2\, M_Z^2\, \Re\mathfrak{e}\Big[M_1\, \mu\, s_\mathrm{w}^2 + M_2\, \mu\, c_\mathrm{w}^2\Big] \\
& \qquad + \tfrac{1}{2} \left(M_Z^2\, s_{2\beta}\, s_{2\mathrm{w}}\right)^2 + |M_1|^2 \left(|\mu|^2 + M_Z^2\, c_{2\mathrm{w}}\right) + |M_2|^2 \left(|\mu|^2 - M_Z^2\, c_{2\mathrm{w}}\right) \Big\} \\
& - x_0^3 \left\{|M_1|^2 + |M_2|^2 + 2\, M_Z^2 + 2\, |\mu|^2\right\} \\
& + x_0^4\ .
\end{aligned}
\tag{3.17}
$$

As mentioned above, the mass eigenstates of the Higgs-boson sector are derived in Chapter 6.

4. Higher-order calculations

Renormalizable quantum field theories allow precise calculations of observables by successive evaluation of the corresponding Feynman diagrams with an increasing number of closed loops. Since the momentum inside a loop is not fixed, all possible values have to be taken into account, which is realized by integration over the loop momentum in the respective Feynman diagram.

4.1. One-loop order

At the one-loop level the propagators with their corresponding masses m_i appear together with the external momenta p_j and the loop momentum q inside a loop diagram, leading to an expression $\tilde{f}_1(q,\, p_j,\, m_i)$. The evaluated Feynman diagram $\tilde{F}_1(p_j,\, m_i)$ is obtained by integration:

$$\tilde{F}_1(p_j,\, m_i) = \int\limits_{\mathbb{R}^4} \frac{\mathrm{d}^4 q}{(2\pi)^4}\, \tilde{f}_1(q,\, p_j,\, m_i)\ . \tag{4.1}$$

As can be verified already for simple integrands, e. g. $\tilde{f}\,(q,\, p_j,\, m_i) = 1/(q^2 - m^2)$, the integration leads to divergent results for $|q| \to \infty$ (ultra-violet divergences). To avoid this problem the divergent parts of the integral have to be controlled by an additional mechanism which is called regularization. Widely used methods are dimensional regularization (DREG) [tV72; BG72; CM72; Ash72] or dimensional reduction (DRED) [Sie79; CJN80]. As described in e. g. Ref. [Wei09] the integration measure and dimension are modified leading to

$$F_1(p_j,\, m_i,\, D) = \int\limits_{\mathbb{R}^D} \frac{\mathrm{d}^D q}{\boldsymbol{i}\,\pi^2\,(2\pi\mu_{\mathrm{D}})^{D-4}}\, f_1(q,\, p_j,\, m_i,\, D) \tag{4.2}$$

in $D = 4 - 2\epsilon$ dimensions with the regularization mass parameter μ_{D}; the divergent part is parametrized by ϵ and manifestly recovered in the limit $\epsilon \to 0$. Thereby μ_{D} takes care of the necessity to keep the action $\int\limits_{\mathbb{R}^D} \mathrm{d}^D x \, \mathcal{L}(D)$ dimensionless.

In DREG all momenta and fields are treated as D-dimensional objects, changing the number of degrees of freedom asymmetrically for bosons and fermions and thus breaking supersymmetry. DRED prevents this issue by only modifying momenta and integration measures, but keeping other objects, e. g. gamma matrices, four-dimensional. Alternatively, supersymmetry can also be restored when using DREG by adding the missing contributions as demonstrated in Refs. [Var10; SV12]. The final elimination of the ultra-violet divergent parts is taken care of by renormalization as described in Chapter 5.

Moreover, infra-red divergences can occur when massless particles are propagating inside a loop. They can be regularized by introducing a cut-off for the integration or a pseudo-mass for the particle and they are eliminated by adding the corresponding Feynman diagrams with real emission of this massless particle. Since infra-red divergences are not important in the context of this thesis, they are not further considered here.

Besides DREG and DRED several other regularization methods exist like the Pauli–Villars procedure [PV49], lattice field theory, causal perturbation theory [EG73] and others.

Depending on the structure of the kernel f_1 different kinds of loop integrals are distinguished: if the numerator is a number, a mass parameter or another scale which is independent on the loop momentum, the integral is denoted as scalar; if the numerator contains the loop momentum, the integral is called higher-rank or tensor integral. The methods required for calculating scalar one-loop integrals were described first in Ref. [tV79]. The reduction of one-loop tensor integrals to scalar integrals was explained first in Ref. [PV79]. All one-loop n-point functions can be reduced to a basis of scalar one-loop integrals of up to four-point functions.

If only two-point functions are considered, just one external momentum remains. Accordingly, only the two different variables q and $q + p$ can appear in the propagators of the Feynman diagrams. In general, the Feynman integrals for n-point vertex functions with $n > 2$, but just one non-zero external momentum, can be decomposed into the integrals for two-point functions by partial fractioning.

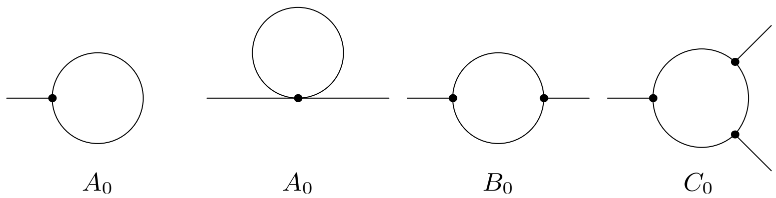

Figure 4.1.: The Feynman diagrams of generic one-loop integrals up to three-point functions.

The basic topologies for the one-loop integrals of up to three-point functions are displayed in Fig. 4.1. The following integrals will be used in this thesis, with the notations given here:

$$A_0\Big(m^2\Big) := \int\limits_{\mathbb{R}^D} \frac{\mathrm{d}^D q}{\boldsymbol{i}\,\pi^2\,(2\pi\mu_\mathrm{D})^{D-4}} \frac{1}{[q^2 - m^2 + \boldsymbol{i}\,\epsilon']} \;, \tag{4.3a}$$

$$B_0\Big(p^2,\, m_1^2,\, m_2^2\Big) := \int\limits_{\mathbb{R}^D} \frac{\mathrm{d}^D q}{\boldsymbol{i}\,\pi^2\,(2\pi\mu_\mathrm{D})^{D-4}} \frac{1}{[q^2 - m_1^2 + \boldsymbol{i}\,\epsilon']\Big[(q+p)^2 - m_2^2 + \boldsymbol{i}\,\epsilon'\Big]} \;, \tag{4.3b}$$

$$\begin{aligned} B_\mu\Big(p,\, m_1^2,\, m_2^2\Big) &:= \int\limits_{\mathbb{R}^D} \frac{\mathrm{d}^D q}{\boldsymbol{i}\,\pi^2\,(2\pi\mu_\mathrm{D})^{D-4}} \frac{q_\mu}{[q^2 - m_1^2 + \boldsymbol{i}\,\epsilon']\Big[(q+p)^2 - m_2^2 + \boldsymbol{i}\,\epsilon'\Big]} \;, \\ &:= p_\mu B_1\Big(p^2,\, m_1^2,\, m_2^2\Big) \;, \end{aligned} \tag{4.3c}$$

$$\begin{aligned} B_{\mu\nu}\Big(p,\, m_1^2,\, m_2^2\Big) &:= \int\limits_{\mathbb{R}^D} \frac{\mathrm{d}^D q}{\boldsymbol{i}\,\pi^2\,(2\pi\mu_\mathrm{D})^{D-4}} \frac{q_\mu q_\nu}{[q^2 - m_1^2 + \boldsymbol{i}\,\epsilon']\Big[(q+p)^2 - m_2^2 + \boldsymbol{i}\,\epsilon'\Big]} \;, \\ &:= g_{\mu\nu} B_{00}\Big(p^2,\, m_1^2,\, m_2^2\Big) + p_\mu p_\nu B_{11}\Big(p^2,\, m_1^2,\, m_2^2\Big) \;, \end{aligned} \tag{4.3d}$$

$$\begin{aligned} &C_0\Big(p_1^2,\, p_2^2,\, (p_1+p_2)^2,\, m_1^2,\, m_2^2,\, m_3^2\Big) := \\ &\int\limits_{\mathbb{R}^D} \frac{\mathrm{d}^D q}{\boldsymbol{i}\,\pi^2\,(2\pi\mu_\mathrm{D})^{D-4}} \frac{1}{[q^2 - m_1^2 + \boldsymbol{i}\,\epsilon']\Big[(q+p_1)^2 - m_2^2 + \boldsymbol{i}\,\epsilon'\Big]\Big[(q+p_2)^2 - m_3^2 + \boldsymbol{i}\,\epsilon'\Big]} \end{aligned} \tag{4.3e}$$

with $\epsilon' > 0$ being the infinitesimal deviation from the real axis to obtain causal Feynman propagators. Explicit solutions of the integrals are listed in Appendix B.1.

4.2. Two-loop order

For higher precision two-loop calculations are required and the formalism has to be extended to two-loop Feynman diagrams. Besides the external momenta p_j, two independent loop momenta q_1 and q_2 appear now and both integrations have to be regularized.

A general two-loop Feynman integral is given by

$$F_2(p_j,\, m_i,\, D) = \int\limits_{\mathbb{R}^D}\int\limits_{\mathbb{R}^D} \frac{\mathrm{d}^D q_1\, \mathrm{d}^D q_2}{\left(\boldsymbol{i}\,\pi^2\,(2\pi\mu_{\mathrm{D}})^{D-4}\right)^2}\, f_2(q_1,\, q_2,\, p_j,\, m_i,\, D)\ . \tag{4.4}$$

Possible higher-rank tensor structures of the integrand f_2 can be reduced to scalar terms as described in Ref. [WSB94b]. In contrast to the one-loop case, neither a complete basis of master integrals is known, nor full analytical solutions for all possible scalar two-loop integrals exist. However, different numerical methods are available to evaluate these integrals [BCH13; Smi13; Glu+11; BW08; Fre12; UF08].

Regarding only two-point vertex functions, the external momentum and the two loop momenta form a set of five different kinematic variables:

$$k_1 = q_1\ ,\quad k_2 = q_1 + p\ ,\quad k_3 = q_2 - q_1\ ,\quad k_4 = q_2\ ,\quad k_5 = q_2 + p\ . \tag{4.5}$$

In analogy to the one-loop case, the integrals for n-point vertex functions with $n > 2$, but just one non-zero external momentum, can be decomposed into two-loop integrals with a maximum of five different denominators corresponding to the five different kinematic variables of Eq. (4.5).

The different topologies of the one-particle irreducible two-point functions and their corresponding notations are displayed in Fig. 4.2.1. The symbols used for scalar two-point functions with n propagators are defined as follows:

$$\begin{aligned}&\mathrm{T}_{a_1\ldots a_n}\!\left(p^2;\, m_1^2,\, \ldots,\, m_n^2\right) = \\ &\qquad\int\limits_{\mathbb{R}^D}\int\limits_{\mathbb{R}^D} \frac{\mathrm{d}^D q_1\, \mathrm{d}^D q_2}{\left(\boldsymbol{i}\,\pi^2\,(2\pi\mu_{\mathrm{D}})^{D-4}\right)^2} \frac{1}{\left[k_{a_1}^2 - m_1^2 + \boldsymbol{i}\,\epsilon'\right]\cdots\left[k_{a_n}^2 - m_n^2 + \boldsymbol{i}\,\epsilon'\right]}\ ,\end{aligned} \tag{4.6}$$

with $a_i \in \{1,\, 2,\, 3,\, 4,\, 5\}$ and k_{a_i} corresponding to the kinematic variables in Eq. (4.5).

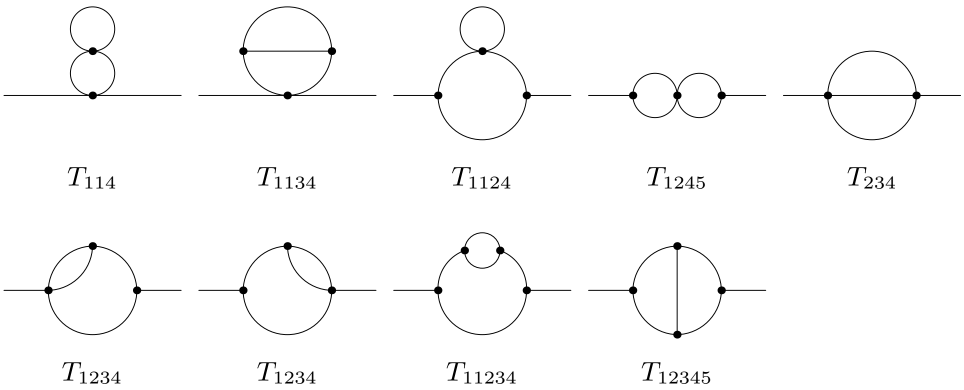

4.2.1: Two-point functions.

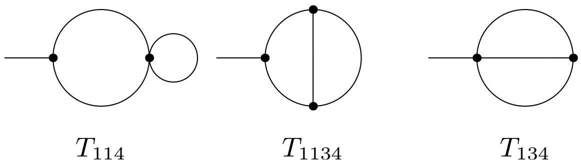

4.2.2: One-point functions.

Figure 4.2.: The Feynman diagrams of generic two-loop integrals for one- and two-point functions.

For the special case of a vanishing external momentum only vacuum diagrams with the variables k_1, k_3 and k_4 remain and all integrals can be derived analytically. Also the one-point functions ($\equiv$ tadpole diagrams), which are depicted in Fig. 4.2.2, can be expressed in terms of these variables. To abbreviate the notation the identity

$$\mathrm{T}_{a_1 \ldots a_n}\Big(p^2 = 0;\, m_1^2, \ldots,\, m_n^2\Big) \equiv \mathrm{T}_{a_1 \ldots a_n}\Big(m_1^2, \ldots,\, m_n^2\Big)\ , \quad a_i \in \{1,\, 3,\, 4\}\ , \tag{4.7}$$

is introduced. The necessary explicit expressions that are used in this thesis are presented in Appendix B.2.

5. Renormalization

In Chapter 4 higher-order Feynman diagrams have been introduced and their divergences have been parametrized by the dimension $D = 4 - 2\epsilon$. Physical observables must not depend on this regulator in the final result; the method used to absorb the ultra-violet divergent parts of the loop integrals is called renormalization. After performing this step the limit $D \to 4$ (or $\epsilon \to 0$) can be taken without problems.

5.1. Renormalization methods

An important renormalization method, giving wide insights into the mathematical foundation of renormalization of quantum field theories, is given by the Bogolyubov–Parasyuk theorem [BP55], which was later completely proven by Hepp and Zimmermann [Hep66; Zim69] and is therefore called BPHZ theorem today. The fundamental observation is that the divergent parts of each loop integral are just polynomials in the external momenta at each level of perturbation theory after canceling possible subdivergences. Thus, renormalization of a divergent loop integral corresponds to the subtraction of the proper terms in the Taylor series of the integrand (named R-operation). The general solution of this procedure contains free constants which are interpreted as counterterms and fixed by a renormalization scheme.

The advantage of BPHZ renormalization is the unnecessity of a preceding regularization of the divergent integrals. However, it is complicated to impose symmetry relations between different counterterms. The used method of renormalization in this thesis is the multiplicative renormalization procedure which is explained in the following sections.

5.2. Renormalization transformation

Multiplicative renormalization can be carried out by the application of the following transformations:

$$m \to m_0 := Z_m \, m = (1 + \delta Z_m) \, m = m + \delta m \ , \tag{5.1a}$$

$$g \to \ g_0 := Z_g \, g \ \ = (1 + \delta Z_g) \, g \ \ = g + \delta g \ , \tag{5.1b}$$

for all masses m and all couplings g, i. e. all parameters inside the Lagrangian. Furthermore, all appearing fields ψ have to be renormalized to obtain finite vertex functions:

$$\psi \to \psi_0 := \sqrt{Z_\psi} \, \psi = \sqrt{1 + \delta Z_\psi} \, \psi \ . \tag{5.2}$$

The parameters and fields before the transformation are called bare (depicted by an index 0), while afterwards there are the renormalization constants (depicted by a δ) and the renormalized parameters and fields. Each renormalization constant can be expanded as a series according to increasing loop order.

Having performed this transformation additional interaction terms are described by the Lagrangian, which are called counterterms. Each renormalized tree-level interaction gets assigned a counterterm; however also new vertices which do not exist at lowest order of perturbation theory could arise. Usually one counterterm consists of several renormalization constants. In gauge theories, gauge invariance is preserved by fixing the renormalization constants in a proper way obeying the Slavnov–Taylor identities [Aok+80; BSH86; Hol+02].

Beyond the one-loop order further complications have to be taken care of. Firstly, all renormalization transformations need to be expanded to higher orders:

$$m \to m_0 := Z_m \, m \ \ = m + \delta^{(1)} m + \delta^{(2)} m + \mathcal{O}\Big(\delta^{(3)} m\Big) \ , \tag{5.3a}$$

$$g \to \ g_0 := Z_g \, g \ \ \ = g + \delta^{(1)} g + \delta^{(2)} g + \mathcal{O}\Big(\delta^{(3)} g\Big) \ , \tag{5.3b}$$

$$\psi \to \ \psi_0 := \sqrt{Z_\psi} \, \psi = \left[1 + \frac{1}{2} \delta^{(1)} Z_\psi + \frac{1}{2} \left(\delta^{(2)} Z_\psi - \Big(\tfrac{1}{2} \delta^{(1)} Z_\psi\Big)^2\right) + \mathcal{O}\Big(\delta^{(3)} Z_\psi\Big)\right] \psi \tag{5.3c}$$

where the notation of kth order renormalization constants indicated by $\delta^{(k)}$ is introduced. In the case of field renormalization the expansion of the square root to higher orders has to be taken into account, which implies the occurence of higher powers of lower-order renormalization constants at a given level of perturbation. Secondly, products of renormalization constants have to be taken into account as can be seen in Chapter 6. And thirdly, loop diagrams with insertions of counterterms must be respected which is shown explicitly in the Feynman-diagrammatic representation in the main part of this thesis in Chapter 7 and the corresponding analytical results in Appendix D.4 and Appendix D.5. Only after computing the sum of all possible diagrams of the same order the resulting vertex functions are free of divergences and observables are additionally gauge-independent.

5.3. Renormalization schemes

Besides the desired property of canceling the unphysical divergences of a theory, additional finite parts can be exchanged between the renormalization constants and the renormalized parameters. Fixing the finite part of a renormalization constant defines its renormalization scheme and thus the relation of the renormalized parameter to physical observables. For practical calculations the most important renormalization schemes are

- the minimal subtraction (MS) scheme:
  the renormalization constant contains only the divergent part of the bare parameter or field and its finite part is equal to zero; DREG is used to separate the divergences of the loop integrals,

- the modified minimal subtraction ($\overline{\text{MS}}$) scheme:
  similar to the MS scheme, but the finite part comprises the combination of the constants $(-\gamma_\text{E} + \log{(4\pi)})$ which emerge from the loop integration, with the Euler–Mascheroni constant $\gamma_\text{E} := \lim\limits_{n \to \infty} \left(\sum\limits_{k=1}^{n} \frac{1}{k} - \ln n \right)$,

- the dimensional reduction (DR) and the modified dimensional reduction ($\overline{\text{DR}}$) schemes:
  in analogy to the MS and the $\overline{\text{MS}}$ schemes, but DRED is used as regularization method,

- the on-shell (OS) scheme:
  in addition to the divergent parts of the bare parameter the renormalization constant contains all finite parts that are necessary to render the renormalized parameter closely connected to a physical observable[6]. This eliminates the dependence on the regularization parameter μ_{D}.

5.4. Renormalization group

The previous section clarifies that each renormalized parameter depends on the regularization parameter μ_{D} unless it is renormalized in the on-shell scheme. Furthermore, μ_{D} appears as coefficient of all couplings and fields in the Lagrangian to keep the action dimensionless (cf. Chapter 4). Therefore, the μ_{D}-invariant quantitites are given by

$$g_{\mathrm{B}} = \mu_{\mathrm{D}}^{\alpha(g_0)\,\epsilon}\, g_0 = \mu_{\mathrm{D}}^{\alpha(g_0)\,\epsilon}\,\sqrt{Z_g(\mu_{\mathrm{D}})}\, g(\mu_{\mathrm{D}}) = \mu_{\mathrm{D}}^{\alpha(g_0)\,\epsilon}\left(g(\mu_{\mathrm{D}}) + \sum_{k=1}^{\infty}\delta^{(k)} g(\mu_{\mathrm{D}})\right) \;, \tag{5.4a}$$

$$\psi_{\mathrm{B}} = \mu_{\mathrm{D}}^{\alpha(\psi_0)\,\epsilon}\,\psi_0 = \mu_{\mathrm{D}}^{\alpha(\psi_0)\,\epsilon}\,\sqrt{Z_\psi(\mu_{\mathrm{D}})}\,\psi(\mu_{\mathrm{D}}) \;. \tag{5.4b}$$

Thereby $\alpha(g_0)$ and $\alpha(\psi_0)$ are the appropriate and consistent numbers to keep the action dimensionless. The independence of the left-hand sides of Eqs. (5.4) on the regularization parameter is used to define running couplings $g(\mu_{\mathrm{D}})$ whose values depend on the scale μ_{D}:

$$\begin{aligned} 0 &\overset{!}{=} \mu_{\mathrm{D}}^{-\alpha(g_0)\,\epsilon}\,\mu_{\mathrm{D}}\,\frac{\partial}{\partial\mu_{\mathrm{D}}}\, g_{\mathrm{B}} \\ &= \alpha(g_0)\,\epsilon\,\sqrt{Z_g}\, g + \left(\mu_{\mathrm{D}}\,\frac{\partial}{\partial\mu_{\mathrm{D}}}\, g\right)\sqrt{Z_g} + \left[\sum_{g_i}\left(\mu_{\mathrm{D}}\,\frac{\partial}{\partial\mu_{\mathrm{D}}}\, g_i\right)\left(\frac{\partial}{\partial g_i}\,\sqrt{Z_g}\right)\right] g \\ &= \alpha(g_0)\,\epsilon\,\sqrt{Z_g}\, g + \beta(g)\,\sqrt{Z_g} + \left(\sum_{g_i}\beta(g_i)\,\partial_{g_i}\sqrt{Z_g}\right) g \;, \end{aligned} \tag{5.5}$$

with the notation $\partial_{g_i} \equiv \partial/\partial g_i$ and the beta functions

$$\beta(g) := \mu_{\mathrm{D}}\,\frac{\partial}{\partial\mu_{\mathrm{D}}}\, g = \sum_{k\,=\,0}^{\infty}\beta^{(k)}(g) \;. \tag{5.6}$$

[6] This can be a pole mass in the case of a mass parameter, but it also can be a coupling at a fixed scale.

The last term on the right-hand side of Eq. (5.5) takes care of possible further running couplings inside of Z_g. The symbol $\beta^{(k)}$ denotes the part of kth order of the beta function.

The extension of this relation to the higher-order one-particle-irreducible bare n-point vertex functions $\Gamma_{\psi_1,\ldots,\psi_n}$ (ψ_i being the interacting fields) yields the renormalization group equations. With the additional constraint of a diagonal matrix for the field-renormalization constants[7] for the investigated theory (in the MSSM realized by the Peccei–Quinn symmetry [PQ77]) the renormalized vertex functions are given by

$$\hat{\Gamma}_{\psi_1,\ldots,\psi_n} = \prod_{i\,=\,1}^{n} \sqrt{Z_{\psi_i}}\, \Gamma_{\psi_1,\ldots,\psi_n} \ . \tag{5.7}$$

The bare vertex functions are independent on the regularization parameter μ_{D}:

$$\mu_{\mathrm{D}} \frac{\partial}{\partial \mu_{\mathrm{D}}} \Gamma_{\psi_1,\ldots,\psi_n} \stackrel{!}{=} 0 \ . \tag{5.8}$$

Consistently with the above definitions it follows

$$\begin{aligned} 0 &= \left(\prod_{i\,=\,1}^{n} \sqrt{Z_{\psi_i}}^{\,-1} \right) \left\{ \left[\mu_{\mathrm{D}} \frac{\partial}{\partial \mu_{\mathrm{D}}} + \sum_{g_i} \left(\mu_{\mathrm{D}} \frac{\partial}{\partial \mu_{\mathrm{D}}} g_i \right) \frac{\partial}{\partial g_i} \right] \hat{\Gamma}_{\psi_1,\ldots,\psi_n} \right\} \\ &\quad + \left[\sum_{i\,=\,1}^{n} \left(\mu_{\mathrm{D}} \frac{\partial}{\partial \mu_{\mathrm{D}}} \sqrt{Z_{\psi_i}}^{\,-1} \right) \left(\prod_{\substack{j\,=\,1 \\ j\,\neq\, i}}^{n} \sqrt{Z_{\psi_j}}^{\,-1} \right) \right] \hat{\Gamma}_{\psi_1,\ldots,\psi_n} \\ &= \left(\prod_{i\,=\,1}^{n} \sqrt{Z_{\psi_i}}^{\,-1} \right) \left\{ \left[\mu_{\mathrm{D}} \frac{\partial}{\partial \mu_{\mathrm{D}}} + \sum_{g_i} \beta(g_i)\, \partial_{g_i} + \sum_{i\,=\,1}^{n} \gamma_i \right] \hat{\Gamma}_{\psi_1,\ldots,\psi_n} \right\} \ , \end{aligned} \tag{5.9}$$

with the anomalous dimension of the field ψ_i given by

$$\gamma_i := \left(\mu_{\mathrm{D}} \frac{\partial}{\partial \mu_{\mathrm{D}}} \sqrt{Z_{\psi_i}}^{\,-1} \right) \sqrt{Z_{\psi_i}} = \sum_{k\,=\,0}^{\infty} \gamma_i^{(k)} \ . \tag{5.10}$$

The symbols $\gamma_i^{(k)}$ depict the part of kth order of the anomalous dimension.

The renormalized quantity $\hat{\Gamma}_{\psi_1,\ldots,\psi_n}$ and all its derivatives are finite in the limit $\epsilon \to 0$. Thus also $\beta(g_i)$ and γ_i, the beta functions and the anomalous dimensions, are finite.

[7] In general the field-renormalization transformation $\psi_a \to \sum_b \sqrt{Z_{\psi_a \psi_b}}\, \psi_b$ is valid. The theories which are considered here possess some additional symmetry (besides gauge symmetries) that allows for the choice of a diagonal field-renormalization matrix $Z_{\psi_a \psi_b} = Z_{\psi_a}\, \delta_{ab}$, i. e. the off-diagonal entries are not required to absorb divergences.

6. Higgs bosons in the MSSM

The Higgs fields of the MSSM have been introduced in Section 3.2. In the following a detailed derivation of the required tree-level and higher-order relations is performed. The presentation of Sections 6.1–6.4 follows Ref. [Fra+07].

6.1. Higgs potential

The non-derivative terms of the Lagrangian that only depend on the Higgs fields are combined to the Higgs potential (cf. Eq. (3.4) and Eq. (3.7)):

$$V_H = V_H^{\text{Higgs}} + V_H^{\text{breaking}} \;, \tag{6.1a}$$

$$V_H^{\text{Higgs}} = \frac{1}{8}\left(g_Y^2 + g_{\text{w}}^2\right)\left(\mathcal{H}_2^\dagger \mathcal{H}_2 - \mathcal{H}_1^\dagger \mathcal{H}_1\right)^2 + \frac{1}{2} g_{\text{w}}^2 \left(\mathcal{H}_1^\dagger \mathcal{H}_2\right)\left(\mathcal{H}_2^\dagger \mathcal{H}_1\right) \;, \tag{6.1b}$$

$$V_H^{\text{breaking}} = m_1^2\, \mathcal{H}_1^\dagger \mathcal{H}_1 + m_2^2\, \mathcal{H}_2^\dagger \mathcal{H}_2 + \left(m_{12}^2\, \mathcal{H}_1 \overset{SU}{\odot} \mathcal{H}_2 + \text{h.c.}\right) \;, \tag{6.1c}$$

where $m_i^2 \equiv \tilde{m}_i^2 + |\mu|^2$ are real and $m_{12}^2 \equiv b_{\mathcal{H}_1\mathcal{H}_2}\, \mu = |m_{12}^2| \boldsymbol{e}^{\boldsymbol{i}\,\zeta'}$ can be complex. The Higgs fields given in Eq. (3.2) are tree-level states. In the most general case an additional CP-violating relative phase ζ appears in one of the doublets:

$$\mathcal{H}_1 = \begin{pmatrix} v_1 + \frac{1}{\sqrt{2}}\left(\phi_1 - \boldsymbol{i}\,\chi_1\right) \\ -\phi_1^- \end{pmatrix}, \quad \mathcal{H}_2 = \boldsymbol{e}^{\boldsymbol{i}\,\zeta} \begin{pmatrix} \phi_2^+ \\ v_2 + \frac{1}{\sqrt{2}}\left(\phi_2 + \boldsymbol{i}\,\chi_2\right) \end{pmatrix}. \tag{6.2}$$

Herein the vacuum expectation values are chosen as real and positive since any imaginary part could either be absorbed in the phase ζ or by redefining the Higgs fields using the gauge invariance of the Lagrangian.

To abbreviate the notation the following symbols are used:

$$s_x \equiv \sin x \;, \quad c_x \equiv \cos x \;, \quad t_x \equiv \tan x \;. \tag{6.3}$$

Inserting the Higgs doublets of Eq. (6.2) explicitly in the potential of Eq. (6.1) and collecting powers of the field components yields

$$V_H = \text{constant} - T_{\phi_1}\,\phi_1 - T_{\phi_2}\,\phi_2 - T_{\chi_1}\,\chi_1 - T_{\chi_2}\,\chi_2 + \text{triple} + \text{quartic} \\ + \frac{1}{2}\left(\phi_1,\, \phi_2,\, \chi_1,\, \chi_2\right) \mathbf{M}_{\phi_1\phi_2\chi_1\chi_2} \begin{pmatrix} \phi_1 \\ \phi_2 \\ \chi_1 \\ \chi_2 \end{pmatrix} + \left(\phi_1^-,\, \phi_2^-\right) \mathbf{M}_{\phi_1^\pm\phi_2^\pm} \begin{pmatrix} \phi_1^+ \\ \phi_2^+ \end{pmatrix} \;, \tag{6.4}$$

with the coefficients of the linear terms (the tadpole coefficients)

$$T_{\phi_1} = -\sqrt{2}\left[m_1^2\, v_1 - |m_{12}^2|\, v_2\, c_{\zeta+\zeta'} + \tfrac{1}{4}\left(g_Y^2 + g_\mathrm{w}^2\right)\left(v_1^2 - v_2^2\right) v_1\right] \;, \tag{6.5a}$$

$$T_{\phi_2} = -\sqrt{2}\left[m_2^2\, v_2 - |m_{12}^2|\, v_1\, c_{\zeta+\zeta'} - \tfrac{1}{4}\left(g_Y^2 + g_\mathrm{w}^2\right)\left(v_1^2 - v_2^2\right) v_2\right] \;, \tag{6.5b}$$

$$T_{\chi_1} = \sqrt{2}\, |m_{12}^2|\, v_2\, s_{\zeta+\zeta'} \;, \tag{6.5c}$$

$$T_{\chi_2} = -\frac{v_1}{v_2}\, T_{\chi_1} = -\sqrt{2}\, |m_{12}^2|\, v_1\, s_{\zeta+\zeta'} \;, \tag{6.5d}$$

and the coefficients of the quadratic terms (the mass matrices)

$$\mathbf{M}_{\phi_1\phi_2\chi_1\chi_2} = \begin{pmatrix} \mathbf{M}_{\phi_1\phi_2} & \mathbf{M}_{\phi\chi} \\ \mathbf{M}_{\phi\chi}^\dagger & \mathbf{M}_{\chi_1\chi_2} \end{pmatrix}, \tag{6.6a}$$

$$\mathbf{M}_{\phi_1\phi_2} = \begin{pmatrix} m_1^2 + \frac{1}{4}\,(g_Y^2 + g_\mathrm{w}^2)\,(3\,v_1^2 - v_2^2) & -|m_{12}^2|\, c_{\zeta+\zeta'} - \frac{1}{2}\,(g_Y^2 + g_\mathrm{w}^2)\, v_1\, v_2 \\ -|m_{12}^2|\, c_{\zeta+\zeta'} - \frac{1}{2}\,(g_Y^2 + g_\mathrm{w}^2)\, v_1\, v_2 & m_2^2 + \frac{1}{4}\,(g_Y^2 + g_\mathrm{w}^2)\,(3\,v_2^2 - v_1^2) \end{pmatrix}, \tag{6.6b}$$

$$\mathbf{M}_{\phi\chi} = \begin{pmatrix} 0 & |m_{12}^2|\, s_{\zeta+\zeta'} \\ -|m_{12}^2|\, s_{\zeta+\zeta'} & 0 \end{pmatrix}, \tag{6.6c}$$

$$\mathbf{M}_{\chi_1\chi_2} = \begin{pmatrix} m_1^2 + \frac{1}{4}\,(g_Y^2 + g_\mathrm{w}^2)\,(v_1^2 - v_2^2) & -|m_{12}^2|\, c_{\zeta+\zeta'} \\ -|m_{12}^2|\, c_{\zeta+\zeta'} & m_2^2 + \frac{1}{4}\,(g_Y^2 + g_\mathrm{w}^2)\,(v_2^2 - v_1^2) \end{pmatrix}, \tag{6.6d}$$

$$\mathbf{M}_{\phi_1^\pm\phi_2^\pm} = \begin{pmatrix} m_1^2 + \frac{g_Y^2}{4}\,(v_1^2 - v_2^2) + \frac{g_\mathrm{w}^2}{4}\,(v_1^2 + v_2^2) & -|m_{12}^2| e^{i\,(\zeta+\zeta')} - \frac{g_\mathrm{w}^2}{2}\, v_1\, v_2 \\ -|m_{12}^2| e^{i\,(\zeta+\zeta')} - \frac{g_\mathrm{w}^2}{2}\, v_1\, v_2 & m_2^2 + \frac{g_Y^2}{4}\,(v_2^2 - v_1^2) + \frac{g_\mathrm{w}^2}{4}\,(v_1^2 + v_2^2) \end{pmatrix}. \tag{6.6e}$$

The matrices $\mathbf{M}_{\phi_1\phi_2}$ and $\mathbf{M}_{\chi_1\chi_2}$ are real and symmetric. The constant, triple and quartic terms of V_H are not considered in the following since they are not needed for the calculation in this thesis. However, it is worth mentioning that the triple and quartic couplings are determined by the positive real gauge couplings g_Y and g_w.

6.2. Minimization conditions

The minimum of the Higgs potential is located at the vacuum described by the vacuum expectation values v_1 and v_2 in Eq. (6.2), i. e.

$$V_H^{\min} \stackrel{!}{=} V_H\big|_{\phi_1\,=\,0,\,\phi_2\,=\,0,\,\chi_1\,=\,0,\,\chi_2\,=\,0} \ . \tag{6.7}$$

The necessary conditions for $V_H^{\min}$ being a minimum are

$$\left.\frac{\partial V_H}{\partial \phi_1}\right|_{\phi_1\,=\,0,\,\phi_2\,=\,0,\,\chi_1\,=\,0,\,\chi_2\,=\,0} = 0 \ , \tag{6.8a}$$

$$\left.\frac{\partial V_H}{\partial \phi_2}\right|_{\phi_1\,=\,0,\,\phi_2\,=\,0,\,\chi_1\,=\,0,\,\chi_2\,=\,0} = 0 \ , \tag{6.8b}$$

$$\left.\frac{\partial V_H}{\partial \chi_1}\right|_{\phi_1\,=\,0,\,\phi_2\,=\,0,\,\chi_1\,=\,0,\,\chi_2\,=\,0} = 0 \ , \tag{6.8c}$$

$$\left.\frac{\partial V_H}{\partial \chi_2}\right|_{\phi_1\,=\,0,\,\phi_2\,=\,0,\,\chi_1\,=\,0,\,\chi_2\,=\,0} = 0 \ . \tag{6.8d}$$

Their evaluation leads to the relations

$$m_1^2 = |m_{12}^2|\,\frac{v_2}{v_1}\,c_{\zeta+\zeta'} - \frac{1}{4}\left(g_Y^2 + g_{\mathrm{w}}^2\right)\left(v_1^2 - v_2^2\right) \ , \tag{6.9a}$$

$$m_2^2 = |m_{12}^2|\,\frac{v_1}{v_2}\,c_{\zeta+\zeta'} + \frac{1}{4}\left(g_Y^2 + g_{\mathrm{w}}^2\right)\left(v_1^2 - v_2^2\right) \ , \tag{6.9b}$$

$$s_{\zeta+\zeta'} = 0 \ , \tag{6.9c}$$

which are equivalent to vanishing tadpole coefficients in Eq. (6.5). By the use of a Peccei–Quinn transformation [PQ77] the parameters μ and $m_{12}^2 = |m_{12}^2|e^{i\,\zeta'}$ can be redefined such that $\zeta' = 0$, hence Eq. (6.9c) implies $\zeta = 0$. As a consequence of this result, the mass matrices in Eqs. (6.6) simplify: $\mathbf{M}_{\phi\chi} = 0$ and $\mathbf{M}_{\phi^\pm\phi^\pm}$ is real and symmetric like the other mass matrices. Since the triple and quartic couplings of the Higgs potential are determined by the real gauge couplings the Higgs sector of the MSSM is CP-conserving at lowest order.

However CP-violation can occur at higher orders in perturbation theory. The dependence on ζ is kept since it has to be renormalized and acquires independent renormalization constants. In contrast, by using a Peccei–Quinn transformation ζ' can always be set to zero. Hence, the parameter m_{12}^2 is treated as a real quantity from now on.

6.3. Tree-level mass-eigenstate basis

The Higgs potential in Eq. (6.1) can be expressed in terms of a new basis which yields the mass eigenstates at lowest order. The necessary transformations of the Higgs fields are given by

$$\begin{pmatrix} h \\ H \end{pmatrix} = \mathbf{D}_\alpha \begin{pmatrix} \phi_1 \\ \phi_2 \end{pmatrix}, \quad \begin{pmatrix} A \\ G \end{pmatrix} = \mathbf{D}_{\beta_n} \begin{pmatrix} \chi_1 \\ \chi_2 \end{pmatrix}, \quad \begin{pmatrix} H^\pm \\ G^\pm \end{pmatrix} = \mathbf{D}_{\beta_c} \begin{pmatrix} \phi_1^\pm \\ \phi_2^\pm \end{pmatrix}, \tag{6.10}$$

with the notation $\phi_1^- = \left(\phi_1^+\right)^\dagger$, $\phi_2^- = \left(\phi_2^+\right)^\dagger$ and the mixing matrices $\mathbf{D}_x = \left(\begin{smallmatrix} -s_x & c_x \\ c_x & s_x \end{smallmatrix}\right)$, writing $s_x \equiv \sin x$ and $c_x \equiv \cos x$.

The mixing angles α, β_n and β_c are not renormalized, but used as tree-level parameters at all orders of perturbation theory. Their explicit occurrence is kept in the following expressions in order to derive the correct counterterms for the Higgs potential.

Applying the transformations of Eq. (6.10) to the Higgs potential in Eq. (6.1) yields

$$\begin{aligned} V_H = {} & \text{constant} - T_h\, h - T_H\, H - T_A\, A - T_G\, G + \text{triple} + \text{quartic} \\ & + \tfrac{1}{2} \left(h,\, H,\, A,\, G\right) \mathbf{M}_{hHAG} \begin{pmatrix} h \\ H \\ A \\ G \end{pmatrix} + \left(H^-,\, G^-\right) \mathbf{M}_{H^\pm G^\pm} \begin{pmatrix} H^+ \\ G^+ \end{pmatrix}, \end{aligned} \tag{6.11}$$

with the corresponding tadpole coefficients T_h, T_H, T_A and T_G and the mass matrices

$$\mathbf{M}_{hHAG} = \begin{pmatrix} m_h^2 & m_{hH}^2 & m_{hA}^2 & m_{hG}^2 \\ m_{hH}^2 & m_H^2 & m_{HA}^2 & m_{HG}^2 \\ m_{hA}^2 & m_{HA}^2 & m_A^2 & m_{AG}^2 \\ m_{hG}^2 & m_{HG}^2 & m_{AG}^2 & m_G^2 \end{pmatrix}, \quad \mathbf{M}_{H^\pm G^\pm} = \begin{pmatrix} m_{H^\pm}^2 & m_{H^-G^+}^2 \\ m_{G^-H^+}^2 & m_{G^\pm}^2 \end{pmatrix}. \tag{6.12}$$

It should be noted that the mass matrix of the neutral Higgs bosons is real and symmetric whereas the one of the charged bosons is complex and hermitian.

Before presenting the explicit expressions of the entries in Eq. (6.11) also the set of the eight independent parameters g_Y, g_w, m_{12}, m_1, m_2, v_1, v_2 and ζ is substituted by the set of the on-shell parameters e, M_W, s_w, $m_{H^\pm}$ (or m_A), T_h, T_H, T_A and t_β.

Thereby the gauge couplings fulfill the following relations:

$$g_Y = \frac{e}{c_\mathrm{w}} \;, \tag{6.13a}$$
$$g_\mathrm{w} = \frac{e}{s_\mathrm{w}} \;, \tag{6.13b}$$
$$c_\mathrm{w} = \frac{M_W}{M_Z} = \sqrt{1 - s_\mathrm{w}^2} \;. \tag{6.13c}$$

According to electroweak symmetry breaking the gauge-boson masses are connected to the vacuum expectation values as follows,

$$M_Z^2 = \tfrac{1}{2}\left(g_Y^2 + g_\mathrm{w}^2\right)\left(v_1^2 + v_2^2\right) \;, \tag{6.14a}$$
$$M_W^2 = \tfrac{1}{2}\, g_\mathrm{w}^2 \left(v_1^2 + v_2^2\right) \;. \tag{6.14b}$$

In addition, the following quantity is defined:

$$\tan(\beta) \equiv t_\beta = \frac{v_2}{v_1} \;. \tag{6.15}$$

The tadpole coefficients in the basis of lowest-order mass eigenstates are derived as follows by applying the rotations in Eqs. (6.10) with the angles α, β_n and β_c to Eqs. (6.5):

$$\begin{aligned} T_h = \sqrt{2}\Big[& m_1^2\, v_1\, s_\alpha - m_2^2\, v_2\, c_\alpha + m_{12}^2\, c_\zeta \left(v_1\, c_\alpha - v_2\, s_\alpha\right) \\ & + \tfrac{1}{4}\left(g_Y^2 + g_\mathrm{w}^2\right)\left(v_1^2 - v_2^2\right)\left(v_1\, s_\alpha + v_2\, c_\alpha\right)\Big] \;, \end{aligned} \tag{6.16a}$$
$$\begin{aligned} T_H = \sqrt{2}\Big[& - m_1^2\, v_1\, c_\alpha - m_2^2\, v_2\, s_\alpha + m_{12}^2\, c_\zeta \left(v_1\, s_\alpha + v_2\, c_\alpha\right) \\ & - \tfrac{1}{4}\left(g_Y^2 + g_\mathrm{w}^2\right)\left(v_1^2 - v_2^2\right)\left(v_1\, c_\alpha - v_2\, s_\alpha\right)\Big] \;, \end{aligned} \tag{6.16b}$$
$$T_A = -\sqrt{2}\, m_{12}^2\, s_\zeta \left(v_1\, c_{\beta_n} + v_2\, s_{\beta_n}\right) \;, \tag{6.16c}$$
$$T_G = -t_{\beta-\beta_n}\, T_A \;, \tag{6.16d}$$

where now T_G is linearly dependent on T_A. Similarly, the relations of m_A and $m_{H^\pm}$ to the previous set of parameters can be computed:

$$m_A^2 = m_1^2\, s_{\beta_n}^2 + m_2^2\, c_{\beta_n}^2 + s_{2\beta_n}\, m_{12}^2\, c_\zeta - c_{2\beta_n}\, \tfrac{1}{4}\left(g_Y^2 + g_\mathrm{w}^2\right)\left(v_1^2 - v_2^2\right) \;, \tag{6.17a}$$
$$\begin{aligned} m_{H^\pm}^2 = {} & m_1^2\, s_{\beta_c}^2 + m_2^2\, c_{\beta_c}^2 + s_{2\beta_c}\, m_{12}^2\, c_\zeta - c_{2\beta_c}\, \tfrac{1}{4}\left(g_Y^2 + g_\mathrm{w}^2\right)\left(v_1^2 - v_2^2\right) \\ & + \tfrac{1}{2} g_\mathrm{w}^2 \left(v_1\, c_{\beta_c} + v_2\, s_{\beta_c}\right)^2 \;. \end{aligned} \tag{6.17b}$$

For the substitution of the original parameters, the relations of Eqs. (6.13)–(6.17) are used, yielding the following identities:

$$v_1 = \frac{\sqrt{2}\, c_\beta\, s_\mathrm{w}\, M_W}{e} \;, \tag{6.18a}$$

$$v_2 = \frac{\sqrt{2}\, s_\beta\, s_\mathrm{w}\, M_W}{e} \;, \tag{6.18b}$$

$$\begin{aligned} m_1^2 = &-\frac{1}{2}\, M_Z^2\, c_{2\beta} + m_A^2\, \frac{s_\beta^2}{c_{\beta-\beta_n}^2} \\ &+ \frac{e\, c_{\beta_n}}{2\, s_\mathrm{w}\, M_W\, c_{\beta-\beta_n}^2} \Big\{ T_h \left[s_\alpha\, c_\beta\, c_{\beta_n} + s_\beta \left(c_\alpha\, c_{\beta_n} + 2\, s_\alpha\, s_{\beta_n} \right) \right] \\ &\qquad - T_H \left(c_{\alpha+\beta}\, c_{\beta_n} + 2\, c_\alpha\, s_\beta\, s_{\beta_n} \right) \Big\} \;, \end{aligned} \tag{6.18c}$$

$$\begin{aligned} m_2^2 = &\,\frac{1}{2}\, M_Z^2\, c_{2\beta} + m_A^2\, \frac{c_\beta^2}{c_{\beta-\beta_n}^2} \\ &+ \frac{e\, s_{\beta_n}}{2\, s_\mathrm{w}\, M_W\, c_{\beta-\beta_n}^2} \Big\{ T_H \left[-s_\alpha\, s_\beta\, s_{\beta_n} + c_\beta \left(c_\alpha\, s_{\beta_n} - 2\, s_\alpha\, c_{\beta_n} \right) \right] \\ &\qquad - T_h \left(s_{\alpha+\beta}\, s_{\beta_n} + 2\, c_\alpha\, c_\beta\, c_{\beta_n} \right) \Big\} \;, \end{aligned} \tag{6.18d}$$

$$\begin{aligned} m_{12}^2\, c_\zeta = m_A^2\, \frac{s_{2\beta}}{2\, c_{\beta-\beta_n}^2} + \frac{e}{4\, s_\mathrm{w}\, M_W\, c_{\beta-\beta_n}^2} &\Big\{ T_h \left(c_{\beta+\alpha} + c_{\beta-\alpha}\, c_{2\beta_n} \right) \\ &\quad + T_H \left(s_{\beta+\alpha} - s_{\beta-\alpha}\, c_{2\beta_n} \right) \Big\} \;, \end{aligned} \tag{6.18e}$$

$$m_{12}^2\, s_\zeta = -\frac{e\, T_A}{2\, s_\mathrm{w}\, M_W\, c_{\beta-\beta_n}} \;. \tag{6.18f}$$

Therein m_A is used instead of $m_{H^\pm}$; as can be seen in Eqs. (6.17) only one of both masses can be used as an independent parameter.

The new set of parameters is now utilized to display the full form of the bilinear expressions of Eq. (6.11). It is convenient to parametrize $\mathbf{M}_{hHAG}$ in terms of m_A and $\mathbf{M}_{H^\pm G^\pm}$ in terms of $m_{H^\pm}$. The results are given by

$$\begin{aligned} m_h^2 = &\, M_Z^2\, s_{\alpha+\beta}^2 + m_A^2\, \frac{c_{\alpha-\beta}^2}{c_{\beta-\beta_n}^2} \\ &+ \frac{e\, s_{\alpha-\beta_n}}{2\, s_\mathrm{w}\, M_W\, c_{\beta-\beta_n}^2} \left[T_H\, c_{\alpha-\beta}\, s_{\alpha-\beta_n} + T_h\, \frac{1}{2} \left(c_{2\alpha-\beta-\beta_n} + 3\, c_{\beta-\beta_n} \right) \right] \;, \end{aligned} \tag{6.19a}$$

$$\begin{aligned} m_{hH}^2 = &-M_Z^2\, s_{\alpha+\beta}\, c_{\alpha+\beta} + m_A^2\, \frac{s_{\alpha-\beta}\, c_{\alpha-\beta}}{c_{\beta-\beta_n}^2} \\ &+ \frac{e}{2\, s_\mathrm{w}\, M_W\, c_{\beta-\beta_n}^2} \left[T_H\, s_{\alpha-\beta}\, s_{\alpha-\beta_n}^2 - T_h\, c_{\alpha-\beta}\, c_{\alpha-\beta_n}^2 \right] \;, \end{aligned} \tag{6.19b}$$

$$\begin{aligned}
m_H^2 &= M_Z^2\, c_{\alpha+\beta}^2 + m_A^2\, \frac{s_{\alpha-\beta}^2}{c_{\beta-\beta_n}^2} \\
&\quad + \frac{e\, c_{\alpha-\beta_n}}{2\, s_\mathrm{w}\, M_W\, c_{\beta-\beta_n}^2} \left[-T_h\, s_{\alpha-\beta}\, c_{\alpha-\beta_n} + T_H\, \frac{1}{2} \left(c_{2\alpha-\beta-\beta_n} - 3\, c_{\beta-\beta_n} \right) \right] \,, \qquad (6.19c)
\end{aligned}$$

$$m_{hA}^2 = m_{HG}^2 = \frac{e}{2\, s_\mathrm{w}\, M_W}\, T_A\, \frac{s_{\alpha-\beta_n}}{c_{\beta-\beta_n}} \,, \qquad (6.19d)$$

$$m_{hG}^2 = -m_{HA}^2 = \frac{e}{2\, s_\mathrm{w}\, M_W}\, T_A\, \frac{c_{\alpha-\beta_n}}{c_{\beta-\beta_n}} \,, \qquad (6.19e)$$

$$m_{AG}^2 = -m_A^2\, t_{\beta-\beta_n} - \frac{e}{2\, s_\mathrm{w}\, M_W\, c_{\beta-\beta_n}} \left(T_H\, s_{\alpha-\beta_n} - T_h\, c_{\alpha-\beta_n} \right) \,, \qquad (6.19f)$$

$$m_G^2 = m_A^2\, t_{\beta-\beta_n}^2 + \frac{e}{2\, s_\mathrm{w}\, M_W\, c_{\beta-\beta_n}^2} \left(-T_H\, c_{\alpha+\beta-2\beta_n} + T_h\, s_{\alpha+\beta-2\beta_n} \right) \,, \qquad (6.19g)$$

$$m_{H^-G^+}^2 = -m_{H^\pm}^2\, t_{\beta-\beta_c} - \frac{e}{2\, s_\mathrm{w}\, M_W} \left(T_H\, \frac{s_{\alpha-\beta_c}}{c_{\beta-\beta_c}} + T_h\, \frac{c_{\alpha-\beta_c}}{c_{\beta-\beta_c}} + \boldsymbol{i}\, T_A\, \frac{1}{c_{\beta-\beta_n}} \right) \,, \qquad (6.19h)$$

$$m_{G^-H^+}^2 = \left(m_{H^-G^+}^2 \right)^* \,, \qquad (6.19i)$$

$$m_{G^\pm}^2 = m_{H^\pm}^2\, t_{\beta-\beta_c}^2 + \frac{e}{2\, s_\mathrm{w}\, M_W\, c_{\beta-\beta_c}^2} \left(-T_H\, c_{\alpha+\beta-2\beta_c} + T_h\, s_{\alpha+\beta-2\beta_c} \right) \,. \qquad (6.19j)$$

6.4. Lowest-order relations

At lowest order, the minimization conditions for the Higgs potential (cf. Section 6.2) impose vanishing tadpole coefficients

$$T_i^{(0)} = 0 \,, \quad i \in \{h,\, H,\, A,\, G\} \,. \qquad (6.20)$$

Accordingly, the relative complex phase of the Higgs doublets is equal to zero,

$$\zeta = 0 \,. \qquad (6.21)$$

Furthermore all couplings of the Higgs potential are real, rendering the Higgs sector CP-conserving at lowest order.

6.4.1. Masses and mixing angles

The tree-level mass matrices of Eq. (6.12) in the chosen mass-eigenstate basis are diagonal, thus the lowest-order Higgs-boson masses are given by

$$\mathbf{M}_{hHAG}^{(0)} = \mathrm{diag}\left(m_h^2,\, m_H^2,\, m_A^2,\, m_G^2 \right) \,, \quad \mathbf{M}_{H^\pm G^\pm}^{(0)} = \mathrm{diag}\left(m_{H^\pm}^2,\, m_{G^\pm}^2 \right) \,. \qquad (6.22)$$

Applying these relations to Eq. (6.19f) and Eq. (6.19h) leads to

$$0 \overset{!}{=} m^2_{AG} = -m^2_A\, t_{\beta-\beta_n} \qquad \Rightarrow \quad \beta = \beta_n \;, \tag{6.23a}$$

$$0 \overset{!}{=} m^2_{H^-G^+} = -m^2_{H^\pm}\, t_{\beta-\beta_c} \qquad \Rightarrow \quad \beta = \beta_c \;. \tag{6.23b}$$

As an immediate consequence the masses of the unphysical Goldstone bosons G and $G^\pm$ given in Eq. (6.19g) and Eq. (6.19j), respectively, are zero. Furthermore, Eq. (6.18e) simplifies to a condition for the mass of the CP-odd A boson:

$$m^2_A = \frac{2\, m^2_{12}}{s_{2\beta}} \;. \tag{6.24}$$

For the charged Higgs boson $H^\pm$ a similar relation is obtained by using Eqs. (6.17) in Eq. (6.18e):

$$m^2_{H^\pm} = \frac{2\, m^2_{12}}{s_{2\beta}} + M^2_W \;. \tag{6.25}$$

Thus, the following mass relation holds:

$$m^2_{H^\pm} = m^2_A + M^2_W \;. \tag{6.26}$$

The tree-level masses of the neutral CP-even Higgs bosons are more easily acquired by diagonalizing the matrix in Eq. (6.6b). The application of Eqs. (6.18) and the usage of the lowest-order relations of Eq. (6.20) and Eq. (6.21) yields

$$\mathbf{M}_{\phi_1\phi_2} = \frac{1}{2}\begin{pmatrix} m^2_A + M^2_Z - (m^2_A - M^2_Z)\, c_{2\beta} & -\,(m^2_A + M^2_Z)\, s_{2\beta} \\ -\,(m^2_A + M^2_Z)\, s_{2\beta} & m^2_A + M^2_Z + (m^2_A - M^2_Z)\, c_{2\beta} \end{pmatrix} . \tag{6.27}$$

The eigenvalues of this matrix are

$$m^2_{h/H} = \frac{1}{2}\left[m^2_A + M^2_Z \mp \sqrt{\left(m^2_A + M^2_Z\right)^2 - 4\, m^2_A\, M^2_Z\, c^2_{2\beta}}\,\right] \;, \tag{6.28}$$

especially yielding the relation $m^2_h + m^2_H = m^2_A + M^2_Z$.

Furthermore, an upper limit on the lightest Higgs-boson mass is obtained,

$$m^2_h < M^2_Z\, c^2_{2\beta} \;, \tag{6.29}$$

although higher-order corrections shift this bound significantly.

Utilizing the properties of the CP-even Higgs-boson mass matrix to be real and symmetric, the following rules for the mixing angle α are derived:

$$s_{2\alpha} = -\frac{m_H^2 + m_h^2}{m_H^2 - m_h^2}\, s_{2\beta}\ , \quad c_{2\alpha} = -\frac{m_A^2 - m_Z^2}{m_H^2 - m_h^2}\, c_{2\beta}\ , \quad t_{2\alpha} = \frac{m_A^2 + m_Z^2}{m_A^2 - m_Z^2}\, t_{2\beta}\ . \tag{6.30}$$

Without loss of generality, β can be defined in the range between 0 and $\pi/2$ [CH03]. For this choice, Eqs. (6.30) constrain α to be in the intervall $-\pi/2 < \alpha < 0$. The third equation of Eqs. (6.30) depends only on the input parameters m_A and t_β.

As can be seen from Eqs. (6.23)–(6.30), the masses and mixing angles of the Higgs sector at lowest order are determined by the two parameters m_A (or $m_{H^\pm}$) and t_β. At higher orders of perturbation theory, mixing of the A boson and the other neutral states is induced by CP-violating couplings from other sectors of the MSSM. In that case A is not a mass eigenstate anymore; instead, the mass of the charged Higgs boson will be used as an input parameter.

6.4.2. Gauge fixing

The Lagrangian of the MSSM at the quantum level incorporates a gauge-fixing part,

$$\mathcal{L}_{\text{fix}} = -\frac{1}{2\xi_A}\, F_A\, F_A^\dagger - \frac{1}{2\xi_Z}\, F_Z\, F_Z^\dagger - \frac{1}{2\xi_W}\, F_W^+\, F_W^-\ . \tag{6.31}$$

The gauge-fixing functions can be chosen in the R_ξ gauge as in Ref. [SSV13],

$$F_A = \partial^\mu A_\mu\ , \tag{6.32a}$$

$$F_Z = \partial^\mu Z_\mu + \xi_Z \xi_Z'\, M_Z\, G\ , \tag{6.32b}$$

$$F_W^\pm = \partial^\mu W_\mu^\pm \pm \boldsymbol{i}\, \xi_W \xi_W'\, M_W\, G^\pm\ . \tag{6.32c}$$

Thus $\mathcal{L}_{\text{fix}}$ introduces additional terms that are bilinear in the Goldstone fields G and $G^\pm$ and hence contribute to their masses. At the tree level they arise as

$$m_G^2 = \xi_Z \xi_Z'^2\, M_Z^2\ , \tag{6.33a}$$

$$m_{G^\pm}^2 = \xi_W \xi_W'^2\, M_W^2\ . \tag{6.33b}$$

For the following analysis the 't Hooft–Feynman gauge is used which is an R_ξ gauge with gauge-fixing parameters $\xi_i = 1$ and $\xi_i' = 1$, $i \in \{A,\, Z,\, W\}$. Thus, the tree-level values of the Goldstone-boson masses are equal to the gauge-boson masses.

6.5. Higher-order relations for masses and mixings

At higher orders the one-point and two-point functions are dressed by loop contributions and have to be renormalized. They are related to higher-order corrections of the tadpole coefficients and masses in Eq. (6.11).

The renormalized one-point functions are equivalent to the renormalized tadpoles. At j-loop order ($j \geq 1$) they are denoted as $\hat{\Upsilon}_i^{(j)}$, $i \in \{h,\, H,\, A,\, G\}$. The lowest-order tadpole coefficients in Eq. (6.20) receive loop contributions up to the kth order ($k \geq 1$) according to

$$T_i^{(k)} = T_i^{(0)} + \sum_{j\,=\,1}^{k} \hat{\Upsilon}_i^{(j)}\ , \quad i \in \{h,\, H,\, A,\, G\}\ . \tag{6.34}$$

The renormalized two-point vertex functions are given by

$$\hat{\mathbf{\Gamma}}_{hHAG}^{(k)}\big(p^2\big) = \boldsymbol{i}\,\Big[p^2\mathbf{1} - \mathbf{M}_{hHAG}^{(k)}\big(p^2\big)\Big]\ , \tag{6.35a}$$

$$\hat{\mathbf{\Gamma}}_{H^\pm G^\pm}^{(k)}\big(p^2\big) = \boldsymbol{i}\,\Big[p^2\mathbf{1} - \mathbf{M}_{H^\pm G^\pm}^{(k)}\big(p^2\big)\Big]\ . \tag{6.35b}$$

In Eq. (6.22) the lowest-order mass matrices are listed. The higher-order corrections up to the kth order ($k \geq 1$) are then given by

$$\mathbf{M}_{hHAG}^{(k)}\big(p^2\big) = \mathbf{M}_{hHAG}^{(0)} - \sum_{j\,=\,1}^{k} \hat{\mathbf{\Sigma}}_{hHAG}^{(j)}\big(p^2\big)\ , \tag{6.36a}$$

$$\mathbf{M}_{H^\pm G^\pm}^{(k)}\big(p^2\big) = \mathbf{M}_{H^\pm G^\pm}^{(0)} - \sum_{j\,=\,1}^{k} \hat{\mathbf{\Sigma}}_{H^\pm G^\pm}^{(j)}\big(p^2\big)\ . \tag{6.36b}$$

Therein, the matrices of self-energies at j-loop order ($j \geq 1$) are denoted as

$$\hat{\mathbf{\Sigma}}_{hHAG}^{(j)}\big(p^2\big) = \begin{pmatrix} \hat{\Sigma}_h^{(j)}(p^2) & \hat{\Sigma}_{hH}^{(j)}(p^2) & \hat{\Sigma}_{hA}^{(j)}(p^2) & \hat{\Sigma}_{hG}^{(j)}(p^2) \\ \hat{\Sigma}_{hH}^{(j)}(p^2) & \hat{\Sigma}_H^{(j)}(p^2) & \hat{\Sigma}_{HA}^{(j)}(p^2) & \hat{\Sigma}_{HG}^{(j)}(p^2) \\ \hat{\Sigma}_{hA}^{(j)}(p^2) & \hat{\Sigma}_{HA}^{(j)}(p^2) & \hat{\Sigma}_A^{(j)}(p^2) & \hat{\Sigma}_{AG}^{(j)}(p^2) \\ \hat{\Sigma}_{hG}^{(j)}(p^2) & \hat{\Sigma}_{HG}^{(j)}(p^2) & \hat{\Sigma}_{AG}^{(j)}(p^2) & \hat{\Sigma}_G^{(j)}(p^2) \end{pmatrix}, \tag{6.37a}$$

$$\hat{\mathbf{\Sigma}}_{H^\pm G^\pm}^{(j)}\big(p^2\big) = \begin{pmatrix} \hat{\Sigma}_{H^\pm}^{(j)}(p^2) & \hat{\Sigma}_{H^- G^+}^{(j)}(p^2) \\ \hat{\Sigma}_{G^- H^+}^{(j)}(p^2) & \hat{\Sigma}_{G^\pm}^{(j)}(p^2) \end{pmatrix}. \tag{6.37b}$$

They include j-loop Feynman diagrams and counterterms and are momentum dependent.

The masses of the Higgs bosons are achieved as the real parts of the poles of the corresponding dressed propagator matrices which are related to the inverse of the irreducible two-point vertex functions in Eq. (6.35a) and Eq. (6.35b), respectively. As soon as $\hat{\mathbf{\Sigma}}^{(j)}_{hHAG}(p^2)$ contains non-vanishing off-diagonal entries at any loop order j, in general also $\hat{\mathbf{\Gamma}}^{(k)}_{hHAG}(p^2)$ has off-diagonal entries at a loop order $k \geq j$.

Thus, the higher-order corrected masses m_{h_1}, m_{h_2} and m_{h_3} of the neutral Higgs bosons are gained as the real parts of the roots of the determinant of $\hat{\mathbf{\Gamma}}^{(k)}_{hHAG}$, i. e.

$$\det\left[\hat{\mathbf{\Gamma}}^{(k)}_{hHAG}\left(p^2\right)\right]_{p^2\,=\,x_i^2} = 0\ , \quad m_{h_i}^2 = \mathfrak{Re}\left[x_i^2\right]\ , \quad i \in \{1,\,2,\,3\}\ . \tag{6.38}$$

This is clearly a non-trivial task since the dependence of the self-energies in $\mathbf{M}^{(k)}_{hHAG}$ on the external momentum p^2 is a complicated function. The fourth solution of Eq. (6.38) belongs to the Goldstone boson, whose mass remains at zero also at higher orders [Hol+02].

Analogously, the mass of the charged Higgs bosons $H^{\pm}$, at higher orders denoted as $m_{h^{\pm}}$, is given by the real part of the root of the determinant of $\hat{\mathbf{\Gamma}}^{(k)}_{H^{\pm}G^{\pm}}$, i. e.

$$\det\left[\hat{\mathbf{\Gamma}}^{(k)}_{H^{\pm}G^{\pm}}\left(p^2\right)\right]_{p^2\,=\,x^2} = 0\ , \quad m_{h^{\pm}}^2 = \mathfrak{Re}\left[x^2\right]\ . \tag{6.39}$$

Again, the second solution of Eq. (6.39) is equal to zero, corresponding to the mass of the charged Goldstone bosons which do not receive higher-order contributions [Hol+02].

In the most general case, also mixings with the longitudinal Z and $W^{\pm}$ have to be considered in Eq. (6.37a) and Eq. (6.37b), respectively. They are correlated with the mixings of G and $G^{\pm}$ by Slavnov–Taylor identities [BBS08; WRW11; Hol+02], thus required to maintain gauge invariance. However, the relevant contributions appear the first time in the gauge parts of two-loop corrections, which are neglected here.

The mixing angles α, β_n and β_c are not renormalized, but kept at their tree-level values. Since the self-energies which contribute to Eq. (6.35a) and Eq. (6.35b) at higher orders are non-diagonal and momentum dependent, mixing angles generally cannot be defined anymore at higher orders.

Moreover, the gauge-fixing sector is not renormalized, i. e. the gauge-boson masses M_W and M_Z as well as the gauge-fixing parameters ξ_i and ξ_i' in Eqs. (6.33) are kept at their tree-level values.

6.6. Renormalization of the Higgs potential

The quantities $\hat{\Upsilon}_i^{(j)}$, $\hat{\mathbf{\Sigma}}_{hHAG}^{(j)}$ and $\hat{\mathbf{\Sigma}}_{H^\pm G^\pm}^{(j)}$ which have been introduced in Eq. (6.34) and Eqs. (6.36) are all renormalized quantities.

The tadpoles can be decomposed according to

$$\hat{\Upsilon}_i^{(j)} = \Upsilon_i^{(j)} + \delta^{(j)} T_i^{\mathbf{Z}}, \quad i \in \{h,\, H,\, A,\, G\} \ , \tag{6.40}$$

with the jth order unrenormalized tadpoles $\Upsilon_i^{(j)}$ and the corresponding tadpole counterterms $\delta^{(j)} T_i^{\mathbf{Z}}$.

Analogously, the self-energy matrices are decomposed according to

$$\hat{\mathbf{\Sigma}}_{hHAG}^{(j)}\Big(p^2\Big) = \mathbf{\Sigma}_{hHAG}^{(j)}\Big(p^2\Big) - \delta^{(j)}\mathbf{M}_{hHAG}^{\mathbf{Z}}\Big(p^2\Big) \ , \tag{6.41a}$$

$$\hat{\mathbf{\Sigma}}_{H^\pm G^\pm}^{(j)}\Big(p^2\Big) = \mathbf{\Sigma}_{H^\pm G^\pm}^{(j)}\Big(p^2\Big) - \delta^{(j)}\mathbf{M}_{H^\pm G^\pm}^{\mathbf{Z}}\Big(p^2\Big) \ . \tag{6.41b}$$

The unrenormalized j-loop order self-energy matrices are denoted as

$$\mathbf{\Sigma}_{hHAG}^{(j)}\Big(p^2\Big) = \begin{pmatrix} \Sigma_h^{(j)}(p^2) & \Sigma_{hH}^{(j)}(p^2) & \Sigma_{hA}^{(j)}(p^2) & \Sigma_{hG}^{(j)}(p^2) \\ \Sigma_{hH}^{(j)}(p^2) & \Sigma_H^{(j)}(p^2) & \Sigma_{HA}^{(j)}(p^2) & \Sigma_{HG}^{(j)}(p^2) \\ \Sigma_{hA}^{(j)}(p^2) & \Sigma_{HA}^{(j)}(p^2) & \Sigma_A^{(j)}(p^2) & \Sigma_{AG}^{(j)}(p^2) \\ \Sigma_{hG}^{(j)}(p^2) & \Sigma_{HG}^{(j)}(p^2) & \Sigma_{AG}^{(j)}(p^2) & \Sigma_G^{(j)}(p^2) \end{pmatrix} , \tag{6.42a}$$

$$\mathbf{\Sigma}_{H^\pm G^\pm}^{(j)}\Big(p^2\Big) = \begin{pmatrix} \Sigma_{H^\pm}^{(j)}(p^2) & \Sigma_{H^- G^+}^{(j)}(p^2) \\ \Sigma_{G^- H^+}^{(j)}(p^2) & \Sigma_{G^\pm}^{(j)}(p^2) \end{pmatrix} . \tag{6.42b}$$

For the corresponding counterterms of jth order the following notation is used:

$$\delta^{(j)}\mathbf{M}_{hHAG}^{\mathbf{Z}}\Big(p^2\Big) = \begin{pmatrix} \delta^{(j)} m_h^{\mathbf{Z}}(p^2) & \delta^{(j)} m_{hH}^{\mathbf{Z}}(p^2) & \delta^{(j)} m_{hA}^{\mathbf{Z}}(p^2) & \delta^{(j)} m_{hG}^{\mathbf{Z}}(p^2) \\ \delta^{(j)} m_{hH}^{\mathbf{Z}}(p^2) & \delta^{(j)} m_H^{\mathbf{Z}}(p^2) & \delta^{(j)} m_{HA}^{\mathbf{Z}}(p^2) & \delta^{(j)} m_{HG}^{\mathbf{Z}}(p^2) \\ \delta^{(j)} m_{hA}^{\mathbf{Z}}(p^2) & \delta^{(j)} m_{HA}^{\mathbf{Z}}(p^2) & \delta^{(j)} m_A^{\mathbf{Z}}(p^2) & \delta^{(j)} m_{AG}^{\mathbf{Z}}(p^2) \\ \delta^{(j)} m_{hG}^{\mathbf{Z}}(p^2) & \delta^{(j)} m_{HG}^{\mathbf{Z}}(p^2) & \delta^{(j)} m_{AG}^{\mathbf{Z}}(p^2) & \delta^{(j)} m_G^{\mathbf{Z}}(p^2) \end{pmatrix} , \tag{6.43a}$$

$$\delta^{(j)}\mathbf{M}_{H^\pm G^\pm}^{\mathbf{Z}}\Big(p^2\Big) = \begin{pmatrix} \delta^{(j)} m_{H^\pm}^{\mathbf{Z}}(p^2) & \delta^{(j)} m_{H^- G^+}^{\mathbf{Z}}(p^2) \\ \delta^{(j)} m_{G^- H^+}^{\mathbf{Z}}(p^2) & \delta^{(j)} m_{G^\pm}^{\mathbf{Z}}(p^2) \end{pmatrix} . \tag{6.43b}$$

The counterterms include parameter and field-renormalization constants and are dependent on the external momentum.

The independent renormalization constants for the parameters of the Higgs potential are introduced by the renormalization transformations

$$
\begin{aligned}
&e \to e + \sum_{j=1}^{k} \delta^{(j)} e \,, \qquad t_\beta \to t_\beta + \sum_{j=1}^{k} \delta^{(j)} t_\beta \,, \qquad M_W \to M_W + \sum_{j=1}^{k} \delta^{(j)} M_W \,, \\
&M_Z \to M_Z + \sum_{j=1}^{k} \delta^{(j)} M_Z \qquad \text{or} \qquad s_\mathrm{w} \to s_\mathrm{w} + \sum_{j=1}^{k} \delta^{(j)} s_\mathrm{w} \,, \\
&m_A^2 \to m_A^2 + \sum_{j=1}^{k} \delta^{(j)} m_A^2 \qquad \text{or} \qquad m_{H^\pm}^2 \to m_{H^\pm}^2 + \sum_{j=1}^{k} \delta^{(j)} m_{H^\pm}^2 \,, \\
&T_h \to T_h + \sum_{j=1}^{k} \delta^{(j)} T_h \,, \quad T_H \to T_H + \sum_{j=1}^{k} \delta^{(j)} T_H \,, \quad T_A \to T_A + \sum_{j=1}^{k} \delta^{(j)} T_A \,.
\end{aligned}
\tag{6.44}
$$

Therein "or" means that the parameters of jth order on the left- and right-hand side are not independent, thus only one of them can be fixed by an independent renormalization condition; M_Z and s_w are related to each other by Eq. (6.13), and the masses m_A and $m_{H^\pm}$ have to respect Eq. (6.26). The tadpole counterterms $\delta^{(j)} T_G$ are not appearing in Eq. (6.44), since they are already fixed by $\delta^{(j)} T_A$ via the linear relation between T_A and T_G in Eq. (6.16d).

The parameter $t_\beta = v_2/v_1$ is renormalized since it originates from the vacuum expectation values of the Higgs fields. On the other hand, the mixing angles β_n, β_c and also α, although related to t_β at lowest order, are not renormalized; they do not absorb divergences. As a consequence of keeping the mixing angles at their tree-level values, the self-energy counterterms can be evaluated in the basis of the lowest-order mass eigenstates.

In addition to parameter renormalization, also renormalization of the Higgs fields as described in Eqs. (5.3) is required in order to achieve finite self-energies for an arbitrary external momentum.

In our choice, each doublet acquires one field-renormalization constant:

$$
\mathcal{H}_1 \to \mathcal{H}_1 \sqrt{Z_{\mathcal{H}_1}} \,, \quad Z_{\mathcal{H}_1} = 1 + \sum_{j=1}^{k} \delta^{(j)} Z_{\mathcal{H}_1} \,, \tag{6.45a}
$$

$$
\mathcal{H}_2 \to \mathcal{H}_2 \sqrt{Z_{\mathcal{H}_2}} \,, \quad Z_{\mathcal{H}_2} = 1 + \sum_{j=1}^{k} \delta^{(j)} Z_{\mathcal{H}_2} \,. \tag{6.45b}
$$

Since the Higgs fields are transformed into mass eigenstates according to Eq. (6.10), also the field-renormalization constants are transformed to the new basis. Using the rotation matrices $\mathbf{D}_x := \left(\begin{smallmatrix} -s_x & c_x \\ c_x & s_x \end{smallmatrix}\right)$ yields

$$\begin{pmatrix} h \\ H \end{pmatrix} \to \mathbf{D}_\alpha \begin{pmatrix} \sqrt{Z_{\mathcal{H}_1}} & 0 \\ 0 & \sqrt{Z_{\mathcal{H}_2}} \end{pmatrix} \mathbf{D}_\alpha^{-1} \begin{pmatrix} h \\ H \end{pmatrix} =: \mathbf{Z}_{hH} \begin{pmatrix} h \\ H \end{pmatrix} , \tag{6.46a}$$

$$\begin{pmatrix} A \\ G \end{pmatrix} \to \mathbf{D}_{\beta_n} \begin{pmatrix} \sqrt{Z_{\mathcal{H}_1}} & 0 \\ 0 & \sqrt{Z_{\mathcal{H}_2}} \end{pmatrix} \mathbf{D}_{\beta_n}^{-1} \begin{pmatrix} A \\ G \end{pmatrix} =: \mathbf{Z}_{AG} \begin{pmatrix} A \\ G \end{pmatrix} , \tag{6.46b}$$

$$\begin{pmatrix} H^\pm \\ G^\pm \end{pmatrix} \to \mathbf{D}_{\beta_c} \begin{pmatrix} \sqrt{Z_{\mathcal{H}_1}} & 0 \\ 0 & \sqrt{Z_{\mathcal{H}_2}} \end{pmatrix} \mathbf{D}_{\beta_c}^{-1} \begin{pmatrix} H^\pm \\ G^\pm \end{pmatrix} =: \mathbf{Z}_{H^\pm G^\pm} \begin{pmatrix} H^\pm \\ G^\pm \end{pmatrix} . \tag{6.46c}$$

Thereby the new objects $\mathbf{Z}_{hH}$, $\mathbf{Z}_{AG}$ and $\mathbf{Z}_{H^\pm G^\pm}$ are introduced. They are field-renormalization matrices for the Higgs fields in the basis of lowest-order mass eigenstates, but depend on the original field-renormalization constants in Eq. (6.45).

An expansion of these (2×2) matrices to loop order k defines the terms

$$\mathbf{Z}_{hH} = \mathbf{1} + \sum_{j=1}^{k} \delta^{(j)}\mathbf{Z}_{hH} , \qquad \delta^{(j)}\mathbf{Z}_{hH} = \frac{1}{2} \begin{pmatrix} \delta^{(j)} Z_{hh} & \delta^{(j)} Z_{hH} \\ \delta^{(j)} Z_{Hh} & \delta^{(j)} Z_{HH} \end{pmatrix} , \tag{6.47a}$$

$$\mathbf{Z}_{AG} = \mathbf{1} + \sum_{j=1}^{k} \delta^{(j)}\mathbf{Z}_{AG} , \qquad \delta^{(j)}\mathbf{Z}_{AG} = \frac{1}{2} \begin{pmatrix} \delta^{(j)} Z_{AA} & \delta^{(j)} Z_{AG} \\ \delta^{(j)} Z_{GA} & \delta^{(j)} Z_{GG} \end{pmatrix} , \tag{6.47b}$$

$$\mathbf{Z}_{H^\pm G^\pm} = \mathbf{1} + \sum_{j=1}^{k} \delta^{(j)}\mathbf{Z}_{H^\pm G^\pm} , \quad \delta^{(j)}\mathbf{Z}_{H^\pm G^\pm} = \frac{1}{2} \begin{pmatrix} \delta^{(j)} Z_{H^\pm H^\pm} & \delta^{(j)} Z_{H^- G^+} \\ \delta^{(j)} Z_{G^- H^+} & \delta^{(j)} Z_{G^\pm G^\pm} \end{pmatrix} . \tag{6.47c}$$

It is noteworthy that no field-renormalization constant for the transition between the tree-level CP-even and CP-odd states exist at all orders in perturbation theory, which is an immediate consequence of CP-conservation at the tree level.

For the following general formulas of the tadpole counterterms in Eq. (6.40) and the self-energy counterterms in Eqs. (6.43) some conventions are introduced:

$$\delta^{(0)}\mathbf{Z}_{hH} = \mathbf{1} , \quad \delta^{(0)}\mathbf{Z}_{AG} = \mathbf{1} , \quad \delta^{(0)}\mathbf{Z}_{H^\pm G^\pm} = \mathbf{1} , \tag{6.48a}$$

$$\delta^{(0)}\mathbf{M}_{hHAG} = \mathbf{M}_{hHAG}^{(0)} , \quad \delta^{(0)}\mathbf{M}_{H^\pm G^\pm} = \mathbf{M}_{H^\pm G^\pm}^{(0)} , \tag{6.48b}$$

$$\delta^{(0)}T_i = T_i^{(0)} , \quad i \in \{h,\, H,\, A,\, G\} . \tag{6.48c}$$

The tadpole counterterms in Eq. (6.40) can be expressed as the sum of the matrix products of the tadpole renormalization constants in Eq. (6.44) and the field-renormalization constants in Eq. (6.47). At each loop order k the separate counterterms of various orders j_1 and j_2 are combined:

$$\begin{pmatrix} \delta^{(k)}T_h^{\mathbf{Z}} \\ \delta^{(k)}T_H^{\mathbf{Z}} \\ \delta^{(k)}T_A^{\mathbf{Z}} \\ \delta^{(k)}T_G^{\mathbf{Z}} \end{pmatrix} = \sum_{\substack{j_1,\, j_2 \,=\, 0 \\ j_1 + j_2 \,=\, k}}^{k} \begin{pmatrix} \delta^{(j_1)}\mathbf{Z}_{hH} & \mathbf{0} \\ \mathbf{0} & \delta^{(j_1)}\mathbf{Z}_{AG} \end{pmatrix} \begin{pmatrix} \delta^{(j_2)}T_h \\ \delta^{(j_2)}T_H \\ \delta^{(j_2)}T_A \\ \delta^{(j_2)}T_G \end{pmatrix} . \tag{6.49}$$

Similarly, the mass counterterms in Eqs. (6.43) can be achieved from sums of matrix products of the field and genuine mass counterterms. Again, the separate counterterms of various orders j_1, j_2 (and j_3) are combined:

$$\begin{aligned} \delta^{(k)}\mathbf{M}_{hHAG}^{\mathbf{Z}} = & \sum_{\substack{j_1,\, j_2,\, j_3 \,=\, 0 \\ j_1 + j_2 + j_3 \,=\, k}}^{k} \begin{pmatrix} \delta^{(j_1)}\mathbf{Z}_{hH}^T & \mathbf{0} \\ \mathbf{0} & \delta^{(j_1)}\mathbf{Z}_{AG}^T \end{pmatrix} \delta^{(j_2)}\mathbf{M}_{hHAG} \begin{pmatrix} \delta^{(j_3)}\mathbf{Z}_{hH} & \mathbf{0} \\ \mathbf{0} & \delta^{(j_3)}\mathbf{Z}_{AG} \end{pmatrix} \\ & - \sum_{\substack{j_1,\, j_2 \,=\, 0 \\ j_1 + j_2 \,=\, k}}^{k} \begin{pmatrix} \delta^{(j_1)}\mathbf{Z}_{hH}^T & \mathbf{0} \\ \mathbf{0} & \delta^{(j_1)}\mathbf{Z}_{AG}^T \end{pmatrix} \left(p^2\mathbf{1}\right) \begin{pmatrix} \delta^{(j_2)}\mathbf{Z}_{hH} & \mathbf{0} \\ \mathbf{0} & \delta^{(j_2)}\mathbf{Z}_{AG} \end{pmatrix} , \end{aligned} \tag{6.50a}$$

$$\begin{aligned} \delta^{(k)}\mathbf{M}_{H^\pm G^\pm}^{\mathbf{Z}} = & \sum_{\substack{j_1,\, j_2,\, j_3 \,=\, 0 \\ j_1 + j_2 + j_3 \,=\, k}}^{k} \delta^{(j_1)}\mathbf{Z}_{H^\pm G^\pm}^T\, \delta^{(j_2)}\mathbf{M}_{H^\pm G^\pm}\, \delta^{(j_3)}\mathbf{Z}_{H^\pm G^\pm} \\ & - \sum_{\substack{j_1,\, j_2 \,=\, 0 \\ j_1 + j_2 \,=\, k}}^{k} \delta^{(j_1)}\mathbf{Z}_{H^\pm G^\pm}^T \left(p^2\mathbf{1}\right) \delta^{(j_2)}\mathbf{Z}_{H^\pm G^\pm} \ . \end{aligned} \tag{6.50b}$$

In this representation of the counterterms the momentum-dependent parts are separated from the momentum-independent parts.

The matrices of the genuine j-loop mass counterterms are denoted as

$$\delta^{(j)}\mathbf{M}_{hHAG} = \begin{pmatrix} \delta^{(j)}m_h^2 & \delta^{(j)}m_{hH}^2 & \delta^{(j)}m_{hA}^2 & \delta^{(j)}m_{hG}^2 \\ \delta^{(j)}m_{hH}^2 & \delta^{(j)}m_H^2 & \delta^{(j)}m_{HA}^2 & \delta^{(j)}m_{HG}^2 \\ \delta^{(j)}m_{hA}^2 & \delta^{(j)}m_{HA}^2 & \delta^{(j)}m_A^2 & \delta^{(j)}m_{AG}^2 \\ \delta^{(j)}m_{hG}^2 & \delta^{(j)}m_{HG}^2 & \delta^{(j)}m_{AG}^2 & \delta^{(j)}m_G^2 \end{pmatrix} , \tag{6.51a}$$

$$\delta^{(j)}\mathbf{M}_{H^\pm G^\pm} = \begin{pmatrix} \delta^{(j)}m_{H^\pm}^2 & \delta^{(j)}m_{H^-G^+}^2 \\ \delta^{(j)}m_{G^-H^+}^2 & \delta^{(j)}m_{G^\pm}^2 \end{pmatrix} . \tag{6.51b}$$

6.7. One-loop renormalization

To demonstrate renormalization and to introduce the notation for Chapter 7 the counterterms are derived at the one-loop order in the following. Furthermore, at higher orders the one-loop counterterms are necessary for the evaluation of the tadpole and mass counterterms in Eq. (6.49) and Eq. (6.50), respectively.

6.7.1. Field renormalization

Expanding Eqs. (6.44) and Eqs. (6.47) to the order $k = 1$ and comparing the entries in Eq. (6.46) yields

$$\delta^{(1)} Z_{hh} = \left(s_\alpha^2 \delta^{(1)} Z_{\mathcal{H}_1} + c_\alpha^2 \delta^{(1)} Z_{\mathcal{H}_2}\right) \,, \tag{6.52a}$$
$$\delta^{(1)} Z_{HH} = \left(c_\alpha^2 \delta^{(1)} Z_{\mathcal{H}_1} + s_\alpha^2 \delta^{(1)} Z_{\mathcal{H}_2}\right) \,, \tag{6.52b}$$
$$\delta^{(1)} Z_{hH} = \delta^{(1)} Z_{Hh} = c_\alpha s_\alpha \left(\delta^{(1)} Z_{\mathcal{H}_2} - \delta^{(1)} Z_{\mathcal{H}_1}\right) \,, \tag{6.52c}$$
$$\delta^{(1)} Z_{AA} = \left(s_{\beta_n}^2 \delta^{(1)} Z_{\mathcal{H}_1} + c_{\beta_n}^2 \delta^{(1)} Z_{\mathcal{H}_2}\right) \,, \tag{6.52d}$$
$$\delta^{(1)} Z_{GG} = \left(c_{\beta_n}^2 \delta^{(1)} Z_{\mathcal{H}_1} + s_{\beta_n}^2 \delta^{(1)} Z_{\mathcal{H}_2}\right) \,, \tag{6.52e}$$
$$\delta^{(1)} Z_{AG} = \delta^{(1)} Z_{GA} = c_{\beta_n} s_{\beta_n} \left(\delta^{(1)} Z_{\mathcal{H}_2} - \delta^{(1)} Z_{\mathcal{H}_1}\right) \,, \tag{6.52f}$$
$$\delta^{(1)} Z_{H^\pm H^\pm} = \left(s_{\beta_c}^2 \delta^{(1)} Z_{\mathcal{H}_1} + c_{\beta_c}^2 \delta^{(1)} Z_{\mathcal{H}_2}\right) \,, \tag{6.52g}$$
$$\delta^{(1)} Z_{G^\pm G^\pm} = \left(c_{\beta_c}^2 \delta^{(1)} Z_{\mathcal{H}_1} + s_{\beta_c}^2 \delta^{(1)} Z_{\mathcal{H}_2}\right) \,, \tag{6.52h}$$
$$\delta^{(1)} Z_{H^- G^+} = \delta^{(1)} Z_{G^- H^+} = c_{\beta_c} s_{\beta_c} \left(\delta^{(1)} Z_{\mathcal{H}_2} - \delta^{(1)} Z_{\mathcal{H}_1}\right) \,. \tag{6.52i}$$

The two independent renormalization constants $\delta^{(1)} Z_{\mathcal{H}_1}$ and $\delta^{(1)} Z_{\mathcal{H}_2}$ have to be determined. This is done by imposing $\overline{\text{DR}}$ conditions to avoid potentially large contributions from the finite parts [Bri92; Fra+02; FS02]. Using Eq. (6.10), they can be obtained from the self-energies in the basis of lowest-order interaction or mass eigenstates:

$$\delta^{(1)} Z_{\mathcal{H}_1} = -\Re\mathfrak{e}\left[\frac{\partial \Sigma_{\phi_1}^{(1)}(p^2)}{\partial p^2}\right]_{\text{div}} = -\Re\mathfrak{e}\left[\frac{\partial \Sigma_H^{(1)}\big|_{\alpha\,=\,0}(p^2)}{\partial p^2}\right]_{\text{div}} \,, \tag{6.53a}$$
$$\delta^{(1)} Z_{\mathcal{H}_2} = -\Re\mathfrak{e}\left[\frac{\partial \Sigma_{\phi_2}^{(1)}(p^2)}{\partial p^2}\right]_{\text{div}} = -\Re\mathfrak{e}\left[\frac{\partial \Sigma_h^{(1)}\big|_{\alpha\,=\,0}(p^2)}{\partial p^2}\right]_{\text{div}} \,. \tag{6.53b}$$

6.7.2. Mass and tadpole renormalization

The tadpole counterterms of Eq. (6.49) at the one-loop order yield

$$\begin{pmatrix} \delta^{(1)}T_h^{\mathbf{Z}} \\ \delta^{(1)}T_H^{\mathbf{Z}} \\ \delta^{(1)}T_A^{\mathbf{Z}} \\ \delta^{(1)}T_G^{\mathbf{Z}} \end{pmatrix} = \begin{pmatrix} \delta^{(1)}\mathbf{Z}_{hH} & \mathbf{0} \\ \mathbf{0} & \delta^{(1)}\mathbf{Z}_{AG} \end{pmatrix} \begin{pmatrix} T_h^{(0)} \\ T_H^{(0)} \\ T_A^{(0)} \\ T_G^{(0)} \end{pmatrix} + \begin{pmatrix} \delta^{(1)}T_h \\ \delta^{(1)}T_H \\ \delta^{(1)}T_A \\ \delta^{(1)}T_G \end{pmatrix} . \tag{6.54}$$

With the lowest-order tadpoles $T_i^{(0)} = 0$, $i \in \{h,\, H,\, A,\, G\}$ (cf. Eq. (6.20)) the explicit form of Eq. (6.54) is given by

$$\delta^{(1)}T_i^{\mathbf{Z}} = \delta^{(1)}T_i \ , \quad i \in \{h,\, H,\, A,\, G\} \ . \tag{6.55}$$

The tadpole counterterms $\delta^{(1)}T_i$, $i \in \{h,\, H,\, A\}$ are fixed by requiring the minimum of the Higgs potential not to be shifted by the renormalized one-loop tadpoles, i. e. $\hat{\Upsilon}_i^{(1)} = 0$. Thus, Eq. (6.40) with $j = 1$, and Eq. (6.55) provide the tadpole counterterms according to

$$0 \overset{!}{=} \hat{\Upsilon}_i^{(1)} = \Upsilon_i^{(1)} + \delta^{(1)}T_i^{\mathbf{Z}} \ , \quad \delta^{(1)}T_i = -\Upsilon_i^{(1)} \ , \quad i \in \{h,\, H,\, A\} \ . \tag{6.56}$$

The fourth tadpole counterterm $\delta^{(1)}T_G$ is fixed by $\delta^{(1)}T_A$ via the linear dependence of T_G on T_A in Eq. (6.16d), i. e.

$$\delta^{(1)}T_G = -\delta^{(1)}T_A \ . \tag{6.57}$$

The evaluation of the mass counterterms of Eqs. (6.50) for $k = 1$ leads to

$$\begin{aligned} \delta^{(1)}\mathbf{M}_{hHAG}^{\mathbf{Z}} = & \begin{pmatrix} \delta^{(1)}\mathbf{Z}_{hH}^T & \mathbf{0} \\ \mathbf{0} & \delta^{(1)}\mathbf{Z}_{AG}^T \end{pmatrix} \left(\mathbf{M}_{hHAG}^{(0)} - p^2\mathbf{1}\right) \\ & + \left(\mathbf{M}_{hHAG}^{(0)} - p^2\mathbf{1}\right) \begin{pmatrix} \delta^{(1)}\mathbf{Z}_{hH} & \mathbf{0} \\ \mathbf{0} & \delta^{(1)}\mathbf{Z}_{AG} \end{pmatrix} \\ & + \delta^{(1)}\mathbf{M}_{hHAG} \ , \end{aligned} \tag{6.58a}$$

$$\begin{aligned} \delta^{(1)}\mathbf{M}_{H^\pm G^\pm}^{\mathbf{Z}} = & \, \delta^{(1)}\mathbf{Z}_{H^\pm G^\pm}^T \left(\mathbf{M}_{H^\pm G^\pm}^{(0)} - p^2\mathbf{1}\right) + \left(\mathbf{M}_{H^\pm G^\pm}^{(0)} - p^2\mathbf{1}\right) \delta^{(1)}\mathbf{Z}_{H^\pm G^\pm} \\ & + \delta^{(1)}\mathbf{M}_{H^\pm G^\pm} \ . \end{aligned} \tag{6.58b}$$

The usage of the lowest-order mass matrices which are listed in Eq. (6.22) results in the following expressions for the components of $\delta^{(1)}\mathbf{M}^{\mathbf{Z}}_{hHAG}$ and $\delta^{(1)}\mathbf{M}^{\mathbf{Z}}_{H^\pm G^\pm}$ in Eqs. (6.58) with the same notation as in Eq. (6.43):

$$\delta^{(1)}m^{\mathbf{Z}}_{h} = \left(m_h^2 - p^2\right)\delta^{(1)}Z_{hh} + \delta^{(1)}m_h^2\;, \tag{6.59a}$$
$$\delta^{(1)}m^{\mathbf{Z}}_{H} = \left(m_H^2 - p^2\right)\delta^{(1)}Z_{HH} + \delta^{(1)}m_H^2\;, \tag{6.59b}$$
$$\delta^{(1)}m^{\mathbf{Z}}_{A} = \left(m_A^2 - p^2\right)\delta^{(1)}Z_{AA} + \delta^{(1)}m_A^2\;, \tag{6.59c}$$
$$\delta^{(1)}m^{\mathbf{Z}}_{G} = \left(m_G^2 - p^2\right)\delta^{(1)}Z_{GG} + \delta^{(1)}m_G^2\;, \tag{6.59d}$$
$$\delta^{(1)}m^{\mathbf{Z}}_{hH} = \left(\tfrac{m_h^2+m_H^2}{2} - p^2\right)\delta^{(1)}Z_{hH} + \delta^{(1)}m_{hH}^2\;, \tag{6.59e}$$
$$\delta^{(1)}m^{\mathbf{Z}}_{hA} = \delta^{(1)}m_{hA}^2\;, \tag{6.59f}$$
$$\delta^{(1)}m^{\mathbf{Z}}_{hG} = \delta^{(1)}m_{hG}^2\;, \tag{6.59g}$$
$$\delta^{(1)}m^{\mathbf{Z}}_{HA} = \delta^{(1)}m_{HA}^2\;, \tag{6.59h}$$
$$\delta^{(1)}m^{\mathbf{Z}}_{HG} = \delta^{(1)}m_{HG}^2\;, \tag{6.59i}$$
$$\delta^{(1)}m^{\mathbf{Z}}_{AG} = \left(\tfrac{m_A^2+m_G^2}{2} - p^2\right)\delta^{(1)}Z_{AG} + \delta^{(1)}m_{AG}^2\;, \tag{6.59j}$$
$$\delta^{(1)}m^{\mathbf{Z}}_{H^\pm} = \left(m_{H^\pm}^2 - p^2\right)\delta^{(1)}Z_{H^\pm H^\pm} + \delta^{(1)}m_{H^\pm}^2\;, \tag{6.59k}$$
$$\delta^{(1)}m^{\mathbf{Z}}_{G^\pm} = \left(m_{G^\pm}^2 - p^2\right)\delta^{(1)}Z_{G^\pm G^\pm} + \delta^{(1)}m_{G^\pm}^2\;, \tag{6.59l}$$
$$\delta^{(1)}m^{\mathbf{Z}}_{H^-G^+} = \left(\tfrac{m_{H^\pm}^2+m_{G^\pm}^2}{2} - p^2\right)\delta^{(1)}Z_{H^-G^+} + \delta^{(1)}m_{H^-G^+}^2\;, \tag{6.59m}$$
$$\delta^{(1)}m^{\mathbf{Z}}_{G^-H^+} = \left(\tfrac{m_{G^\pm}^2+m_{H^\pm}^2}{2} - p^2\right)\delta^{(1)}Z_{G^-H^+} + \delta^{(1)}m_{G^-H^+}^2\;. \tag{6.59n}$$

Furthermore, depending on the chosen input parameter being m_A or $m_{H^\pm}$, the appropriate renormalization condition has to be imposed.

- If m_A is chosen as an input parameter, then the on-shell condition for the renormalized self-energy reads

$$\mathfrak{Re}\Big[\hat{\Sigma}^{(1)}_A\left(p^2\right)\Big]_{p^2\,=\,m_A^2} = 0\;. \tag{6.60}$$

  Applying this relation to Eq. (6.41a) with $j = 1$, and using Eq. (6.59c) yields

$$\delta^{(1)}m_A^2 = \mathfrak{Re}\Big[\Sigma^{(1)}_A\left(m_A^2\right)\Big]\;. \tag{6.61}$$

  This option is not available in the case of CP-violation, since m_A^2 is not an on-shell parameter anymore.

- On the other hand, if the charged Higgs-boson mass $m_{H^\pm}$ is chosen as an input parameter, the condition

$$\mathfrak{Re}\Big[\hat{\Sigma}^{(1)}_{H^\pm}\Big(p^2\Big)\Big]_{p^2\,=\,m^2_{H^\pm}} = 0 \tag{6.62}$$

is imposed on Eq. (6.41b). With the additional result of Eq. (6.59k), the renormalization constant $\delta^{(1)}m^2_{H^\pm}$ is fixed by

$$\delta^{(1)}m^2_{H^\pm} = \mathfrak{Re}\Big[\Sigma^{(1)}_{H^\pm}\Big(m^2_{H^\pm}\Big)\Big] \ . \tag{6.63}$$

For either choice the other counterterm is determined by Eq. (6.26) yielding

$$\delta^{(1)}m^2_{H^\pm} = \delta^{(1)}m^2_A + \delta^{(1)}M^2_W \ . \tag{6.64}$$

The other genuine mass counterterms follow from applying the renormalization transformations in Eq. (6.44) with $k = 1$ to the expressions in Eqs. (6.19). Having inserted the lowest-order relations of Eq. (6.20) and Eqs. (6.22) they are given by

$$\begin{aligned}
\delta^{(1)}m^2_h &= \delta^{(1)}m^2_A\, c^2_{\alpha-\beta} + \delta^{(1)}M^2_Z\, s^2_{\alpha+\beta} \\
&\quad + \frac{e\, s_{\alpha-\beta}}{2\, s_{\mathrm{w}}\, M_W}\Big[\delta^{(1)}T_H\, c_{\alpha-\beta}\, s_{\alpha-\beta} + \delta^{(1)}T_h\Big(1 + c^2_{\alpha-\beta}\Big)\Big] \qquad (6.65\mathrm{a}) \\
&\quad + \delta^{(1)}t_\beta\, c^2_\beta\Big(m^2_A\, s_{2(\alpha-\beta)} + M^2_Z\, s_{2(\alpha+\beta)}\Big) \ , \\
\delta^{(1)}m^2_H &= \delta^{(1)}m^2_A\, s^2_{\alpha-\beta} + \delta^{(1)}M^2_Z\, c^2_{\alpha+\beta} \\
&\quad - \frac{e\, c_{\alpha-\beta}}{2\, s_{\mathrm{w}}\, M_W}\Big[\delta^{(1)}T_H\Big(1 + s^2_{\alpha-\beta}\Big) + \delta^{(1)}T_h\, s_{\alpha-\beta}\, c_{\alpha-\beta}\Big] \qquad (6.65\mathrm{b}) \\
&\quad - \delta^{(1)}t_\beta\, c^2_\beta\Big(m^2_A\, s_{2(\alpha-\beta)} + M^2_Z\, s_{2(\alpha+\beta)}\Big) \ , \\
\delta^{(1)}m^2_G &= \frac{e}{2\, s_{\mathrm{w}}\, M_W}\Big(-\delta^{(1)}T_H\, c_{\alpha-\beta} + \delta^{(1)}T_h\, s_{\alpha-\beta}\Big) \ , \qquad (6.65\mathrm{c}) \\
\delta^{(1)}m^2_{hH} &= \frac{1}{2}\Big(\delta^{(1)}m^2_A\, s_{2(\alpha-\beta)} - \delta^{(1)}M^2_Z\, s_{2(\alpha+\beta)}\Big) \\
&\quad + \frac{e}{2\, s_{\mathrm{w}}\, M_W}\Big[\delta^{(1)}T_H\, s^3_{\alpha-\beta} - \delta^{(1)}T_h\, c^3_{\alpha-\beta}\Big] \qquad (6.65\mathrm{d}) \\
&\quad - \delta^{(1)}t_\beta\, c^2_\beta\Big(m^2_A\, c_{2(\alpha-\beta)} + M^2_Z\, c_{2(\alpha+\beta)}\Big) \ , \\
\delta^{(1)}m^2_{hA} &= \frac{e}{2\, s_{\mathrm{w}}\, M_W}\delta^{(1)}T_A\, s_{\alpha-\beta} \ , \qquad (6.65\mathrm{e}) \\
\delta^{(1)}m^2_{hG} &= \frac{e}{2\, s_{\mathrm{w}}\, M_W}\delta^{(1)}T_A\, c_{\alpha-\beta} \ , \qquad (6.65\mathrm{f}) \\
\delta^{(1)}m^2_{HA} &= -\delta^{(1)}m^2_{hG} \ , \qquad (6.65\mathrm{g}) \\
\delta^{(1)}m^2_{HG} &= \delta^{(1)}m^2_{hA} \ , \qquad (6.65\mathrm{h})
\end{aligned}$$

$$\delta^{(1)} m^2_{AG} = \frac{e}{2\, s_\mathrm{w}\, M_W} \left[-\delta^{(1)} T_H\, s_{\alpha-\beta} - \delta^{(1)} T_h\, c_{\alpha-\beta}\right] - \delta^{(1)} t_\beta\, m_A^2\, c_\beta^2 \ , \tag{6.65i}$$

$$\delta^{(1)} m^2_{G^\pm} = \frac{e}{2\, s_\mathrm{w}\, M_W} \left[-\delta^{(1)} T_H\, c_{\alpha-\beta} + \delta^{(1)} T_h\, s_{\alpha-\beta}\right] \ , \tag{6.65j}$$

$$\delta^{(1)} m^2_{H^- G^+} = -\frac{e}{2\, s_\mathrm{w}\, M_W} \left[\delta^{(1)} T_H\, s_{\alpha-\beta} + \delta^{(1)} T_h\, c_{\alpha-\beta} + i\, \delta^{(1)} T_A\right] - \delta^{(1)} t_\beta\, m^2_{H^\pm}\, c_\beta^2 \ , \tag{6.65k}$$

$$\delta^{(1)} m^2_{G^- H^+} = \left(\delta^{(1)} m^2_{H^- G^+}\right)^* \ . \tag{6.65l}$$

As can be seen, renormalization of e is not necessary for the one-loop Higgs-mass counterterms. This is due to the fact that $\delta^{(1)} e$ would only appear as a factor of a tree-level tadpole which are however equal to zero.

The W-boson mass is an input parameter for Eq. (6.64) and has to be renormalized. Together with the renormalization constant for the Z-boson mass it is fixed by the on-shell conditions

$$\begin{aligned} 0 &\stackrel{!}{=} \mathfrak{Re}\left[\hat{\Sigma}^{(1)}_{WW}\left(p^2\right)\right]_{p^2\,=\,M_W^2} \ , \\ &= \mathfrak{Re}\left[\Sigma^{(1)}_{WW}\left(p^2\right) + \left(p^2 - M_W^2\right) \delta^{(1)} Z_{WW} - \delta^{(1)} M_W^2\right]_{p^2\,=\,M_W^2} \ , \end{aligned} \tag{6.66a}$$

$$\begin{aligned} 0 &\stackrel{!}{=} \mathfrak{Re}\left[\hat{\Sigma}^{(1)}_{ZZ}\left(p^2\right)\right]_{p^2\,=\,M_W^2} \ , \\ &= \mathfrak{Re}\left[\Sigma^{(1)}_{ZZ}\left(p^2\right) + \left(p^2 - M_Z^2\right) \delta^{(1)} Z_{ZZ} - \delta^{(1)} M_Z^2\right]_{p^2\,=\,M_Z^2} \ , \end{aligned} \tag{6.66b}$$

leading to

$$\delta^{(1)} M_W^2 = \mathfrak{Re}\left[\Sigma^{(1)}_{WW}\left(M_W^2\right)\right] \ , \tag{6.67a}$$

$$\delta^{(1)} M_Z^2 = \mathfrak{Re}\left[\Sigma^{(1)}_{ZZ}\left(M_Z^2\right)\right] \ , \tag{6.67b}$$

with the one-loop self-energy diagrams $\Sigma^{(1)}_{WW}$ and $\Sigma^{(1)}_{ZZ}$ for the W and Z boson respectively. In this scheme $\delta^{(1)} s_\mathrm{w}$ is a dependent quantity which is fixed by Eqs. (6.13), i. e.

$$\delta^{(1)} s_\mathrm{w} = \frac{c_\mathrm{w}^2}{2\, s_\mathrm{w}} \left(\frac{\delta^{(1)} M_Z^2}{M_Z^2} - \frac{\delta^{(1)} M_W^2}{M_W^2}\right) \ . \tag{6.68}$$

6.7.3. Renormalization of tan(β)

The last remaining renormalization constant is $\delta^{(1)} t_\beta$. It originates from the renormalization of Eq. (6.15) where the property of the vacuum expectation values of acting like fields as well as parameters is respected, i. e.

$$v_i \to \sqrt{Z_{\mathcal{H}_i}}\left(v_i + \delta^{(1)} v_i\right) = v_i + \delta^{(1)} v_i + \frac{1}{2}\, v_i\, \delta^{(1)} Z_{\mathcal{H}_i} \;, \quad i \in \{1,\, 2\} \;, \tag{6.69a}$$

$$\delta^{(1)}\left(\frac{v_2}{v_1}\right) = \frac{v_2}{v_1}\left[\frac{\delta^{(1)} v_2}{v_2} - \frac{\delta^{(1)} v_1}{v_1} + \frac{1}{2}\left(\delta^{(1)} Z_{\mathcal{H}_2} - \delta^{(1)} Z_{\mathcal{H}_1}\right)\right] \;. \tag{6.69b}$$

Conveniently $\delta^{(1)} t_\beta$ is fixed in the $\overline{\mathrm{DR}}$ scheme which has emerged as the best choice in Ref. [FS02]; different process-dependent renormalization schemes have been applied in Ref. [BBS08]. With the additional observation [CPR92; Dab95] of

$$\left.\frac{\delta^{(1)} v_1}{v_1}\right|_{\mathrm{div}} = \left.\frac{\delta^{(1)} v_2}{v_2}\right|_{\mathrm{div}} \;, \tag{6.70a}$$

it follows that

$$\delta^{(1)} t_\beta = \delta^{(1)}\left.\left(\frac{v_2}{v_1}\right)\right|_{\mathrm{div}} = \frac{1}{2}\, t_\beta \left(\delta^{(1)} Z_{\mathcal{H}_2} - \delta^{(1)} Z_{\mathcal{H}_1}\right) \;. \tag{6.70b}$$

Thereby Eq. (6.70a) follows from $\mathcal{H}_1$ and $\mathcal{H}_2$ having the same $SU(2)_{\mathrm{L}}$ and $U(1)_Y$ quantum numbers, up to a sign. The field-renormalization constants have already been determined in Eqs. (6.53) by $\overline{\mathrm{DR}}$ conditions.

The divergence in Eq. (6.70b) is related to the beta function for t_β at the one-loop order:

$$\frac{\delta^{(1)} t_\beta}{t_\beta} = \frac{\beta^{(1)}(t_\beta)}{2\, t_\beta}\frac{1}{\epsilon} = -\frac{1}{2\,(4\pi)^2}\frac{1}{\epsilon}\left[N_{\mathrm{c}}\,\mathrm{Tr}\left(\mathbf{h}_u \mathbf{h}_u^\dagger\right) - N_{\mathrm{c}}\,\mathrm{Tr}\left(\mathbf{h}_d \mathbf{h}_d^\dagger\right) - \mathrm{Tr}\left(\mathbf{h}_e \mathbf{h}_e^\dagger\right)\right] \;, \tag{6.71}$$

which solely depends on the Yukawa-coupling matrices $\mathbf{h}_u$, $\mathbf{h}_d$ and $\mathbf{h}_e$ that are introduced in Eq. (3.5). The constant $N_{\mathrm{c}} = 3$ denotes the number of colors. For a detailed study on the evaluation of the beta function of t_β refer to [SSV13]. Some general remarks on the origin of the beta function of t_β and its relation to renormalization of t_β are given at the end of this chapter.

Having set up full one-loop renormalization of the linear and bilinear terms in the Higgs potential leaves the evaluation of all necessary self-energy and tadpole Feynman diagrams, which can be expressed by the standard scalar one-loop functions as defined in Chapter 4. Latest results of the full one-loop calculation have been presented in Ref. [Fra+07].

6.8. Two-loop renormalization

As the formal basis for the concrete two-loop calculation in Chapter 7 the results for two-loop renormalization of the Higgs tadpoles and masses are presented in this section.

6.8.1. Field renormalization

The field-renormalization transformation introduced by Eqs. (6.45) has to be expanded to the second order, leading to

$$\begin{aligned}\mathcal{H}_i \to \mathcal{H}_i\sqrt{Z_{\mathcal{H}_i}} &= \mathcal{H}_i\sqrt{1+\delta^{(1)}Z_{\mathcal{H}_i}+\delta^{(2)}Z_{\mathcal{H}_i}} \\ &= \mathcal{H}_i\left(1+\frac{1}{2}\delta^{(1)}Z_{\mathcal{H}_i}+\frac{1}{2}\Delta^{(2)}Z_{\mathcal{H}_i}\right) ,\end{aligned} \tag{6.72a}$$

with the abbreviation

$$\Delta^{(2)}Z_{\mathcal{H}_i} := \delta^{(2)}Z_{\mathcal{H}_i} - \frac{1}{4}\left(\delta^{(1)}Z_{\mathcal{H}_i}\right)^2 . \tag{6.72b}$$

The full two-loop content of $\sqrt{Z_{\mathcal{H}_i}}$ is contained in $\Delta^{(2)}Z_{\mathcal{H}_i}$, $i \in \{1,\, 2\}$.

According to Eqs. (6.46) the two-loop field-renormalization constants in the basis of lowest-order mass eigenstates are given by

$$\delta^{(2)}Z_{hh} = \left(s_\alpha^2\,\Delta^{(2)}Z_{\mathcal{H}_1} + c_\alpha^2\,\Delta^{(2)}Z_{\mathcal{H}_2}\right) , \tag{6.73a}$$

$$\delta^{(2)}Z_{HH} = \left(c_\alpha^2\,\Delta^{(2)}Z_{\mathcal{H}_1} + s_\alpha^2\,\Delta^{(2)}Z_{\mathcal{H}_2}\right) , \tag{6.73b}$$

$$\delta^{(2)}Z_{hH} = \delta^{(2)}Z_{Hh} = c_\alpha\,s_\alpha\left(\Delta^{(2)}Z_{\mathcal{H}_2} - \Delta^{(2)}Z_{\mathcal{H}_1}\right) , \tag{6.73c}$$

$$\delta^{(2)}Z_{AA} = \left(s_{\beta_n}^2\,\Delta^{(2)}Z_{\mathcal{H}_1} + c_{\beta_n}^2\,\Delta^{(2)}Z_{\mathcal{H}_2}\right) , \tag{6.73d}$$

$$\delta^{(2)}Z_{GG} = \left(c_{\beta_n}^2\,\Delta^{(2)}Z_{\mathcal{H}_1} + s_{\beta_n}^2\,\Delta^{(2)}Z_{\mathcal{H}_2}\right) , \tag{6.73e}$$

$$\delta^{(2)}Z_{AG} = \delta^{(2)}Z_{GA} = c_{\beta_n}\,s_{\beta_n}\left(\Delta^{(2)}Z_{\mathcal{H}_2} - \Delta^{(2)}Z_{\mathcal{H}_1}\right) , \tag{6.73f}$$

$$\delta^{(2)}Z_{H^\pm H^\pm} = \left(s_{\beta_c}^2\,\Delta^{(2)}Z_{\mathcal{H}_1} + c_{\beta_c}^2\,\Delta^{(2)}Z_{\mathcal{H}_2}\right) , \tag{6.73g}$$

$$\delta^{(2)}Z_{G^\pm G^\pm} = \left(c_{\beta_c}^2\,\Delta^{(2)}Z_{\mathcal{H}_1} + s_{\beta_c}^2\,\Delta^{(2)}Z_{\mathcal{H}_2}\right) , \tag{6.73h}$$

$$\delta^{(2)}Z_{H^\pm G^\pm} = \delta^{(2)}Z_{G^\pm H^\pm} = c_{\beta_c}\,s_{\beta_c}\left(\Delta^{(2)}Z_{\mathcal{H}_2} - \Delta^{(2)}Z_{\mathcal{H}_1}\right) . \tag{6.73i}$$

Two independent renormalization conditions are required for $\delta^{(2)} Z_{\mathcal{H}_i}$. In analogy to Eqs. (6.53), they are determined by the $\overline{\mathrm{DR}}$ conditions

$$\delta^{(2)} Z_{\mathcal{H}_1} = -\Re\mathfrak{e}\left[\frac{\partial \Sigma_H^{(2)}\Big|_{\alpha\,=\,0}(p^2)}{\partial p^2}\right]_{\text{div}} , \tag{6.74a}$$

$$\delta^{(2)} Z_{\mathcal{H}_2} = -\Re\mathfrak{e}\left[\frac{\partial \Sigma_h^{(2)}\Big|_{\alpha\,=\,0}(p^2)}{\partial p^2}\right]_{\text{div}} . \tag{6.74b}$$

6.8.2. Mass and tadpole renormalization

For $k = 2$ the tadpole counterterms in Eqs. (6.49) amount to

$$\begin{pmatrix} \delta^{(2)} T_h^{\mathbf{Z}} \\ \delta^{(2)} T_H^{\mathbf{Z}} \\ \delta^{(2)} T_A^{\mathbf{Z}} \\ \delta^{(2)} T_G^{\mathbf{Z}} \end{pmatrix} = \begin{pmatrix} \delta^{(2)}\mathbf{Z}_{hH} & \mathbf{0} \\ \mathbf{0} & \delta^{(2)}\mathbf{Z}_{AG} \end{pmatrix} \begin{pmatrix} T_h^{(0)} \\ T_H^{(0)} \\ T_A^{(0)} \\ T_G^{(0)} \end{pmatrix} + \begin{pmatrix} \delta^{(1)}\mathbf{Z}_{hH} & \mathbf{0} \\ \mathbf{0} & \delta^{(1)}\mathbf{Z}_{AG} \end{pmatrix} \begin{pmatrix} \delta^{(1)} T_h \\ \delta^{(1)} T_H \\ \delta^{(1)} T_A \\ \delta^{(1)} T_G \end{pmatrix} + \begin{pmatrix} \delta^{(2)} T_h \\ \delta^{(2)} T_H \\ \delta^{(2)} T_A \\ \delta^{(2)} T_G \end{pmatrix} . \tag{6.75}$$

The evaluation of the mass counterterms in Eqs. (6.50) for $k = 2$ yields

$$\begin{aligned} \delta^{(2)}\mathbf{M}_{hHAG}^{\mathbf{Z}} = &\begin{pmatrix} \delta^{(2)}\mathbf{Z}_{hH}^T & \mathbf{0} \\ \mathbf{0} & \delta^{(2)}\mathbf{Z}_{AG}^T \end{pmatrix} \left(\mathbf{M}_{hHAG}^{(0)} - p^2\mathbf{1}\right) \\ &+ \left(\mathbf{M}_{hHAG}^{(0)} - p^2\mathbf{1}\right) \begin{pmatrix} \delta^{(2)}\mathbf{Z}_{hH} & \mathbf{0} \\ \mathbf{0} & \delta^{(2)}\mathbf{Z}_{AG} \end{pmatrix} \\ &+ \begin{pmatrix} \delta^{(1)}\mathbf{Z}_{hH}^T & \mathbf{0} \\ \mathbf{0} & \delta^{(1)}\mathbf{Z}_{AG}^T \end{pmatrix} \delta^{(1)}\mathbf{M}_{hHAG} + \delta^{(1)}\mathbf{M}_{hHAG} \begin{pmatrix} \delta^{(1)}\mathbf{Z}_{hH} & \mathbf{0} \\ \mathbf{0} & \delta^{(1)}\mathbf{Z}_{AG} \end{pmatrix} \\ &+ \begin{pmatrix} \delta^{(1)}\mathbf{Z}_{hH}^T & \mathbf{0} \\ \mathbf{0} & \delta^{(1)}\mathbf{Z}_{AG}^T \end{pmatrix} \left(\mathbf{M}_{hHAG}^{(0)} - p^2\mathbf{1}\right) \begin{pmatrix} \delta^{(1)}\mathbf{Z}_{hH} & \mathbf{0} \\ \mathbf{0} & \delta^{(1)}\mathbf{Z}_{AG} \end{pmatrix} \\ &+ \delta^{(2)}\mathbf{M}_{hHAG} , \end{aligned} \tag{6.76a}$$

$$\begin{aligned}\delta^{(2)}\mathbf{M}^{\mathbf{Z}}_{H^\pm G^\pm} = {} & \delta^{(2)}\mathbf{Z}^T_{H^\pm G^\pm}\left(\mathbf{M}^{(0)}_{H^\pm G^\pm} - p^2\mathbf{1}\right) + \left(\mathbf{M}^{(0)}_{H^\pm G^\pm} - p^2\mathbf{1}\right)\delta^{(2)}\mathbf{Z}_{H^\pm G^\pm} \\ & + \delta^{(1)}\mathbf{Z}^T_{H^\pm G^\pm}\delta^{(1)}\mathbf{M}_{H^\pm G^\pm} + \delta^{(1)}\mathbf{M}_{H^\pm G^\pm}\delta^{(1)}\mathbf{Z}_{H^\pm G^\pm} \\ & + \delta^{(1)}\mathbf{Z}^T_{H^\pm G^\pm}\left(\mathbf{M}^{(0)}_{H^\pm G^\pm} - p^2\mathbf{1}\right)\delta^{(1)}\mathbf{Z}_{H^\pm G^\pm} + \delta^{(2)}\mathbf{M}_{H^\pm G^\pm}\ ,\end{aligned} \tag{6.76b}$$

By expanding the matrix products and applying the lowest-order and symmetry relations the expressions for each component can be achieved; the explicit results are listed in Appendix C.

Besides the genuine two-loop mass and tadpole counterterms, the results of Eqs. (6.76) contain also products of the genuine one-loop mass and tadpole counterterms with one-loop field-renormalization constants; in addition, products of different field-renormalization constants occur, too. Again, the explicit expressions of the genuine two-loop mass counterterms are recorded in Appendix C.

The independent renormalization constants can be fixed in the same way as at the one-loop order, i. e.

- the tadpoles do not shift the minimum of the Higgs potential:

$$\delta^{(2)}T_i^{\mathbf{Z}} = -\Upsilon_i^{(2)}\ , \quad i \in \{h, H, A\}\ ; \tag{6.77}$$

- the gauge-boson masses are renormalized on-shell:

$$\delta^{(2)}M_W^2 = \mathfrak{Re}\left[\Sigma^{(2)}_{WW}\left(M_W^2\right)\right]\ , \tag{6.78a}$$
$$\delta^{(2)}M_Z^2 = \mathfrak{Re}\left[\Sigma^{(2)}_{ZZ}\left(M_Z^2\right)\right]\ ; \tag{6.78b}$$

- and either the A-boson mass or the $H^\pm$-boson mass is on-shell, depending on the chosen input parameter m_A or $m_{H^\pm}$:

$$\delta^{(2)}m_A^2 = \mathfrak{Re}\left[\Sigma^{(2)}_{A}\left(m_A^2\right)\right]\ , \tag{6.79a}$$
$$\delta^{(2)}m_{H^\pm}^2 = \mathfrak{Re}\left[\Sigma^{(2)}_{H^\pm}\left(m_{H^\pm}^2\right)\right]\ . \tag{6.79b}$$

  Again, m_A cannot be chosen as an input parameter in the case of CP-violation. The mass counterterms are correlated via

$$\delta^{(2)}m_{H^\pm}^2 = \delta^{(2)}m_A^2 + \delta^{(2)}M_W^2\ . \tag{6.80}$$

At the two-loop level also $\delta^{(1)}e$ is appearing for the first time. It occurs always in combination with $\delta^{(1)}s_\mathrm{w}$ and $\delta^{(1)}M_W$ as can be seen in the explicit expressions in Appendix C.2.

The relation

$$\frac{\delta^{(1)}e}{e} = -\frac{1}{2}\left(\delta^{(1)}Z_{AA} - \frac{s_\mathrm{w}}{c_\mathrm{w}}\delta^{(1)}Z_{ZA}\right) \tag{6.81a}$$

determines $\delta^{(1)}e$ by the field-renormalization constants of the photon,

$$\delta^{(1)}Z_{AA} = -\mathfrak{Re}\left[\frac{\partial\Sigma^{(1)}_{AA}(p^2)}{\partial p^2}\right]_{p^2\,=\,0}\,, \tag{6.81b}$$

and photon–Z mixing,

$$\delta^{(1)}Z_{ZA} = -\mathfrak{Re}\left[\frac{2\Sigma^{(1)}_{ZA}(0)}{M_Z^2}\right]\,, \tag{6.81c}$$

as in the Standard Model [Den93].

6.8.3. Renormalization of tan(β)

Renormalization of t_β at the two-loop order is more involved. Applying the renormalization transformation

$$v_i \to v_i + \delta^{(1)}v_i + \frac{1}{2}v_i\delta^{(1)}Z_{\mathcal{H}_i} + \delta^{(2)}v_i + \frac{1}{2}v_i\left[\delta^{(2)}Z_{\mathcal{H}_i} - \frac{1}{4}\left(\delta^{(1)}Z_{\mathcal{H}_i}\right)^2\right]\,, \quad i\in\{1,\,2\}\,, \tag{6.82}$$

at Eq. (6.15) renders the two-loop part

$$\begin{aligned}\delta^{(2)}\left(\frac{v_2}{v_1}\right) = \frac{v_2}{v_1}\Bigg[&\frac{\delta^{(2)}v_2}{v_2} - \frac{\delta^{(2)}v_1}{v_1} + \frac{1}{2}\left(\delta^{(2)}Z_{\mathcal{H}_2} - \delta^{(2)}Z_{\mathcal{H}_1}\right)\\ &+\left(\frac{\delta^{(1)}v_2}{v_2} - \frac{\delta^{(1)}v_1}{v_1}\right)\left(-\frac{\delta^{(1)}v_1}{v_1} + \frac{1}{2}\left(\delta^{(1)}Z_{\mathcal{H}_2} - \delta^{(1)}Z_{\mathcal{H}_1}\right)\right)\\ &-\frac{1}{2}\left(\delta^{(1)}Z_{\mathcal{H}_2} - \delta^{(1)}Z_{\mathcal{H}_1}\right)\left(\frac{1}{4}\left(\delta^{(1)}Z_{\mathcal{H}_2} - \delta^{(1)}Z_{\mathcal{H}_1}\right) + \delta^{(1)}Z_{\mathcal{H}_1}\right)\Bigg]\,.\end{aligned} \tag{6.83}$$

Again, $\delta^{(2)}t_\beta$ is defined in the $\overline{\text{DR}}$ scheme. The renormalization condition

$$\frac{\delta^{(1)}v_1}{v_1} = \frac{\delta^{(1)}v_2}{v_2} \tag{6.84}$$

is an extension of Eq. (6.70a) and simplifies Eq. (6.83). Furthermore, the one-loop relation for renormalization of t_β in the $\overline{\text{DR}}$ scheme in Eq. (6.70b) is utilized, yielding

$$\begin{aligned}\delta^{(2)}t_\beta = \delta^{(2)}\left(\frac{v_2}{v_1}\right)\bigg|_{\text{div}} = t_\beta \Bigg[&\left(\frac{\delta^{(2)}v_2}{v_2} - \frac{\delta^{(2)}v_1}{v_1}\right)\bigg|_{\text{div}} + \frac{1}{2}\left(\delta^{(2)}Z_{\mathcal{H}_2} - \delta^{(2)}Z_{\mathcal{H}_1}\right) \\ &- \frac{1}{2}\left(\frac{\delta^{(1)}t_\beta}{t_\beta}\right)^2 - \frac{\delta^{(1)}t_\beta}{t_\beta}\delta^{(1)}Z_{\mathcal{H}_1}\Bigg] .\end{aligned} \tag{6.85}$$

Thereby the field-renormalization constants are fixed by Eqs. (6.74).

The divergent part of the combination $\left(\delta^{(2)}v_2\big/v_2 - \delta^{(2)}v_1\big/v_1\right)$ is in general not equal to zero and even gauge-dependent as can be seen in the following result of the two-loop beta function of t_β.

In addition to the one-loop beta function of t_β given in Eq. (6.71) the corresponding two-loop function is necessary to determine $\delta^{(2)}t_\beta$. Its full form is taken from Ref. [SSV14]:

$$\begin{aligned}\frac{\beta^{(2)}(t_\beta)}{t_\beta} = &\frac{1}{(4\pi)^4}\Big\{ -\left(\tfrac{4}{15}\tfrac{5}{3}g_Y^2 + \tfrac{16}{3}g_\text{s}^2\right) N_\text{c}\,\text{Tr}\left(\mathbf{h}_u\mathbf{h}_u^\dagger\right) \\ &\qquad + \left(-\tfrac{2}{15}\tfrac{5}{3}g_Y^2 + \tfrac{16}{3}g_\text{s}^2\right) N_\text{c}\,\text{Tr}\left(\mathbf{h}_d\mathbf{h}_d^\dagger\right) + \tfrac{6}{5}\tfrac{5}{3}g_Y^2\,\text{Tr}\left(\mathbf{h}_e\mathbf{h}_e^\dagger\right)\Big\} \\ &+ \frac{3}{(4\pi)^4}\left[N_\text{c}\,\text{Tr}\left(\mathbf{h}_u\mathbf{h}_u^\dagger\mathbf{h}_u\mathbf{h}_u^\dagger\right) - N_\text{c}\,\text{Tr}\left(\mathbf{h}_d\mathbf{h}_d^\dagger\mathbf{h}_d\mathbf{h}_d^\dagger\right) - \text{Tr}\left(\mathbf{h}_e\mathbf{h}_e^\dagger\mathbf{h}_e\mathbf{h}_e^\dagger\right)\right] \\ &+ \frac{1}{(4\pi)^2}\,\xi\,\xi'\left(\tfrac{3}{10}\tfrac{5}{3}g_Y^2 + \tfrac{3}{2}g_\text{w}^2\right)\frac{\beta^{(1)}(t_\beta)}{t_\beta} ,\end{aligned} \tag{6.86}$$

wherein $\xi \equiv \xi_i$ and $\xi' \equiv \xi_i'$, $i \in \{A,\ Z,\ W\}$ are universal gauge-fixing parameters of an R_ξ gauge function (cf. Section 6.4.2) and g_s is the strong gauge coupling.

The last term on the right-hand side of Eq. (6.86) is gauge-dependent. It purely originates from parameter renormalization of the vacuum expectation values v_i. All other terms on the right-hand side of Eq. (6.86) are induced by the anomalous dimensions of $\mathcal{H}_1$ and $\mathcal{H}_2$.

The connection between the beta functions (i. e. the running) and the renormalization constants for t_β can be derived as follows:

- the beta function of t_β at kth order (cf. Section 5.4) is defined by the relation

$$\frac{\beta^{(k)}(t_\beta)}{t_\beta} = \gamma_2^{(k)} - \gamma_1^{(k)} + \hat{\gamma}_2^{(k)} - \hat{\gamma}_1^{(k)} \tag{6.87}$$

  where a similar notation as in Ref. [SSV13] is used, i. e. $\gamma_2^{(k)}$ and $\gamma_1^{(k)}$ are the anomalous dimensions of $\mathcal{H}_2$ and $\mathcal{H}_1$ at kth order (cf. Section 5.4), and $\hat{\gamma}_2^{(k)}$ and $\hat{\gamma}_1^{(k)}$ are the analogous quantities for parameter renormalization of v_2 and v_1.

- the beta function of a given order k is directly related to the coefficient of the $\frac{1}{\epsilon}$ pole of $\delta^{(k)} t_\beta$,

- the higher-order poles in ϵ for each $\delta^{(k)} t_\beta$ can be achieved by products of lower-order γs and $\hat{\gamma}$s (e. g. Ref. [Spe13]).

In Ref. [Spe13] the following equations can be found (here specified for the field-renormalization constants of the Higgs doublets in the MSSM):[8]

$$\delta^{(1)} Z_{\mathcal{H}_i} = \gamma_i^{(1)} \frac{1}{\epsilon}, \tag{6.88a}$$

$$\delta^{(2)} Z_{\mathcal{H}_i} = \frac{1}{2} \gamma_i^{(2)} \frac{1}{\epsilon} + \frac{1}{4} \sum_{g_j} \beta^{(1)}(g_j)\, \partial_{g_j} \gamma_i^{(1)} \frac{1}{\epsilon^2} + \frac{1}{2} \left(\gamma_i^{(1)} \frac{1}{\epsilon} \right)^2 . \tag{6.88b}$$

The second term on the right-hand side of Eq. (6.88b) sums all contributions by the beta functions of the gauge couplings and other running couplings g_j inside of $\gamma_i^{(1)}$.

[8] Different conventions for the definition of $\delta^{(2)} Z_{\mathcal{H}_i}$ are used in Ref. [Spe13] and in this thesis.

7. Two-loop top-Yukawa-coupling corrections

Following the general discussions of the mass shifts for the Higgs bosons at higher orders in Section 6.5, the focus is set on the irreducible $\mathcal{O}(\alpha_t^2)$ terms for the neutral and charged physical Higgs bosons now. Thereby mixings of all neutral, physical tree-level mass eigenstates h, H and A are in general possible as can be seen in Eqs. (6.36); consequently all contributing self-energies to $\mathbf{\Sigma}^{(2)}_{hHA}$, including transitions, must be evaluated. The self-energy matrix $\mathbf{\Sigma}^{(2)}_{hHA}$ denotes the upper left submatrix with rank three of $\mathbf{\Sigma}^{(2)}_{hHAG}$ defined in Eq. (6.42a). Mixing with the Goldstone boson G yields subleading two-loop contributions; also G–Z mixing occurs in principle, which is related to the other mixings of the Goldstone boson by Slavnov–Taylor identities [BBS08; WRW11] and of subleading type as well [Hol+02]. However, A–G mixing has to be taken into account in intermediate steps for consistent renormalization. Analogously, only the upper left entry of the charged Higgs-boson mass matrix $\mathbf{\Sigma}^{(2)}_{H^\pm G^\pm}$ given in Eq. (6.42b) is considered and mixings with the charged Goldstone bosons are neglected. The $H^\pm$–$G^\pm$ mixing only enters in the renormalization procedure.

7.1. Outline of the calculation

The considered class of two-loop Feynman diagrams is created with the help of the `Mathematica` package `FeynArts` [Hah01] using the model file of Ref. [Fri+13] and an additional add-on model file to introduce unique symbols for the Goldstone-boson masses (cf. Section 7.2); Fig. 7.1 shows all contributing diagrams. As can be seen each diagram contains top particles t and/or stop/sbottom particles $\tilde{t}_1$, $\tilde{t}_2$, $\tilde{b}_\mathrm{L}$ which are connected to the external Higgs bosons. In addition bottoms b, charginos $\tilde{\chi}^\pm$, neutralinos $\tilde{\chi}^0$ and all Higgs and unphysical Goldstone bosons appear in internal lines.

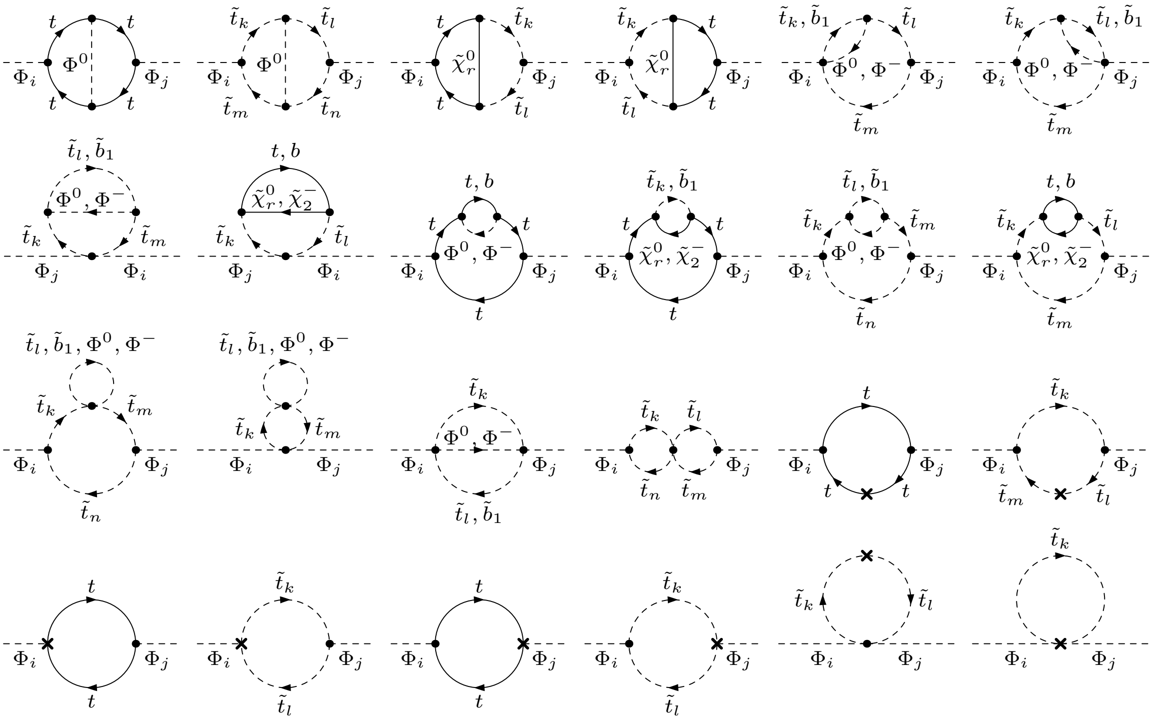

Figure 7.1.: Full list of two-loop self-energy diagrams for the neutral Higgs bosons. The crosses denote one-loop counterterm insertions. $\Phi_i = h,\, H,\, A$; $\Phi^0 = h,\, H,\, A,\, G$; $\Phi^- = H^-,\, G^-$.

Those two-loop diagrams which are composed of an one-loop diagram and a counterterm insertion are part of $\mathbf{\Sigma}^{(2)}_{hHAG}$; they are referred to as subrenormalization diagrams. The genuine two-loop counterterms and required renormalization constants are presented in detail in Section 7.4. The couplings and one-loop counterterms for each interaction vertex are depicted in Section 7.7 with their corresponding analytical expressions. Thereby some approximations are used; they are explained in Section 7.2. Since these simplifications also affect the MSSM sectors of the other internally appearing particles mentioned above, they are revisited in Section 7.5 and Section 7.6.

For the reduction of the subrenormalization diagrams and the one-loop renormalization constants to the set of one-loop functions presented in Appendix B.1 the `Mathematica` package `FormCalc` [HP99] is used. The appearing two-loop diagrams are reduced to the scalar integrals which are displayed in Appendix B.2 with the help of the `Mathematica` package `TwoCalc` [WSB94a]. The subsequent evaluation of all loop functions is done completely analytically, with the help of `Mathematica`. All Feynman diagrams are created with the help of `FeynEdit` [HL08].

7.2. Approximations

The dominant parts of the $\mathcal{O}(\alpha_t^2)$ contributions are enhanced by an additional factor m_t^2. Thus, the following approximations are applied to their evaluation:[9]

- The external momentum is set to zero, i. e. the two-loop self-energies in $\mathbf{\Sigma}^{(2)}_{hHAG}$ are calculated at $p^2 = 0$. Furthermore also the counterterms $\delta^{(2)}\mathbf{M}^{\mathbf{Z}}_{hHAG}$ which are introduced in Eq. (6.41a) are calculated at $p^2 = 0$. As an immediate consequence all appearing two-loop integrals are independent of p^2 leading to vacuum diagrams that are known analytically (cf. Section 4.2); all two-loop integrals can be reduced to T_{134} or factorized into a product of two one-loop integrals.

- The gauge-less limit is applied. It is an approximation where pure gauge couplings are neglected, i. e. $g_Y = 0$, $g_\mathrm{w} = 0$. Furthermore, the strong gauge coupling is neglected, $g_\mathrm{s} = 0$. Within this scenario, gauge bosons do not receive any mass terms, i. e. $M_W = 0$ and $M_Z = 0$. However the weak mixing angle θ_w which appears in s_w and c_w keeps its original tree-level value. Caution has to be taken when applying this limit to the used `FeynArts` model file since all couplings, especially the Yukawa couplings, are expressed in terms of e, s_w, c_w, M_W and M_Z (g_s is the only coupling that occurs directly).

- The bottom-quark mass m_b is set to zero. Thus, the $\mathcal{O}(\alpha_t\alpha_b)$ and $\mathcal{O}(\alpha_b^2)$ contributions are neglected and the $\mathcal{O}(\alpha_t^2)$ contributions build a supersymmetric and gauge-invariant class of two-loop corrections to the Higgs-boson masses.

The implementation of the vanishing external momentum can be easily introduced after the evaluation of amplitudes for the Feynman diagrams. As mentioned before difficulties in assembling the gauge-less limit arise from the parametrization of the gauge and Yukawa couplings in terms of the same quantities. To avoid this problem at first M_Z is expressed as M_W/c_w. Then the routine stated in Tab. 7.1 is applied at each coupling in the amplitudes created by `FeynArts`. Therein `simprules` contains the simplifications of the MSSM sectors that are explained in Section 7.5 and Section 7.6. The variable `yt` = `MT/MW` $\equiv m_t/M_W$ is related to the top-Yukawa coupling h_t. Successively negative powers of $M_W \equiv$ `MW` are parametrized by `yt`: `t1` contains the part that is proportional to M_W^{-2}, `t2` adds the term of the order M_W^{-1}, and `t3` further keeps track of the M_W^0 contribution. At each step higher powers of M_W are set to zero, effectively eliminating all gauge contributions.

[9] These approximations were also used for the evaluation of the $\mathcal{O}(\alpha_t\alpha_s)$ contributions [Hei+07].

However another caveat has to be taken care of: in the model file of Ref. [Fri+13] the tree-level Goldstone-boson masses are explicitly set to $m_G = M_Z$ and $m_{G^\pm} = M_W$, thus, the routine above would obliterate them. To have the possibility of identifying their contributions during the whole calculation they need to acquire unique symbols for their masses. This is achieved by the `FeynArts` add-on model file given in Tab. 7.2 that introduces the tree-level mass parameters `MG0` $\equiv m_G$ and `MGp` $\equiv m_{G^\pm}$.

Table 7.1.: The used function to elimininate all gauge couplings.

```
nogaugecoupling[term_] :=
  Block[{t1, t2, t3, simprules},
    t1 = yt^2 (Collect[term*MW^2/MT^2, MW, Simplify] /. MW -> 0);
    t2 = t1 + yt (Collect[(term - t1 /. yt -> MT/MW)*MW/MT,
                          MW, Simplify] /. MW -> 0);
    t3 = t2 + Simplify[term - t2 /. yt -> MT/MW] /. MW -> 0;
    Simplify[t3 /. GS -> 0 /. MB -> 0 /. simprules]
  ];
```

Table 7.2.: The add-on model file for `FeynArts` to handle Goldstone-boson masses.

```
newMass[{field_, mass_}] :=
  (field == def_) :>
    (field == def /. (Mass -> _) -> (Mass -> mass));
M$ClassesDescription =
  M$ClassesDescription /.
    Map[newMass, {{S[4], MG0}, {S[6], MGp}}];
```

7.3. Simplified lowest-order relations

Due to the applied approximations as described in Section 7.2 the lowest-order relations of the Higgs-boson sector which are derived in Section 6.4 are modified; this comes solely by neglecting all gauge contributions.

Hence, Eq. (6.26) and Eq. (6.28) are simplified to

$$m_h^2 = 0 \; , \quad m_H^2 = m_A^2 \; , \quad m_{H^\pm}^2 = m_A^2 \; . \tag{7.1}$$

Furthermore, also the masses of the unphysical Goldstone bosons that are originating from gauge-fixing terms (cf. Section 6.4.2) are zero in the gauge-less limit:

$$m_G^2 = 0 \ , \quad m_{G^\pm}^2 = 0 \ . \tag{7.2}$$

The lowest-order relations between the mixing angles β_c and β_n with the ratio of the vacuum expectation values t_β as derived in Eqs. (6.23) are still valid:

$$\beta_c = \beta_n = \beta. \tag{7.3}$$

For the third parameter α Eqs. (6.30) now yield

$$s_{2\alpha} = -s_{2\beta} \ , \quad c_{2\alpha} = -c_{2\beta} \ , \quad t_{2\alpha} = t_{2\beta} \ , \tag{7.4}$$

which can be summarized easier in the equation $\alpha = \beta - \pi/2$.

Thus for the evaluation of the $\mathcal{O}(\alpha_t^2)$ contributions with complex parameters the occuring lowest-order values for the masses of h, G and $G^\pm$ are set to zero, the masses of H, A and $H^\pm$ are set equal to each other and the mixing angle α is substituted by β.

7.4. Renormalization

In this section the effects of the approximations which are introduced in Section 7.2 on two-loop renormalization of the Higgs potential of the $\mathcal{O}(\alpha_t^2)$ calculation are discussed.

The tadpoles as defined by Eq. (6.34) for $k = 2$ yield

$$T_i^{(2)} = T_i^{(0)} + \hat{\Upsilon}_i^{(1)} + \hat{\Upsilon}_i^{(2)} \ , \quad T_i^{(0)} = 0 \ , \quad i \in \{h,\, H,\, A\} \ . \tag{7.5}$$

The tadpole $T_G^{(2)}$ of the unphysical Goldstone boson G is not necessary for the calculation of the physical Higgs-boson masses at the two-loop level.

The explicit forms of Eqs. (6.36) are given by

$$\mathbf{M}_{hHAG}^{(2)}\left(p^2\right) = \mathbf{M}_{hHAG}^{(0)} - \hat{\mathbf{\Sigma}}_{hHAG}^{(1)}\left(p^2\right) - \hat{\mathbf{\Sigma}}_{hHAG}^{(2)}(0) \ , \tag{7.6a}$$

$$\mathbf{M}_{H^\pm G^\pm}^{(2)}\left(p^2\right) = \mathbf{M}_{H^\pm G^\pm}^{(0)} - \hat{\mathbf{\Sigma}}_{H^\pm G^\pm}^{(1)}\left(p^2\right) - \hat{\mathbf{\Sigma}}_{H^\pm G^\pm}^{(2)}(0) \ . \tag{7.6b}$$

Therein, the dependence on the external momentum is neglected at the two-loop order, i. e. the computed $\mathcal{O}(\alpha_t^2)$ contributions shift the entries of the matrices by a constant value. However, it is stressed that the momentum-dependent parts of the one-loop corrections remain; thus, the masses of the Higgs bosons at higher orders have to be computed with Eq. (6.35a) and Eq. (6.35b), respectively.

7.4.1. Counterterms

The counterterms for the tadpoles and self-energies which are introduced by Eq. (6.40) and Eqs. (6.41), respectively, are displayed for the two-loop case in matrix notation in Eqs. (6.76) and explicitly in Appendix C. In the following, the formulas are expressed within the present approximations and choosing $m_{H^\pm}$ as an input quantity, providing a common mass for the heavy Higgs bosons.

The tadpole counterterms are given by

$$\delta^{(2)}T_h^{\mathbf{Z}} = \tfrac{1}{2}\left(\delta^{(1)}Z_{hh}\,\delta^{(1)}T_h + \delta^{(1)}Z_{hH}\,\delta^{(1)}T_H\right) + \delta^{(2)}T_h\ , \tag{7.7a}$$

$$\delta^{(2)}T_H^{\mathbf{Z}} = \tfrac{1}{2}\left(\delta^{(1)}Z_{HH}\,\delta^{(1)}T_H + \delta^{(1)}Z_{hH}\,\delta^{(1)}T_h\right) + \delta^{(2)}T_H\ , \tag{7.7b}$$

$$\delta^{(2)}T_A^{\mathbf{Z}} = \tfrac{1}{2}\left(\delta^{(1)}Z_{AA}\,\delta^{(1)}T_A + \delta^{(1)}Z_{AG}\,\delta^{(1)}T_G\right) + \delta^{(2)}T_A\ . \tag{7.7c}$$

The results for the required self-energy counterterms are

$$\delta^{(2)}m_h^{\mathbf{Z}} = \tfrac{1}{4}\,m_{H^\pm}^2\left(\delta^{(1)}Z_{hH}\right)^2 + \delta^{(1)}Z_{hh}\,\delta^{(1)}m_h^2 + \delta^{(1)}Z_{hH}\,\delta^{(1)}m_{hH}^2 + \delta^{(2)}m_h^2\ , \tag{7.8a}$$

$$\begin{aligned}\delta^{(2)}m_H^{\mathbf{Z}} = {} & m_{H^\pm}^2\left[\delta^{(2)}Z_{HH} + \tfrac{1}{4}\left(\delta^{(1)}Z_{HH}\right)^2\right] \\ & + \delta^{(1)}Z_{HH}\,\delta^{(1)}m_H^2 + \delta^{(1)}Z_{hH}\,\delta^{(1)}m_{hH}^2 + \delta^{(2)}m_H^2\ ,\end{aligned} \tag{7.8b}$$

$$\begin{aligned}\delta^{(2)}m_A^{\mathbf{Z}} = {} & m_{H^\pm}^2\left[\delta^{(2)}Z_{AA} + \tfrac{1}{4}\left(\delta^{(1)}Z_{AA}\right)^2\right] \\ & + \delta^{(1)}Z_{AA}\,\delta^{(1)}m_A^2 + \delta^{(1)}Z_{AG}\,\delta^{(1)}m_{AG}^2 + \delta^{(2)}m_A^2\ ,\end{aligned} \tag{7.8c}$$

$$\begin{aligned}\delta^{(2)}m_{hH}^{\mathbf{Z}} = {} & \tfrac{1}{2}\left[\left(\delta^{(1)}Z_{hh} + \delta^{(1)}Z_{HH}\right)\delta^{(1)}m_{hH}^2 + \delta^{(1)}Z_{hH}\left(\delta^{(1)}m_h^2 + \delta^{(1)}m_H^2\right)\right] \\ & + \tfrac{1}{4}\,m_{H^\pm}^2\,\delta^{(1)}Z_{HH}\,\delta^{(1)}Z_{hH} + \tfrac{m_{H^\pm}^2}{2}\,\delta^{(2)}Z_{hH} + \delta^{(2)}m_{hH}^2\ ,\end{aligned} \tag{7.8d}$$

$$\begin{aligned}\delta^{(2)}m_{hA}^{\mathbf{Z}} = {} & \tfrac{1}{2}\Big[\left(\delta^{(1)}Z_{hh} + \delta^{(1)}Z_{AA}\right)\delta^{(1)}m_{hA}^2 \\ & \quad + \delta^{(1)}Z_{hH}\,\delta^{(1)}m_{HA}^2 + \delta^{(1)}Z_{AG}\,\delta^{(1)}m_{hG}^2\Big] + \delta^{(2)}m_{hA}^2\ ,\end{aligned} \tag{7.8e}$$

$$\begin{aligned} \delta^{(2)} m^{\mathbf{Z}}_{HA} = \tfrac{1}{2} \Big[&\left(\delta^{(1)} Z_{HH} + \delta^{(1)} Z_{AA}\right) \delta^{(1)} m^2_{HA} \\ &+ \delta^{(1)} Z_{hH}\, \delta^{(1)} m^2_{hA} + \delta^{(1)} Z_{AG}\, \delta^{(1)} m^2_{HG} \Big] + \delta^{(2)} m^2_{HA} \ , \end{aligned} \tag{7.8f}$$

$$\begin{aligned} \delta^{(2)} m^{\mathbf{Z}}_{H^\pm} = m^2_{H^\pm} &\left[\delta^{(2)} Z_{H^\pm H^\pm} + \tfrac{1}{4} \left(\delta^{(1)} Z_{H^\pm H^\pm}\right)^2\right] + \delta^{(1)} Z_{H^\pm H^\pm}\, \delta^{(1)} m^2_{H^\pm} \\ &+ \tfrac{1}{2}\, \delta^{(1)} Z_{H^- G^+} \left(\delta^{(1)} m^2_{H^- G^+} + \delta^{(1)} m^2_{G^- H^+}\right) + \delta^{(2)} m^2_{H^\pm} \ . \end{aligned} \tag{7.8g}$$

Therein the field-renormalization constants are those from Eqs. (6.52) and Eqs. (6.73) for the one-loop and two-loop case, respectively. Furthermore, genuine two-loop mass counterterms appear: for the general case they are listed in Appendix C. Applying the approximations of Section 7.2 and their consequences on the lowest-order relations as shown in Section 7.3 yields the expressions

$$\begin{aligned} \delta^{(2)} m^2_h = &\ m^2_{H^\pm}\, c^4_\beta \left(\delta^{(1)} t_\beta\right)^2 - \frac{e}{2\, M_W\, s_\mathrm{w}}\, c^2_\beta\, \delta^{(1)} t_\beta\, \delta^{(1)} T_H \\ &- \frac{e}{2\, M_W\, s_\mathrm{w}} \left[\delta^{(2)} T_h + \delta^{(1)} T_h\, \delta^{(1)} Z_\mathrm{w}\right] \ , \end{aligned} \tag{7.9a}$$

$$\delta^{(2)} m^2_H = \delta^{(2)} m^2_{H^\pm} \ , \tag{7.9b}$$

$$\delta^{(2)} m^2_A = \delta^{(2)} m^2_{H^\pm} \ , \tag{7.9c}$$

$$\begin{aligned} \delta^{(2)} m^2_{hH} = &\ m^2_{H^\pm}\, c^2_\beta\, \delta^{(2)} t_\beta + c^2_\beta\, \delta^{(1)} m^2_{H^\pm}\, \delta^{(1)} t_\beta - m^2_{H^\pm}\, c^3_\beta\, s_\beta \left(\delta^{(1)} t_\beta\right)^2 \\ &- \frac{e}{2\, M_W\, s_\mathrm{w}} \left[\delta^{(2)} T_H + \delta^{(1)} T_H\, \delta^{(1)} Z_\mathrm{w}\right] \ , \end{aligned} \tag{7.9d}$$

$$\delta^{(2)} m^2_{hA} = -\frac{e}{2\, M_W\, s_\mathrm{w}} \left[\delta^{(2)} T_A + \delta^{(1)} T_A\, \delta^{(1)} Z_\mathrm{w}\right] \ , \tag{7.9e}$$

$$\delta^{(2)} m^2_{HA} = 0 \ , \tag{7.9f}$$

$$\delta^{(1)} Z_\mathrm{w} = \frac{\delta^{(1)} e}{e} - \frac{\delta^{(1)} M_W}{M_W} - \frac{\delta^{(1)} s_\mathrm{w}}{s_\mathrm{w}} \ . \tag{7.9g}$$

The use of $\delta^{(1)} Z_\mathrm{w}$ underlines that $\delta^{(1)} e$, $\delta^{(1)} M_W$ and $\delta^{(1)} s_\mathrm{w}$ are always occuring together in this combination. However in the gauge-less limit $\delta^{(1)} e$ is equal to zero.

In Eqs. (7.8) also several genuine one-loop mass counterterms are needed and applying the simplifications to the general expressions in Eqs. (6.65) yields

$$\delta^{(1)} m^2_h = -\frac{e}{2\, s_\mathrm{w}\, M_W}\, \delta^{(1)} T_h \ , \tag{7.10a}$$

$$\delta^{(1)} m^2_H = \delta^{(1)} m^2_{H^\pm} \ , \tag{7.10b}$$

$$\delta^{(1)} m^2_A = \delta^{(1)} m^2_{H^\pm} \ , \tag{7.10c}$$

$$\delta^{(1)} m^2_{hH} = -\frac{e}{2\, s_\mathrm{w}\, M_W}\, \delta^{(1)} T_H + m^2_{H^\pm}\, c^2_\beta\, \delta^{(1)} t_\beta \ , \tag{7.10d}$$

$$\delta^{(1)} m^2_{hA} = -\frac{e}{2\, s_\mathrm{w}\, M_W}\, \delta^{(1)} T_A \ , \tag{7.10e}$$

$$\delta^{(1)} m^2_{hG} = 0 \ , \tag{7.10f}$$

$$\delta^{(1)} m^2_{HA} = 0 \ , \tag{7.10g}$$

$$\delta^{(1)} m^2_{HG} = \delta^{(1)} m^2_{hA} \ , \tag{7.10h}$$

$$\delta^{(1)} m^2_{H^-G^+} = \frac{e}{2\, s_\mathrm{w}\, M_W} \Big[\delta^{(1)} T_H - \boldsymbol{i}\, \delta^{(1)} T_A\Big] - m^2_{H^\pm}\, c^2_\beta\, \delta^{(1)} t_\beta \ , \tag{7.10i}$$

$$\delta^{(1)} m^2_{G^-H^+} = \Big(\delta^{(1)} m^2_{H^-G^+}\Big)^* \ . \tag{7.10j}$$

7.4.2. Renormalization conditions

The independent renormalization constants are fixed similarly as described in Section 6.7 and Section 6.8. Differences are emphasized in the following while redundant conditions are written again for completeness but in short form:

- The tadpole renormalization constants $\delta^{(k)} T_i$, $k \in \{1, 2\}$ are fixed by requiring the minimum of the Higgs potential not shifted, i. e.[10]

$$\Upsilon^{(1)}_i + \delta^{(1)} T_i = 0 \ , \quad \Upsilon^{(2)}_i + \delta^{(2)} T^{\mathbf{Z}}_i = 0 \ , \quad i \in \{h,\, H,\, A\} \ . \tag{7.11}$$

  The $\delta^{(2)} T^{\mathbf{Z}}_i$ are listed in Eqs. (7.7). The two-loop diagrams contributing to $\Upsilon^{(2)}_i$ are displayed in Fig. 7.2 and written down in Appendix D.3 and Appendix D.5.

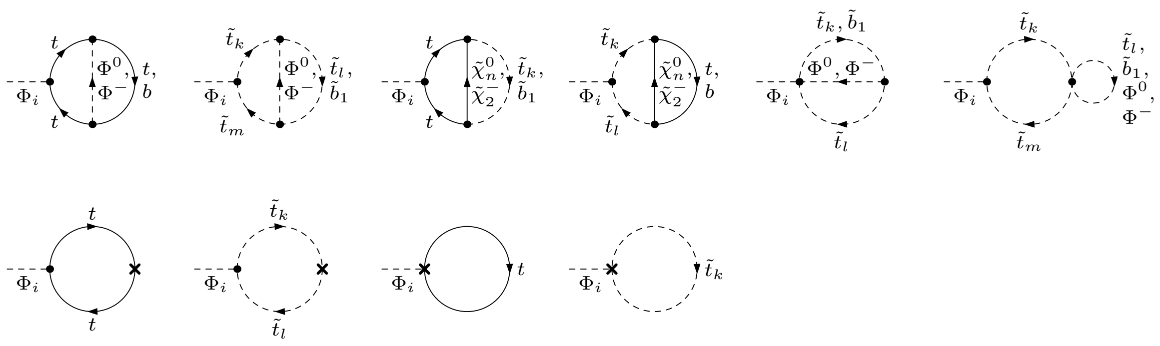

Figure 7.2.: Full list of two-loop tadpole diagrams contributing to $\Upsilon^{(2)}_i$. The crosses denote one-loop counterterm insertions. $\Phi_i = h,\, H,\, A$; $\Phi^0 = h,\, H,\, A,\, G$; $\Phi^- = H^-,\, G^-$.

[10] The counterterms $\delta^{(k)} T_G$ are not independent and do not need separate renormalization conditions

- (i) The charged Higgs-boson mass $m_{H^\pm}$ is the only independent mass parameter of the Higgs sector with complex parameters and thus used as an input quantity.

  Accordingly, the corresponding mass counterterms are fixed by independent renormalization conditions, chosen as on-shell conditions, which in the $p^2 = 0$ approximation are given by

$$\mathfrak{Re}\Big[\hat{\Sigma}^{(k)}_{H^\pm}(0)\Big] = 0 \quad \Rightarrow \quad \delta^{(k)} m^{\mathbf{Z}}_{H^\pm} = \mathfrak{Re}\Big[\Sigma^{(k)}_{H^\pm}(0)\Big] \ , \quad k \in \{1, 2\} \ . \tag{7.12}$$

  Imposing this conditions on the general one-loop result in Eq. (6.59k) and the two-loop result in Eq. (7.8g) yields

$$\delta^{(1)} m^2_{H^\pm} = \mathfrak{Re}\Big[\Sigma^{(1)}_{H^\pm}(0)\Big] - m^2_{H^\pm}\delta^{(1)} Z_{H^\pm H^\pm} \ , \tag{7.13a}$$

$$\begin{aligned}\delta^{(2)} m^2_{H^\pm} = \mathfrak{Re}\Big[\Sigma^{(2)}_{H^\pm}(0)\Big] &- m^2_{H^\pm}\left[\delta^{(2)} Z_{H^\pm H^\pm} + \tfrac{1}{4}\left(\delta^{(1)} Z_{H^\pm H^\pm}\right)^2\right] \\ &- \tfrac{1}{2}\delta^{(1)} Z_{H^- G^+}\left(\delta^{(1)} m^2_{H^- G^+} + \delta^{(1)} m^2_{G^- H^+}\right) \\ &- \delta^{(1)} Z_{H^\pm H^\pm}\, \delta^{(1)} m^2_{H^\pm} \ .\end{aligned} \tag{7.13b}$$

  The other required one-loop counterterms are given in Eqs. (7.10) and the field-renormalization constants are listed in Eqs. (6.52).

  The analytical result for the $\mathcal{O}(\alpha_t^2)$ contributions to the charged Higgs-boson self-energy can be found in Appendix D.2 and Appendix D.4. The contributing Feynman diagrams to the two-loop self-energy are depicted in Fig. 7.3.

  (ii) For the comparison of the $\mathcal{O}(\alpha_t^2)$ corrections with the existing result for real parameters the charged Higgs-boson mass is replaced by the A-boson mass as the independent mass parameter of the Higgs sector and thus taken as input quantity.

  Hence, the mass counterterms are fixed by independent renormalization conditions, chosen as on-shell conditions. In the $p^2 = 0$ approximation they yield

$$\mathfrak{Re}\Big[\hat{\Sigma}^{(k)}_{A}(0)\Big] = 0 \quad \Rightarrow \quad \delta^{(k)} m^{\mathbf{Z}}_{A} = \mathfrak{Re}\Big[\Sigma^{(k)}_{A}(0)\Big] \ , \quad k \in \{1, 2\} \ . \tag{7.14}$$

The corresponding counterterms for the A-boson self-energies are given by Eq. (7.8c) at the two-loop level and by Eq. (6.59c) with $p^2 = 0$ at the one-loop level. The genuine mass counterterms therein arise from the renormalization conditions of Eqs. (7.14) for the one-loop and two-loop cases, respectively:

$$\delta^{(1)} m_A^2 = \Re\mathfrak{e}\Big[\Sigma_A^{(1)}(0)\Big] - m_A^2 \delta^{(1)} Z_{AA} \,, \tag{7.15a}$$

$$\begin{aligned}\delta^{(2)} m_A = \Re\mathfrak{e}\Big[\Sigma_A^{(2)}(0)\Big] &- m_A^2 \left[\delta^{(2)} Z_{AA} + \tfrac{1}{4}\left(\delta^{(1)} Z_{AA}\right)^2\right] \\ &- \delta^{(1)} Z_{AA} \delta^{(1)} m_A^2 - \delta^{(1)} Z_{AG} \delta^{(1)} m_{AG}^2 \,.\end{aligned} \tag{7.15b}$$

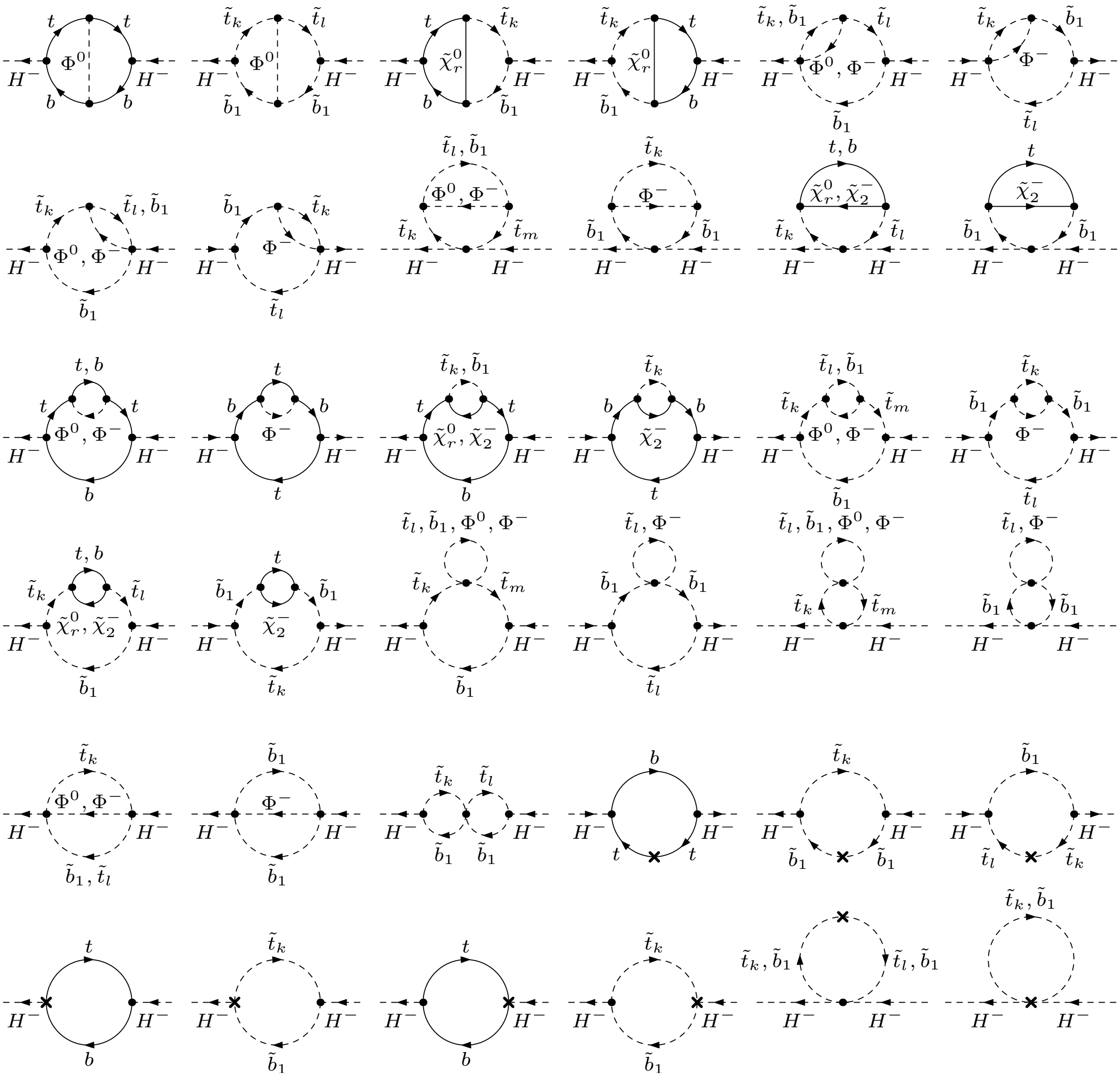

Figure 7.3.: Full list of two-loop self-energy diagrams for the charged Higgs bosons. The crosses denote one-loop counterterm insertions. $\Phi^0 = h,\, H,\, A,\, G$; $\Phi^- = H^-,\, G^-$.

For a quick permutation between $m_{H^\pm}$ and m_A being an input parameter as well as the appropriate corresponding renormalization scheme, a switch is introduced into the evaluation of the self-energies and counterterms. The implementation in `Mathematica` is carried out by the commands given in Tab. 7.3: the first two lines define the two-loop mass counterterms for the charged and CP-odd Higgs bosons, respectively. The symbols `dMHpsq2` and `dMA0sq2` are the two-loop renormalization constants which are defined in lines three and four with the switch `$MA0Input` set to its proper value. The expressions `dMCHiggsZ2[5, 5]` and `dMNHiggsZ2[3, 3]` contain all parts of Eq. (7.13b) and Eq. (7.15b) with field-renormalization constants. Lines five and six are the definitions for the one-loop counterterms evaluated by `FormCalc`.

Table 7.3.: Implementation of a switch for the chosen input parameter being m_A or $m_{H^\pm}$ and applying the corresponding renormalization condition.

```
dMCHiggs2[5, 5] := $MA0Input dMA0sq2 + (1 - $MA0Input) dMHpsq2;
dMNHiggs2[3, 3] := $MA0Input dMA0sq2 + (1 - $MA0Input) dMHpsq2;
dMHpsq2 := SEHp2 - dMCHiggsZ2[5, 5] /. $MA0Input -> 0;
dMA0sq2 := SEA02 - dMNHiggsZ2[3, 3] /. $MA0Input -> 1;

RenConst[dMCHiggs1[5, 5]] :=
  $MA0Input (ReTilde[SelfEnergy[S[3] -> S[3], 0]]
             - MA0^2 dZNHiggs1[3, 3])
  + (1 - $MA0Input) (ReTilde[SelfEnergy[S[5] -> S[5], 0]]
                     - MHp^2 dZCHiggs1[5, 5]);
RenConst[dMNHiggs1[3, 3]] :=
  $MA0Input (ReTilde[SelfEnergy[S[3] -> S[3], 0]]
             - MA0^2 dZNHiggs1[3, 3])
  + (1 - $MA0Input) (ReTilde[SelfEnergy[S[5] -> S[5], 0]]
                     - MHp^2 dZCHiggs1[5, 5]);
```

- The independent field-renormalization constants are fixed in the $\overline{\mathrm{DR}}$ scheme at the one-loop and the two-loop order as explained by Eqs. (6.53) and Eqs. (6.74), respectively. The relations to the field-renormalization constants in the lowest-order mass-eigenstate basis are identically equal to Eqs. (6.52) and Eqs. (6.73).

  However for the present simplifications the result $\delta^{(1)}Z_{\mathcal{H}_1} = 0$ is obtained. This arises from the fact that only the p^2-dependent divergences of $\Sigma^{(1)}_{\phi_1}$ contribute to $\delta^{(1)}Z_{\mathcal{H}_1}$. The occurrence of these divergences requires the propagation of non-scalar particles in $\Sigma^{(1)}_{\phi_1}$. The only available one which couples to ϕ_1 is the bottom quark whose mass is set to zero, thus canceling all contributions to $\delta^{(1)}Z_{\mathcal{H}_1}$.

- t_β is renormalized in the $\overline{\mathrm{DR}}$ scheme at the one-loop and two-loop order. Within the top-Yukawa approximation the divergences originating from parameter renormalization of the vacuum expectation values cancel, i. e.

$$\left.\frac{\delta^{(k)}v_1}{v_1}\right|_{\mathrm{div}} = \left.\frac{\delta^{(k)}v_2}{v_2}\right|_{\mathrm{div}} , \quad k \in \{1,\, 2\} \,. \tag{7.16}$$

By imposing the renormalization condition

$$\frac{\delta^{(1)}v_1}{v_1} = \frac{\delta^{(1)}v_2}{v_2} \tag{7.17}$$

the remaining parts of Eq. (6.70b) and Eq. (6.85) simplify to

$$\frac{\delta^{(1)}t_\beta}{t_\beta} = \frac{1}{2}\delta^{(1)}Z_{\mathcal{H}_2} \,, \tag{7.18a}$$

$$\frac{\delta^{(2)}t_\beta}{t_\beta} = \frac{1}{2}\left[\delta^{(2)}Z_{\mathcal{H}_2} - \delta^{(2)}Z_{\mathcal{H}_1} - \frac{1}{4}\left(\delta^{(1)}Z_{\mathcal{H}_2}\right)^2\right] \,. \tag{7.18b}$$

On the other hand, the results in terms of beta functions which are presented by Eq. (6.71) and Eq. (6.86) can be utilized. Applying the approximations to both expressions yields

$$\frac{\beta^{(1)}(t_\beta)}{t_\beta} = -\frac{3h_t^2}{(4\pi)^2} \,, \tag{7.19a}$$

$$\frac{\beta^{(2)}(t_\beta)}{t_\beta} = \frac{9h_t^4}{(4\pi)^4} = \left(\frac{\beta^{(1)}(t_\beta)}{t_\beta}\right)^2 \,. \tag{7.19b}$$

As can be derived from the anomalous dimensions of $\mathcal{H}_1$ and $\mathcal{H}_2$ at the two-loop order, given in Ref. [SSV14], the pure top-Yukawa-coupling term of Eq. (7.19b) solely stems from $\gamma_2^{(2)}$, whereas $\gamma_1^{(2)}$ is equal to zero (analogously at the one-loop order). Thus, by the use of Eq. (6.88b) the result $\delta^{(2)}Z_{\mathcal{H}_1} = 0$ for the two-loop field-renormalization constant is found.

For the evaluation of $\delta^{(2)}Z_{\mathcal{H}_2}$ by Eq. (6.88b) the one-loop beta function for the only appearing coupling, the top-Yukawa-coupling, is necessary. The result is taken from Ref. [CPR94]:

$$\frac{\beta(h_t)}{h_t} = \frac{1}{(4\pi)^2}\left[-\tfrac{13}{15}\tfrac{5}{3}g_Y^2 - 3g_{\mathrm{w}}^2 - \tfrac{16}{3}g_{\mathrm{s}}^2 + 3h_t^2 + h_b^2 + 3\left(h_u^2 + h_c^2 + h_t^2\right)\right] \,. \tag{7.20}$$

Thus, in the top-Yukawa approximation the second term on the right-hand side of Eq. (6.88b) yields

$$\frac{1}{4}\,\beta(h_t)\,\partial_{h_t}\,\delta^{(1)}Z_{\mathcal{H}_2}\,\frac{1}{\epsilon} = -\frac{9h_t^4}{(4\pi)^4}\,\frac{1}{\epsilon^2} = -\left(\frac{\beta^{(1)}(t_\beta)}{t_\beta}\right)^2\frac{1}{\epsilon^2} \tag{7.21}$$

Hence, using the relations of Eq. (6.87) and Eqs. (6.88) in Eqs. (7.18) and inserting the results of $\delta^{(2)}Z_{\mathcal{H}_2}$ and $\delta^{(2)}Z_{\mathcal{H}_1}$ yields the following connections between the renormalization constants and beta functions for t_β:

$$\frac{\delta^{(1)}t_\beta}{t_\beta} = \frac{1}{2}\delta^{(1)}Z_{\mathcal{H}_2} = \frac{\beta^{(1)}(t_\beta)}{2t_\beta}\frac{1}{\epsilon}\ , \tag{7.22}$$

$$\begin{aligned}\frac{\delta^{(2)}t_\beta}{t_\beta} &= \frac{1}{2}\left[\frac{\beta^{(2)}(t_\beta)}{2t_\beta}\frac{1}{\epsilon} + \frac{1}{4}\,\beta(h_t)\,\partial_{h_t}\delta^{(1)}Z_{\mathcal{H}_2}\,\frac{1}{\epsilon} + \frac{1}{2}\left(\delta^{(1)}Z_{\mathcal{H}_2}\right)^2 - \frac{1}{4}\left(\delta^{(1)}Z_{\mathcal{H}_2}\right)^2\right]\\ &= \frac{1}{2}\left[2\left(\frac{\beta^{(1)}(t_\beta)}{2t_\beta}\right)^2\frac{1}{\epsilon} - 4\left(\frac{\beta^{(1)}(t_\beta)}{2t_\beta}\right)^2\frac{1}{\epsilon^2} + \left(\frac{\beta^{(1)}(t_\beta)}{2t_\beta}\right)^2\frac{1}{\epsilon^2}\right]\\ &= \left(\frac{\beta^{(1)}(t_\beta)}{2t_\beta}\right)^2\left(\frac{1}{\epsilon} - \frac{3}{2}\frac{1}{\epsilon^2}\right)\ .\end{aligned} \tag{7.23}$$

Applying these results to Eq. (7.18b) and using $\delta^{(2)}Z_{\mathcal{H}_1} = 0$ allows to derive the following result:

$$\delta^{(2)}Z_{\mathcal{H}_2} = 2\left(\frac{\beta^{(1)}(t_\beta)}{2t_\beta}\right)^2\left(\frac{1}{\epsilon} - \frac{1}{\epsilon^2}\right)\ . \tag{7.24}$$

The explicit formulas for $\delta^{(2)}t_\beta$ and $\delta^{(2)}Z_{\mathcal{H}_2}$ are just given for completeness; in the final result of the renormalized self-energies they cancel.

- In the on-shell scheme, also the counterterms $\delta^{(1)}M_W^2/M_W^2$ and $\delta^{(1)}M_Z^2/M_Z^2$ are required for renormalizing the top-Yukawa coupling

$$h_t = \frac{m_t}{v_2} = \frac{e\,m_t}{\sqrt{2}\,s_\beta\,s_\mathrm{w}\,M_W}\ . \tag{7.25}$$

Although in the gauge-less limit, the ratios $\delta^{(1)}M_W^2/M_W^2$ and $\delta^{(1)}M_Z^2/M_Z^2$ have remaining finite and divergent contributions arising from the Yukawa couplings, which have to be included as one-loop quantities $\sim h_t^2$. They are evaluated from the W- and Z-boson self-energies whose corresponding Feynman graphs are depicted in Fig. 7.4.

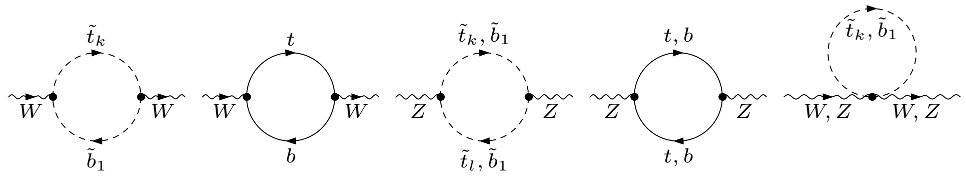

Figure 7.4.: Feynman diagrams for the renormalization constants $\delta^{(1)}M_W \Big/ M_W$ and $\delta^{(1)}M_Z \Big/ M_Z$ of the gauge-boson sector.

The on-shell renormalization conditions in the gauge-less limit are given by[11]

$$\left.\frac{\hat{\Sigma}^{(1)}_{WW}(p^2)}{M_W^2}\right|_{p^2=0} = 0 \;, \quad \frac{\hat{\Sigma}^{(1)}_{WW}(0)}{M_W^2} = \frac{\Sigma^{(1)}_{WW}(0)}{M_W^2} - \frac{\delta^{(1)}M_W^2}{M_W^2} \;, \tag{7.26a}$$

$$\left.\frac{\hat{\Sigma}^{(1)}_{ZZ}(p^2)}{M_Z^2}\right|_{p^2=0} = 0 \;, \quad \frac{\hat{\Sigma}^{(1)}_{ZZ}(0)}{M_Z^2} = \frac{\Sigma^{(1)}_{ZZ}(0)}{M_Z^2} - \frac{\delta^{(1)}M_Z^2}{M_Z^2} \;, \tag{7.26b}$$

resulting in

$$\frac{\delta^{(1)}M_W^2}{M_W^2} = \frac{\Sigma^{(1)}_{WW}(0)}{M_W^2} \;, \quad \frac{\delta^{(1)}M_Z^2}{M_Z^2} = \frac{\Sigma^{(1)}_{ZZ}(0)}{M_Z^2} \;. \tag{7.27}$$

In this scheme $\delta^{(1)}s_\mathrm{w}^2$ is determined by

$$\delta^{(1)}s_\mathrm{w}^2 = c_\mathrm{w}^2 \left(\frac{\delta^{(1)}M_Z^2}{M_Z^2} - \frac{\delta^{(1)}M_W^2}{M_W^2} \right) \;. \tag{7.28}$$

In the top-Yukawa approximation $\delta^{(1)}s_\mathrm{w}^2$ is finite.

7.4.3. Parametrization

The appearance of δs_w^2 in the $\mathcal{O}(\alpha_t^2)$ terms, as specified above, is a consequence of the on-shell scheme where the top-Yukawa coupling $h_t = m_t/v_2 = m_t/(v\, s_\beta)$ is expressed in terms of

$$\frac{1}{v} = \frac{g_\mathrm{w}}{\sqrt{2}\, M_W} = \frac{e}{\sqrt{2}\, s_\mathrm{w}\, M_W}. \tag{7.29}$$

Accordingly, the one-loop self-energies have to be parametrized in terms of this representation for h_t when added to the two-loop self-energies in Eq. (7.6).

[11] The field-renormalization constants $\delta^{(1)}Z_{WW}$ and $\delta^{(1)}Z_{ZZ}$ that occur in Eqs. (6.66) do not contribute in the gauge-less limit.

On the other hand, if the Fermi constant G_F is used for parametrization of the one-loop self-energies, as performed by `FeynHiggs`, the relation

$$\sqrt{2}\, G_\mathrm{F} = \frac{e^2}{4\, s_\mathrm{w}^2\, M_W^2} \left(1 + \Delta^{(k)} r\right) \tag{7.30}$$

has to be applied, which gets loop contributions also in the gauge-less limit, at the one-loop order given by

$$\Delta^{(1)} r = -\frac{c_\mathrm{w}^2}{s_\mathrm{w}^2} \left(\frac{\delta^{(1)} M_Z^2}{M_Z^2} - \frac{\delta^{(1)} M_W^2}{M_W^2} \right) = -\frac{\delta^{(1)} s_\mathrm{w}^2}{s_\mathrm{w}^2} \ . \tag{7.31}$$

This finite shift in the one-loop self-energies induces two-loop $\mathcal{O}(\alpha_t^2)$ terms and has to be taken into account, effectively canceling all occurrences of $\delta^{(1)} s_\mathrm{w}^2$.

7.5. Neutralino and chargino sectors

The $\mathcal{O}(\alpha_t^2)$ contributions to the Higgs-boson self-energies involve Feynman diagrams with internal charginos and neutralinos.

7.5.1. Tree-level relations

The mass matrices given in Eq. (3.16) and Eq. (3.14), respectively, are simplified to

$$\mathbf{Y} = \begin{pmatrix} \begin{matrix} M_1 & 0 \\ 0 & M_2 \end{matrix} & \mathbf{0} \\ \mathbf{0} & \begin{matrix} 0 & -\mu \\ -\mu & 0 \end{matrix} \end{pmatrix}, \quad \mathbf{X} = \begin{pmatrix} M_2 & 0 \\ 0 & \mu \end{pmatrix}, \tag{7.32}$$

according to our approximations explained in Section 7.2. Although $\mathbf{X}$ is already diagonal, the singular-value decomposition $\mathbf{U}^* \mathbf{X} \mathbf{V}^\dagger$ with the unitary matrices $\mathbf{U}$ and $\mathbf{V}$ is performed to gain positive real chargino masses. The choice

$$\mathbf{U} = \begin{pmatrix} e^{i\,\phi_{M_2}} & 0 \\ 0 & e^{i\,\phi_\mu} \end{pmatrix}, \quad \mathbf{V} = \mathbf{1} \ , \tag{7.33}$$

with the complex phases ϕ_{M_2} and ϕ_μ of M_2 and μ, respectively, satisfies this requirement.

The deduced singular values (cf. Eq. (3.15a)) are the masses

$$m_{\tilde{\chi}_1^\pm} = |M_2| \ , \quad m_{\tilde{\chi}_2^\pm} = |\mu| \ . \tag{7.34}$$

Similarly, the singular-value decomposition $\mathbf{N}^*\mathbf{Y}\mathbf{N}^\dagger$ with the unitary matrix

$$\mathbf{N} = \begin{pmatrix} \begin{matrix} e^{\frac{i}{2}\phi_{M_1}} & 0 \\ 0 & e^{\frac{i}{2}\phi_{M_2}} \end{matrix} & \mathbf{0} \\ \mathbf{0} & \frac{1}{\sqrt{2}} e^{\frac{i}{2}\phi_\mu} \begin{pmatrix} 1 & -1 \\ i & i \end{pmatrix} \end{pmatrix} \tag{7.35}$$

is performed. Here, the additional complex phase ϕ_{M_1} of M_1 occurs. The singular values are achieved as solutions of Eq. (3.17) in this special case for our approximations. They are the masses

$$m_{\tilde{\chi}_1^0} = |M_1| \ , \quad m_{\tilde{\chi}_2^0} = |M_2| \ , \quad m_{\tilde{\chi}_{3/4}^0} = |\mu| \ . \tag{7.36}$$

As a consequence, the charginos and neutralinos $\tilde{\chi}_1^0$, $\tilde{\chi}_2^0$ and $\tilde{\chi}_1^\pm$ do not contribute to the Higgs-boson self-energies in the top-Yukawa approximation. The remaining charginos and neutralinos $\tilde{\chi}_3^0$, $\tilde{\chi}_4^0$ and $\tilde{\chi}_2^\pm$ are the original higgsinos with degenerate masses equal to $|\mu|$ which is also the only independent parameter of this sector in addition to those of the Higgs sector.

7.5.2. Renormalization

In the $\mathcal{O}(\alpha_t^2)$ contributions, Feynman diagrams with higgsinos appear at the two-loop level for the first time, thus there was no need to renormalize their mass parameter μ. However, μ also occurs as part of the couplings in the squark sector already at the one-loop level, hence its renormalization $\mu \to \mu + \delta^{(1)}\mu$ has to be respected in the calculation of the $\mathcal{O}(\alpha_t^2)$ contributions.

A convenient choice to define μ, M_1 and M_2 at higher orders is given by on-shell conditions for either both charginos and one neutralino, or one chargino and two neutralinos [Cha+12b; BB09; Bha+12]. However, since only $\delta^{(1)}\mu$ is required here, it is sufficient to impose a single renormalization condition, chosen as on-shell condition for the mass of $\tilde{\chi}_2^\pm$:

$$\mathfrak{Re}\left[\hat{\Sigma}^{(1)}_{\tilde{\chi}_2^\pm}(p)\right]_{\not p = |\mu|} = 0 \ , \quad \mathfrak{Re}\left[\hat{\Sigma}^{(1)}_{\tilde{\chi}_2^\pm}(|\mu|)\right] = \mathfrak{Re}\left[\Sigma^{(1)}_{\tilde{\chi}_2^\pm}(|\mu|)\right] - \delta^{(1)}\mu \ . \tag{7.37}$$

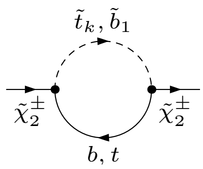

Figure 7.5.: Feynman diagrams for renormalization of the neutralino–chargino sector, i. e. for the renormalization constant $\delta^{(1)}\mu$.

With the Lorentz decomposition

$$\Sigma^{(1)}_{\tilde{\chi}_2^\pm}(p) = \not{p}\left[\tfrac{1-\gamma_5}{2}\Sigma^{(1)\,\mathrm{L}}_{\tilde{\chi}_2^\pm}\left(p^2\right) + \tfrac{1+\gamma_5}{2}\Sigma^{(1)\,\mathrm{R}}_{\tilde{\chi}_2^\pm}\left(p^2\right)\right] + |\mu|\left[\Sigma^{(1)\,\mathrm{S}}_{\tilde{\chi}_2^\pm}\left(p^2\right) + \gamma_5\,\Sigma^{(1)\,\mathrm{PS}}_{\tilde{\chi}_2^\pm}\left(p^2\right)\right] \tag{7.38}$$

of the self-energy for the higgsino-like chargino $\tilde{\chi}_2^\pm$ renormalization of μ is determined as follows:

$$\delta^{(1)}\mu = e^{i\,\phi_\mu}\,\delta^{(1)}|\mu|\;, \tag{7.39a}$$

$$\delta^{(1)}|\mu| = |\mu|\left\{\tfrac{1}{2}\mathfrak{Re}\left[\Sigma^{(1)\,\mathrm{L}}_{\tilde{\chi}_2^\pm}(|\mu|^2) + \Sigma^{(1)\,\mathrm{R}}_{\tilde{\chi}_2^\pm}(|\mu|^2)\right] + \mathfrak{Re}\left[\Sigma^{(1)\,\mathrm{S}}_{\tilde{\chi}_2^\pm}(|\mu|^2)\right]\right\}, \tag{7.39b}$$

The contributing Feynman diagrams are depicted in Fig. 7.5.

Another option is $\overline{\mathrm{DR}}$ renormalization of μ, which defines the counterterm $\delta^{(1)}\mu$ in the $\overline{\mathrm{DR}}$ scheme, i. e. by the divergent part of the expression in Eqs. (7.39). For the numerical analysis and the comparison with the previous result of Ref. [Bri+02] the $\overline{\mathrm{DR}}$ scheme is chosen at the renormalization scale m_t, if not stated otherwise.

7.6. Colored sector

The most important one-loop contributions to the Higgs-boson tadpoles and self-energies are induced by the top and bottom particles and their superpartners stop and sbottom, respectively. The $\mathcal{O}(\alpha_t^2)$ terms are corrections to this class of Feynman diagrams, hence the stop and sbottom sectors appear again and have to be renormalized at the one-loop order.

7.6.1. Tree-level relations

The general mass matrix of the squarks given in Eq. (3.9) is simplified by the approximations of the gauge-less limit and the vanishing bottom mass (cf. Section 7.2).

In the stop mass matrix the gauge contributions are dropped, resulting in

$$\mathbf{M}_{\tilde{t}} = \begin{pmatrix} m_{\tilde{t}_\mathrm{L}}^2 + m_t^2 & m_t\, X_t \\ m_t\, X_t^* & m_{\tilde{q}_\mathrm{R}}^2 + m_q^2 \end{pmatrix}, \tag{7.40a}$$

$$X_t = A_t^* - \frac{\mu}{t_\beta}\;. \tag{7.40b}$$

The application of the unitary transformation

$$\mathbf{U}_{\tilde{t}}\, \mathbf{M}_{\tilde{t}}\, \mathbf{U}_{\tilde{t}}^\dagger = \mathrm{diag}\Big(m_{\tilde{t}_1}^2, m_{\tilde{t}_2}^2\Big) \tag{7.41}$$

yields the stop masses squared as the eigenvalues of Eq. (7.40) in a simplified version of Eq. (3.10):

$$m_{\tilde{t}_{1/2}}^2 = \frac{1}{2}\left[m_{\tilde{t}_\mathrm{L}}^2 + m_{\tilde{t}_\mathrm{R}}^2 + 2m_t^2 \mp \sqrt{\Big(m_{\tilde{t}_\mathrm{L}}^2 - m_{\tilde{t}_\mathrm{R}}^2\Big)^2 + 4m_t^2|X_t|^2}\,\right]\;. \tag{7.42}$$

Since A_t and μ are complex parameters in general, the unitary matrix $\mathbf{U}_{\tilde{t}}$ consists of one mixing angle $\theta_{\tilde{t}}$ and one phase $\varphi_{\tilde{t}}$:

$$\mathbf{U}_{\tilde{t}} = \begin{pmatrix} \mathbf{U}_{\tilde{t}\,11} & \mathbf{U}_{\tilde{t}\,12} \\ \mathbf{U}_{\tilde{t}\,21} & \mathbf{U}_{\tilde{t}\,22} \end{pmatrix} = \begin{pmatrix} c_{\theta_{\tilde{t}}} & e^{i\,\varphi_{\tilde{t}}} s_{\theta_{\tilde{t}}} \\ -e^{-i\,\varphi_{\tilde{t}}} s_{\theta_{\tilde{t}}} & c_{\theta_{\tilde{t}}} \end{pmatrix}. \tag{7.43}$$

The sbottom mass matrix becomes diagonal for $m_b \to 0$:

$$\mathbf{M}_{\tilde{b}} = \begin{pmatrix} m_{\tilde{t}_\mathrm{L}}^2 & 0 \\ 0 & m_{\tilde{b}_\mathrm{R}}^2 \end{pmatrix}. \tag{7.44}$$

In the couplings of the used `FeynArts` model file the sbottom mixing matrix is set to

$$\mathbf{U}_{\tilde{b}} = \mathbf{1}\;. \tag{7.45}$$

The invariance under $SU(2)_\mathrm{L}$ transformations imposes the condition $m_{\tilde{b}_\mathrm{L}}^2 = m_{\tilde{t}_\mathrm{L}}^2$ in Eq. (7.44). Thus, just one additional independent parameter is introduced by the sbottom sector: $m_{\tilde{b}_\mathrm{R}}$. However, all couplings of $\tilde{b}_\mathrm{R}$ are proportional to m_b or m_b^2 which are equal to zero within our approximations. Hence $\tilde{b}_\mathrm{R}$ does not appear and $m_{\tilde{b}_\mathrm{R}}$ is not needed. Only one sbottom particle $\tilde{b}_1 \equiv \tilde{b}_\mathrm{L}$ remains in the Feynman diagrams and its properties are completely determined by the stop-sector entries.

7.6.2. Renormalization

Five independent parameters relevant for our calculation are introduced by the quark–squark sector: the top mass m_t, the real soft SUSY-breaking parameters $m_{\tilde{t}_\mathrm{L}} \equiv m_{\tilde{q}_3}$ and $m_{\tilde{t}_\mathrm{R}}$, and the complex soft-breaking mixing parameter $A_t = |A_t| e^{i\phi_{A_t}}$.

These parameters have to be renormalized at the one-loop level according to

$$m_t \to m_t + \delta^{(1)} m_t \ , \tag{7.46a}$$
$$m^2_{\tilde{t}_\mathrm{L/R}} \to m^2_{\tilde{t}_\mathrm{L/R}} + \delta^{(1)} m^2_{\tilde{t}_\mathrm{L/R}} \ , \tag{7.46b}$$
$$A_t \to A_t + \delta^{(1)} A_t \ . \tag{7.46c}$$

Thus, the stop mass matrix in Eq. (7.40) is renormalized by

$$\mathbf{M}_{\tilde{t}} \to \mathbf{M}_{\tilde{t}} + \delta^{(1)} \mathbf{M}_{\tilde{t}} \tag{7.47}$$

with the counterterm of the stop mass matrix given by

$$\delta^{(1)} \mathbf{M}_{\tilde{t}} = \begin{pmatrix} \delta^{(1)} m^2_{\tilde{t}_\mathrm{L}} + 2\, m_t\, \delta^{(1)} m_t & X_t\, \delta^{(1)} m_t + m_t\, \delta^{(1)} X_t \\ X_t^*\, \delta^{(1)} m_t + m_t\, \delta^{(1)} X_t^* & \delta^{(1)} m^2_{\tilde{t}_\mathrm{R}} + 2\, m_t\, \delta^{(1)} m_t \end{pmatrix} , \tag{7.48a}$$
$$\delta^{(1)} X_t = \delta^{(1)} A_t^* - \frac{\delta^{(1)} \mu}{t_\beta} + \frac{\mu}{t_\beta} \frac{\delta^{(1)} t_\beta}{t_\beta} \ . \tag{7.48b}$$

The other free parameter μ is related to the higgsino sector and its renormalization constant is already determined in Section 7.5.

The independent renormalization conditions for the colored sector are formulated as on-shell conditions in the following way:

- The mass of the top quark is defined on-shell, i. e.[12]

  $$\widetilde{\mathfrak{Re}} \Big[\hat{\Sigma}^{(1)}_t(p) \Big]_{\not{p}\, =\, m_t} = 0 \ , \quad \widetilde{\mathfrak{Re}} \Big[\hat{\Sigma}^{(1)}_t(m_t) \Big] = \widetilde{\mathfrak{Re}} \Big[\Sigma^{(1)}_t(m_t) \Big] - \delta^{(1)} m_t \ , \tag{7.49a}$$
  $$\delta^{(1)} m_t = m_t\, \widetilde{\mathfrak{Re}} \Big[\tfrac{1}{2} \Big(\Sigma^{(1)\,\mathrm{L}}_t\big(m_t^2\big) + \Sigma^{(1)\,\mathrm{R}}_t\big(m_t^2\big) \Big) + \Sigma^{(1)\,\mathrm{S}}_t\big(m_t^2\big) \Big] \ , \tag{7.49b}$$

  according to the Lorentz decomposition (analogously to Eq. (7.38)) of the self-energy of the top quark whose contributions are depicted in Fig. 7.6.

[12] $\widetilde{\mathfrak{Re}}$ denotes the real part of all loop integrals, but leaves the couplings unaffected.

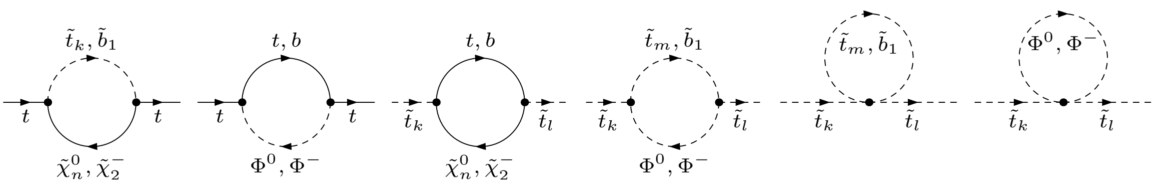

Figure 7.6.: Feynman diagrams for renormalization of the quark–squark sector. $\Phi^0 = h$, H, A, G; $\Phi^- = H^-$, G^-.

- $m^2_{\tilde{t}_\mathrm{L}}$ and $m^2_{\tilde{t}_\mathrm{R}}$ are traded for $m^2_{\tilde{t}_1}$ and $m^2_{\tilde{t}_2}$, which are then fixed by on-shell conditions for the top-squarks,

$$\tilde{\mathfrak{Re}}\Big[\hat{\Sigma}^{(1)}_{\tilde{t}_i\tilde{t}_i}\big(p^2\big)\Big]_{p^2\,=\,m^2_{\tilde{t}_i}} = 0\ , \quad \tilde{\mathfrak{Re}}\Big[\hat{\Sigma}^{(1)}_{\tilde{t}_i\tilde{t}_i}\big(m^2_{\tilde{t}_i}\big)\Big] = \tilde{\mathfrak{Re}}\Big[\Sigma^{(1)}_{\tilde{t}_i\tilde{t}_i}\big(m^2_{\tilde{t}_i}\big)\Big] - \delta^{(1)}m^2_{\tilde{t}_i\tilde{t}_i}\ , \tag{7.50a}$$

$$\delta^{(1)}m^2_{\tilde{t}_i\tilde{t}_i} = \tilde{\mathfrak{Re}}\Big[\Sigma^{(1)}_{\tilde{t}_i\tilde{t}_i}\big(m^2_{\tilde{t}_i}\big)\Big]\ , \quad i \in \{1,\, 2\}\ , \tag{7.50b}$$

involving the diagonal $\tilde{t}_1$ and $\tilde{t}_2$ self-energies (diagrammatically visualized in Fig. 7.6). The off-diagonal entry of the top-squark self-energy matrix is used to impose the renormalization condition

$$\tilde{\mathfrak{Re}}\Big[\hat{\Sigma}^{(1)}_{\tilde{t}_1\tilde{t}_2}\big(p^2\big)\Big]_{p^2\,=\,m^2_{\tilde{t}_1}} + \tilde{\mathfrak{Re}}\Big[\hat{\Sigma}^{(1)}_{\tilde{t}_1\tilde{t}_2}\big(p^2\big)\Big]_{p^2\,=\,m^2_{\tilde{t}_2}} = 0\ , \tag{7.51a}$$

$$\tilde{\mathfrak{Re}}\Big[\hat{\Sigma}^{(1)}_{\tilde{t}_1\tilde{t}_2}\big(p^2\big)\Big] = \tilde{\mathfrak{Re}}\Big[\Sigma^{(1)}_{\tilde{t}_1\tilde{t}_2}\big(p^2\big)\Big] - \delta^{(1)}m^2_{\tilde{t}_1\tilde{t}_2}\ , \tag{7.51b}$$

as in Ref. [Hei+07]. Its evaluation determines the off-diagonal counterterm for the stop masses according to

$$\delta^{(1)}m^2_{\tilde{t}_1\tilde{t}_2} = \frac{1}{2}\,\tilde{\mathfrak{Re}}\Big[\Sigma^{(1)}_{\tilde{t}_1\tilde{t}_2}\big(m^2_{\tilde{t}_1}\big) + \Sigma^{(1)}_{\tilde{t}_1\tilde{t}_2}\big(m^2_{\tilde{t}_2}\big)\Big]\ . \tag{7.52}$$

These on-shell conditions determine the counterterm matrix

$$\mathbf{U}_{\tilde{t}}\,\delta^{(1)}\mathbf{M}_{\tilde{t}}\,\mathbf{U}^\dagger_{\tilde{t}} = \begin{pmatrix} \delta^{(1)}m^2_{\tilde{t}_1\tilde{t}_1} & \delta^{(1)}m^2_{\tilde{t}_1\tilde{t}_2} \\ \delta^{(1)}m^{2\,*}_{\tilde{t}_1\tilde{t}_2} & \delta^{(1)}m^2_{\tilde{t}_2\tilde{t}_2} \end{pmatrix}. \tag{7.53}$$

Inverting Eq. (7.53) and using Eqs. (7.48) yields

$$\begin{aligned} \delta^{(1)}m^2_{\tilde{q}_3} \equiv \delta^{(1)}m^2_{\tilde{t}_\mathrm{L}} = {} & |\mathbf{U}_{\tilde{t}\,11}|^2\,\delta^{(1)}m^2_{\tilde{t}_1\tilde{t}_1} + |\mathbf{U}_{\tilde{t}\,21}|^2\,\delta^{(1)}m^2_{\tilde{t}_2\tilde{t}_2} \\ & + 2\,\mathfrak{Re}\Big[\mathbf{U}_{\tilde{t}\,21}\,\mathbf{U}^*_{\tilde{t}\,11}\,\delta^{(1)}m^2_{\tilde{t}_1\tilde{t}_2}\Big] - 2\,m_t\,\delta^{(1)}m_t\ , \end{aligned} \tag{7.54a}$$

$$\begin{aligned}\delta^{(1)} m^2_{\tilde{t}_\mathrm{R}} &= |\mathbf{U}_{\tilde{t}\,12}|^2\, \delta^{(1)} m^2_{\tilde{t}_1\tilde{t}_1} + |\mathbf{U}_{\tilde{t}\,22}|^2\, \delta^{(1)} m^2_{\tilde{t}_2\tilde{t}_2} \\ &\quad + 2\,\mathfrak{Re}\Big[\mathbf{U}_{\tilde{t}\,22}\, \mathbf{U}^*_{\tilde{t}\,12}\, \delta^{(1)} m^2_{\tilde{t}_1\tilde{t}_2}\Big] - 2\, m_t\, \delta^{(1)} m_t\ .\end{aligned} \tag{7.54b}$$

- The mixing parameter A_t is correlated with the $\tilde{t}$-mass eigenvalues, t_β, and μ, through Eq. (7.41). Exploiting Eq. (7.53), the unitarity of $\mathbf{U}_{\tilde{t}}$ and Eqs. (7.48) yields the expression

$$\begin{aligned}X_t\, \delta^{(1)} m_t + m_t\, \delta^{(1)} X_t &= \mathbf{U}_{\tilde{t}\,22}\, \mathbf{U}^*_{\tilde{t}\,11}\, \delta^{(1)} m^2_{\tilde{t}_1\tilde{t}_2} + \mathbf{U}_{\tilde{t}\,12}\, \mathbf{U}^*_{\tilde{t}\,21} \left(\delta^{(1)} m^2_{\tilde{t}_1\tilde{t}_2}\right)^* \\ &\quad + \mathbf{U}_{\tilde{t}\,12}\, \mathbf{U}^*_{\tilde{t}\,11} \left(\delta^{(1)} m^2_{\tilde{t}_1\tilde{t}_1} - \delta^{(1)} m^2_{\tilde{t}_2\tilde{t}_2}\right)\ .\end{aligned} \tag{7.55}$$

By utilizing the definitions of the top-mass and stop-mass counterterms of Eq. (7.49b), Eq. (7.50b) and Eq. (7.52) the counterterm $\delta^{(1)} X_t$ is determined; further using Eq. (7.48b) fixes $\delta^{(1)} A_t$. Actually this yields two separate conditions, one for the absolute value $|A_t|$ and one for the phase ϕ_{A_t}:

$$\begin{aligned}\delta^{(1)}|A_t| = \ \mathfrak{Re}\bigg\{\frac{e^{i\,\phi_{A_t}}}{m_t}\bigg[&\mathbf{U}_{\tilde{t}\,22}\, \mathbf{U}^*_{\tilde{t}\,11}\, \delta^{(1)} m^2_{\tilde{t}_1\tilde{t}_2} + \mathbf{U}_{\tilde{t}\,12}\, \mathbf{U}^*_{\tilde{t}\,21} \left(\delta^{(1)} m^2_{\tilde{t}_1\tilde{t}_2}\right)^* \\ &+ \mathbf{U}_{\tilde{t}\,12}\, \mathbf{U}^*_{\tilde{t}\,11} \left(\delta^{(1)} m^2_{\tilde{t}_1\tilde{t}_1} - \delta^{(1)} m^2_{\tilde{t}_2\tilde{t}_2}\right) \\ &- X_t\, \delta^{(1)} m_t + \frac{\delta^{(1)}\mu}{t_\beta} - \frac{\mu}{t_\beta}\frac{\delta^{(1)} t_\beta}{t_\beta}\bigg]\bigg\}\ ,\end{aligned} \tag{7.56a}$$

$$\begin{aligned}\delta^{(1)}\phi_{A_t} = -\,\mathfrak{Im}\bigg\{\frac{e^{i\,\phi_{A_t}}}{m_t|A_t|}\bigg[&\mathbf{U}_{\tilde{t}\,22}\, \mathbf{U}^*_{\tilde{t}\,11}\, \delta^{(1)} m^2_{\tilde{t}_1\tilde{t}_2} + \mathbf{U}_{\tilde{t}\,12}\, \mathbf{U}^*_{\tilde{t}\,21} \left(\delta^{(1)} m^2_{\tilde{t}_1\tilde{t}_2}\right)^* \\ &+ \mathbf{U}_{\tilde{t}\,12}\, \mathbf{U}^*_{\tilde{t}\,11} \left(\delta^{(1)} m^2_{\tilde{t}_1\tilde{t}_1} - \delta^{(1)} m^2_{\tilde{t}_2\tilde{t}_2}\right) \\ &- X_t\, \delta^{(1)} m_t + \frac{\delta^{(1)}\mu}{t_\beta} - \frac{\mu}{t_\beta}\frac{\delta^{(1)} t_\beta}{t_\beta}\bigg]\bigg\}\ .\end{aligned} \tag{7.56b}$$

The additionally required mass counterterm $\delta^{(1)}\mu$ has already been obtained in Section 7.5.

- As already mentioned, the relevant sbottom mass is not an independent parameter, but determined by $SU(2)_\mathrm{L}$ invariance. Hence its counterterm introduced by $m^2_{\tilde{b}_\mathrm{L}} \to m^2_{\tilde{b}_\mathrm{L}} + \delta^{(1)} m^2_{\tilde{b}_\mathrm{L}}$ is a derived quantity:

$$\delta^{(1)} m^2_{\tilde{b}_\mathrm{L}} \equiv \delta^{(1)} m^2_{\tilde{q}_3} \tag{7.57}$$

which is already fixed by Eq. (7.54a).

7.7. Couplings and counterterm insertions

Having defined all necessary sectors of the MSSM, the required couplings for the two-loop diagrams including the counterterms for subrenormalization are written down in the following.

7.7.1. Tree-level vertices

The tree-level vertices contain the top-Yukawa coupling $h_t = m_t/v_2$. In the case of the Higgs bosons, their different couplings are accommodated by explicit factors $c\,(\ldots)$. The symbols Φ^0 and $\Phi^\pm$ are used as generic expressions for the Higgs bosons, i. e. $\Phi^0 \in \{h,\, H,\, A,\, G\}$ and $\Phi^\pm \in \{H^\pm,\, G^\pm\}$. For fermion couplings, the left-chiral part is the first and the right-chiral part the second entry of the column. The approximations mentioned in Section 7.2 have already been applied to this expressions, leaving only those parts proportional to h_t or h_t^2. The mixing matrix $\mathbf{U}$ of the charginos does not appear in the following; $\mathbf{V} = \mathbf{1}$ is already inserted.

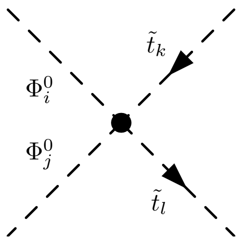

$$
\begin{aligned}
&= -\boldsymbol{i}\; C\Big(\Phi_i^0,\, \Phi_j^0,\, \tilde{t}_k,\, \tilde{t}_l\Big) \\
&= -\boldsymbol{i}\; h_t^2 \Big[c_4\Big(\Phi_i^0,\, \Phi_j^0\Big)\, (\mathbf{U}^*_{\tilde{t}\,k1}\, \mathbf{U}_{\tilde{t}\,l1} + \mathbf{U}^*_{\tilde{t}\,k2}\, \mathbf{U}_{\tilde{t}\,l2})\Big]\ , \\
c_4(h,\, h) &= c_\alpha^2\ , \\
c_4(H,\, H) &= s_\alpha^2\ , \\
c_4(A,\, A) &= c_\beta^2\ , \\
c_4(G,\, G) &= s_\beta^2\ , \\
c_4(h,\, H) &= c_\alpha\, s_\alpha\ , \\
c_4(A,\, G) &= c_\beta\, s_\beta\ .
\end{aligned}
\tag{7.58a}
$$

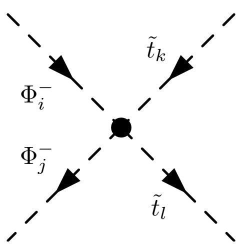

$$
\begin{aligned}
&= -\boldsymbol{i}\; C\Big(\Phi_i^-,\, \Phi_j^+,\, \tilde{t}_k,\, \tilde{t}_l\Big) \\
&= -\boldsymbol{i}\; h_t^2 \Big[c_4^{\tilde{t}}\Big(\Phi_i^-,\, \Phi_j^+\Big)\, \mathbf{U}^*_{\tilde{t}\,k2}\, \mathbf{U}_{\tilde{t}\,l2}\Big]\ , \\
c_4^{\tilde{t}}\Big(H^-,\, H^+\Big) &= c_\beta^2\ , \\
c_4^{\tilde{t}}\Big(G^-,\, G^+\Big) &= s_\beta^2\ , \\
c_4^{\tilde{t}}\Big(H^-,\, G^+\Big) &= c_\beta\, s_\beta\ , \\
c_4^{\tilde{t}}\Big(G^-,\, H^+\Big) &= c_\beta\, s_\beta\ .
\end{aligned}
\tag{7.58b}
$$

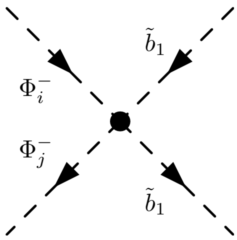

$$
\begin{aligned}
&= -\boldsymbol{i}\; C\Big(\Phi_i^-,\, \Phi_j^+,\, \tilde{b}_1,\, \tilde{b}_1\Big) = -\boldsymbol{i}\; h_t^2\Big[c_4^{\tilde{b}}\Big(\Phi_i^-,\, \Phi_j^+\Big)\Big]\;, \\
&\quad c_4^{\tilde{b}}\Big(H^-,\, H^+\Big) = c_\beta^2\;, \\
&\quad c_4^{\tilde{b}}\Big(G^-,\, G^+\Big) = s_\beta^2\;, \\
&\quad c_4^{\tilde{b}}\Big(H^-,\, G^+\Big) = c_\beta\, s_\beta\;, \\
&\quad c_4^{\tilde{b}}\Big(G^-,\, H^+\Big) = c_\beta\, s_\beta\;.
\end{aligned}
\tag{7.58c}
$$

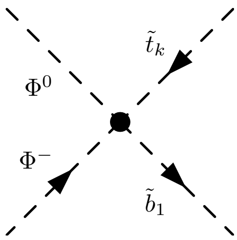

$$
\begin{aligned}
&= -\boldsymbol{i}\; C\Big(\Phi^0,\, \Phi^-,\, \tilde{t}_k,\, \tilde{b}_1\Big) = -\boldsymbol{i}\; C\Big(\Phi^0,\, \Phi^+,\, \tilde{t}_k,\, \tilde{b}_1\Big)^* \\
&= -\boldsymbol{i}\; h_t^2\Big[c_4\Big(\Phi^0,\, \Phi^-\Big)\,\mathbf{U}^*_{\tilde{t}\,k1}\Big]\;, \\
&\quad c_4\Big(h,\, H^-\Big) = \tfrac{-c_\alpha\, c_\beta}{\sqrt{2}}\;, \quad c_4\Big(H,\, H^-\Big) = \tfrac{-s_\alpha\, c_\beta}{\sqrt{2}}\;, \\
&\quad c_4\Big(h,\, G^-\Big) = \tfrac{-c_\alpha\, s_\beta}{\sqrt{2}}\;, \quad c_4\Big(H,\, G^-\Big) = \tfrac{-s_\alpha\, s_\beta}{\sqrt{2}}\;, \\
&\quad c_4\Big(A,\, H^-\Big) = \tfrac{-\boldsymbol{i}\; c_\beta^2}{\sqrt{2}}\;, \quad c_4\Big(G,\, H^-\Big) = \tfrac{-\boldsymbol{i}\; c_\beta\, s_\beta}{\sqrt{2}}\;, \\
&\quad c_4\Big(A,\, G^-\Big) = \tfrac{-\boldsymbol{i}\; c_\beta\, s_\beta}{\sqrt{2}}\;, \quad c_4\Big(G,\, G^-\Big) = \tfrac{-\boldsymbol{i}\; s_\beta^2}{\sqrt{2}}\;.
\end{aligned}
\tag{7.58d}
$$

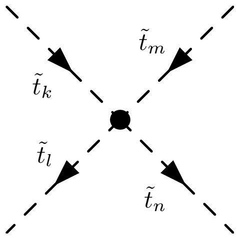

$$
\begin{aligned}
&= -\boldsymbol{i}\; C\Big(\tilde{t}_k,\, \tilde{t}_l,\, \tilde{t}_m,\, \tilde{t}_n\Big) \\
&= -\boldsymbol{i}\; h_t^2\Big[\,(\mathbf{U}^*_{\tilde{t}\,k1}\,\mathbf{U}^*_{\tilde{t}\,m2} + \mathbf{U}^*_{\tilde{t}\,k2}\,\mathbf{U}^*_{\tilde{t}\,m1}) \\
&\qquad\qquad (\mathbf{U}_{\tilde{t}\,l1}\,\mathbf{U}_{\tilde{t}\,n2} + \mathbf{U}_{\tilde{t}\,l2}\,\mathbf{U}_{\tilde{t}\,n1})\Big]\;.
\end{aligned}
\tag{7.58e}
$$

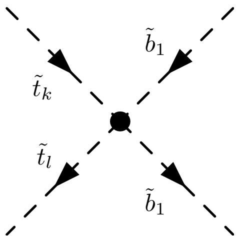

$$
= -\boldsymbol{i}\; C\Big(\tilde{t}_k,\, \tilde{t}_l,\, \tilde{b}_1,\, \tilde{b}_1\Big) = -\boldsymbol{i}\; h_t^2\Big[\mathbf{U}^*_{\tilde{t}\,k2}\,\mathbf{U}_{\tilde{t}\,l2}\Big]\;. \tag{7.58f}
$$

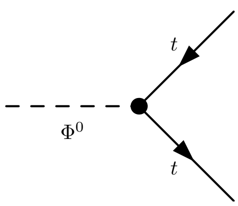

$$
\begin{aligned}
&= -\boldsymbol{i}\; C\Big(\Phi^0,\, t,\, t\Big) = -\boldsymbol{i}\; h_t\Big[c_3\Big(\Phi^0\Big)\Big]\begin{pmatrix} 1 \\ \mathrm{sign}(\Phi^0)\end{pmatrix}, \\
&\quad \{c_3(h),\, \mathrm{sign}(h)\} = \Big\{\tfrac{c_\alpha}{\sqrt{2}},\, 1\Big\}\;, \\
&\quad \{c_3(H),\, \mathrm{sign}(H)\} = \Big\{\tfrac{s_\alpha}{\sqrt{2}},\, 1\Big\}\;, \\
&\quad \{c_3(A),\, \mathrm{sign}(A)\} = \Big\{\tfrac{\boldsymbol{i}\, c_\beta}{\sqrt{2}},\, -1\Big\}\;, \\
&\quad \{c_3(G),\, \mathrm{sign}(G)\} = \Big\{\tfrac{\boldsymbol{i}\, s_\beta}{\sqrt{2}},\, -1\Big\}\;.
\end{aligned}
\tag{7.58g}
$$

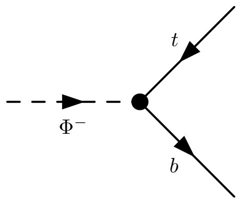

$$= -\boldsymbol{i}\; C\Big(\Phi^-,\, t,\, \bar{b}\Big) = -\boldsymbol{i}\; h_t\Big[c_3\Big(\Phi^-\Big)\Big]\begin{pmatrix}0\\1\end{pmatrix}\,,$$
$$c_3\Big(H^-\Big) = -c_\beta\;,$$
$$c_3\Big(G^-\Big) = -s_\beta\;. \tag{7.58h}$$

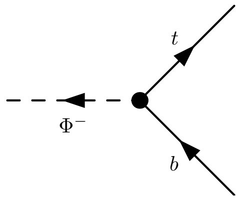

$$= -\boldsymbol{i}\; C\Big(\Phi^+,\, \bar{t},\, b\Big) = -\boldsymbol{i}\; h_t\Big[\bar{c}_3\Big(\Phi^+\Big)\Big]\begin{pmatrix}1\\0\end{pmatrix}\,,$$
$$\bar{c}_3\Big(H^+\Big) = -c_\beta\;,$$
$$\bar{c}_3\Big(G^+\Big) = -s_\beta\;. \tag{7.58i}$$

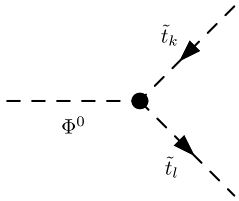

$$\begin{aligned}
&= -\boldsymbol{i}\; C\Big(\Phi^0,\, \tilde{t}_k,\, \tilde{t}_l\Big)\\
&= -\boldsymbol{i}\; h_t\Big[\, c_m\Big(\Phi^0\Big)\,(\mathbf{U}^*_{\tilde{t}\,k1}\,\mathbf{U}_{\tilde{t}\,l1} + \mathbf{U}^*_{\tilde{t}\,k2}\,\mathbf{U}_{\tilde{t}\,l2})\, m_t\\
&\qquad + c_\mu\Big(\Phi^0\Big)\,\Big(\mathrm{sign}\Big(\Phi^0\Big)\,\mathbf{U}^*_{\tilde{t}\,k2}\,\mathbf{U}_{\tilde{t}\,l1}\,\mu + \mathbf{U}^*_{\tilde{t}\,k1}\,\mathbf{U}_{\tilde{t}\,l2}\,\mu^*\Big)\\
&\qquad + c_A\Big(\Phi^0\Big)\,\Big(\mathrm{sign}\Big(\Phi^0\Big)\,\mathbf{U}^*_{\tilde{t}\,k2}\,\mathbf{U}_{\tilde{t}\,l1}\,A_t^* + \mathbf{U}^*_{\tilde{t}\,k1}\,\mathbf{U}_{\tilde{t}\,l2}\,A_t\Big)\Big]\,,
\end{aligned}$$
$$\{c_m(h),\, c_\mu(h),\, c_A(h),\, \mathrm{sign}(h)\} = \Big\{\sqrt{2}\,c_\alpha,\, \tfrac{s_\alpha}{\sqrt{2}},\, \tfrac{c_\alpha}{\sqrt{2}},\, 1\Big\}\;,$$
$$\{c_m(H),\, c_\mu(H),\, c_A(H),\, \mathrm{sign}(H)\} = \Big\{\sqrt{2}\,s_\alpha,\, \tfrac{-c_\alpha}{\sqrt{2}},\, \tfrac{s_\alpha}{\sqrt{2}},\, 1\Big\}\;,$$
$$\{c_m(A),\, c_\mu(A),\, c_A(A),\, \mathrm{sign}(A)\} = \Big\{0,\, \tfrac{\boldsymbol{i}\,s_\beta}{\sqrt{2}},\, \tfrac{\boldsymbol{i}\,c_\beta}{\sqrt{2}},\, -1\Big\}\;,$$
$$\{c_m(G),\, c_\mu(G),\, c_A(G),\, \mathrm{sign}(G)\} = \Big\{0,\, \tfrac{-\boldsymbol{i}\,c_\beta}{\sqrt{2}},\, \tfrac{\boldsymbol{i}\,s_\beta}{\sqrt{2}},\, -1\Big\}\;. \tag{7.58j}$$

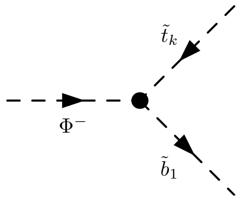

$$\begin{aligned}
&= -\boldsymbol{i}\; C\Big(\Phi^-,\, \tilde{t}_k,\, \tilde{b}_1\Big) = -\boldsymbol{i}\; C\Big(\Phi^+,\, \tilde{t}_k,\, \tilde{b}_1\Big)^*\\
&= -\boldsymbol{i}\; h_t\Big[c_m\Big(\Phi^-\Big)\,\mathbf{U}^*_{\tilde{t}\,k1}\,m_t + c_\mu\Big(\Phi^-\Big)\,\mathbf{U}^*_{\tilde{t}\,k2}\,\mu + c_A\Big(\Phi^-\Big)\,\mathbf{U}^*_{\tilde{t}\,k2}\,A_t^*\Big]\,,
\end{aligned}$$
$$\Big\{c_m\Big(H^-\Big),\, c_\mu\Big(H^-\Big),\, c_A\Big(H^-\Big)\Big\} = \{-c_\beta,\, -s_\beta,\, -c_\beta\}\;,$$
$$\Big\{c_m\Big(G^-\Big),\, c_\mu\Big(G^-\Big),\, c_A\Big(G^-\Big)\Big\} = \{-s_\beta,\, c_\beta,\, -s_\beta\}\;. \tag{7.58k}$$

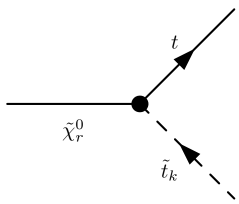

$$= -\boldsymbol{i}\; C\Big(\tilde{\chi}^0_r,\, \bar{t},\, \tilde{t}_k\Big) = -\boldsymbol{i}\; h_t\begin{pmatrix}\mathbf{U}^*_{\tilde{t}\,k1}\,\mathbf{N}^*_{r4}\\ \mathbf{U}^*_{\tilde{t}\,k2}\,\mathbf{N}_{r4}\end{pmatrix}. \tag{7.58l}$$

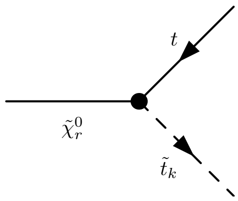

$$= -\boldsymbol{i}\; C\Big(\tilde{\chi}_r^0,\, t,\, \tilde{t}_k\Big) = -\boldsymbol{i}\; h_t \begin{pmatrix} \mathbf{U}_{\tilde{t}\,k2}\, \mathbf{N}^*_{r4} \\ \mathbf{U}_{\tilde{t}\,k1}\, \mathbf{N}_{r4} \end{pmatrix}. \tag{7.58m}$$

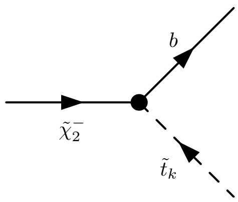

$$= -\boldsymbol{i}\; C\Big(\tilde{\chi}_2^-,\, \bar{b},\, \tilde{t}_k\Big) = -\boldsymbol{i}\; h_t \begin{pmatrix} 0 \\ -\mathbf{U}^*_{\tilde{t}\,k2} \end{pmatrix}. \tag{7.58n}$$

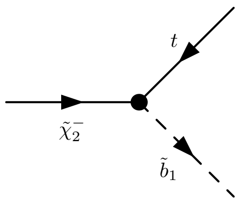

$$= -\boldsymbol{i}\; C\Big(\tilde{\chi}_2^-,\, t,\, \tilde{b}_1\Big) = -\boldsymbol{i}\; h_t \begin{pmatrix} 0 \\ -1 \end{pmatrix}. \tag{7.58o}$$

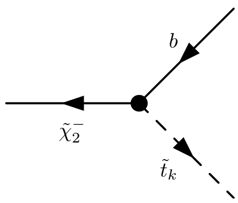

$$= -\boldsymbol{i}\; C\Big(\tilde{\chi}_2^+,\, b,\, \tilde{t}_k\Big) = -\boldsymbol{i}\; h_t \begin{pmatrix} -\mathbf{U}_{\tilde{t}\,k2} \\ 0 \end{pmatrix}. \tag{7.58p}$$

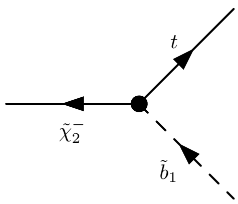

$$= -\boldsymbol{i}\; C\Big(\tilde{\chi}_2^+,\, \bar{t},\, \tilde{b}_1\Big) = -\boldsymbol{i}\; h_t \begin{pmatrix} -1 \\ 0 \end{pmatrix}. \tag{7.58q}$$

7.7.2. Counterterm vertices

The following one-loop counterterm vertices appear as insertions in the two-loop diagrams with subrenormalization at one of their vertices. To shorten the notation, the previously defined tree-level couplings $C(\,\dots)$ are re-utilized. Their corresponding one-loop counterterms are named $\delta^{(1)}C(\,\dots)$. Since each of the used vertices contains the top-Yukawa coupling h_t, its renormalization is given once as the definition of $\delta^{(1)}h_t$ and then reused in the coupling counterterms. Also the field-renormalization constants of the Higgs bosons are considered; all other field-renormalization constants cancel out in the sum of the full set of Feynman diagrams, since the corresponding particles exclusively appear in internal propagators.

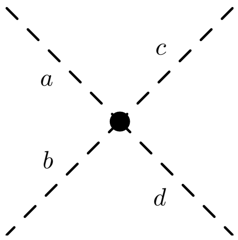

$= -i\, C(a,\, b,\, c,\, d)$,

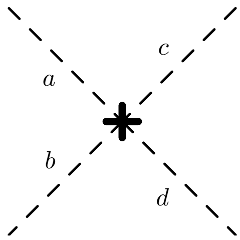

$= -i\, \delta^{(1)}C(a,\, b,\, c,\, d)$, (7.59a)

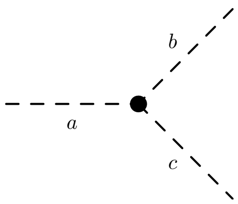

$= -i\, C(a,\, b,\, c)$,

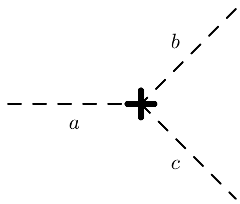

$= -i\, \delta^{(1)}C(a,\, b,\, c)$, (7.59b)

$$\delta^{(1)}h_t = h_t \left(\frac{\delta^{(1)}m_t}{m_t} - \frac{\delta^{(1)}M_W}{M_W} - \frac{\delta^{(1)}s_\mathrm{w}}{s_\mathrm{w}} - \frac{\delta^{(1)}s_\beta}{s_\beta} \right) \,, \tag{7.60a}$$

$$\delta^{(1)}C\Big(\Phi_i^0,\, \Phi_j^0,\, \tilde{t}_k,\, \tilde{t}_l\Big) = C\Big(\Phi_i^0,\, \Phi_j^0,\, \tilde{t}_k,\, \tilde{t}_l\Big) \left(\frac{2\, \delta^{(1)}h_t}{h_t} + \delta^{(1)}Z_{\mathcal{H}_2} \right) \,, \tag{7.61a}$$

$$\delta^{(1)}C\Big(\Phi_i^-,\, \Phi_j^+,\, \tilde{t}_k,\, \tilde{t}_l\Big) = C\Big(\Phi_i^-,\, \Phi_j^+,\, \tilde{t}_k,\, \tilde{t}_l\Big) \left(\frac{2\, \delta^{(1)}h_t}{h_t} + \delta^{(1)}Z_{\mathcal{H}_2} \right) \,, \tag{7.61b}$$

$$\delta^{(1)}C\Big(\Phi_i^-,\, \Phi_j^+,\, \tilde{b}_1,\, \tilde{b}_1\Big) = C\Big(\Phi_i^-,\, \Phi_j^+,\, \tilde{b}_1,\, \tilde{b}_1\Big) \left(\frac{2\, \delta^{(1)}h_t}{h_t} + \delta^{(1)}Z_{\mathcal{H}_2} \right) \,, \tag{7.61c}$$

$$\delta^{(1)}C\Big(\Phi^0,\, \Phi^-,\, \tilde{t}_k,\, \tilde{b}_1\Big) = C\Big(\Phi^0,\, \Phi^-,\, \tilde{t}_k,\, \tilde{b}_1\Big) \left(\frac{2\, \delta^{(1)}h_t}{h_t} + \delta^{(1)}Z_{\mathcal{H}_2} \right) \,, \tag{7.61d}$$

$$\delta^{(1)}C\Big(\tilde{t}_k,\, \tilde{t}_l,\, \tilde{t}_m,\, \tilde{t}_n\Big) = C\Big(\tilde{t}_k,\, \tilde{t}_l,\, \tilde{t}_m,\, \tilde{t}_n\Big) \left(\frac{2\, \delta^{(1)}h_t}{h_t} \right) \,, \tag{7.61e}$$

$$\delta^{(1)}C\Big(\tilde{t}_k,\, \tilde{t}_l,\, \tilde{b}_1,\, \tilde{b}_1\Big) = C\Big(\tilde{t}_k,\, \tilde{t}_l,\, \tilde{b}_1,\, \tilde{b}_1\Big) \left(\frac{2\, \delta^{(1)}h_t}{h_t} \right) \,, \tag{7.61f}$$

$$\delta^{(1)}C\Big(\Phi^0,\, t,\, t\Big) = C\Big(\Phi^0,\, t,\, t\Big) \left(\frac{\delta^{(1)}h_t}{h_t} + \frac{1}{2}\, \delta^{(1)}Z_{\mathcal{H}_2} \right) \,, \tag{7.61g}$$

$$\delta^{(1)}C\Big(\Phi^-,\, t,\, \bar{b}\Big) = C\Big(\Phi^-,\, t,\, \bar{b}\Big) \left(\frac{\delta^{(1)}h_t}{h_t} + \frac{1}{2}\, \delta^{(1)}Z_{\mathcal{H}_2} \right) \,, \tag{7.61h}$$

$$\delta^{(1)}C\Big(\Phi^+,\, \bar{t},\, b\Big) = C\Big(\Phi^+,\, \bar{t},\, b\Big) \left(\frac{\delta^{(1)}h_t}{h_t} + \frac{1}{2}\, \delta^{(1)}Z_{\mathcal{H}_2} \right) \,, \tag{7.61i}$$

$$\begin{aligned}
\delta^{(1)}C\Big(\Phi^0,\, \tilde{t}_k,\, \tilde{t}_l\Big) = C\Big(\Phi^0,\, \tilde{t}_k,\, \tilde{t}_l\Big)\left(\frac{\delta^{(1)}h_t}{h_t}\right) \\
+\; h_t\Bigg\{\, c_\mu\Big(\Phi^0\Big)\Bigg[\mathrm{sign}\Big(\Phi^0\Big)\,\mathbf{U}^*_{\tilde{t}\,k2}\,\mathbf{U}_{\tilde{t}\,l1}\,\mu\left(\frac{\delta^{(1)}\mu}{\mu}+\frac{1}{2}\,\delta^{(1)}Z_{\mathcal{H}_1}\right) \\
+\,\mathbf{U}^*_{\tilde{t}\,k1}\,\mathbf{U}_{\tilde{t}\,l2}\,\mu^*\left(\frac{\delta^{(1)}\mu^*}{\mu^*}+\frac{1}{2}\,\delta^{(1)}Z_{\mathcal{H}_1}\right)\Bigg] \\
+\; c_A\Big(\Phi^0\Big)\Bigg[\mathrm{sign}\Big(\Phi^0\Big)\,\mathbf{U}^*_{\tilde{t}\,k2}\,\mathbf{U}_{\tilde{t}\,l1}\,A_t^* \\
\times\left(\frac{\delta^{(1)}A_t^*}{A_t^*}+\frac{1}{2}\,\delta^{(1)}Z_{\mathcal{H}_2}\right) \\
+\,\mathbf{U}^*_{\tilde{t}\,k1}\,\mathbf{U}_{\tilde{t}\,l2}\,A_t\left(\frac{\delta^{(1)}A_t}{A_t}+\frac{1}{2}\,\delta^{(1)}Z_{\mathcal{H}_2}\right)\Bigg] \\
+\,c_m\Big(\Phi^0\Big)\left(\mathbf{U}^*_{\tilde{t}\,k1}\,\mathbf{U}_{\tilde{t}\,l1}+\mathbf{U}^*_{\tilde{t}\,k2}\,\mathbf{U}_{\tilde{t}\,l2}\right) \\
\times\, m_t\left(\frac{\delta^{(1)}m_t}{m_t}+\frac{1}{2}\,\delta^{(1)}Z_{\mathcal{H}_2}\right)\Bigg\}\,,
\end{aligned} \tag{7.61j}$$

$$\begin{aligned}
\delta^{(1)}C\Big(\Phi^-,\, \tilde{t}_k,\, \tilde{b}_1\Big) = C\Big(\Phi^-,\, \tilde{t}_k,\, \tilde{b}_1\Big)\left(\frac{\delta^{(1)}h_t}{h_t}\right) \\
+\; h_t\Bigg[c_\mu\Big(\Phi^-\Big)\,\mathbf{U}^*_{\tilde{t}\,k2}\,\mu\left(\frac{\delta^{(1)}\mu}{\mu}+\frac{1}{2}\,\delta^{(1)}Z_{\mathcal{H}_1}\right) \\
+\,c_A\Big(\Phi^-\Big)\,\mathbf{U}^*_{\tilde{t}\,k2}\,A_t^*\left(\frac{\delta^{(1)}A_t^*}{A_t^*}+\frac{1}{2}\,\delta^{(1)}Z_{\mathcal{H}_2}\right) \\
+\,c_m\Big(\Phi^-\Big)\,\mathbf{U}^*_{\tilde{t}\,k1}\,m_t\left(\frac{\delta^{(1)}m_t}{m_t}+\frac{1}{2}\,\delta^{(1)}Z_{\mathcal{H}_2}\right)\Bigg]\,,
\end{aligned} \tag{7.61k}$$

$$\delta^{(1)}C\Big(\tilde{\chi}^0_r,\, \bar{t},\, \tilde{t}_k\Big) = C\Big(\tilde{\chi}^0_r,\, \bar{t},\, \tilde{t}_k\Big)\left(\frac{\delta^{(1)}h_t}{h_t}\right)\,, \tag{7.61l}$$

$$\delta^{(1)}C\Big(\tilde{\chi}^0_r,\, t,\, \tilde{t}_k\Big) = C\Big(\tilde{\chi}^0_r,\, t,\, \tilde{t}_k\Big)\left(\frac{\delta^{(1)}h_t}{h_t}\right)\,, \tag{7.61m}$$

$$\delta^{(1)}C\Big(\tilde{\chi}^-_2,\, \bar{b},\, \tilde{t}_k\Big) = C\Big(\tilde{\chi}^-_2,\, \bar{b},\, \tilde{t}_k\Big)\left(\frac{\delta^{(1)}h_t}{h_t}\right)\,, \tag{7.61n}$$

$$\delta^{(1)}C\Big(\tilde{\chi}^-_2,\, t,\, \tilde{t}_k\Big) = C\Big(\tilde{\chi}^-_2,\, t,\, \tilde{t}_k\Big)\left(\frac{\delta^{(1)}h_t}{h_t}\right)\,, \tag{7.61o}$$

$$\delta^{(1)}C\Big(\tilde{\chi}^+_2,\, b,\, \tilde{t}_k\Big) = C\Big(\tilde{\chi}^+_2,\, b,\, \tilde{t}_k\Big)\left(\frac{\delta^{(1)}h_t}{h_t}\right)\,, \tag{7.61p}$$

$$\delta^{(1)}C\Big(\tilde{\chi}^+_2,\, \bar{t},\, \tilde{b}_1\Big) = C\Big(\tilde{\chi}^+_2,\, \bar{t},\, \tilde{b}_1\Big)\left(\frac{\delta^{(1)}h_t}{h_t}\right)\,. \tag{7.61q}$$

The counterterms of Eq. (7.61j) and Eq. (7.61k) should be emphasized, because they are the only ones which cannot be simply expressed as a product of a tree-level coupling and the counterterm of the top-Yukawa coupling and field renormalization.

In addition, also counterterms for two-point vertices are required. The necessary expressions are given in the following:

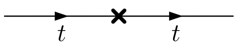

$$= -i\, C(t,\, t) = i\, \delta^{(1)} m_t \ . \tag{7.62a}$$

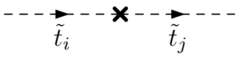

$$= -i\, C\Big(\tilde{t}_i,\, \tilde{t}_j\Big) = i\, \delta^{(1)} m^2_{\tilde{t}_i \tilde{t}_j} \ . \tag{7.62b}$$

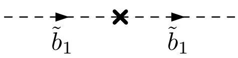

$$= -i\, C\Big(\tilde{b}_1,\, \tilde{b}_1\Big) = i\, \delta^{(1)} m^2_{\tilde{b}_1} \equiv i\, \delta^{(1)} m^2_{\tilde{q}_3} \ . \tag{7.62c}$$

7.8. Special aspects of the analytical calculation

The evaluation of the $\mathcal{O}(\alpha_t^2)$ contributions to the Higgs-boson masses has been performed completely analytical, which allows for a better control of the divergences and understanding of the dependence on different MSSM parameters. Some special aspects that emerged during the computation are mentioned in the following.

7.8.1. One-loop integrals at two-loop order

Products of two one-loop integrals occur in some two-loop diagrams, in diagrams with subrenormalization, and in genuine two-loop counterterms. Each infra-red finite one-loop function $F_{1,\,a}$ can be expressed as a Laurent series

$$F_{1,\,a} = \frac{a_{-1}}{\epsilon} + a_0 + a_1\, \epsilon + \mathcal{O}\Big(\epsilon^2\Big) \tag{7.63}$$

around the regulator ϵ of the ultra-violet divergence. Within a one-loop calculation only the coefficient a_{-1} of the pole and the finite part a_0 are required; the term a_1 and coefficients of higher orders in ϵ vanish in the limit $\epsilon \to 0$ after renormalization. However, in the product of two functions $F_{1,\,a}$ and $F_{1,\,b}$ at the two-loop level the coefficients of higher powers in ϵ are necessary:

$$F_{1,\,a}\, F_{1,\,b} = \frac{a_{-1}\, b_{-1}}{\epsilon^2} + \frac{a_{-1}\, b_0 + a_0\, b_{-1}}{\epsilon} + (a_{-1}\, b_1 + a_0\, b_0 + a_1\, b_{-1}) + \mathcal{O}(\epsilon) \ . \tag{7.64}$$

The finite part of a two-loop result includes contributions from the $\mathcal{O}(\epsilon)$ coefficients of each one-loop integral. The used expressions for the one-loop functions expanded up to the $\mathcal{O}(\epsilon)$ are presented in Appendix B.1.

As explained in Section 7.2 only a single type of two-loop integrals remains, denoted as $\mathrm{T}_{134}(m_1^2, m_2^2, m_3^2)$. Its full form is displayed in Eq. (B.8a); however its ultra-violet divergent parts and some finite terms are solely given through products of expressions from the one-loop function

$$A_0\left(m^2\right) = \frac{A_0(m^2)|_{\frac{1}{\epsilon}}}{\epsilon} + A_0\left(m^2\right)\Big|_{\epsilon^0}\epsilon^0 + A_0\left(m^2\right)\Big|_{\epsilon^1}\epsilon^1 + \mathcal{O}\left(\epsilon^2\right) . \tag{7.65}$$

Here, $A_0(m^2)|_{\frac{1}{\epsilon}}$, $A_0(m^2)|_{\epsilon^0}$ and $A_0(m^2)|_{\epsilon^1}$ are the coefficients of $\frac{1}{\epsilon}$, ϵ^0 and ϵ^1, respectively.

The expansion of Eq. (B.8a) with the usage of Eq. (7.65) yields the following result which is ordered in powers of ϵ:

$$\begin{aligned}
\mathrm{T}_{134}\left(m_1^2, m_2^2, m_3^2\right) = &\sum_{i=1}^{3}\left\{\frac{1}{2}\frac{\left[A_0(m_i^2)|_{\frac{1}{\epsilon}}\right]^2}{m_i^2}\right\}\frac{1}{\epsilon^2} \\
&+\sum_{i=1}^{3}\left\{\frac{1}{2}\frac{\left[A_0(m_i^2)|_{\frac{1}{\epsilon}}\right]^2}{m_i^2} + \frac{A_0(m_i^2)|_{\frac{1}{\epsilon}}\, A_0(m_i^2)|_{\epsilon^0}}{m_i^2}\right\}\frac{1}{\epsilon} \\
&+\sum_{i=1}^{3}\left\{\frac{\left[A_0(m_i^2)|_{\frac{1}{\epsilon}}\right]^2}{m_i^2} + \frac{A_0(m_i^2)|_{\frac{1}{\epsilon}}\, A_0(m_i^2)|_{\epsilon^0}}{m_i^2}\right. \\
&\qquad + \frac{1}{2}\frac{\left[A_0(m_i^2)|_{\epsilon^0}\right]^2}{m_i^2} + \frac{A_0(m_i^2)|_{\frac{1}{\epsilon}}\, A_0(m_i^2)|_{\epsilon^1}}{m_i^2} \\
&\qquad \left. + \Phi^{\mathrm{cyc}}\left(m_1^2, m_2^2, m_3^2\right)\right\}\epsilon^0 \\
&+\mathcal{O}\left(\epsilon^1\right) .
\end{aligned} \tag{7.66}$$

The function Φ^{cyc} contains only finite parts and is given in Eqs. (B.8b)–(B.8e).

By using this form of T_{134} two advantages emerge:

- the cancelation of the $\frac{1}{\epsilon^2}$ and $\frac{1}{\epsilon}$ poles in the renormalized self-energies of the Higgs bosons can be checked analytically,

- the finite contributions to the self-energies which are induced by the coefficients of $\mathcal{O}(\epsilon)$ drop out of the Higgs-boson self-energies.

7.8.2. Real-valued self-energies

Our calculation of the Higgs-boson self-energies takes care of the complex-valued parameters μ, A_t and the stop-mixing matrix $\mathbf{U}_{\tilde{t}}$ as well as the corresponding renormalization constants. However, by replacing the complex parameters with the real quantities

$$|\mathbf{U}_{\tilde{t}\,11}|^2\ , \quad |X_t|^2\ , \quad |\mu|^2\ , \quad \frac{\delta^{(1)}\mu}{\mu}\ , \quad \mathfrak{Re}\Big[\frac{\delta^{(1)}X_t}{X_t}\Big], \quad \mathfrak{Re}\left[\frac{\delta^{(1)}m^2_{\tilde{t}_i\tilde{t}_j}\,\mathbf{U}_{\tilde{t}\,2j}\,\mathbf{U}^*_{\tilde{t}\,1i}}{m_t\,X_t}\right]\ , \tag{7.67a}$$

$$|\mathbf{U}_{\tilde{t}\,12}|^2\ , \quad |Y_t|^2\ , \quad \mathfrak{Im}[X_t\,\mu^*]\ , \quad \mathfrak{Im}\Big[\frac{\delta^{(1)}X_t}{X_t}\Big]\ , \quad \mathfrak{Im}\left[\frac{\delta^{(1)}m^2_{\tilde{t}_i\tilde{t}_j}\,\mathbf{U}_{\tilde{t}\,2j}\,\mathbf{U}^*_{\tilde{t}\,1i}}{m_t\,X_t}\right]\ , \tag{7.67b}$$

with the combinations

$$X_t = A_t^* - \frac{\mu}{t_\beta}\ , \tag{7.68a}$$

$$Y_t = A_t^* + \mu\, t_\beta\ , \tag{7.68b}$$

$$\delta^{(1)}X_t = \delta^{(1)}A_t^* - \frac{\delta^{(1)}\mu}{t_\beta} + \frac{\mu}{t_\beta}\frac{\delta^{(1)}t_\beta}{t_\beta}\ , \tag{7.68c}$$

all coefficients of the loop integrals turn out to be real.[13] The full expressions are depicted in Appendix D.

For the applied approximation of a vanishing external momentum, all integrals in the Higgs-boson self-energies are real. Furthermore, in the definition of the renormalization constants only the real parts of the appearing loop integrals are used.

Thus, each computed self-energy generates a real shift to the corresponding Higgs-boson mass-matrix element. Furthermore, the CP-violating mixings of the lowest-order mass eigenstates h and H with the lowest-order mass eigenstate A turn out to be proportional to $\mathfrak{Im}[X_t\mu^*]$, i. e. no CP-violation is induced by the $\mathcal{O}(\alpha_t^2)$ contributions, if the phases ϕ_μ and ϕ_{X_t} add up to 0 or $\pm\pi$.

[13]Some more manifestly real combinations of complex parameters appear in the renormalization constants in Appendix D.6.

8. Numerical investigation of the top-Yukawa corrections

The following numerical evaluation of the Higgs-boson masses includes the full one-loop result, the $\mathcal{O}(\alpha_t\alpha_s)$ contributions, and the new $\mathcal{O}(\alpha_t^2)$ contributions which are derived in this thesis. The one-loop results and the $\mathcal{O}(\alpha_t\alpha_s)$ terms are obtained from `FeynHiggs`, while the $\mathcal{O}(\alpha_t^2)$ terms are computed by means of the corresponding two-loop self-energies specified in the previous chapter. Thereby, the new $\mathcal{O}(\alpha_t^2)$ self-energies are combined with the results of the other available self-energies according to Eq. (7.6) within `FeynHiggs`, and the Higgs-boson masses are derived via Eq. (6.38). For comparison with previous results, G_{F} is chosen for normalization of the top-Yukawa corrections, as mentioned at the end of Section 7.4.

The SM parameters are put together in Tab. 8.1, as well as those MSSM parameters that are kept for the analyses which are performed in this chapter. The residual input parameters of the MSSM are shown in the figures or their captions. The parameters μ, t_β and the Higgs field-renormalization constants are defined in the $\overline{\mathrm{DR}}$ scheme at the scale m_t if not stated otherwise.

Table 8.1.: Default input values of the MSSM and SM parameters.

MSSM input	SM input
$M_2 = 200$ GeV,	$m_t = 173.2$ GeV,
$M_1 = (5s_{\mathrm{w}}^2)/(3c_{\mathrm{w}}^2)\, M_2\,,$	$m_b = 4.2$ GeV,
$m_{\tilde{l}_1} = m_{\tilde{e}_{\mathrm{R}}} = 2000$ GeV,	$m_\tau = 1.77703$ GeV,
$m_{\tilde{q}_1} = m_{\tilde{u}_{\mathrm{R}}} = m_{\tilde{d}_{\mathrm{R}}} = 2000$ GeV,	$M_W = 80.385$ GeV,
$A_u = A_d = A_e = 0$ GeV,	$M_Z = 91.1876$ GeV,
$m_{\tilde{l}_2} = m_{\tilde{\mu}_{\mathrm{R}}} = 2000$ GeV,	$G_{\mathrm{F}} = 1.16639 \cdot 10^{-5}$,
$m_{\tilde{q}_2} = m_{\tilde{c}_{\mathrm{R}}} = m_{\tilde{s}_{\mathrm{R}}} = 2000$ GeV,	$\alpha_s = 0.118$,
$A_c = A_s = A_\mu = 0$ GeV,	$1/\alpha = 128.944742392237$.

8.1. Neutral Higgs masses in the real MSSM

As a first application, the MSSM with real parameters is studied. The A-boson mass is chosen as an input and renormalized on-shell at higher orders. The only non-vanishing off-diagonal entries of the renormalized self-energy matrix in Eq. (6.37a) are the $\hat{\Sigma}^{(j)}_{hH}$, $j \in \{1, 2\}$, thus the lowest-order mass eigenstates h and H mix to new Higgs bosons at higher orders. The corresponding masses which are calculated via Eq. (6.38) are sorted in ascending order, i. e. $m_h < m_H$. However, a diagonalization of the propagator matrix is not possible anymore because of the p^2-dependent mixing in Eq. (6.35a). Nevertheless, it is convenient to define an effective mixing angle α_{eff} in the approximation $\hat{\mathbf{\Sigma}}^{(j)}_{hHAG}(p^2) \to \hat{\mathbf{\Sigma}}^{(j)}_{hHAG}(0)$, $j \in \{1, 2\}$. It describes the mixing of ϕ_1 and ϕ_2 into h and H via the matrix $\mathbf{D}_{\alpha_{\text{eff}}}$ in analogy to Eq. (6.10).[14]

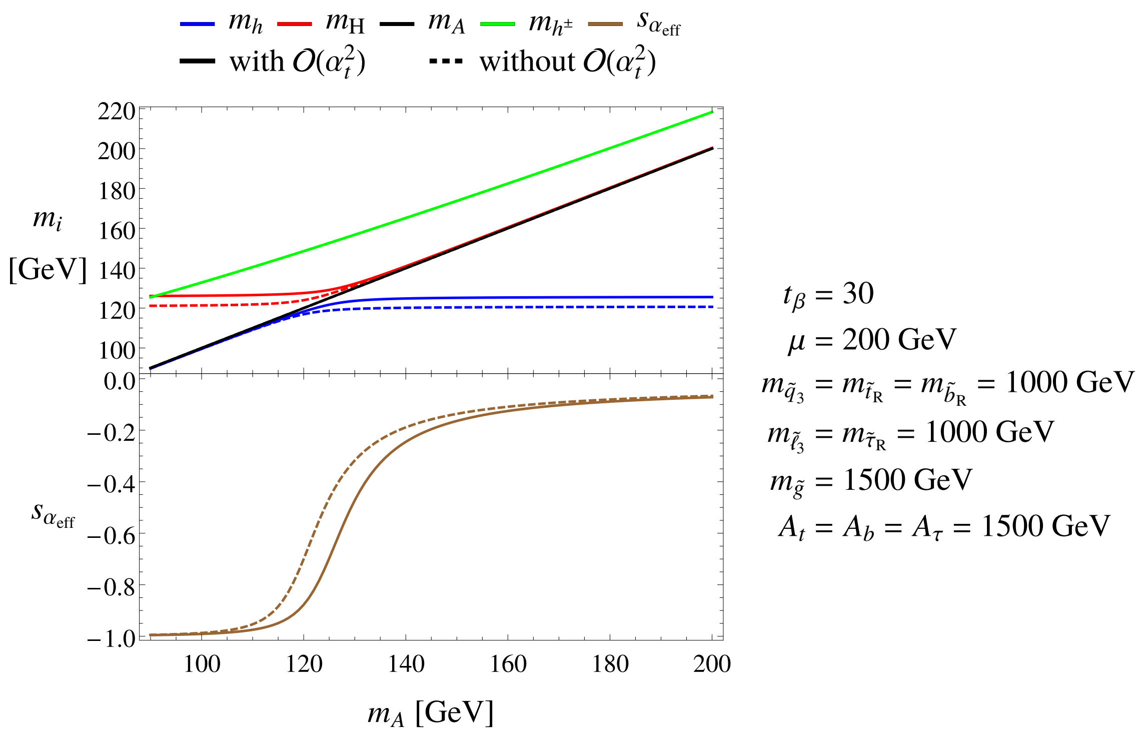

Figure 8.1.: Up: The dependence of the Higgs masses m_i, $i \in \{h, H, A, h^\pm\}$ on m_A with the color coding given above the plot is depicted including the $\mathcal{O}(\alpha_t^2)$ terms calculated in the Feynman diagrammatic approach (straight lines) or discarding this contribution (dashed lines). Down: The effective mixing angle $s_{\alpha_{\text{eff}}}$ for the approximation $p^2 = 0$ is shown with (straight) and without (dashed) the $\mathcal{O}(\alpha_t^2)$ contributions.

[14]This approximation corresponds to the effective potential approach [HHW00b; Hei+01].

In Fig. 8.1 the dependence of the Higgs-boson masses m_h (blue) and m_H (red) on the input value of m_A (depicted in black for your guidance) is visualized. For low masses, h has a similar mass compared to that of the A boson, and in the high-mass region H has a similar mass compared to that of the A boson. In both cases the mass of h or H that is different from the A-boson mass saturates and becomes independent of m_A. Around $m_A \approx 125$ GeV a transition between these two scenarios takes place. The contribution of the $\mathcal{O}(\alpha_t^2)$ corrections to the Higgs-boson masses is illustrated by the difference between the dashed and straight lines. The charged Higgs-boson mass $m_{h^\pm}$ (green) gets only small contributions from the $\mathcal{O}(\alpha_t^2)$ corrections in the depicted parameter region.

Furthermore, the effective mixing angle $s_{\alpha_{\text{eff}}}$ is close to zero for large m_A, i. e. in the approximation of $p^2 = 0$ for the renormalized self-energies $h \approx \phi_2$ and $H \approx \phi_1$; also the couplings of h are similar to the Higgs boson of the SM in this case, whereas H has suppressed couplings (decoupling limit). In contrast, $s_{\alpha_{\text{eff}}}$ is close to -1 for small m_A, hence $h \approx \phi_1$ and $H \approx \phi_2$ and the heavy Higgs boson H behaves more like the SM Higgs boson.

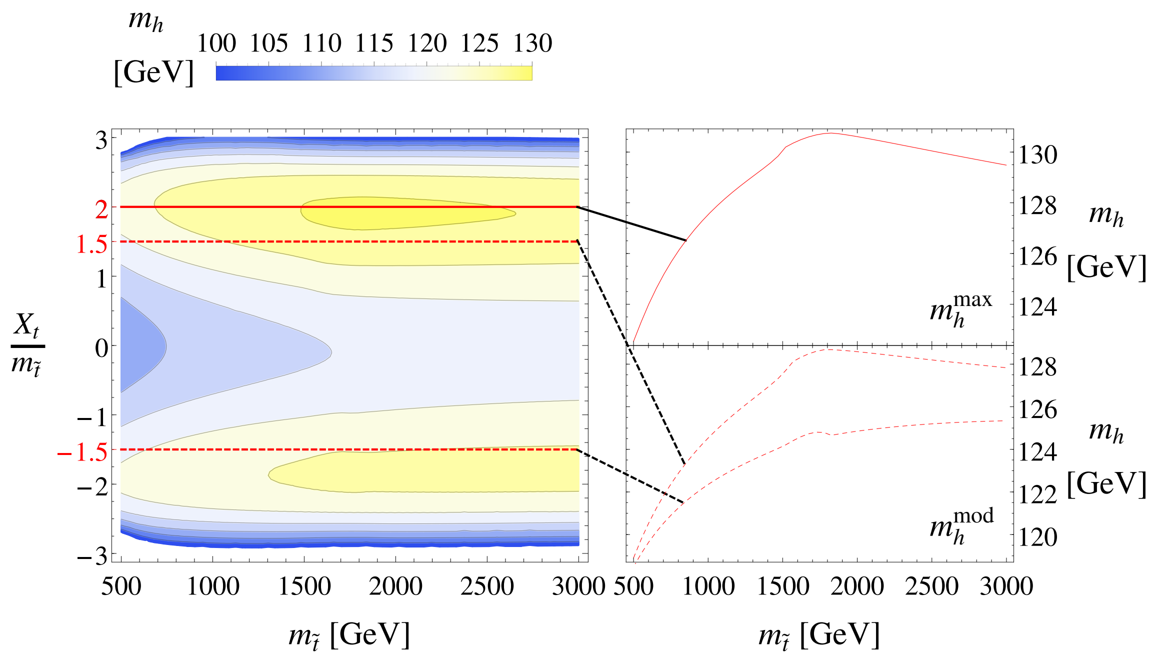

Figure 8.2.: The dependence of the light Higgs-boson mass m_h on the stop-sector parameters $m_{\tilde{t}} \equiv m_{\tilde{q}_3} = m_{\tilde{t}_R}$ and X_t. The three specially marked values of $X_t/m_{\tilde{t}}$ are used to define the m_h^{max} ($X_t = 2\, m_{\tilde{t}}$) and $m_h^{\text{mod},\pm}$ scenarios ($X_t = \pm 1.5\, m_{\tilde{t}}$, respectively). The other parameters are fixed at: $t_\beta = 10$, $\mu = 200$ GeV, $m_A = 500$ GeV, $m_{\tilde{\ell}_3} = m_{\tilde{\tau}_R} = m_{\tilde{b}_R} = 1000$ GeV, $A_b = A_\tau = 0$, $m_{\tilde{g}} = 1500$ GeV.

The maximal mass of the light Higgs boson h in the region of large m_A strongly depends on the stop-sector parameters $m_{\tilde{t}} \equiv m_{\tilde{q}_3} = m_{\tilde{t}_R}$ and $X_t = A_t - \mu/t_\beta$.

The dependence of m_h on $m_{\tilde{t}}$ and $X_t/m_{\tilde{t}}$ for degenerate soft-breaking parameters and sufficiently large $m_A = 500$ GeV, i. e. the light Higgs is SM-like, as depicted in Fig. 8.2 (the other parameters are given in the caption). For a fixed value of $m_{\tilde{t}}$ the dependence of the Higgs-boson mass m_{h_1} on $X_t/m_{\tilde{t}}$ has a local minimum at zero, local maxima at $\approx \pm 2$ and a steep gradient for larger $|X_t|/m_{\tilde{t}}$ (which is also depicted explicitly in Fig. 8.4). For a rising $m_{\tilde{t}}$ and fixed $X_t/m_{\tilde{t}}$ the mass quickly increases to its maximum value and slowly declines subsequently. This is an effect of the fixed-order calculation and is not found, if higher-order logarithms of the type $\log(m_{\tilde{t}}/m_t)$ are included [Hah+14]. The kinks correspond to thresholds for decays into gluinos.

The case with $X_t = 2\, m_{\tilde{t}}$ is named m_h^{max} scenario [Sch+06; Car+03; HHW00a]; more moderate cases for lower values of $X_t = \pm 1.5\, m_{\tilde{t}}$ have been proposed in Ref. [Car+13] and are named $m_h^{\text{mod},\pm}$ scenarios, respectively.

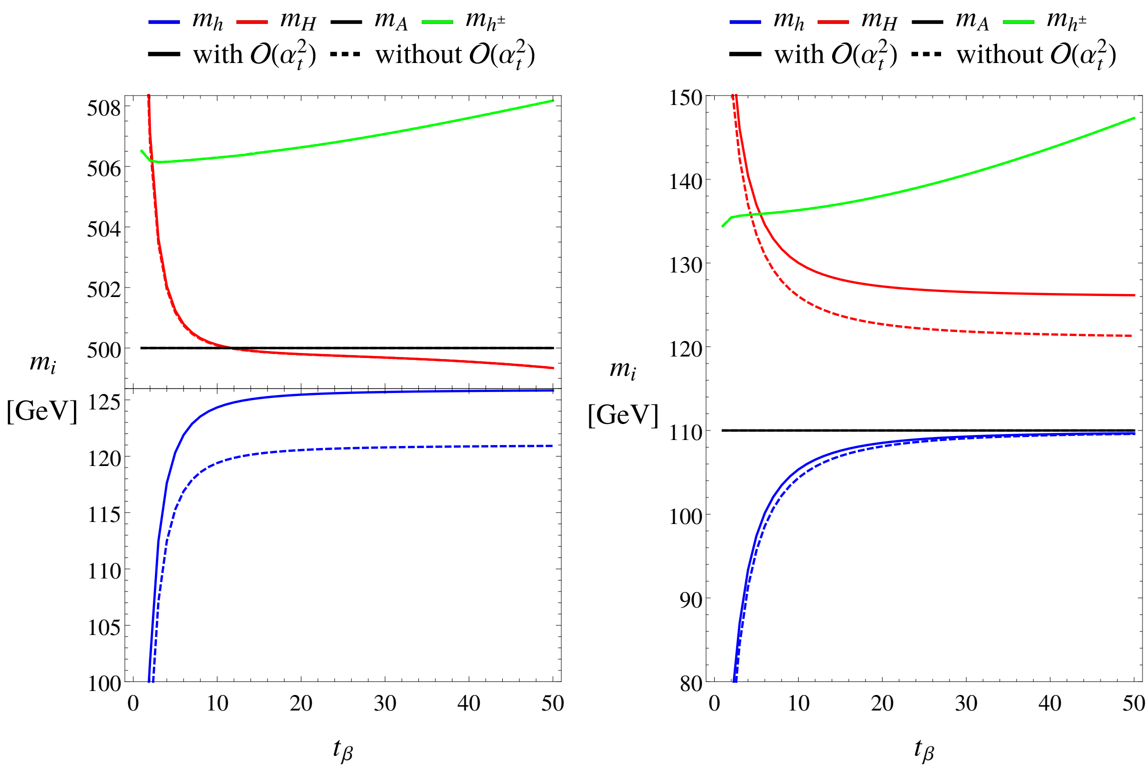

Figure 8.3.: The dependence of the Higgs-boson masses m_i, $i \in \{h, H, A, h^\pm\}$ on t_β with (straight) and without (dashed) the $\mathcal{O}(\alpha_t^2)$ contributions. Left: $m_A = 500$ GeV. Right: $m_A = 110$ GeV. The other parameters are fixed at: $m_{\tilde{q}_3} = m_{\tilde{t}_R} = m_{\tilde{b}_R} = 1000$ GeV, $\mu = 200$ GeV, $m_{\tilde{g}} = 1500$ GeV, $m_{\tilde{\ell}_3} = m_{\tilde{\tau}_R} = 1000$ GeV, $A_t = A_b = A_\tau = 1.5\, m_{\tilde{q}_3}$.

Another important parameter is t_β, which affects the values of m_h and m_H already at the tree level (cf. Eq. (6.28)). But also the loop contributions are influenced by t_β, e. g. by its appearance inside of the mass matrices of the sfermions in Eq. (3.9). As can be seen in Fig. 8.3, the influence of t_β on the mass predictions for h and H is strong, especially for low values. The effect on the heavy Higgs mass m_H is less pronounced for a larger input of m_A. Depending on the specific parameters the $\mathcal{O}(\alpha_t^2)$ terms are important for a precise prediction of m_h or m_H or both.

Comparison with a previous result

A previous analytic result of the $\mathcal{O}(\alpha_t^2)$ contributions to the neutral Higgs-boson masses in the real MSSM already exists from a calculation making use of the effective-potential method [Bri+02]. The version of `FeynHiggs` for real parameters has this result included, making thus a direct comparison with the prediction of the new diagrammatic calculation possible. Thereby all parameters and renormalization have been adapted to agree with Ref. [Bri+02], i. e. the A-boson mass is used as input quantity and renormalized on-shell as explained in Section 7.4.2, and $\delta^{(1)} s_\mathrm{w}$ is absorbed by the corrections to the Fermi constant G_F as described in Section 7.4.3.

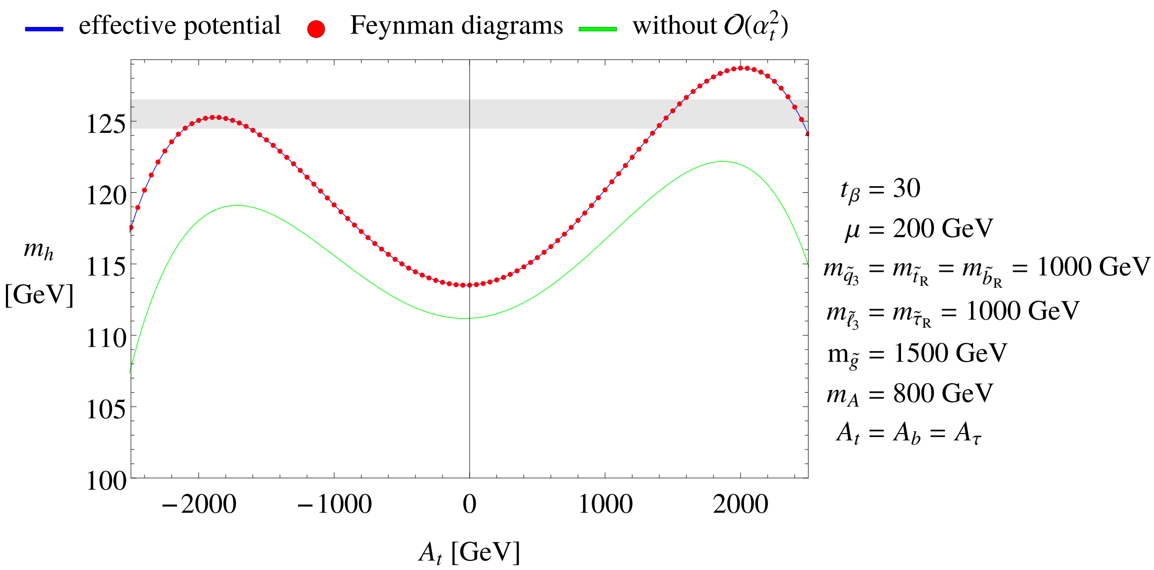

Figure 8.4.: Comparison of the results for the light Higgs-boson mass evaluated in the effective potential approach (blue) and the Feynman-diagrammatic approach (red). For reference the result without the $\mathcal{O}(\alpha_t^2)$ contributions is shown (green). The gray area depicts the mass range between 124.5 GeV and 126.5 GeV.

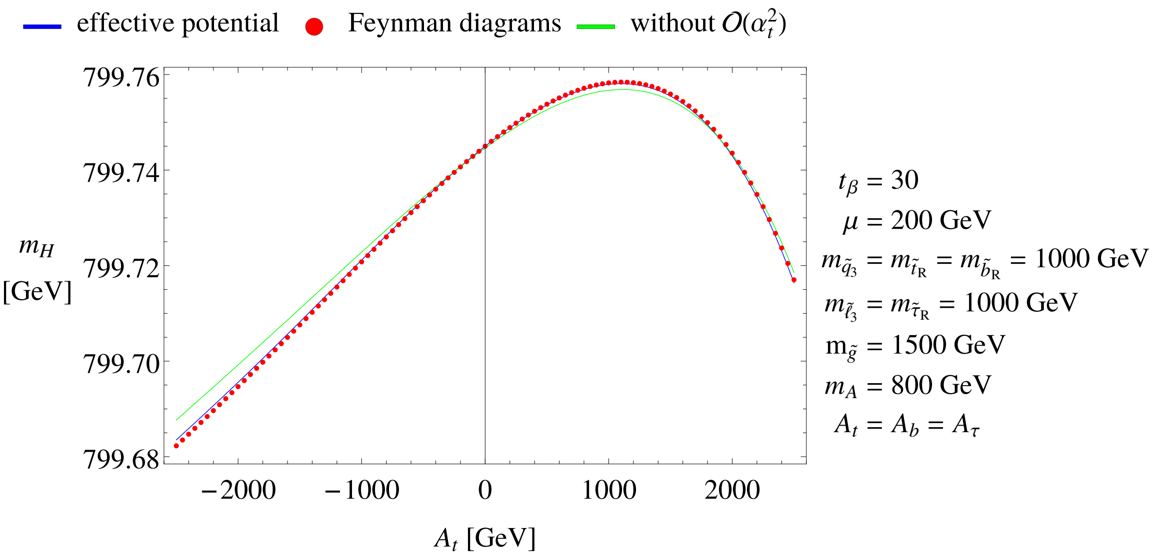

Figure 8.5.: Comparison of the results evaluated in the effective potential approach (blue) and the Feynman-diagrammatic approach (red) for the heavy Higgs-boson mass. For reference the result without the $\mathcal{O}(\alpha_t^2)$ contributions is shown (green).

Very good agreement is found between the two results that have been obtained in completely independent ways. As an example, this feature is displayed in Fig. 8.4, where the shift of the light Higgs-boson mass by the $\mathcal{O}(\alpha_t^2)$ terms in the two approaches is shown on top of the mass prediction without these terms. The gray band depicts the mass range 125.5 ± 1 GeV around the Higgs signal measured by ATLAS and CMS. The mass shifts displayed in Fig. 8.4 underline the importance of the two-loop top-Yukawa contributions for a reliable prediction of the light Higgs boson mass.

In Fig. 8.5 the mass shift for the heavy Higgs boson is depicted for the same parameters. It is in general small and also the variation with A_t is below 0.1 GeV which is an immediate consequence of the suppressed couplings of the heavy Higgs boson in this region. Nevertheless the very good agreement of the Feynman diagrammatic and the effective potential approach is emphasized again. The very small deviation for large $|A_t|$ is inside the limits of the computational accuracy.

Inverted Higgs-boson mass hierarchy

A possibility to interpret the measured Higgs-like state around 125.5 GeV as the heavy Higgs boson H has been pointed out in Refs. [HSW12; Ben+12; BFS12].

To arrange the mass m_H in an appropriate intervall, the input parameter m_A also has to be low as can be seen in Fig. 8.1. In that case the charged Higgs boson becomes light, too; the light CP-even Higgs-boson mass m_h becomes very low, which introduces the name m_h^{low} scenario for this case. Thereby h has strongly suppressed couplings to gauge bosons thus having been invisible for past experiments. Despite strong constraints by experimental data on the allowed parameter space of the MSSM in this scenario [col13a; col13b], it cannot be excluded yet as is shown in the following.

In Ref. [Car+13] this case is labeled differently as "low-M_H scenario". Therein two allowed parameter regions are identified: one for $t_\beta \approx 5.5$, $\mu \approx 1500$ GeV and one for $t_\beta \approx 7.5$, $\mu \approx 2800$ GeV. The available range for t_β is constrained from above by Higgs-to-τ^+-τ^- searches at the LHC and from below by searches for a charged Higgs boson or the LEP experiment. Furthermore strong experimental bounds exist in the $t_\beta(m_A)$ and $t_\beta(m_{H^\pm})$ plane which are however only given for Higgs cross sections evaluated in the m_h^{max} scenario. Nevertheless, the A-boson mass is kept as light as possible to meet the limits of CMS [col13a]. Also the resulting charged Higgs-boson mass is chosen to be heavier than 140 GeV which is the current limit of ATLAS [col13b]. For large μ the latter requirement becomes more difficult to achieve due to the negative $\mathcal{O}(\alpha_t^2)$ contributions to the charged Higgs-boson mass; this effect is explained in more detail in Section 8.3.

Both parameter regions which are mentioned above are depicted in Fig. 8.6 with a degenerate stop soft-breaking value $m_{\tilde{t}} \equiv m_{\tilde{t}_\text{L}} = m_{\tilde{t}_\text{R}}$ varied at the vertical axis and the quantity $X_t/m_{\tilde{t}}$ varied at the horizontal axis. The red (yellow) band shows the $125.5 \pm 2\,(\pm 3)$ GeV contour for the mass of the heavy CP-even state m_H. This range corresponds to an estimated theoretical uncertainty of the light Higgs-boson mass due to presently not calculated two-loop and three-loop contributions [Deg+03]; it is assumed to also be valid for m_H in the m_h^{low} scenario. The blue (light-blue) region indicates a charged Higgs-boson mass of more than 140 (138) GeV at higher orders (cf. Section 8.3). The parameter region which fits the constraints best is found in the intersection of the blue and red regions. As can be seen there are two possibilities in each case: a very large $X_t \approx 2.5\, m_{\tilde{t}}$ and a moderate negative X_t. For the upper plot in Fig. 8.6 only a narrow band is allowed for $m_{\tilde{t}}$ at the low-A_t region due to the strong gradient for the Higgs mass m_H at very low t_β. In contrast, for the lower plot of Fig. 8.6 the high-A_t region is constrained by the low value of the charged Higgs-boson mass.

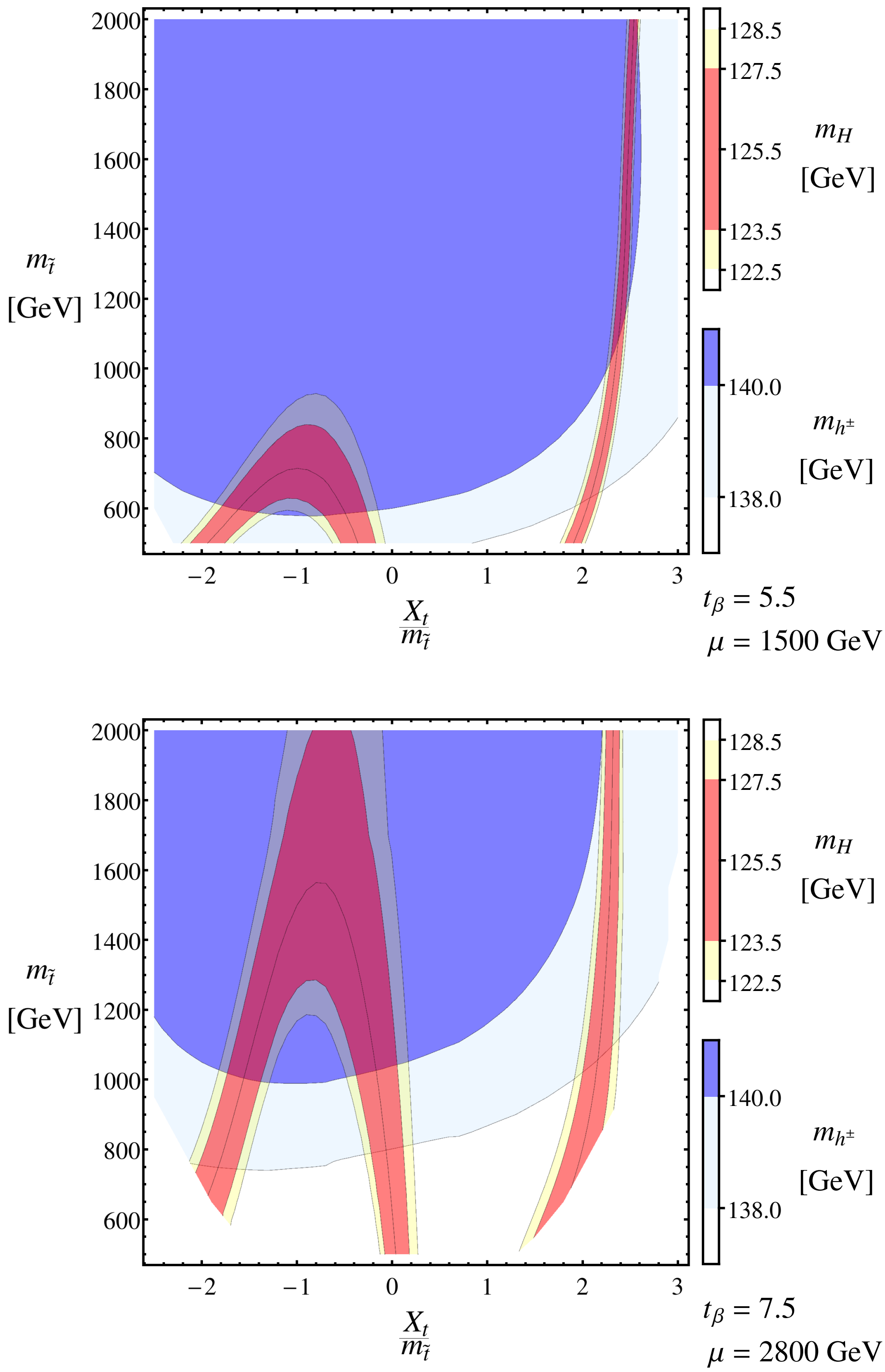

Figure 8.6.: Contour plots for the dependences of m_H and $m_{h^\pm}$ on $X_t/m_{\tilde{t}}$ and $m_{\tilde{t}} \equiv m_{\tilde{q}_3} = m_{\tilde{t}_R}$ are shown. The red (yellow) band indicates where H can be interpreted as the experimentally measured Higgs-like particle with a mass of $m_H = 125.5 \pm 2\,(\pm 3)$ GeV. The blue area shows the mass of the charged Higgs boson with contours at $m_{h^\pm} = 140$ GeV and $m_{h^\pm} = 138$ GeV. Two different parameter regions are shown as derived in Ref. [Car+13]. Up: $t_\beta = 5.5$, $\mu = 1500$ GeV. Down: $t_\beta = 7.5$, $\mu = 2800$ GeV. The other parameters are $m_{\tilde{g}} = 1500$ GeV, $A_b = A_\tau = 0$, $m_{\tilde{b}_R} = m_{\tilde{\ell}_3} = m_{\tilde{\tau}_R} = 1000$ GeV.

8.2. Neutral Higgs masses in the complex MSSM

In the following, the MSSM parameters A_t, μ and $m_{\tilde{g}}$ are considered as complex-valued quantities. In this case also $\hat{\Sigma}^{(j)}_{hA}$ and $\hat{\Sigma}^{(j)}_{HA}$, $j \in \{1, 2\}$ contribute to the self-energy matrices in Eq. (6.37a), thus all neutral lowest-order Higgs bosons h, H and A mix at higher orders in general. The resulting masses m_{h_1}, m_{h_2} and m_{h_3} are acquired from the p^2-dependent Eq. (6.38) and sorted in the order $m_{h_1} < m_{h_2} < m_{h_3}$. Accordingly, the charged Higgs-boson mass $m_{H^\pm}$ is chosen as an input parameter and renormalized on-shell at higher orders.

8.2.1. Comparison with a previous interpolation

Until now, the $\mathcal{O}(\alpha_t^2)$ terms were not available for complex parameters. Instead, in the present version of `FeynHiggs`, the dependence of the $\mathcal{O}(\alpha_t^2)$ contributions on the phases ϕ_{A_t} and ϕ_μ is approximated by an interpolation between the real results for the phases 0 and $\pm\pi$ [Hah+07; Hah+09].

A comparison with the full diagrammatic calculation yields deviations that can be notable, in particular for large $|A_t|$ and large μ. Fig. 8.7 displays the quality of the interpolation as a function of ϕ_{A_t} and shows that the deviations become more pronounced with rising μ, which is kept real. Also the admixture of the CP-odd part in h_1 is increasing with μ, but in the depicted parameter range it is in general small, below 2%. The asymmetric behaviour with respect to ϕ_{A_t} is caused by the phase of the gluino mass in the $\mathcal{O}(\alpha_t\alpha_s)$ contributions. The shaded area again illustrates the range from 124.5 GeV to 126.5 GeV.

However a caveat has to be issued: since $m_{H^\pm}$ is used as an input in the case of complex parameters, it is also renormalized on-shell; in particular, for the $\mathcal{O}(\alpha_t^2)$ corrections Eqs. (7.13) have to be used. Accordingly, the counterterms for the A-boson mass at the one-loop and two-loop level are determined by Eq. (6.64) and Eq. (6.80), respectively. Particularly, the genuine mass counterterms in Eq. (7.9c) and Eq. (7.10c) have to be used as input for Eq. (7.8c) to renormalize the $\mathcal{O}(\alpha_t^2)$ contributions to $\Sigma^{(2)}_A$ in Eq. (7.6a), i. e. the explicit expressions for the $\mathcal{O}(\alpha_t^2)$ contributions to $\Sigma^{(2)}_{H^\pm}$ are required. However, the previous result of the $\mathcal{O}(\alpha_t^2)$ corrections in the effective potential approach is only available for m_A being renormalized on-shell, especially the contributions to the charged Higgs-boson self-energy are not contained in `FeynHiggs` (instead the terms of the A-boson self-energy are used). Thus, by

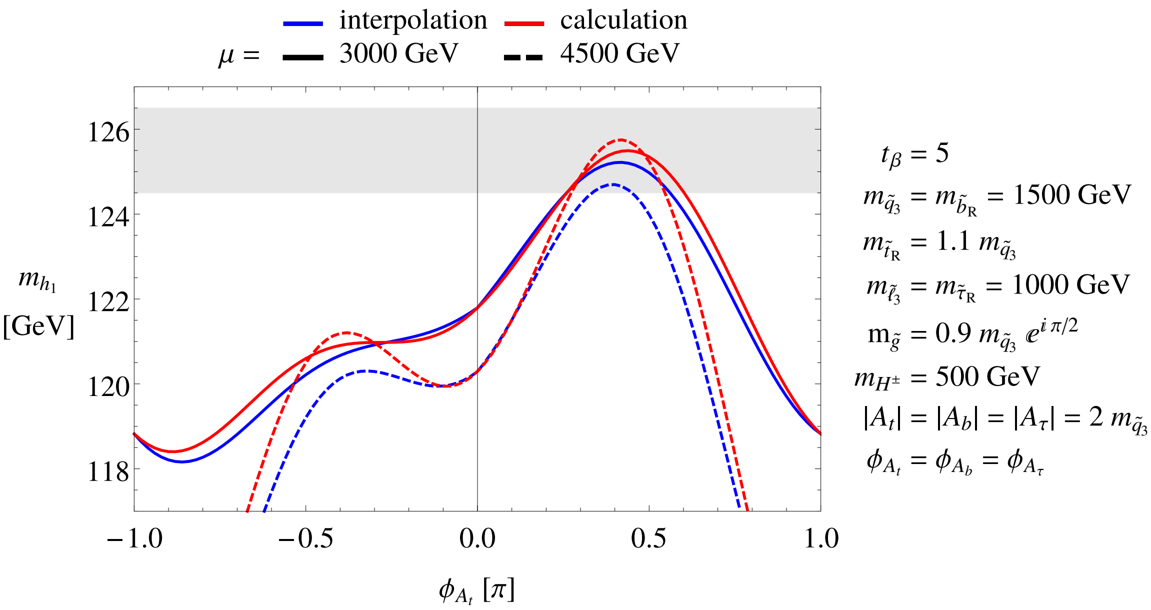

Figure 8.7.: The result for m_{h_1} in the diagrammatic calculation (red), in comparison with the approximate result from an interpolation between the phases $\phi_{A_t} = 0, \pm\pi$ (blue) for different values of a real μ. The gray area depicts the mass range between 124.5 GeV and 126.5 GeV.

using the interpolation in `FeynHiggs` the renormalized self-energies are calculated incorrectly, whenever the $\mathcal{O}(\alpha_t^2)$ terms in the difference $\Sigma_A^{(2)} - \Sigma_{H^\pm}^{(2)}$ are large. The depicted example in Fig. 8.7 is situated in a parameter region where the heavy Higgs bosons practically do not mix with h, i. e. renormalization of either m_A or $m_{H^\pm}$ has a negligible influence on the prediction of m_{h_1}.

This is not the case for the other two neutral Higgs bosons in this scenario. In Fig. 8.8 the masses m_{h_2} (red) and m_{h_3} (green) are depicted for the Feynman diagrammatic calculation (straight) and for the effective potential interpolation (dashed) on top of the result without the $\mathcal{O}(\alpha_t^2)$ contributions (dotted). A clear deviation between the two different calculations is visible and even for the case of real parameters at $\phi_{A_t} = 0, \pm\pi$ big shifts occur, originating from the different renormalization schemes[15] (the size is controlled by μ as is illustrated in Section 8.3); and moreover these deviations are passed on to the lightest Higgs-boson mass as soon as large mixings between h and H, A occur. In the present scenario, close to the real values of A_t the masses m_{h_2} and m_{h_3} can be identified as the masses of H and A, respectively. For a large imaginary part of A_t the situation is vice versa because of a strong CP-mixing. This feature is illustrated in Section 8.2.2.

[15]Similar effects have been observed in the calculation of the $\mathcal{O}(\alpha_t\alpha_s)$ corrections [Fra+13].

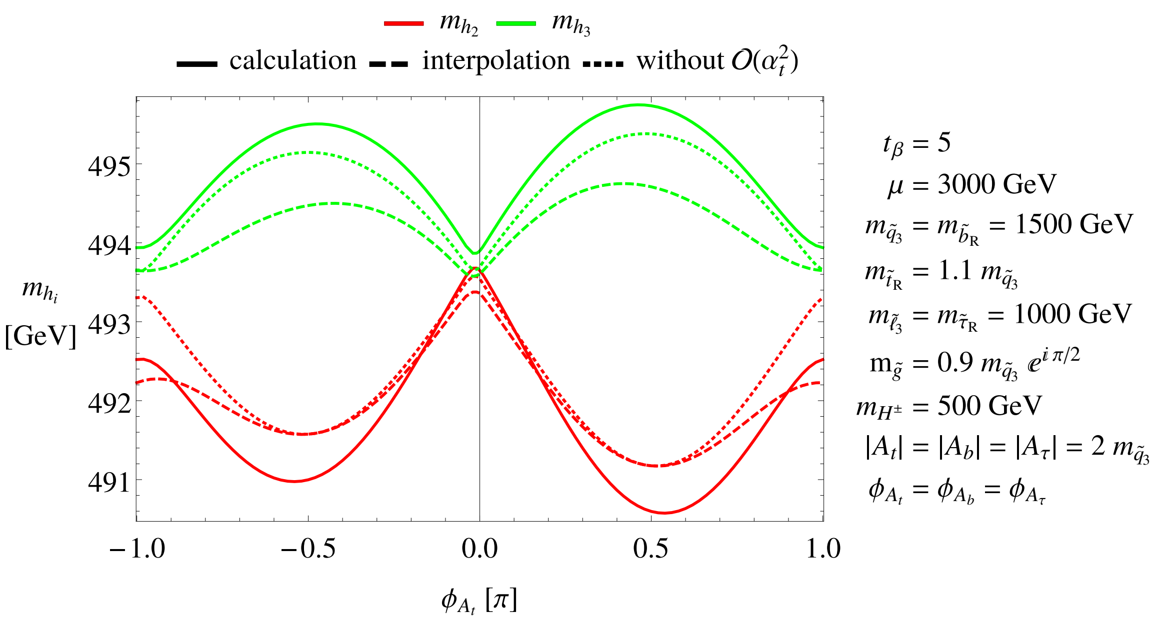

Figure 8.8.: Results for m_{h_2} (red) and m_{h_3} (green) in the diagrammatic calculation (straight) in comparison with the approximate result from an interpolation between the phases $\phi_{A_t} = 0, \pm\pi$ (dashed). For reference the result without the $\mathcal{O}(\alpha_t^2)$ terms is shown (dotted).

8.2.2. *CP*-mixing

As mentioned before, all three neutral lowest-order Higgs bosons, i. e. the CP-even h and H, and the CP-odd A, in general mix at higher orders. They are no mass eigenstates and in general CP-mixed states. Furthermore, the mixing of h, H and A is p^2-dependent, hence also the CP-violating mixing features depend on the external momentum.

A convenient approximation for the discussion of the CP-mixing is given by assuming $p^2 = 0$ in the renormalized self-energies of the Higgs bosons. In this case, Eq. (6.38) simplifies to the eigenvalue equation for the matrix $\mathbf{M}^{(2)}_{hHAG}(0)$ in Eq. (7.6a). The real mixing matrix which diagonalizes $\mathbf{M}^{(2)}_{hHA}(0)$, i. e. the upper-left (3×3) submatrix of $\mathbf{M}^{(2)}_{hHAG}(0)$ neglecting mixings with the Goldstone boson, is denoted as $\mathbf{U}_H$ in the following. It allows to define an approximate mass-eigenstate basis according to

$$\begin{pmatrix} h_1 \\ h_2 \\ h_3 \end{pmatrix} = \mathbf{U}_H \begin{pmatrix} h \\ H \\ A \end{pmatrix}, \quad \mathbf{U}_H = \begin{pmatrix} U_{H,11} & U_{H,12} & U_{H,13} \\ U_{H,21} & U_{H,22} & U_{H,23} \\ U_{H,31} & U_{H,32} & U_{H,33} \end{pmatrix}. \tag{8.1}$$

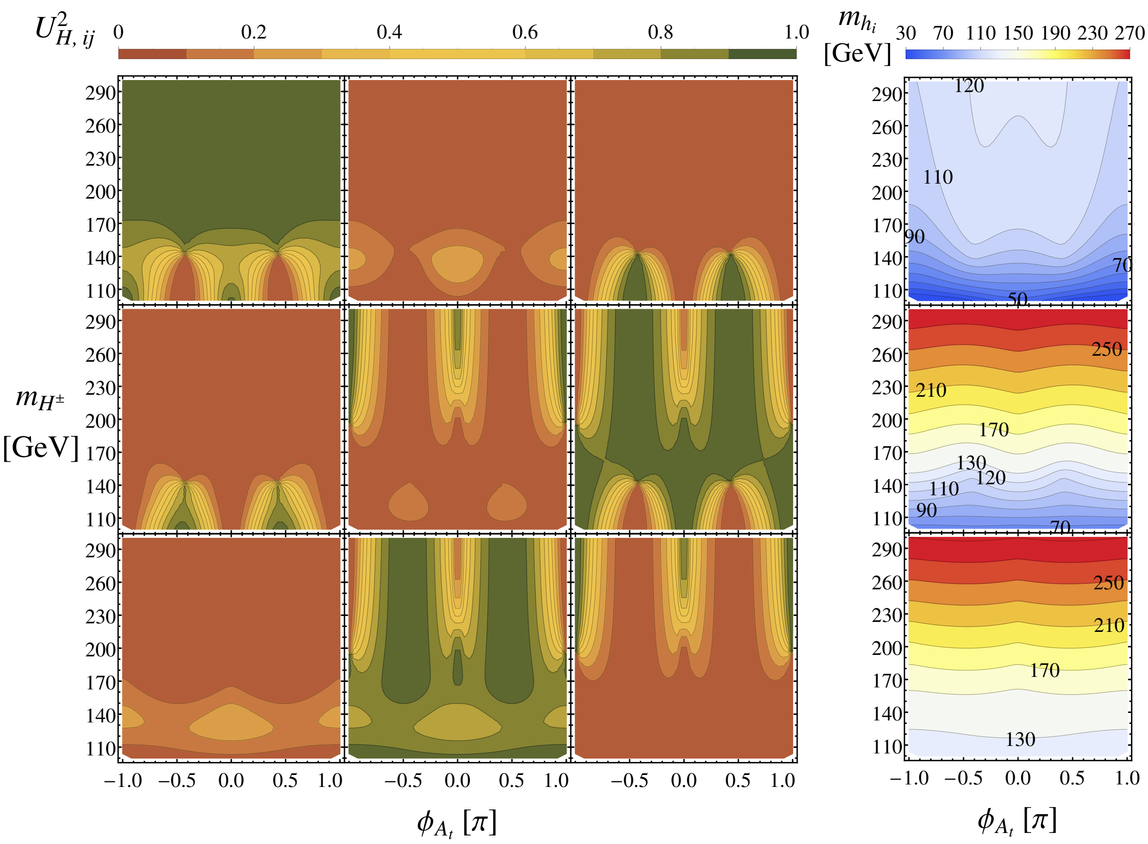

Figure 8.9.: The mixing-matrix elements squared $U^2_{H,\,ij}$, $i, j \in \{1,\, 2,\, 3\}$ (left) and masses m_{h_i} (right), where i is the index of the row and j is the index of the column, are illustrated with the phase ϕ_{A_t} and the input mass $m_{H^\pm}$ being varied. The color coding is explained in the labels at the top of the figures; for convenience some contours of the mass plots are signed with their corresponding mass values. The input parameters are fixed at $\mu = 2000$ GeV, $t_\beta = 5$, $m_{\tilde{\ell}_3} = m_{\tilde{\tau}_R} = 1000$ GeV, $m_{\tilde{q}_3} = m_{\tilde{t}_R} = m_{\tilde{b}_R} = 1000$ GeV, $|A_t| = |A_b| = |A_\tau| = 2\, m_{\tilde{q}_3}$, $m_{\tilde{g}} = 1500$ GeV.

In general, the h_i, $i \in \{1,\, 2,\, 3\}$ are no longer CP-eigenstates since they are composed of the tree-level CP-even bosons h and H and the tree-level CP-odd boson A. The squared elements $U^2_{H,\,i3}$ of Eq. (8.1) tell the amount of the A boson inside of $h_i = U_{H,\,i1}\, h + U_{H,\,i2}\, H + U_{H,\,i3}\, A$.

The dependence of the mixing-matrix elements squared $U^2_{H,\,ij}$ and the Higgs-boson masses m_{h_i} on the input value of the charged Higgs-boson mass $m_{H^\pm}$ and the basically unconstrained complex phase ϕ_{A_t} [FO96] is presented in Fig. 8.9. Thereby the tiles on the left-hand side are ordered according to the matrix form of $U^2_{H,\,ij}$, i and j being the indices of the row and the column, respectively. The masses m_{h_i} on the right-hand side are in ascending order from the first to the third row.

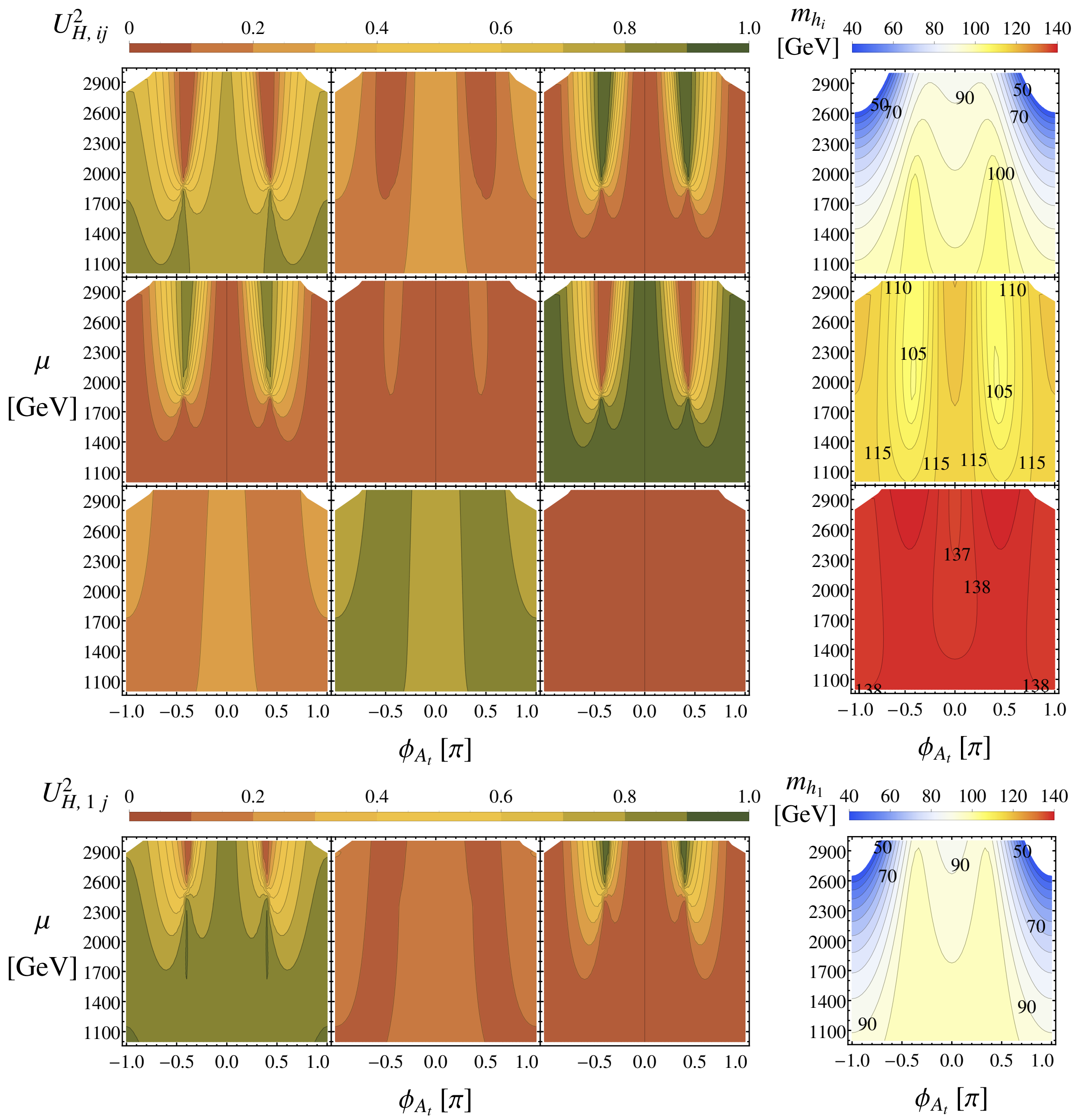

Figure 8.10.: The mixing-matrix elements squared $U^2_{H,ij}$, $i, j \in \{1, 2, 3\}$ (up left) and masses m_{h_i} (up right), where i is the index of the row and j is the index of the column, are illustrated with the phase ϕ_{A_t} and the real-valued μ being varied. For comparison the mixing-matrix elements squared $U^2_{H,1j}$, $j \in \{1, 2, 3\}$ (down left) and mass m_{h_1} (down right) are depicted without the contributions of the $\mathcal{O}(\alpha_t^2)$ terms. The color coding is explained in the labels at the top of the figures; for convenience some contours of the mass plots are signed with their corresponding mass values. The input parameters are fixed at $m_{H^\pm} = 140$ GeV, $t_\beta = 5$, $m_{\tilde{\ell}_3} = m_{\tilde{\tau}_R} = 1000$ GeV, $m_{\tilde{q}_3} = m_{\tilde{t}_R} = m_{\tilde{b}_R} = 1000$ GeV, $|A_t| = |A_b| = |A_\tau| = 2\,m_{\tilde{q}_3}$, $m_{\tilde{g}} = 1500$ GeV.

Whenever two masses $m^2_{h_i}$ and $m^2_{h_j}$ are close to each other or even equal, the $U^2_{H,ij}$ change from zero to one very quickly, i. e. two fields h_i and h_j interchange their meaning. For a large charged Higgs mass the lightest Higgs h_1 is basically equal to h. In contrast, the heavier Higgs bosons can be composed of H and A in all possible variations, depending on the phase, thus yielding the possibility of very large CP-mixing. Especially eye-catching are the nodal points close to the real values of A_t for $\phi_{A_t} = \pm\pi$ and $m_{H^\pm} \approx 205$ GeV. They correspond to the parameter points where the masses of h_2 and h_3 are equal; slightly above or below the nodes h_2 and h_3 can exactly be identified as H or A. A similar, but not as strong, effect is visible close to the real value of A_t for $\phi_{A_t} \approx 0$. Besides this special situations, h_3 is mostly composed of H. At $m_{H^\pm} \approx 170$ GeV an extreme situation is observed: each h_i is almost equal to h, H or A for any complex phase. However the situation changes for low input values of $m_{H^\pm}$ where a large admixture of A to the lightest Higgs boson h_1 is predicted, depending on the complex phase ϕ_{A_t}. In the same parameter range the heaviest state h_3 is nearly CP-even for any phase. The strongest gradients for the mixing of h and A to h_1 and h_2 appear at $\phi_{A_t} \approx \pm 0.4$ and $m_{H^\pm} \approx 140$ GeV; for the present choice of parameters the masses m_{h_1} and m_{h_2} come closest to each other at this points.

Another interesting feature is the dependence of CP-mixing on the higgsino-mass parameter μ. For the input value $m_{H^\pm} = 140$ GeV the dependence on a real μ is depicted in Fig. 8.10. Thereby the mixing-matrix elements squared and masses use the same conventions as in Fig. 8.9. As can be seen, μ has to be large to induce varying mixing effects for different complex phases ϕ_{A_t}. In the whole depicted parameter range h_3 essentially consists of H and the admixture of A to h_3 is practically negligible. However big gradients can be seen in the other mixings which have the same origin as in Fig. 8.9 and which appear again at the phases $\phi_{A_t} \approx \pm 0.4$: here the difference of the masses m_{h_1} and m_{h_2} becomes very small. For a comparison of the result with and without the $\mathcal{O}(\alpha_t^2)$ terms the latter is depicted for the lightest Higgs boson h_1 in the lower two tiles of Fig. 8.10. Apparently, the regions with a large gradient in the mixing are shifted by the $\mathcal{O}(\alpha_t^2)$ contributions to lower values of μ. Besides that, the mixing-matrix elements squared without the $\mathcal{O}(\alpha_t^2)$ contributions are smaller in the whole parameter region; this is a consequence of the additional dependence on the stop sector (and therefore on ϕ_{A_t}), which is introduced by the $\mathcal{O}(\alpha_t^2)$ corrections. However, the general phase dependence of the mixing-matrix elements squared for large values of μ remains the same, even though their extreme points are shifted to slightly higher $|\phi_{X_t}|$ by the new contributions.

8.2.3. Inverted Higgs-boson mass hierarchy

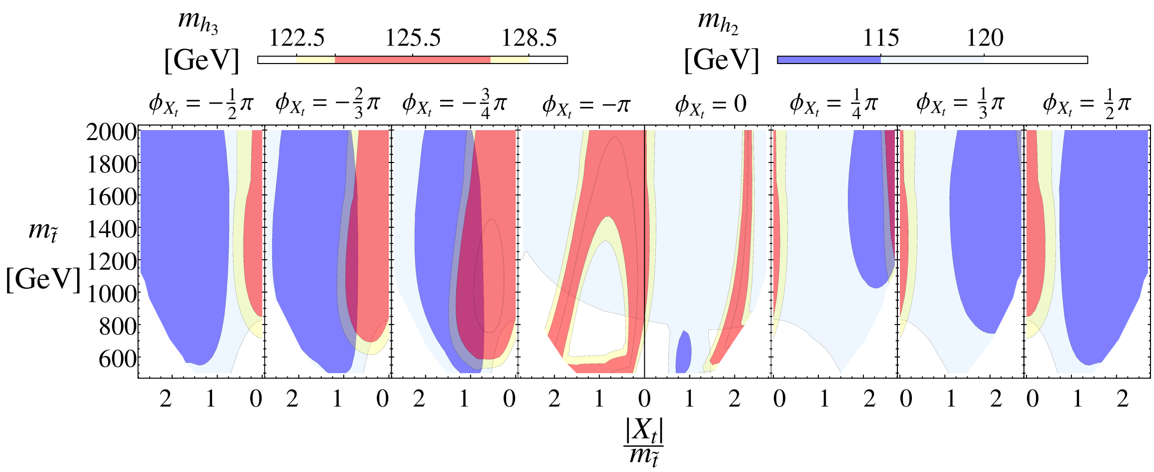

Figure 8.11.: Contour plots for the dependences of m_{h_2} and m_{h_3} on $|X_t|/m_{\tilde{t}}$ and $m_{\tilde{t}} \equiv m_{\tilde{q}_3} = m_{\tilde{t}_R}$ are shown. The red (yellow) band indicates where m_{h_3} has a value of $m_{h_3} = 125.5 \pm 2(\pm 3)$ GeV. The blue (light-blue) area shows the mass m_{h_2} of the other heavy Higgs boson with contours at $m_{h_2} = 115\,(120)$ GeV. The charged Higgs-boson mass is an input parameter and fixed at $m_{H^\pm} = 140$ GeV. The color coding is given at the top of the figure. Here the parameter region at $t_\beta = 7.5$, $\mu = 2800$ GeV is shown with the complex phase of X_t varied as indicated at the top of each tile. The other input parameters are $m_{\tilde{b}_R} = m_{\tilde{\ell}_3} = m_{\tilde{\tau}_R} = 1000$ GeV, $A_b = A_\tau = 0$, $m_{\tilde{g}} = 1500$ GeV.

In analogy to the real MSSM, the m_h^{low} scenario can also be investigated in the case of complex parameters. To arrange for low masses of the heavy neutral Higgs bosons, the input value $m_{H^\pm}$ has to be small.

As has been pointed out in Section 8.2.2 all neutral lowest-order Higgs bosons mix at higher orders, in general violating CP-symmetry. The experimentally measured Higgs-like particle with a mass of ≈ 125.5 GeV has been shown to be at most 68% CP-odd [DM13]. In Fig. 8.9 it can be seen that the Higgs boson h_3 is the one which corresponds best to a CP-even boson for a low input of $m_{H^\pm}$. Thus, the possibility of $m_{h_3} \approx 125.5$ GeV is investigated in the following.

Imposing the additional constraints $m_{h_2} < 120$ GeV and $m_{H^\pm} > 140$ GeV to fulfill the current experimental bounds, leaves only one of the two scenarios that were discussed in the real case: $t_\beta \approx 7.5$ and $\mu \approx 2800$ GeV. In the other scenario either m_{h_2} or m_{h_3} is too large in the depicted parameter range.

In Fig. 8.11 the dependences of m_{h_2} and m_{h_3} on $|X_t|/m_{\tilde{t}}$ and $m_{\tilde{t}} \equiv m_{\tilde{q}_3} = m_{\tilde{t}_\mathrm{R}}$ are illustrated for different phases ϕ_{X_t}. Compared to the case with real parameters only the possibility for small values of $|X_t|$ remains; the former available large-$|X_t|$ region is shifted to even higher values. However, due to the additional mixing with the third neutral Higgs boson a larger range for the stop-mass parameter $m_{\tilde{t}} \equiv m_{\tilde{q}_3} = m_{\tilde{t}_\mathrm{R}}$ is allowed now. The regions which agree best with the conditions that are imposed on m_{h_2} and m_{h_3} are the overlapping red and blue areas. Hence, the preferred ϕ_{X_t} is found to be close to $-3\pi/4$. In contrast, phases close to zero result in difficulties to fulfill both conditions at the same time for the investigated parameter space. The outer-most tiles are mirrored since the results only depend on $|\phi_{X_t}|$ for the chosen parameters. Furthermore, the tiles with a phase difference of π are continuous in $|X_t|$ if they were combined at the origin. Also very remarkable are the heavy changes of the mass predictions between the phases zero and $\pi/4$ on the one hand and between the phases $-\pi$ and $-3\pi/4$ on the other hand, compared to the small changes among all the other tiles.

8.2.4. Scenario with a complex-valued μ

In this section the dependence of the mass predictions on the complex phase ϕ_μ of the bilinear superpotential parameter μ is investigated. In the $\mathcal{O}(\alpha_t^2)$ terms the phase appears in the mixing matrices of the higgsinos and along with μ in the couplings of top squarks and their mixing matrices. Although strong constraints by electric dipole moments exist on ϕ_μ [MS97] the regions close to real values are still allowed [BGK99; Brh+99] and therefore of special interest.

Again, pronounced effects are found in the m_h^low scenario; for larger input values of $m_{H^\pm}$ the mass shifts induced by small phases of μ are tiny for each neutral Higgs boson. The investigated parameter range is illustrated in Fig. 8.12 for phases $\phi_\mu \approx 0$ and in Fig. 8.13 for phases $\phi_\mu \approx \pi$. Fig. 8.12 contains contour plots for $\phi_\mu = 0$ and $\phi_\mu = \pi/5$ and Fig. 8.13 contains contour plots for $\phi_\mu = \pi$ and $\phi_\mu = 4\pi/5$. The varied parameters are $X_t/m_{\tilde{t}}$, with $m_{\tilde{t}} \equiv m_{\tilde{q}_3} = m_{\tilde{t}_\mathrm{R}}$, on the horizontal axis, and $|\mu|$ on the vertical axis. In each case the complex phase of X_t is set equal to zero, i. e. the parameter A_t is modified accordingly.

However, as can be seen in Fig. 8.14, the phase of A_t is close to 0 or π for any value of ϕ_μ as long as $|X_t|$ is sufficiently large compared to $|\mu|/t_\beta$. In contrast, for comparably low $|X_t|$ the phase ϕ_{A_t} has the opposite sign and a similar size as ϕ_μ.

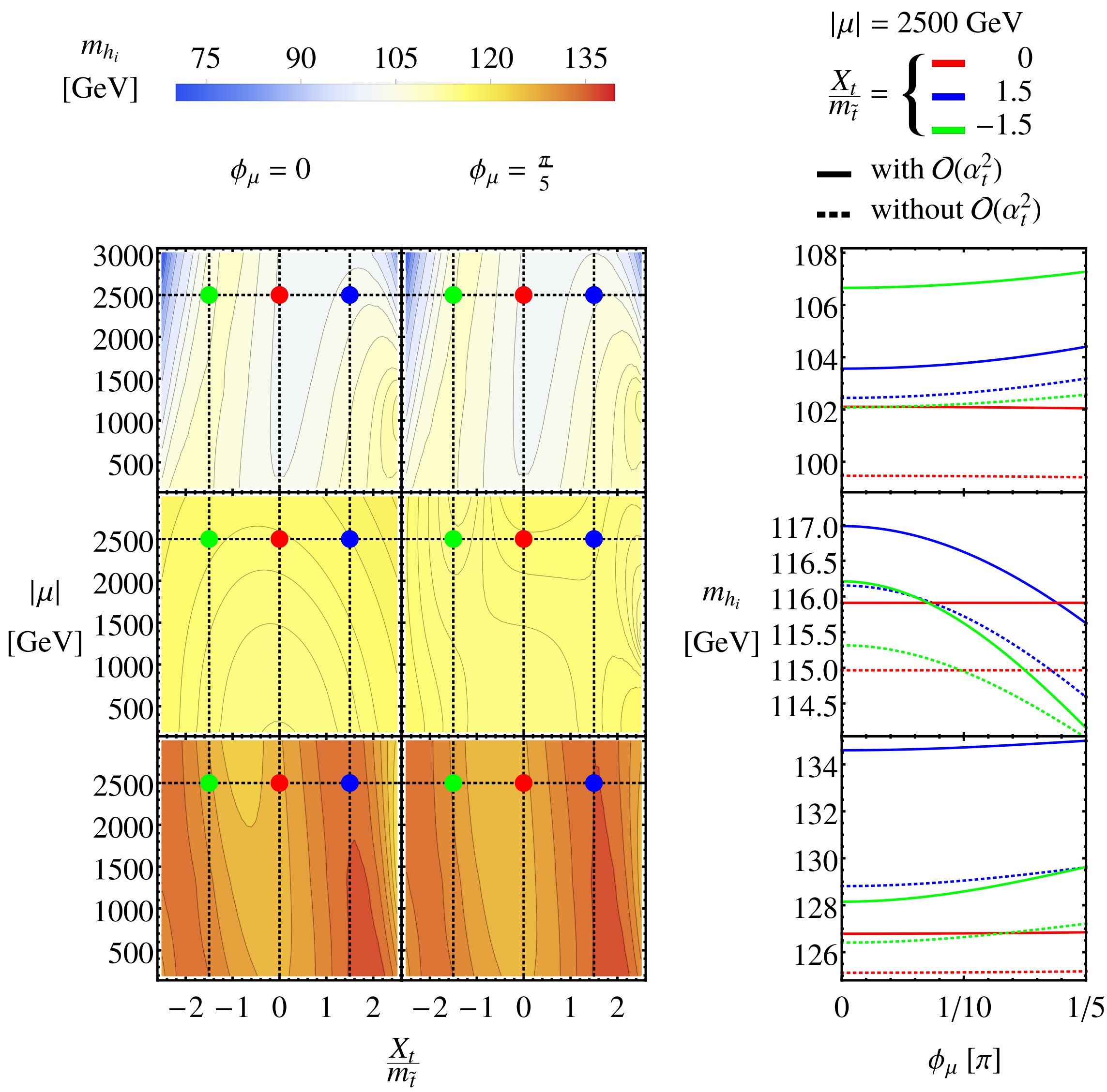

Figure 8.12.: Left: Contour plots for the scenario with a complex μ at low $\phi_\mu \approx 0$ are shown. The plots are arranged from top to bottom in ascending order of the neutral Higgs-boson masses. The color coding and the value of ϕ_μ is given above the tiles. The green, red and blue circles define the input parameters for the plots on the right. Right: The colors of the curves agree with their corresponding points inside the contour plots. The ordering of the masses is the same. The input parameters are $t_\beta = 7.5$, $m_{H^\pm} = 140$ GeV, $m_{\tilde{t}} \equiv m_{\tilde{q}_3} = m_{\tilde{t}_R} = m_{\tilde{b}_R} = 1500$ GeV, $m_{\tilde{\ell}_3} = m_{\tilde{\tau}_R} = 1500$ GeV, $A_b = A_\tau = 0$, $m_{\tilde{g}} = 1500$ GeV.

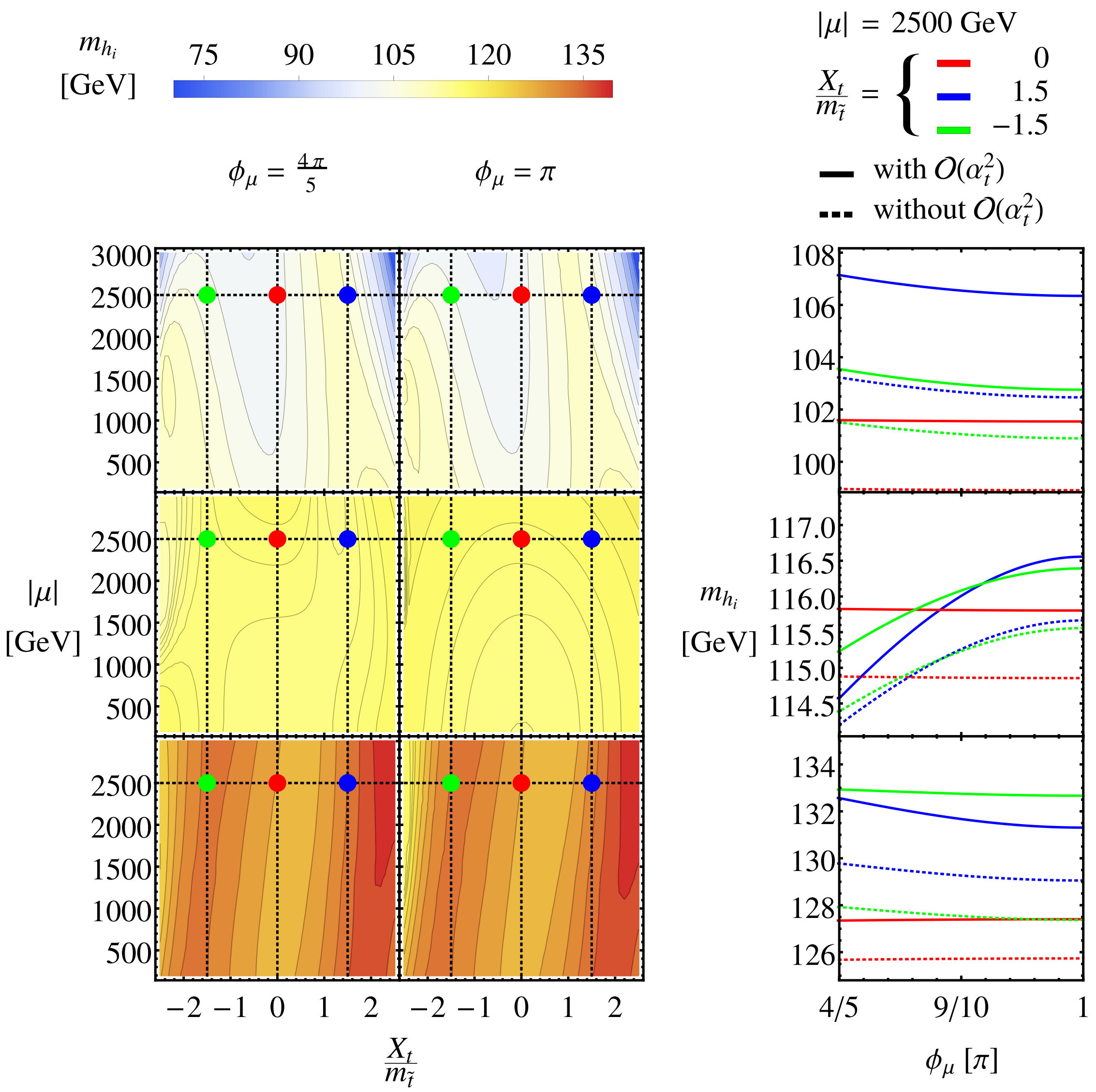

Figure 8.13.: Left: Contour plots for the scenario with a complex μ at high $\phi_\mu \approx \pi$ are shown. The plots are arranged from top to bottom in ascending order of the neutral Higgs-boson masses. The color coding and the value of ϕ_μ is given above the tiles. The green, red and blue circles define the input parameters for the plots on the right. Right: The colors of the curves agree with their corresponding points inside the contour plots. The ordering of the masses is the same. The input parameters are $t_\beta = 7.5$, $m_{H^\pm} = 140$ GeV, $m_{\tilde{t}} \equiv m_{\tilde{q}_3} = m_{\tilde{t}_R} = m_{\tilde{b}_R} = 1500$ GeV, $m_{\tilde{\ell}_3} = m_{\tilde{\tau}_R} = 1500$ GeV, $A_b = A_\tau = 0$, $m_{\tilde{g}} = 1500$ GeV.

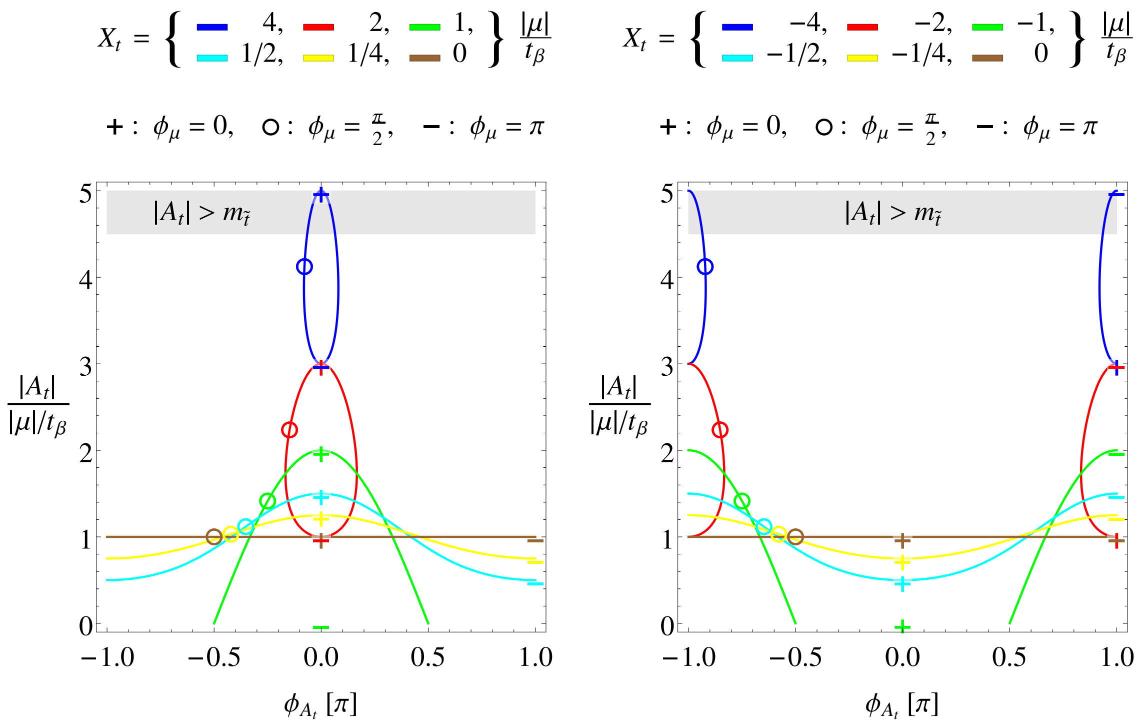

Figure 8.14.: The dependence of $|A_t|$ and ϕ_{A_t} on ϕ_μ is depicted for different real values of $X_t > 0$ (left) and $X_t < 0$ (right) with the color coding corresponding to the legend. Thereby ϕ_μ is varied between $-\pi$ and π yielding the curves. For your guidance the symbols $+$, $\circ$ and $-$, which are explained in the caption, are attached to each line. For some pairs of curves $+$ and $-$ are lying on top of each other. The cases $X_t = \pm\,|\mu|/t_\beta$ are special: for $\phi_\mu = \mp\pi$ the phase of A_t jumps to zero. The gray area illustrates the range of $|A_t| > m_{\tilde{t}}$. The input parameters are $t_\beta = 7.5$, $|\mu| = 2500$ GeV, $m_{\tilde{t}} \equiv m_{\tilde{q}_3} = m_{\tilde{t}_\mathrm{R}} = 1500$ GeV.

The rows of Fig. 8.12 and Fig. 8.13 are sorted from up to down in ascending order of the Higgs-boson masses m_{h_i} with their corresponding values given as indicated by the color coding in the legend. The dependence of m_{h_1} and m_{h_3} on $X_t/m_{\tilde{t}}$ mimics the result for the real case in Fig. 8.2 with two local maxima at $X_t \approx \pm 2\, m_{\tilde{t}}$ and one local minimum close to $X_t = 0$, whereas m_{h_2} shows just a shallow dependence on $X_t/m_{\tilde{t}}$ in the depicted range; only for a large complex μ stronger variations are visible. For low input values of $|\mu|$ none of the masses is significantly shifted by different phases ϕ_μ; however, the situation becomes different for increasing $|\mu|$. There is a tendency for a decreasing m_{h_1} with rising $|\mu|$, while m_{h_3} is decreasing for $\phi_\mu \approx 0$ and increasing for $\phi_\mu \approx \pi$ with rising $|\mu|$; as mentioned before, the case of m_{h_2} depends on the chosen phase.

Three special points are selected in each contour plot as illustrated by the red, blue and green spots with the coordinates $|\mu| = 2500$ GeV and $X_t = 0, \pm 1.5\, m_{\tilde{t}}$. On the right-hand sides of both figures the same color coding is used to show the dependence of the Higgs-boson masses m_{h_i} on the phase ϕ_μ at these three parameter points. Thereby the straight lines depict the results which include the $\mathcal{O}(\alpha_t^2)$ corrections, in contrast to the dotted lines. Since no visible shift occurs for $X_t = 0$ (red), but large shifts appear in the other cases for $X_t = 1.5\, m_{\tilde{t}}$ (blue) and $X_t = -1.5\, m_{\tilde{t}}$ (green), these effects must be induced by the μ-dependence of the stop sector; the contributing ϕ_μ-dependence of the higgsino mixing matrices is negligible in the depicted parameter range. The masses m_{h_1} and m_{h_3} are rising with an increasing imaginary part of μ, while m_{h_2} is falling.

8.3. Charged Higgs-boson mass in the real MSSM

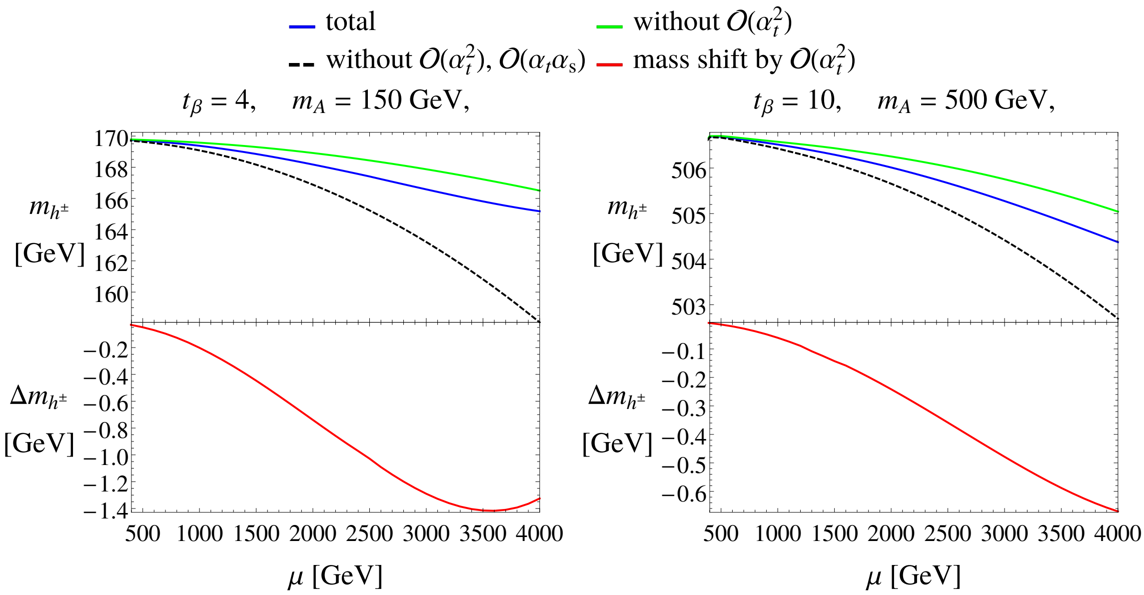

Figure 8.15.: In the upper parts of both plots, the prediction for the charged Higgs-boson mass $m_{h^\pm}$ including all known contributions (blue), without the $\mathcal{O}(\alpha_t^2)$ contributions (green) and without any two-loop corrections (black dashed) is depicted. In the lower parts of both plots, the mass shift $\Delta m_{h^\pm}$ by the $\mathcal{O}(\alpha_t^2)$ contributions is shown (red). Left: $t_\beta = 4$, $m_A = 150$ GeV. Right: $t_\beta = 10$, $m_A = 500$ GeV. The other input parameters are $m_{\tilde{q}_3} = m_{\tilde{t}_\mathrm{R}} = m_{\tilde{b}_\mathrm{R}} = 1000$ GeV, $m_{\tilde{\ell}_3} = m_{\tilde{\tau}_\mathrm{R}} = 1000$ GeV, $A_t = A_b = A_\tau = 1.5\, m_{\tilde{q}_3}$, $m_{\tilde{g}} = 1500$ GeV.

For the calculation of the $\mathcal{O}(\alpha_t^2)$ contributions to the neutral Higgs-boson masses in the complex MSSM the charged Higgs-boson mass $m_{H^\pm}$ has to be chosen as an input parameter and is renormalized on-shell accordingly. Therefore the $\mathcal{O}(\alpha_t^2)$ terms of the charged Higgs-boson self-energy have to be computed. They have been derived in this thesis and were not known before. In the real MSSM the A-boson mass m_A is conventionally chosen as an input parameter. In this case, the $\mathcal{O}(\alpha_t^2)$ self-energies contribute to the mass matrix of the charged Higgs bosons at higher orders according to Eq. (7.6b). The corresponding mass $m_{h^\pm}$ is derived via Eq. (6.39). The present status of the mass prediction for the charged Higgs bosons without the $\mathcal{O}(\alpha_t^2)$ contributions is described in Ref. [Fra+13].

The contributions to $m_{h^\pm}$ induced by the $\mathcal{O}(\alpha_t^2)$ corrections are small over a large parameter space. Two typical m_h^{mod} scenarios which are compatible with current exclusion limits are shown in Fig. 8.15. Above the black dashed line which shows the charged Higgs-boson mass including the one-loop corrections are the curves for the $\mathcal{O}(\alpha_t\alpha_s)$ contributions (green) and both known two-loop contributions comprising the $\mathcal{O}(\alpha_t^2)$ terms (blue). The sum of both two-loop corrections is lowered, i. e. the $\mathcal{O}(\alpha_t^2)$ corrections are negative (red). However, the total two-loop shift still yields a higher mass of the charged Higgs-boson compared to the one-loop result. For large values of μ the charged Higgs-boson mass $m_{h^\pm}$ becomes smaller, but the absolute value of the mass shift $\Delta m_{h^\pm}$ which is induced by the $\mathcal{O}(\alpha_t^2)$ contributions becomes larger. In the scenario with a large m_A (right) the top-Yukawa corrections are smaller compared to the scenario with a low m_A (left).

9. Conclusions

The discovery of a Higgs-like particle with a mass around 125.5 GeV [Cha+14; Aad+14] at the LHC by the experiments ATLAS [Aad+12] and CMS [Cha+12a] has initiated intensive efforts in improving the theory predictions for the Higgs-boson mass of various models. Therefore, higher-order corrections in perturbation theory are an important tool.

The main subject of this thesis is the Feynman-diagrammatic computation and analysis of the top-Yukawa-coupling enhanced two-loop contributions of $\mathcal{O}(\alpha_t^2)$ for the Higgs-boson spectrum in the Minimal Supersymmetric Standard Model (MSSM) with complex parameters. Accordingly, two-loop renormalization of the Higgs tadpoles and self-energies for complex parameters is carried out. So far, these corrections were only available for real parameters evaluated in the effective-potential approach. The Higgs-boson sector of the MSSM is CP-conserving at lowest order and is independent of complex parameters. However, at higher orders in perturbation theory complex parameters are introduced from other sectors of the MSSM leading to mixing of the CP-even neutral Higgs bosons h and H with the CP-odd neutral Higgs boson A at higher orders.

In analogy to the significant phase dependence of the $\mathcal{O}(\alpha_t\alpha_s)$ corrections in the complex MSSM, large contributions by the complex $\mathcal{O}(\alpha_t^2)$ terms can occur. For a precise prediction of the Higgs-boson masses and mixings the exact knowledge of these corrections is necessary. Following the applied approximations in the evaluation of the $\mathcal{O}(\alpha_t\alpha_s)$ terms, the $\mathcal{O}(\alpha_t^2)$ contributions are also calculated in the gauge-less limit with the external momentum and the bottom-quark mass set equal to zero.

For the numerical analysis of the Higgs-boson masses and mixings the new $\mathcal{O}(\alpha_t^2)$ corrections are combined with the other known contributions with the help of `FeynHiggs`. It contains the full complex one-loop result and the complex two-loop $\mathcal{O}(\alpha_t\alpha_s)$ terms. The previously known real $\mathcal{O}(\alpha_t^2)$ terms are also contained in `FeynHiggs`: they are compared with the $\mathcal{O}(\alpha_t^2)$ results of this thesis and replaced by them afterwards.

At first, a comparison of the $\mathcal{O}(\alpha_t^2)$ contributions with the previously existing result for real parameters is carried out. Very good agreement of both results is found for the masses of the CP-even Higgs bosons as long as m_A is chosen as an input; the $\mathcal{O}(\alpha_t^2)$ corrections to the neutral Higgs-boson masses can easily amount to a shift of $+5$ GeV.

For the $\mathcal{O}(\alpha_t^2)$ contributions the significant complex parameters of the MSSM are the trilinear top-squark coupling A_t and the bilinear higgsino-mass parameter μ with the phases ϕ_{A_t} and ϕ_μ, respectively. For the case of non-zero phases, `FeynHiggs` supplies the possibility of an interpolation of the $\mathcal{O}(\alpha_t^2)$ terms from the effective-potential calculation. A comparison with the exact result which is obtained in this thesis reveals partially large deviations of $\mathcal{O}(1\text{ GeV})$, especially for large values of μ. The heavier Higgs-boson masses are in general more affected due to the different renormalization scheme.

The phase ϕ_{A_t} has a strong influence on CP-mixing. As has been clarified, this mixing always happens either among A and h or among A and H; a region with simultaneous CP-mixing of all three Higgs bosons at higher orders could not be found. Thereby, large mixing between h and A is found for small $m_{H^\pm} < 150$ GeV and large μ, whereas large mixings of H and A occur at large $m_{H^\pm}$. The mass shifts in both cases can amount to several GeV when changing the phase ϕ_{A_t} from 0 or $\pm\pi$ to $\pm\pi/2$. Interestingly, there is also the possibility to have just tiny mixing effects, thus little CP-violation, in spite of large imaginary parts of A_t.

The dependence of the Higgs-boson masses on the phase ϕ_μ is investigated only for small imaginary parts of μ. The main effect is induced by the couplings of the stop sector; the occurence of ϕ_μ in the higgsino mixing matrix has just a negligible influence. Furthermore, the investigated parameter range at $X_t = \pm 1.5\, m_{\tilde{t}}$ is basically independent of ϕ_{A_t}. Sizable contributions of $\mathcal{O}(0.5\text{ GeV})$ are found for low values of $m_{H^\pm}$ and large values of $|\mu|$.

The phenomenological interpretation of scenarios with low input values of m_A or $m_{H^\pm}$ is special in the sense that a heavy neutral Higgs boson is identified with the measured boson at the LHC. Although, the progress of measurements at the experiments ATLAS and CMS in the recent years already excluded wide parts of the parameter space of the MSSM, for this scenario some regions are still allowed and investigated. However, if a stricter lower limit on the charged Higgs-boson mass can be set, this scenario will be ruled out.

For the evaluation of the $\mathcal{O}(\alpha_t^2)$ contributions to the Higgs-boson sector in the complex MSSM the corresponding corrections of the charged Higgs-boson self-energy have to be calculated for on-shell renormalization of the charged Higgs-boson mass. These terms are determined in this thesis and were not known before. As a side effect, in the MSSM with real parameters and on-shell renormalization of the A-boson mass they yield a shift of the charged Higgs-boson mass. In general this mass correction is negative and for large values of μ it can exceed a contribution of -1 GeV.

The derived results clearly show the necessity for a precise calculation of the top-Yukawa-coupling enhanced two-loop corrections including the full dependence on complex phases. The overall mass shift by these contributions for real parameters is positive, commonly around 5 GeV for one of the two CP-even lowest-order states h and H. Depending on choosing either the A-boson mass or the charged Higgs-boson mass as an input either m_A or $m_{H^\pm}$ is renormalized on-shell, accordingly. The other mass receives a negative shift of $\mathcal{O}(1\text{ GeV})$, respectively. In the complex MSSM, the dependence on the phases ϕ_{A_t} and ϕ_μ of the complex parameters A_t and μ, respectively, can add further 1 to 2 GeV to the masses of the predominantly CP-even Higgs bosons and a negative shift to the third neutral Higgs-boson mass; the charged Higgs-boson mass is an input parameter and has to be renormalized on-shell in this case.

Because of these large contributions, and in the light of a present experimental accuracy for the mass measurement of the discovered Higgs-like particle at the LHC of about 0.4 GeV,[16] a further reduction of the theory uncertainty for the prediction of the Higgs-boson masses in the MSSM is desirable, especially the yet missing two-loop contributions by gauge bosons should be evaluated.

[16] Currently, the experimental accuracy is predominantly limited by the statistical uncertainty. The systematic uncertainty is about 0.2 GeV [Cha+14; Aad+14].

A. Supersymmetry notations

A.1. Conventions

The metric of a four dimensional flat Minkowski spacetime is defined as

$$g^{\mu\nu} = g_{\mu\nu} = \begin{pmatrix} 1 & 0 & 0 & 0 \\ 0 & -1 & 0 & 0 \\ 0 & 0 & -1 & 0 \\ 0 & 0 & 0 & -1 \end{pmatrix}. \tag{A.1}$$

The applications of Lorentz transformations

$$x'^{\mu} = \left(\delta^{\mu}{}_{\nu} + r^{\mu}{}_{\nu}\right) x^{\nu} \tag{A.2}$$

with a second rank antisymmetric constant tensor $r^{\mu}{}_{\nu}$, or translations

$$x'^{\mu} = t^{\mu} + x^{\mu} \tag{A.3}$$

with a constant four vector t^{μ} on a spacetime element x^{μ} leave physical observables globally invariant. By defining the corresponding unitary operators $U(t) = e^{i\, t_{\mu} P^{\mu}}$ and $U(r) = e^{-\frac{i}{2} r_{\mu\nu} J^{\mu\nu}}$ with their respective generators P^{μ} and $J^{\mu\nu}$ the Poincaré algebra of Eqs. (2.1) is satisfied.

A realization of the Poincaré algebra for spinors is given by the (4×4) matrices γ^{μ}, $\mu \in \{0,\, 1,\, 2,\, 3\}$ with the (anti)commutation relations

$$\{\gamma^{\mu},\, \gamma^{\nu}\} = 2g^{\mu\nu}\mathbf{1}, \tag{A.4a}$$

$$[\gamma^{\mu},\, \gamma^{\nu}] = -4i \begin{pmatrix} \sigma^{\mu\nu} & 0 \\ 0 & \bar{\sigma}^{\mu\nu} \end{pmatrix}. \tag{A.4b}$$

In the Weyl representation they are defined by

$$\gamma^\mu = \begin{pmatrix} \mathbf{0} & \sigma^\mu \\ \bar{\sigma}^\mu & \mathbf{0} \end{pmatrix} \tag{A.5}$$

with the four matrices

$$\sigma^\mu = \left(\mathbf{1},\, \sigma^1,\, \sigma^2,\, \sigma^3\right), \tag{A.6a}$$
$$\bar{\sigma}^\mu = \left(\mathbf{1},\, -\sigma^1,\, -\sigma^2,\, -\sigma^3\right), \tag{A.6b}$$

σ^i, $i \in \{1, 2, 3\}$ being the Pauli matrices and

$$\gamma_5 = \gamma^5 = \boldsymbol{i}\,\gamma^0\gamma^1\gamma^2\gamma^3 = \begin{pmatrix} \mathbf{-1} & \mathbf{0} \\ \mathbf{0} & \mathbf{1} \end{pmatrix}. \tag{A.7}$$

The spin matrices in that representation are given by

$$\sigma^{\mu\nu} = \boldsymbol{i}\,\left(\sigma^\mu\bar{\sigma}^\nu - \sigma^\nu\bar{\sigma}^\mu\right), \tag{A.8a}$$
$$\bar{\sigma}^{\mu\nu} = \boldsymbol{i}\,\left(\bar{\sigma}^\mu\sigma^\nu - \bar{\sigma}^\nu\sigma^\mu\right). \tag{A.8b}$$

A.2. Grassmann variables

Grassmann variables α_i are defined by the anticommutator

$$\{\alpha_i,\, \alpha_j\} = 0 \tag{A.9}$$

among each other while they commute with complex variables. Thus, a general function f of the two Grassmann variables θ and $\bar{\theta}$ has the form

$$f\left(\theta,\, \bar{\theta}\right) = f_0 + f_1\theta + f_2\bar{\theta} + f_3\theta\bar{\theta}. \tag{A.10}$$

The complex numbers f_0, f_1, f_2 and f_3 can be evaluated by using the Berezin integration rules [Ber66]

$$0 = \int \mathrm{d}\theta, \qquad 0 = \int \mathrm{d}\bar{\theta}, \tag{A.11a}$$
$$1 = \int \mathrm{d}\theta\,\theta, \qquad 1 = \int \mathrm{d}\bar{\theta}\,\bar{\theta} \tag{A.11b}$$

and the identities $\theta^2 = 0$ and $\bar{\theta}^2 = 0$. The extension to more independent Grassmann variables is obvious.

A.3. Two-component spinors

Massive Dirac four spinors transform as the direct sum of the two fundamental representations $\left(\frac{1}{2},\, 0\right) \oplus \left(0,\, \frac{1}{2}\right)$ of the groups $SU(2)_+$ and $SU(2)_-$ respectively, with $SU(2)_+ \otimes SU(2)_-$ being homomorphic to the Lorentz group. Two-component Weyl spinors ξ_A and $\bar{\chi}_{\dot{A}}$ can be constructed which transform as $\left(\frac{1}{2},\, 0\right)$ and $\left(0,\, \frac{1}{2}\right)$ respectively. They obey the relations

$$\xi^A = \epsilon^{AB}\xi_B, \qquad \xi_A = \epsilon_{AB}\xi^B, \tag{A.12a}$$

$$\bar{\chi}^{\dot{A}} = \epsilon^{\dot{A}\dot{B}}\bar{\chi}_{\dot{B}}, \qquad \bar{\chi}_{\dot{A}} = \epsilon_{\dot{A}\dot{B}}\bar{\chi}^{\dot{B}} \tag{A.12b}$$

with the totally antisymmetric tensor $\epsilon^{AB} = -\epsilon_{AB} = \left(\begin{smallmatrix} 0 & 1 \\ -1 & 0 \end{smallmatrix}\right)$. The relation between both representations can be expressed by

$$\xi^A = \left(\bar{\xi}^{\dot{A}}\right)^\dagger, \qquad \xi_A = \left(\bar{\xi}_{\dot{A}}\right)^\dagger, \tag{A.13a}$$

$$\bar{\chi}^{\dot{A}} = \left(\chi^A\right)^\dagger, \qquad \bar{\chi}_{\dot{A}} = \left(\chi_A\right)^\dagger. \tag{A.13b}$$

The following combinations form covariant and $SL(2,\, \mathbb{C})$ invariant (being the covering group of the Lorentz group) bilinear forms:

$$\xi\chi = \xi^A\chi_A = \left(\bar{\chi}\bar{\xi}\right)^\dagger, \tag{A.14a}$$

$$\xi\sigma^\mu\bar{\chi} = \xi^A\sigma^\mu_{A\dot{B}}\bar{\chi}^{\dot{B}} = \left(\chi\sigma^\mu\bar{\xi}\right)^\dagger, \tag{A.14b}$$

$$\bar{\chi}\bar{\sigma}^\mu\xi = \bar{\chi}_{\dot{A}}\bar{\sigma}^{\mu\,\dot{A}B}\xi_B = \left(\bar{\xi}\bar{\sigma}^\mu\chi\right)^\dagger. \tag{A.14c}$$

The components of the Weyl spinors are anticommuting. With the additional conjugate Grassmann-variable doublets θ_A and $\bar{\theta}^{\dot{A}}$ the following relations are valid:

$$\xi\sigma^\mu\bar{\chi} = -\bar{\chi}\bar{\sigma}^\mu\xi, \tag{A.15a}$$

$$\xi\sigma^{\mu\nu}\chi = -\chi\sigma^{\mu\nu}\xi, \qquad \bar{\xi}\bar{\sigma}^{\mu\nu}\bar{\chi} = -\bar{\chi}\bar{\sigma}^{\mu\nu}\bar{\xi}, \tag{A.15b}$$

$$\theta^A\theta^B = -\frac{1}{2}\epsilon^{AB}\theta\theta, \qquad \theta_A\theta_B = \frac{1}{2}\epsilon_{AB}\theta\theta, \tag{A.15c}$$

$$\bar{\theta}^{\dot{A}}\bar{\theta}^{\dot{B}} = \frac{1}{2}\epsilon^{\dot{A}\dot{B}}\bar{\theta}\bar{\theta}, \qquad \bar{\theta}_{\dot{A}}\bar{\theta}_{\dot{B}} = -\frac{1}{2}\epsilon_{\dot{A}\dot{B}}\bar{\theta}\bar{\theta}, \tag{A.15d}$$

$$\theta\xi\ \theta\chi = -\frac{1}{2}\xi\chi\ \theta\theta, \qquad \bar{\theta}\bar{\xi}\ \bar{\theta}\bar{\chi} = -\frac{1}{2}\bar{\xi}\bar{\chi}\ \bar{\theta}\bar{\theta}, \tag{A.15e}$$

$$\xi\zeta\ \bar{\chi}\bar{\tau} = \frac{1}{2}\xi\sigma^\mu\bar{\chi}\ \zeta\sigma_\mu\bar{\tau}, \qquad \bar{\xi}\bar{\zeta}\ \chi\tau = \frac{1}{2}\bar{\xi}\bar{\sigma}^\mu\chi\ \bar{\zeta}\bar{\sigma}_\mu\tau, \tag{A.15f}$$

$$\theta\sigma^\mu\bar{\theta}\ \theta\sigma^\nu\bar{\theta} = \frac{1}{2}g^{\mu\nu}\theta\theta\bar{\theta}\bar{\theta}, \tag{A.15g}$$

$$\zeta\xi\ \chi\sigma^\mu\bar{\tau} = -\tfrac{1}{2}\zeta\chi\ \xi\sigma^\mu\bar{\tau} + \zeta\sigma^{\mu\nu}\chi\ \xi\sigma_\nu\bar{\tau}, \qquad \zeta\xi\ \bar{\chi}\bar{\sigma}^\mu\tau = -\tfrac{1}{2}\tau\xi\ \bar{\chi}\bar{\sigma}^\mu\zeta - \tau\sigma^{\mu\nu}\xi\ \bar{\chi}\bar{\sigma}_\nu\zeta, \tag{A.15h}$$

$$\left(\sigma^\mu\bar{\theta}\right)_A \theta\sigma^\nu\bar{\theta} = \bar{\theta}\bar{\theta}\left[\tfrac{1}{2}g^{\mu\nu}\theta_A - \boldsymbol{i}\left(\sigma^{\mu\nu}\theta\right)_A\right], \quad \left(\theta\sigma^\mu\right)_{\dot{A}}\bar{\theta}\bar{\sigma}^\nu\theta = -\theta\theta\left[\tfrac{1}{2}\bar{\theta}_{\dot{A}}g^{\mu\nu} + \boldsymbol{i}\left(\bar{\theta}\bar{\sigma}^{\mu\nu}\right)_{\dot{A}}\right]. \tag{A.15i}$$

A.4. Superfields

Superfields are functions on the superspace which contains Minkowski spacetime vectors x^μ and two additional conjugate Grassmann-valued coordinate doublets θ^A and $\bar{\theta}_{\dot{A}}$. The most general expression for superfields is stated by Eq. (2.7). The infinitesimal transformation of general superfields is performed in Eq. (2.11). Inserting the full expression yields the infinitesimal transformations of its components:

$$\delta f = \sqrt{2}\left(\tau\xi + \bar{\tau}\bar{\chi}\right), \tag{A.16a}$$

$$\delta\xi_A = \sqrt{2}\tau_A M + \frac{\sqrt{2}}{2}\left(\sigma^\mu\bar{\tau}\right)_A\left(-\boldsymbol{i}\,\partial_\mu f + A_\mu\right), \tag{A.16b}$$

$$\delta\bar{\chi}^{\dot{A}} = \sqrt{2}\bar{\tau}^{\dot{A}}N - \frac{\sqrt{2}}{2}\left(\bar{\sigma}^\mu\tau\right)^{\dot{A}}\left(\boldsymbol{i}\,\partial_\mu f + A_\mu\right), \tag{A.16c}$$

$$\delta M = \bar{\tau}\bar{\lambda} + \frac{\boldsymbol{i}\sqrt{2}}{2}\partial_\mu\xi\sigma^\mu\bar{\tau}, \tag{A.16d}$$

$$\delta N = \tau\zeta - \frac{\boldsymbol{i}\sqrt{2}}{2}\tau\sigma^\mu\partial_\mu\bar{\chi}, \tag{A.16e}$$

$$\delta A_\mu = \tau\sigma_\mu\bar{\lambda} + \zeta\sigma_\mu\bar{\tau} - \frac{\boldsymbol{i}\sqrt{2}}{2}\left[\tau\partial_\mu\xi - \partial_\mu\bar{\chi}\bar{\tau}\right] + \sqrt{2}\left[\tau\sigma_{\mu\nu}\partial^\nu\xi - \bar{\tau}\bar{\sigma}_{\mu\nu}\partial^\nu\bar{\chi}\right], \tag{A.16f}$$

$$\delta\bar{\lambda}^{\dot{A}} = \bar{\tau}^{\dot{A}}D - \frac{\boldsymbol{i}}{2}\bar{\tau}^{\dot{A}}\partial^\mu A_\mu - \boldsymbol{i}\left(\bar{\sigma}^\mu\tau\right)^{\dot{A}}\partial_\mu M + \left(\bar{\sigma}^{\mu\nu}\bar{\tau}\right)^{\dot{A}}\partial_\mu A_\nu, \tag{A.16g}$$

$$\delta\zeta_A = \tau_A D + \frac{\boldsymbol{i}}{2}\tau_A\partial^\mu A_\mu - \boldsymbol{i}\left(\sigma^\mu\bar{\tau}\right)_A\partial_\mu N - \left(\sigma^{\mu\nu}\tau\right)_A\partial_\mu A_\nu, \tag{A.16h}$$

$$\delta D = \boldsymbol{i}\left(\partial_\mu\zeta\sigma^\mu\bar{\tau} + \partial_\mu\bar{\lambda}\bar{\sigma}^\mu\tau\right). \tag{A.16i}$$

Thus, the D term of any superfield transforms solely as a derivative. Similarly it can be shown, that the F components of chiral superfields given by Eq. (2.14) transform as a derivative.

A supersymmetric Lagrangian density constructed out of these superfields must remain invariant under each supersymmetry transformation up to a total derivative to keep the action constant. The only possible contributions are thus the D terms of superfields and the F terms of chiral superfields leading to the general form

$$\mathcal{L} = \int \mathrm{d}\theta\,\mathrm{d}\theta\,\mathrm{d}\bar{\theta}\,\mathrm{d}\bar{\theta}\,\Phi_i^\dagger \Phi_i + \int \mathrm{d}\theta\,\mathrm{d}\theta\,\mathcal{W}(\Phi_i) + \int \mathrm{d}\bar{\theta}\,\mathrm{d}\bar{\theta}\,\mathcal{W}\Big(\Phi_i^\dagger\Big). \tag{A.17}$$

However, it is noteworthy that covariant derivatives of superfields can create additional F term contributions as shown in the special case given by Eq. (2.25).

B. Loop integrals

The analytical evaluation of the $\mathcal{O}(\alpha_t^2)$ contributions requires the following explicit expressions for one-loop and two-loop integrals.

B.1. One-loop functions

In the following all required one-loop integrals are listed up to $\mathcal{O}(\epsilon^1)$, where $\epsilon = (4-D)/2$ parametrizes the divergent parts. D is the dimension of the integrated momentum and μ_D depicts the regularization parameter, so that

$$\int \mathrm{d}^4 q \to \mu_\mathrm{D}^{4-D} \int \mathrm{d}^D q \ . \tag{B.1}$$

The reduction to scalar integrals as described first by Ref. [PV79] has been used. The scalar integrals have been re-evaluated by using the technique of Feynman parameters.

$$A_0(0) = 0, \tag{B.2a}$$

$$A_0\big(m^2\big) = \frac{m^2}{\epsilon} - m^2\left\{\mathrm{L}\left(m^2\right)\right\} + m^2\epsilon\left\{\frac{1}{2} + \frac{\pi^2}{12} + \frac{1}{2}\left[\mathrm{L}\left(m^2\right)\right]^2\right\}, \tag{B.2b}$$

$$\begin{aligned} B_0\big(p^2,0,0\big) = {} & \frac{1}{\epsilon} + \left\{1 + C + \log\left(-\tfrac{\mu_\mathrm{D}}{p^2 - i\,\epsilon'}\right)\right\} \\ & + \epsilon\left\{2 - \frac{\pi^2}{12} + \frac{1}{2}\left[1 + C + \log\left(-\tfrac{\mu_\mathrm{D}}{p^2 - i\,\epsilon'}\right)\right]^2\right\}, \end{aligned} \tag{B.3a}$$

$$B_0\big(0,0,m^2\big) = B_0\big(0,m^2,0\big) = \frac{A_0\big(m^2\big)}{m^2}, \tag{B.3b}$$

$$B_0\big(0,m^2,m^2\big) = (1-\epsilon)\,\frac{A_0\big(m^2\big)}{m^2}, \tag{B.3c}$$

$$B_0\big(0,m_1^2,m_2^2\big) = \frac{A_0\big(m_1^2\big) - A_0\big(m_2^2\big)}{m_1^2 - m_2^2}, \tag{B.3d}$$

$$B_0\big(m^2,0,m^2\big) = \frac{1}{\epsilon} + \left\{1 - \mathrm{L}\left(m^2\right)\right\} + \epsilon\left\{2 + \frac{\pi^2}{12} + \frac{1}{2}\left[1 - \mathrm{L}\left(m^2\right)\right]^2\right\}, \tag{B.3e}$$

$$B_0\big(m^2,m^2,0\big) = B_0\big(m^2,0,m^2\big), \tag{B.3f}$$

$$
\begin{aligned}
B_0\big(m_1^2,0,m_2^2\big) &= \frac{1}{\epsilon} + \left\{\frac{m_2^2}{m_1^2}\left[1-\mathrm{L}\left(m_2^2\right)\right] + \frac{m_1^2-m_2^2}{m_1^2}\left[1+C+\log\left(\tfrac{\mu_{\mathrm{D}}}{m_2^2-m_1^2}\right)\right]\right\} \\
&\quad + \epsilon\left\{\frac{m_1^2-m_2^2}{2m_1^2}\left[\left(1+C+\log\left(\tfrac{\mu_{\mathrm{D}}}{m_2^2-m_1^2}\right)\right)^2 - 2\,\mathrm{Li}_2\left(\tfrac{-m_1^2}{m_2^2-m_1^2}\right)\right]\right. \\
&\qquad\left. + 2 + \frac{\pi^2}{12} + \frac{m_2^2}{2m_1^2}\left[1-\mathrm{L}\left(m_2^2\right)\right]^2\right\},
\end{aligned} \tag{B.3g}
$$

$$
B_0\big(m_1^2,m_2^2,0\big) = B_0\big(m_1^2,0,m_2^2\big), \tag{B.3h}
$$

$$
\begin{aligned}
&B_0\Big((m_1\pm m_2)^2,m_1^2,m_2^2\Big) = \\
&\qquad \frac{1}{\epsilon} + \left\{\frac{m_1\left[1-\mathrm{L}\left(m_1^2\right)\right] \pm m_2\left[1-\mathrm{L}\left(m_2^2\right)\right]}{m_1\pm m_2}\right\} \\
&\qquad + \epsilon\left\{2+\frac{\pi^2}{12} + \frac{m_1\left[1-\mathrm{L}\left(m_1^2\right)\right]^2 \pm m_2\left[1-\mathrm{L}\left(m_2^2\right)\right]^2}{2\left(m_1\pm m_2\right)}\right\},
\end{aligned} \tag{B.3i}
$$

$$
\begin{aligned}
B_0\big(p^2,m_1^2,m_2^2\big) &= \frac{1}{\epsilon} + \left\{\frac{m_1^2-m_2^2+p^2}{2p^2}\left[1-\mathrm{L}\left(m_1^2\right)\right] + \frac{m_2^2-m_1^2+p^2}{2p^2}\left[1-\mathrm{L}\left(m_2^2\right)\right]\right. \\
&\qquad\left. + \frac{R}{2p^2}\left[\log\left(m_1^2+m_2^2-p^2+R\right) + \log\left(\tfrac{1}{m_1^2+m_2^2-p^2-R}\right)\right]\right\} \\
&\quad + \epsilon\left\{2+\frac{\pi^2}{12} + \tfrac{m_1^2-m_2^2+p^2}{4p^2}\left[1-\mathrm{L}\left(m_1^2\right)\right]^2 + \tfrac{m_2^2-m_1^2+p^2}{4p^2}\left[1-\mathrm{L}\left(m_2^2\right)\right]^2\right. \\
&\qquad - \frac{R}{4p^2}\Big[\left(1-\mathrm{L}\left(m_1^2\right)\right)\left(\log\left(m_1^2-m_2^2+p^2+R\right) - \log\left(m_2^2-m_1^2-p^2+R\right)\right) \\
&\qquad\qquad + \left(1-\mathrm{L}\left(m_2^2\right)\right)\left(\log\left(m_2^2-m_1^2+p^2+R\right) - \log\left(m_1^2-m_2^2-p^2+R\right)\right) \\
&\qquad\qquad + \left(-1-\mathrm{L}\left(-p^2\right)+2\,\mathrm{L}\left(R\right)\right) \\
&\qquad\qquad\quad \left(\log\left(m_1^2+m_2^2-p^2+R\right) + \log\left(\tfrac{1}{m_1^2+m_2^2-p^2-R}\right)\right) \\
&\qquad\qquad + 2\left(\mathrm{Li}_2\left(\tfrac{m_1^2-m_2^2-p^2+R}{2R}\right) - \mathrm{Li}_2\left(\tfrac{m_2^2-m_1^2+p^2+R}{2R}\right)\right) \\
&\qquad\qquad \left. + 2\left(\mathrm{Li}_2\left(\tfrac{m_2^2-m_1^2-p^2+R}{2R}\right) - \mathrm{Li}_2\left(\tfrac{m_1^2-m_2^2+p^2+R}{2R}\right)\right)\Big]\right\},
\end{aligned} \tag{B.3j}
$$

$$
B_1\big(0,m_1^2,m_2^2\big) = -\frac{1}{2}B_0\big(0,m_1^2,m_2^2\big) + \frac{m_2^2-m_1^2}{2}B_0'\big(0,m_1^2,m_2^2\big), \tag{B.4a}
$$

$$
B_1\big(p^2,m_1^2,m_2^2\big) = \frac{1}{2p^2}\left[A_0\big(m_1^2\big) - A_0\big(m_2^2\big) - \left(p^2-m_2^2+m_1^2\right)B_0\big(p^2,m_1^2,m_2^2\big)\right], \tag{B.4b}
$$

$$
\begin{aligned}
B_{00}\big(p^2,m_1^2,m_2^2\big) = &\frac{1}{2\left(3-2\epsilon\right)}\Big[A_0\big(m_2^2\big) + 2m_1^2 B_0\big(p^2,m_1^2,m_2^2\big) \\
&\qquad + \left(p^2-m_2^2+m_1^2\right)B_1\big(p^2,m_1^2,m_2^2\big)\Big],
\end{aligned} \tag{B.4c}
$$

$$
B_0'(0,0,0) = 0, \tag{B.5a}
$$

$$
B_0'\big(0,0,m^2\big) = \frac{1}{2m^2} + \frac{\epsilon}{2m^2}\left\{\frac{1}{2} - \mathrm{L}\left(m^2\right)\right\}, \tag{B.5b}
$$

$$
B_0'\big(0,m^2,0\big) = B_0'\big(0,0,m^2\big), \tag{B.5c}
$$

$$
B_0'\big(0,m^2,m^2\big) = \frac{1}{6m^2} + \frac{\epsilon}{6m^2}\left\{-1-\mathrm{L}\left(m^2\right)\right\}, \tag{B.5d}
$$

$$B_0'\big(0,m_1^2,m_2^2\big) = \frac{1}{2\left(m_1^2-m_2^2\right)^3}\left\{m_1^4 - m_2^4 + 2m_1^2m_2^2\log\left(\tfrac{m_2^2}{m_1^2}\right)\right\}$$
$$+\frac{\epsilon}{2\left(m_1^2-m_2^2\right)^3}\bigg\{m_1^4\left[\frac{1}{2}-\mathrm{L}\left(m_1^2\right)\right] - m_2^4\left[\frac{1}{2}-\mathrm{L}\left(m_2^2\right)\right] \qquad \text{(B.5e)}$$
$$+m_1^2m_2^2\left[\left(\mathrm{L}\left(m_1^2\right)\right)^2-\left(\mathrm{L}\left(m_2^2\right)\right)^2\right]\bigg\},$$

$$C_0\big(0,0,0,m^2,m^2,m^2\big) = -\frac{\epsilon}{2m^2}B_0\big(0,m^2,m^2\big), \qquad \text{(B.6a)}$$

$$\mathrm{L}\left(m^2\right) = \log\left(\tfrac{m^2}{\mu_{\mathrm{D}}}\right) - C, \qquad \text{(B.7a)}$$
$$C = 1-\gamma_{\mathrm{E}} + \log\left(4\pi\right), \qquad \text{(B.7b)}$$
$$R = \sqrt{m_1^4+m_2^4+p^4-2m_1^2m_2^2-2m_2^2p^2-2p^2m_1^2}. \qquad \text{(B.7c)}$$

B.2. Two-loop functions

The notation of the two-loop integrals follows the conventions which have been introduced by Refs. [WSB94b; Wei+95]. After reducing the appearing two-loop integrals to a set of master integrals and applying the approximation of a vanishing external momentum, only the following function is left which cannot be completely expressed in terms of one-loop functions. The result is taken from Ref. [BT94] and reordered in the given way. Up to $\mathcal{O}(\epsilon^0)$ it reads:

$$\mathrm{T}_{134}\big(m_1^2,m_2^2,m_3^2\big) = \frac{1-\epsilon}{2\left(1-2\epsilon\right)}\left\{\frac{\left[A_0\big(m_1^2\big)\right]^2}{m_1^2}+\frac{\left[A_0\big(m_2^2\big)\right]^2}{m_2^2}+\frac{\left[A_0\big(m_3^2\big)\right]^2}{m_3^2}\right\} \qquad \text{(B.8a)}$$
$$+\Phi^{\mathrm{cyc}}\big(m_1^2,m_2^2,m_3^2\big)\ ,$$
$$\Phi^{\mathrm{cyc}}\big(m^2,0,0\big) = m^2\frac{\pi^2}{6}, \qquad \text{(B.8b)}$$
$$\Phi^{\mathrm{cyc}}\big(m_1^2,m_2^2,0\big) = m_1^2\,\mathrm{Li}_2\left(\tfrac{m_1^2-m_2^2}{m_1^2}\right) + m_2^2\,\mathrm{Li}_2\left(\tfrac{m_2^2-m_1^2}{m_2^2}\right)\ , \qquad \text{(B.8c)}$$
$$\Phi^{\mathrm{cyc}}\big(m_1^2,m_2^2,m_3^2\big) = -\frac{m_1^2}{2}\log\left(\tfrac{m_1^2}{m_2^2}\right)\log\left(\tfrac{m_1^2}{m_3^2}\right) - \frac{m_2^2}{2}\log\left(\tfrac{m_2^2}{m_3^2}\right)\log\left(\tfrac{m_2^2}{m_1^2}\right) - \frac{m_3^2}{2}\log\left(\tfrac{m_3^2}{m_1^2}\right)\log\left(\tfrac{m_3^2}{m_2^2}\right)$$
$$+R\Bigg[\frac{\pi^2}{6}-\frac{1}{2}\log\left(\tfrac{m_1^2}{m_3^2}\right)\log\left(\tfrac{m_2^2}{m_3^2}\right)+\log\left(\tfrac{m_1^2-m_2^2+m_3^2-R}{2m_3^2}\right)\log\left(\tfrac{m_2^2-m_1^2+m_3^2-R}{2m_3^2}\right)$$
$$-\mathrm{Li}_2\left(\tfrac{m_1^2-m_2^2+m_3^2-R}{2m_3^2}\right)-\mathrm{Li}_2\left(\tfrac{m_2^2-m_1^2+m_3^2-R}{2m_3^2}\right)\Bigg]\ , \qquad \text{(B.8d)}$$
$$R = \sqrt{m_1^4+m_2^4+m_3^4-2m_1^2m_2^2-2m_2^2m_3^2-2m_3^2m_1^2}\ . \qquad \text{(B.8e)}$$

The function Φ^{cyc} is cyclic in its arguments and contains only finite parts.

Originally the two-loop Feynman diagrams contain up to five propagators and two loop momenta. Since the external momentum is set to zero only vacuum integrals which depend on up to three different kinematic variables remain. The used notation is introduced in Section 4.2.

During the reduction to master integrals some terms can be expressed as products of one-loop integrals:

$$\mathrm{T}_{ab}\big(m_1^2, m_2^2\big) = A_0\big(m_1^2\big) A_0\big(m_2^2\big), \tag{B.9a}$$

$$\mathrm{T}_{a^x b^y}\Big(\underbrace{m_1^2, \dots, m_1^2}_{x}, \underbrace{m_2^2, \dots, m_2^2}_{y}\Big) = \frac{x-3+\epsilon}{(1-x)\, m_1^2} \mathrm{T}_{a^{x-1} b^y}\Big(\underbrace{m_1^2, \dots, m_1^2}_{x-1}, \underbrace{m_2^2, \dots, m_2^2}_{y}\Big) \tag{B.9b}$$
$$\text{for } x > 1,\ y \geq 1,$$

$$\mathrm{T}_{a^x b^y}\Big(\underbrace{m_1^2, \dots, m_1^2}_{x}, \underbrace{m_2^2, \dots, m_2^2}_{y}\Big) = \frac{y-3+\epsilon}{(1-y)\, m_2^2} \mathrm{T}_{a^x b^{y-1}}\Big(\underbrace{m_1^2, \dots, m_1^2}_{x}, \underbrace{m_2^2, \dots, m_2^2}_{y-1}\Big) \tag{B.9c}$$
$$\text{for } x \geq 1,\ y > 1,$$

with $a \neq b$ and $a,\, b \in \{1,\ 3,\ 4\}$.

All other appearing integrals can be reduced to Eq. (B.8a) or Eq. (B.9) by using the following formulas:

$$\mathrm{T}_{11334}\big(m_1^2, m_1^2, m_1^2, m_1^2, 0\big) = \frac{2}{m_1^2} \mathrm{T}_{1113}\big(m_1^2, m_1^2, m_1^2, m_1^2\big) - 2\mathrm{T}_{11134}\big(m_1^2, m_1^2, m_1^2, m_1^2, 0\big), \tag{B.10a}$$

$$\begin{aligned}
\mathrm{T}_{11334}\big(m_1^2, m_1^2, m_2^2, m_2^2, m_3^2\big) = &- \tfrac{\left(m_1^2-m_2^2\right)^2 - m_3^4}{\left(m_1^2-m_2^2\right)^2 + m_3^4} \Big[\mathrm{T}_{11134}\big(m_1^2, m_1^2, m_1^2, m_2^2, m_3^2\big) \\
&\qquad + \mathrm{T}_{11134}\big(m_2^2, m_2^2, m_2^2, m_1^2, m_3^2\big)\Big] \\
&+ \tfrac{m_3^2}{\left(m_1^2-m_2^2\right)^2 + m_3^4} \\
&\quad \times \Big[\mathrm{T}_{1134}\big(m_1^2, m_1^2, m_2^2, m_3^2\big) + \mathrm{T}_{1134}\big(m_2^2, m_2^2, m_1^2, m_3^2\big)\Big] \\
&- \tfrac{m_3^2}{\left(m_1^2-m_2^2\right)^2 + m_3^4} \mathrm{T}_{1133}\big(m_1^2, m_1^2, m_2^2, m_2^2\big) \\
&+ \tfrac{m_1^4\left(m_1^2-m_2^2+m_3^2\right) + m_2^4\left(m_2^2-m_1^2+m_3^2\right)}{2\left[\left(m_1^2-m_2^2\right)^2 + m_3^4\right]} \\
&\quad \times \left[\frac{\mathrm{T}_{1113}\big(m_1^2, m_1^2, m_1^2, m_2^2\big)}{m_2^4} + \frac{\mathrm{T}_{1113}\big(m_2^2, m_2^2, m_2^2, m_1^2\big)}{m_1^4}\right] \\
&- \tfrac{m_2^2-m_1^2+m_3^2}{\left(m_1^2-m_2^2\right)^2 + m_3^4} \mathrm{T}_{1114}\big(m_1^2, m_1^2, m_1^2, m_3^2\big) \\
&- \tfrac{m_1^2-m_2^2+m_3^2}{\left(m_1^2-m_2^2\right)^2 + m_3^4} \mathrm{T}_{1114}\big(m_2^2, m_2^2, m_2^2, m_3^2\big),
\end{aligned} \tag{B.10b}$$

$$\mathrm{T}_{11134}\big(m_1^2, m_1^2, m_1^2, m_1^2, 0\big) = -\frac{3}{1+2\epsilon}\mathrm{T}_{11113}\big(m_1^2, m_1^2, m_1^2, m_1^2, m_1^2\big), \tag{B.10c}$$

$$\begin{aligned}\mathrm{T}_{11134}\big(m_1^2, m_1^2, m_1^2, m_2^2, m_3^2\big) = {}& \tfrac{\left(m_2^2-m_1^2+m_3^2\right)\epsilon}{\left[(m_1+m_2)^2-m_3^2\right]\left[(m_1-m_2)^2-m_3^2\right]}\mathrm{T}_{1134}\big(m_1^2, m_1^2, m_2^2, m_3^2\big)\\ &+ \tfrac{m_2^2}{\left[(m_1+m_2)^2-m_3^2\right]\left[(m_1-m_2)^2-m_3^2\right]}\\ &\times\Big[\mathrm{T}_{1134}\big(m_1^2, m_1^2, m_2^2, m_3^2\big) + \mathrm{T}_{1134}\big(m_2^2, m_2^2, m_1^2, m_3^2\big)\Big]\\ &- \tfrac{m_1^2-m_2^2+m_3^2}{\left[(m_1+m_2)^2-m_3^2\right]\left[(m_1-m_2)^2-m_3^2\right]}\mathrm{T}_{1113}\big(m_1^2, m_1^2, m_1^2, m_2^2\big)\\ &- \tfrac{m_1^2+m_2^2-m_3^2}{\left[(m_1+m_2)^2-m_3^2\right]\left[(m_1-m_2)^2-m_3^2\right]}\mathrm{T}_{1114}\big(m_1^2, m_1^2, m_1^2, m_3^2\big)\\ &- \tfrac{1}{\left[(m_1+m_2)^2-m_3^2\right]\left[(m_1-m_2)^2-m_3^2\right]}\mathrm{T}_{113}\big(m_1^2, m_1^2, m_2^2\big),\end{aligned} \tag{B.10d}$$

$$\mathrm{T}_{1134}\big(m_1^2, m_1^2, m_1^2, 0\big) = \frac{1}{2m_1^2}\mathrm{T}_{113}\big(m_1^2, m_1^2, m_1^2\big), \tag{B.10e}$$

$$\begin{aligned}\mathrm{T}_{1134}\big(m_1^2, m_1^2, m_2^2, m_3^2\big) = {}& \tfrac{\left(m_2^2-m_1^2+m_3^2\right)(-1+2\epsilon)}{\left[(m_1+m_2)^2-m_3^2\right]\left[(m_1-m_2)^2-m_3^2\right]}\mathrm{T}_{134}\big(m_1^2, m_2^2, m_3^2\big)\\ &- \tfrac{m_1^2-m_2^2+m_3^2}{\left[(m_1+m_2)^2-m_3^2\right]\left[(m_1-m_2)^2-m_3^2\right]}\mathrm{T}_{113}\big(m_1^2, m_1^2, m_2^2\big)\\ &- \tfrac{m_1^2+m_2^2-m_3^2}{\left[(m_1+m_2)^2-m_3^2\right]\left[(m_1-m_2)^2-m_3^2\right]}\mathrm{T}_{114}\big(m_1^2, m_1^2, m_3^2\big)\\ &+ \tfrac{2m_2^2}{\left[(m_1+m_2)^2-m_3^2\right]\left[(m_1-m_2)^2-m_3^2\right]}\mathrm{T}_{334}\big(m_2^2, m_2^2, m_3^2\big).\end{aligned} \tag{B.10f}$$

Integrals with multiple denominators of the same loop-momentum structure and different masses are simplified by partial fractioning beforehand:

$$\mathrm{T}_{aa\ldots}\big(m_1^2, m_2^2, \ldots\big) = \frac{1}{m_1^2-m_2^2}\left[\mathrm{T}_{a\ldots}\big(m_1^2, \ldots\big) - \mathrm{T}_{a\ldots}\big(m_2^2, \ldots\big)\right] \tag{B.11}$$

for $m_1^2 \neq m_2^2$ and $a \in \{1,\, 3,\, 4\}$.

All displayed integrals are symmetric under exchange of different loop-momentum structures:

$$\mathrm{T}_{a^x b^y \ldots}\Big(\underbrace{m_1^2, \ldots, m_1^2}_{x}, \underbrace{m_2^2, \ldots, m_2^2}_{y}, \ldots\Big) = \mathrm{T}_{b^x a^y \ldots}\Big(\underbrace{m_1^2, \ldots, m_1^2}_{x}, \underbrace{m_2^2, \ldots, m_2^2}_{y}, \ldots\Big) \tag{B.12}$$

for a, $b \in \{1,\, 3,\, 4\}$.

C. Two-loop renormalization of the Higgs tadpoles and self-energies

The two-loop renormalization of the Higgs tadpoles and self-energies is carried out in Section 6.8 where the counterterms are given in matrix form. In the following the explicit expressions for all counterterms are listed.

C.1. Two-loop counterterms

The two-loop counterterms for the tadpoles and self-energies appearing in Eqs. (6.76) are given in the notation of Eqs. (6.43) in components by

$$\delta^{(2)}T_h^{\mathbf{Z}} = \tfrac{1}{2}\left(\delta^{(1)}Z_{hh}\delta^{(1)}T_h + \delta^{(1)}Z_{hH}\delta^{(1)}T_H\right) + \delta^{(2)}T_h \;, \tag{C.1a}$$

$$\delta^{(2)}T_H^{\mathbf{Z}} = \tfrac{1}{2}\left(\delta^{(1)}Z_{HH}\delta^{(1)}T_H + \delta^{(1)}Z_{hH}\delta^{(1)}T_h\right) + \delta^{(2)}T_H \;, \tag{C.1b}$$

$$\delta^{(2)}T_A^{\mathbf{Z}} = \tfrac{1}{2}\left(\delta^{(1)}Z_{AA}\delta^{(1)}T_A + \delta^{(1)}Z_{AG}\delta^{(1)}T_G\right) + \delta^{(2)}T_A \;, \tag{C.1c}$$

$$\delta^{(2)}T_G^{\mathbf{Z}} = \tfrac{1}{2}\left(\delta^{(1)}Z_{GG}\delta^{(1)}T_G + \delta^{(1)}Z_{AG}\delta^{(1)}T_A\right) + \delta^{(2)}T_G \;, \tag{C.1d}$$

$$\begin{aligned}\delta^{(2)}m_h^{\mathbf{Z}} = {}& \left(m_h^2 - p^2\right)\left[\delta^{(2)}Z_{hh} + \tfrac{1}{4}\left(\delta^{(1)}Z_{hh}\right)^2\right] + \left(m_H^2 - p^2\right)\tfrac{1}{4}\left(\delta^{(1)}Z_{hH}\right)^2 \\ & + \delta^{(1)}Z_{hh}\,\delta^{(1)}m_h^2 + \delta^{(1)}Z_{hH}\,\delta^{(1)}m_{hH}^2 + \delta^{(2)}m_h^2 \;,\end{aligned} \tag{C.2a}$$

$$\begin{aligned}\delta^{(2)}m_H^{\mathbf{Z}} = {}& \left(m_H^2 - p^2\right)\left[\delta^{(2)}Z_{HH} + \tfrac{1}{4}\left(\delta^{(1)}Z_{HH}\right)^2\right] + \left(m_h^2 - p^2\right)\tfrac{1}{4}\left(\delta^{(1)}Z_{hH}\right)^2 \\ & + \delta^{(1)}Z_{HH}\,\delta^{(1)}m_H^2 + \delta^{(1)}Z_{hH}\,\delta^{(1)}m_{hH}^2 + \delta^{(2)}m_H^2 \;,\end{aligned} \tag{C.2b}$$

$$\begin{aligned}\delta^{(2)}m_A^{\mathbf{Z}} = {}& \left(m_A^2 - p^2\right)\left[\delta^{(2)}Z_{AA} + \tfrac{1}{4}\left(\delta^{(1)}Z_{AA}\right)^2\right] + \left(m_G^2 - p^2\right)\tfrac{1}{4}\left(\delta^{(1)}Z_{AG}\right)^2 \\ & + \delta^{(1)}Z_{AA}\,\delta^{(1)}m_A^2 + \delta^{(1)}Z_{AG}\,\delta^{(1)}m_{AG}^2 + \delta^{(2)}m_A^2 \;,\end{aligned} \tag{C.2c}$$

$$\begin{aligned}\delta^{(2)}m_G^{\mathbf{Z}} = {}& \left(m_G^2 - p^2\right)\left[\delta^{(2)}Z_{GG} + \tfrac{1}{4}\left(\delta^{(1)}Z_{GG}\right)^2\right] + \left(m_A^2 - p^2\right)\tfrac{1}{4}\left(\delta^{(1)}Z_{AG}\right)^2 \\ & + \delta^{(1)}Z_{GG}\,\delta^{(1)}m_G^2 + \delta^{(1)}Z_{AG}\,\delta^{(1)}m_{AG}^2 + \delta^{(2)}m_G^2 \;,\end{aligned} \tag{C.2d}$$

$$\begin{aligned}
\delta^{(2)} m^{\mathbf{Z}}_{hH} &= \tfrac{1}{4}\Big[\left(m_h^2 - p^2\right)\delta^{(1)}Z_{hh}\delta^{(1)}Z_{hH} + \left(m_H^2 - p^2\right)\delta^{(1)}Z_{HH}\delta^{(1)}Z_{hH}\Big] \\
&\quad + \tfrac{1}{2}\Big[\Big(\delta^{(1)}Z_{hh} + \delta^{(1)}Z_{HH}\Big)\delta^{(1)}m^2_{hH} + \delta^{(1)}Z_{hH}\Big(\delta^{(1)}m_h^2 + \delta^{(1)}m_H^2\Big)\Big] \\
&\quad + \Big(\tfrac{m_h^2 + m_H^2}{2} - p^2\Big)\delta^{(2)}Z_{hH} + \delta^{(2)}m^2_{hH}\ ,
\end{aligned} \tag{C.2e}$$

$$\begin{aligned}
\delta^{(2)} m^{\mathbf{Z}}_{hA} &= \tfrac{1}{2}\Big[\Big(\delta^{(1)}Z_{hh} + \delta^{(1)}Z_{AA}\Big)\delta^{(1)}m^2_{hA} + \delta^{(1)}Z_{hH}\,\delta^{(1)}m^2_{HA} + \delta^{(1)}Z_{AG}\,\delta^{(1)}m^2_{hG}\Big] \\
&\quad + \delta^{(2)}m^2_{hA}\ ,
\end{aligned} \tag{C.2f}$$

$$\begin{aligned}
\delta^{(2)} m^{\mathbf{Z}}_{hG} &= \tfrac{1}{2}\Big[\Big(\delta^{(1)}Z_{hh} + \delta^{(1)}Z_{GG}\Big)\delta^{(1)}m^2_{hG} + \delta^{(1)}Z_{hH}\,\delta^{(1)}m^2_{HG} + \delta^{(1)}Z_{AG}\,\delta^{(1)}m^2_{hA}\Big] \\
&\quad + \delta^{(2)}m^2_{hG}\ ,
\end{aligned} \tag{C.2g}$$

$$\begin{aligned}
\delta^{(2)} m^{\mathbf{Z}}_{HA} &= \tfrac{1}{2}\Big[\Big(\delta^{(1)}Z_{HH} + \delta^{(1)}Z_{AA}\Big)\delta^{(1)}m^2_{HA} + \delta^{(1)}Z_{hH}\,\delta^{(1)}m^2_{hA} + \delta^{(1)}Z_{AG}\,\delta^{(1)}m^2_{HG}\Big] \\
&\quad + \delta^{(2)}m^2_{HA}\ ,
\end{aligned} \tag{C.2h}$$

$$\begin{aligned}
\delta^{(2)} m^{\mathbf{Z}}_{HG} &= \tfrac{1}{2}\Big[\Big(\delta^{(1)}Z_{HH} + \delta^{(1)}Z_{AA}\Big)\delta^{(1)}m^2_{HG} + \delta^{(1)}Z_{hH}\,\delta^{(1)}m^2_{hG} + \delta^{(1)}Z_{AG}\,\delta^{(1)}m^2_{HA}\Big] \\
&\quad + \delta^{(2)}m^2_{HG}\ ,
\end{aligned} \tag{C.2i}$$

$$\begin{aligned}
\delta^{(2)} m^{\mathbf{Z}}_{AG} &= \tfrac{1}{4}\Big[\left(m_A^2 - p^2\right)\delta^{(1)}Z_{AA}\,\delta^{(1)}Z_{AG} + \left(m_G^2 - p^2\right)\delta^{(1)}Z_{GG}\,\delta^{(1)}Z_{AG}\Big] \\
&\quad + \tfrac{1}{2}\Big[\Big(\delta^{(1)}Z_{AA} + \delta^{(1)}Z_{GG}\Big)\delta^{(1)}m^2_{AG} + \delta^{(1)}Z_{AG}\Big(\delta^{(1)}m_A^2 + \delta^{(1)}m_G^2\Big)\Big] \\
&\quad + \Big(\tfrac{m_A^2 + m_G^2}{2} - p^2\Big)\delta^{(2)}Z_{AG} + \delta^{(2)}m^2_{AG}\ ,
\end{aligned} \tag{C.2j}$$

$$\begin{aligned}
\delta^{(2)} m^{\mathbf{Z}}_{H^\pm} &= \left(m^2_{H^\pm} - p^2\right)\Big[\delta^{(2)}Z_{H^\pm H^\pm} + \tfrac{1}{4}\Big(\delta^{(1)}Z_{H^\pm H^\pm}\Big)^2\Big] + \left(m^2_{G^\pm} - p^2\right)\tfrac{1}{4}\Big(\delta^{(1)}Z_{H^-G^+}\Big)^2 \\
&\quad + \delta^{(1)}Z_{H^\pm H^\pm}\,\delta^{(1)}m^2_{H^\pm} + \tfrac{1}{2}\,\delta^{(1)}Z_{H^-G^+}\Big(\delta^{(1)}m^2_{H^-G^+} + \delta^{(1)}m^2_{G^-H^+}\Big) + \delta^{(2)}m^2_{H^\pm}\ ,
\end{aligned} \tag{C.2k}$$

$$\begin{aligned}
\delta^{(2)} m^{\mathbf{Z}}_{G^\pm} &= \left(m^2_{G^\pm} - p^2\right)\Big[\delta^{(2)}Z_{G^\pm G^\pm} + \tfrac{1}{4}\Big(\delta^{(1)}Z_{G^\pm G^\pm}\Big)^2\Big] + \left(m^2_{H^\pm} - p^2\right)\tfrac{1}{4}\Big(\delta^{(1)}Z_{G^-H^+}\Big)^2 \\
&\quad + \delta^{(1)}Z_{G^\pm G^\pm}\,\delta^{(1)}m^2_{G^\pm} + \tfrac{1}{2}\,\delta^{(1)}Z_{G^-H^+}\Big(\delta^{(1)}m^2_{G^-H^+} + \delta^{(1)}m^2_{H^-G^+}\Big) + \delta^{(2)}m^2_{G^\pm}\ ,
\end{aligned} \tag{C.2l}$$

$$\begin{aligned}
\delta^{(2)} m^{\mathbf{Z}}_{H^-G^+} &= \tfrac{1}{4}\Big[\left(m^2_{H^\pm} - p^2\right)\delta^{(1)}Z_{H^\pm H^\pm}\,\delta^{(1)}Z_{H^-G^+} + \left(m^2_{G^\pm} - p^2\right)\delta^{(1)}Z_{G^\pm G^\pm}\,\delta^{(1)}Z_{H^-G^+}\Big] \\
&\quad + \tfrac{1}{2}\Big[\Big(\delta^{(1)}Z_{H^\pm H^\pm} + \delta^{(1)}Z_{G^\pm G^\pm}\Big)\delta^{(1)}m^2_{H^-G^+} + \delta^{(1)}Z_{H^-G^+}\Big(\delta^{(1)}m^2_{H^\pm} + \delta^{(1)}m^2_{G^\pm}\Big)\Big] \\
&\quad + \left(\frac{m^2_{H^\pm} + m^2_{G^\pm}}{2} - p^2\right)\delta^{(2)}Z_{H^-G^+} + \delta^{(2)}m^2_{H^-G^+}\ ,
\end{aligned} \tag{C.2m}$$

$$\begin{aligned}
\delta^{(2)} m^{\mathbf{Z}}_{G^-H^+} &= \tfrac{1}{4}\Big[\left(m^2_{G^\pm} - p^2\right)\delta^{(1)}Z_{G^\pm G^\pm}\,\delta^{(1)}Z_{G^-H^+} + \left(m^2_{H^\pm} - p^2\right)\delta^{(1)}Z_{H^\pm H^\pm}\,\delta^{(1)}Z_{G^-H^+}\Big] \\
&\quad + \tfrac{1}{2}\Big[\Big(\delta^{(1)}Z_{G^\pm G^\pm} + \delta^{(1)}Z_{H^\pm H^\pm}\Big)\delta^{(1)}m^2_{G^-H^+} + \delta^{(1)}Z_{G^-H^+}\Big(\delta^{(1)}m^2_{G^\pm} + \delta^{(1)}m^2_{H^\pm}\Big)\Big] \\
&\quad + \left(\frac{m^2_{G^\pm} + m^2_{H^\pm}}{2} - p^2\right)\delta^{(2)}Z_{G^-H^+} + \delta^{(2)}m^2_{G^-H^+}\ .
\end{aligned} \tag{C.2n}$$

C.2. Genuine two-loop mass counterterms

The genuine two-loop mass counterterms appearing in the expressions of Eqs. (6.76) and in Section C.1 are listed in the following. Thereby $\delta^{(1)}e$, $\delta^{(1)}M_W$ and $\delta^{(1)}s_\mathrm{w}$ always appear in the combination $\delta^{(1)}Z_\mathrm{w} = \delta^{(1)}e\big/e - \delta^{(1)}M_W\big/M_W - \delta^{(1)}s_\mathrm{w}\big/s_\mathrm{w}$:

$$\begin{aligned}
\delta^{(2)}m_h^2 = {} & c_{\alpha-\beta}^2\,\delta^{(2)}m_A^2 + s_{\alpha+\beta}^2\,\delta^{(2)}m_Z^2 + c_\beta^2\,\delta^{(2)}t_\beta\left(s_{2(\alpha-\beta)}\,m_A^2 + s_{2(\alpha+\beta)}\,m_Z^2\right) \\
& + c_\beta^2\,\delta^{(1)}t_\beta\left(s_{2(\alpha-\beta)}\,\delta^{(1)}m_A^2 + s_{2(\alpha+\beta)}\,\delta^{(1)}m_Z^2\right) \\
& + \frac{1}{2}\,c_\beta^3\left(\delta^{(1)}t_\beta\right)^2\left[s_{\alpha-\beta}\left(3\,s_{\alpha-2\beta} - s_\alpha\right)m_A^2 + 2\,c_{2\alpha+3\beta}\,m_Z^2\right] \\
& + \frac{e\,s_{\alpha-\beta}}{2\,M_W\,s_\mathrm{w}}\Bigg[\left(1 + c_{\alpha-\beta}^2\right)\left(\delta^{(2)}T_h + \delta^{(1)}T_h\,\delta^{(1)}Z_\mathrm{w}\right) \\
& \qquad + s_{\alpha-\beta}\,c_{\alpha-\beta}\left(\delta^{(2)}T_H + \delta^{(1)}T_H\,\delta^{(1)}Z_\mathrm{w}\right) \\
& \qquad + s_{\alpha-\beta}\,c_\beta^2\,\delta^{(1)}t_\beta\left(c_{\alpha-\beta}\,\delta^{(1)}T_h + s_{\alpha-\beta}\,\delta^{(1)}T_H\right)\Bigg]\,,
\end{aligned} \tag{C.3a}$$

$$\begin{aligned}
\delta^{(2)}m_H^2 = {} & s_{\alpha-\beta}^2\,\delta^{(2)}m_A^2 + c_{\alpha+\beta}^2\,\delta^{(2)}m_Z^2 - c_\beta^2\,\delta^{(2)}t_\beta\left(s_{2(\alpha-\beta)}\,m_A^2 + s_{2(\alpha+\beta)}\,m_Z^2\right) \\
& - c_\beta^2\,\delta^{(1)}t_\beta\left(s_{2(\alpha-\beta)}\,\delta^{(1)}m_A^2 + s_{2(\alpha+\beta)}\,\delta^{(1)}m_Z^2\right) \\
& + \frac{1}{2}\,c_\beta^3\left(\delta^{(1)}t_\beta\right)^2\left[c_{\alpha-\beta}\left(3\,c_{\alpha-2\beta} - c_\alpha\right)m_A^2 - 2\,c_{2\alpha+3\beta}\,m_Z^2\right] \\
& - \frac{e\,c_{\alpha-\beta}}{2\,M_W\,s_\mathrm{w}}\Bigg[\left(1 + s_{\alpha-\beta}^2\right)\left(\delta^{(2)}T_H + \delta^{(1)}T_H\,\delta^{(1)}Z_\mathrm{w}\right) \\
& \qquad + c_{\alpha-\beta}\,s_{\alpha-\beta}\left(\delta^{(2)}T_h + \delta^{(1)}T_h\,\delta^{(1)}Z_\mathrm{w}\right) \\
& \qquad - c_{\alpha-\beta}\,c_\beta^2\,\delta^{(1)}t_\beta\left(c_{\alpha-\beta}\,\delta^{(1)}T_h + s_{\alpha-\beta}\,\delta^{(1)}T_H\right)\Bigg]\,,
\end{aligned} \tag{C.3b}$$

$$\begin{aligned}
\delta^{(2)}m_G^2 = {} & c_\beta^4\,m_A^2\left(\delta^{(1)}t_\beta\right)^2 \\
& + \frac{e}{2\,M_W\,s_\mathrm{w}}\Bigg[s_{\alpha-\beta}\left(\delta^{(2)}T_h + \delta^{(1)}T_h\,\delta^{(1)}Z_\mathrm{w}\right) \\
& \qquad - c_{\alpha-\beta}\left(\delta^{(2)}T_H + \delta^{(1)}T_H\,\delta^{(1)}Z_\mathrm{w}\right) \\
& \qquad + c_\beta^2\,\delta^{(1)}t_\beta\left(c_{\alpha-\beta}\,\delta^{(1)}T_h + s_{\alpha-\beta}\,\delta^{(1)}T_H\right)\Bigg]\,,
\end{aligned} \tag{C.3c}$$

$$\begin{aligned}
\delta^{(2)}m_{hH}^2 = {} & c_{\alpha-\beta}\,s_{\alpha-\beta}\,\delta^{(2)}m_A^2 - c_\beta^2\,\delta^{(2)}t_\beta\left(c_{2(\alpha-\beta)}\,m_A^2 + c_{2(\alpha+\beta)}\,m_Z^2\right) \\
& - c_{\alpha+\beta}\,s_{\alpha+\beta}\,\delta^{(2)}m_Z^2 - c_\beta^2\,\delta^{(1)}t_\beta\left(c_{2(\alpha-\beta)}\,\delta^{(1)}m_A^2 + c_{2(\alpha+\beta)}\,\delta^{(1)}m_Z^2\right) \\
& + \frac{1}{2}\,c_\beta^3\left(\delta^{(1)}t_\beta\right)^2\left[\left(-3\,c_\beta\,s_{2(\alpha-\beta)} + 2\,s_{2\alpha-\beta}\right)m_A^2 + 2\,s_{2\alpha+3\beta}\,m_Z^2\right] \\
& + \frac{e}{2\,M_W\,s_\mathrm{w}}\Bigg[-c_{\alpha-\beta}^3\left(\delta^{(2)}T_h + \delta^{(1)}T_h\,\delta^{(1)}Z_\mathrm{w}\right) \\
& \qquad + s_{\alpha-\beta}^3\left(\delta^{(2)}T_H + \delta^{(1)}T_H\,\delta^{(1)}Z_\mathrm{w}\right) \\
& \qquad - c_{\alpha-\beta}\,s_{\alpha-\beta}\,c_\beta^2\,\delta^{(1)}t_\beta\left(c_{\alpha-\beta}\,\delta^{(1)}T_h + s_{\alpha-\beta}\,\delta^{(1)}T_H\right)\Bigg]\,,
\end{aligned} \tag{C.3d}$$

$$\delta^{(2)}m^2_{hA} = \frac{e}{2\,M_W\,s_\mathrm{w}}\,s_{\alpha-\beta}\left(\delta^{(2)}T_A + \delta^{(1)}T_A\,\delta^{(1)}Z_\mathrm{w}\right)\;, \tag{C.3e}$$

$$\delta^{(2)}m^2_{hG} = \frac{e}{2\,M_W\,s_\mathrm{w}}\,c_{\alpha-\beta}\left(\delta^{(2)}T_A + \delta^{(1)}T_A\,\delta^{(1)}Z_\mathrm{w}\right)\;, \tag{C.3f}$$

$$\delta^{(2)}m^2_{HA} = -\delta^{(2)}m^2_{hG}\;, \tag{C.3g}$$

$$\delta^{(2)}m^2_{HG} = \delta^{(2)}m^2_{hA}\;, \tag{C.3h}$$

$$\begin{aligned}\delta^{(2)}m^2_{AG} = &-c_\beta^2\,m_A^2\,\delta^{(2)}t_\beta - c_\beta^2\,\delta^{(1)}m_A^2\,\delta^{(1)}t_\beta + c_\beta^3\,s_\beta\,m_A^2\left(\delta^{(1)}t_\beta\right)^2\\ &-\frac{e}{2\,M_W\,s_\mathrm{w}}\Bigg[c_{\alpha-\beta}\left(\delta^{(2)}T_h + \delta^{(1)}T_h\,\delta^{(1)}Z_\mathrm{w}\right)\\ &\qquad\qquad + s_{\alpha-\beta}\left(\delta^{(2)}T_H + \delta^{(1)}T_H\,\delta^{(1)}Z_\mathrm{w}\right)\Bigg]\;,\end{aligned} \tag{C.3i}$$

$$\begin{aligned}\delta^{(2)}m^2_{G^\pm} = &\,c_\beta^4\,m^2_{H^\pm}\left(\delta^{(1)}t_\beta\right)^2\\ &+\frac{e}{2\,M_W\,s_\mathrm{w}}\Bigg[s_{\alpha-\beta}\left(\delta^{(2)}T_h + \delta^{(1)}T_h\,\delta^{(1)}Z_\mathrm{w}\right)\\ &\qquad\qquad - c_{\alpha-\beta}\left(\delta^{(2)}T_H + \delta^{(1)}T_H\,\delta^{(1)}Z_\mathrm{w}\right)\\ &\qquad\qquad + c_\beta^2\,\delta^{(1)}t_\beta\left(c_{\alpha-\beta}\,\delta^{(1)}T_h + s_{\alpha-\beta}\,\delta^{(1)}T_H\right)\Bigg]\;,\end{aligned} \tag{C.3j}$$

$$\begin{aligned}\delta^{(2)}m^2_{H^-G^+} = &-c_\beta^2\,m^2_{H^\pm}\,\delta^{(2)}t_\beta + c_\beta^3\,s_\beta\,m^2_{H^\pm}\left(\delta^{(1)}t_\beta\right)^2\\ &-\frac{e}{2\,M_W\,s_\mathrm{w}}\Bigg[c_{\alpha-\beta}\left(\delta^{(2)}T_h + \delta^{(1)}T_h\,\delta^{(1)}Z_\mathrm{w}\right)\\ &\qquad\qquad + s_{\alpha-\beta}\left(\delta^{(2)}T_H + \delta^{(1)}T_H\,\delta^{(1)}Z_\mathrm{w}\right)\\ &\qquad\qquad + \boldsymbol{i}\left(\delta^{(2)}T_A + \delta^{(1)}T_A\,\delta^{(1)}Z_\mathrm{w}\right)\Bigg]\;,\end{aligned} \tag{C.3k}$$

$$\delta^{(2)}m^2_{G^-H^+} = \left(\delta^{(2)}m^2_{H^-G^+}\right)^*\;. \tag{C.3l}$$

D. Analytical $\mathcal{O}(\alpha_t^2)$ results

The analytical expressions for the leading $\mathcal{O}(\alpha_t^2)$ contributions to the Higgs tadpoles and self-energies that are described in Chapter 7 are listed in the following.

D.1. Symbols and abbreviations

The following symbols and abbreviations are used to express the analytical results in a compact way. To shorten the notation the absolute-value bars of $|X_t|^2$, $|Y_t|^2$ and $|\mu|^2$ are suppressed in the following terms:

$$\Delta_{a,b} = m_a^2 - m_b^2 \ , \tag{D.1a}$$

$$X_t = A_t^* - \tfrac{\mu}{t_\beta} \ , \qquad Y_t = A_t^* + \mu\, t_\beta \ , \tag{D.1b}$$

$$X_t^2 \equiv |X_t|^2 = X_t\, X_t^* \ , \quad x_t^2 = \tfrac{X_t^2}{\Delta_{\tilde{t}_i \tilde{t}_j}} \ , \qquad Y_t^2 \equiv |Y_t|^2 = Y_t\, Y_t^* \ , \quad y_t^2 = \tfrac{Y_t^2}{\Delta_{\tilde{t}_i \tilde{t}_j}} \ , \tag{D.1c}$$

$$\mu^2 \equiv |\mu|^2 = \mu\, \mu^* \ , \qquad \eta = \tfrac{\mu^2}{s_\beta^2 c_\beta^2 \Delta_{\tilde{t}_i \tilde{t}_j}} - x_t^2 - y_t^2 \ , \tag{D.1d}$$

$$U_- = \mathbf{U}_{\tilde{t}\,1i}\, \mathbf{U}_{\tilde{t}\,1i}^* - \mathbf{U}_{\tilde{t}\,1j}\, \mathbf{U}_{\tilde{t}\,1j}^* \ , \qquad U_\times = \tfrac{1-U_-^2}{4} = \tfrac{m_t^2}{\Delta_{\tilde{t}_i \tilde{t}_j}}\, x_t^2 \ , \tag{D.1e}$$

$$h_t = \tfrac{e m_t}{\sqrt{2} s_\beta s_\mathrm{w} M_W} \ , \qquad \delta^{(1)} h_t = h_t \left(\tfrac{\delta^{(1)} m_t}{m_t} - \tfrac{\delta^{(1)} M_W}{M_W} - \tfrac{\delta^{(1)} s_\mathrm{w}}{s_\mathrm{w}} - \tfrac{\delta^{(1)} s_\beta}{s_\beta} \right) \ , \tag{D.1f}$$

$$\tfrac{\delta^{(1)} x_t^2}{x_t^2} = \tfrac{\delta^{(1)} X_t}{X_t} + \tfrac{\delta^{(1)} X_t^*}{X_t^*} \ , \qquad \delta^{(1)} \phi_X = -\tfrac{i}{2} \left(\tfrac{\delta^{(1)} X_t}{X_t} - \tfrac{\delta^{(1)} X_t^*}{X_t^*} \right) \ , \tag{D.1g}$$

$$\delta^{(1)} X_t = \delta^{(1)} A_t^* - \tfrac{\delta^{(1)} \mu}{t_\beta} \ , \qquad \delta^{(1)} X_t^* = \delta^{(1)} A_t - \tfrac{\delta^{(1)} \mu^*}{t_\beta} \ . \tag{D.1h}$$

D.2. Genuine two-loop self-energies

The explicit expressions of the genuine two-loop integrals contributing to the Higgs-boson self-energies are depicted in the following.

$$\begin{aligned}
\Sigma_{hh}^{(2)\,\mathrm{gen}} = {} & \frac{N_c s_\beta^2 h_t^4}{256\pi^4} \Big\{ s_A + 4 m_t^2 s_B \Big\} \\
& + \sum_{\substack{i\,=\,1 \\ j\,\neq\,i}}^{2} \frac{N_c s_\beta^2 h_t^4}{256\pi^4} \Big\{ - x_t^2 \left(1 - 12 U_\times\right) s_D - 2 m_t^2 \left(1 + x_t^2\right)^2 s_E + 4 m_t^2 \left(1 + x_t^2\right) s_F \\
& \qquad - \left(1 - 16 U_\times\right) x_t^2 s_G + \left(1 - 4 U_\times\right) x_t^2 s_H + \left(1 + x_t^2 \left(1 - 4 U_\times\right)\right) s_{I_1} \\
& \qquad + \left(1 + x_t^2 + 4 U_\times\right) s_{I_2} + 2 \left(m_t^2 - U_\times X_t^2\right) s_J + \tfrac{1}{2} s_{K_1} \Big\},
\end{aligned} \tag{D.2a}$$

$$
\begin{aligned}
\Sigma_{HH}^{(2)\,\text{gen}} &= \frac{N_c c_\beta^2 h_t^4}{256\pi^4}\Big\{s_A + 4m_t^2 s_B\Big\} \\
&\quad + \sum_{\substack{i\,=\,1\\ j\,\neq\, i}}^{2} \frac{N_c c_\beta^2 h_t^4}{256\pi^4}\bigg\{\tfrac{3m_t^2\eta^2 - Y_t^2}{\Delta_{\tilde{t}_i\tilde{t}_j}} s_D - \tfrac{m_t^2}{2}\left(\eta-2\right)^2 s_E - 2m_t^2\left(\eta-2\right)s_F + \tfrac{4m_t^2\eta^2 - Y_t^2}{\Delta_{\tilde{t}_i\tilde{t}_j}} s_G \\
&\qquad - \tfrac{\left(m_t^2\eta^2 - Y_t^2\right)}{\Delta_{\tilde{t}_i\tilde{t}_j}} s_H - \left(\tfrac{m_t^2\eta^2 - Y_t^2}{\Delta_{\tilde{t}_i\tilde{t}_j}} - 1\right) s_{I_1} - \left(\tfrac{2m_t^2\eta - Y_t^2}{\Delta_{\tilde{t}_i\tilde{t}_j}} - 1\right) s_{I_2} \\
&\qquad - m_t^2\left(\tfrac{\eta^2}{2} - 2\right) s_J + \tfrac{1}{2} s_{L_1}\bigg\},
\end{aligned}
\tag{D.2b}
$$

$$
\begin{aligned}
\Sigma_{hH}^{(2)\,\text{gen}} &= -\frac{N_c s_\beta c_\beta h_t^4}{256\pi^4}\Big\{s_A + 4m_t^2 s_B\Big\} \\
&\quad - \sum_{\substack{i\,=\,1\\ j\,\neq\, i}}^{2} \frac{N_c s_\beta c_\beta h_t^4}{256\pi^4}\bigg\{ -\tfrac{\eta}{2}\left(1 - 12U_\times\right) s_D + m_t^2\left(\eta - 2\right)\left(1 + x_t^2\right) s_E \\
&\qquad - 2m_t^2\left[\tfrac{\eta}{2} - 1 - \left(1 + x_t^2\right)\right] s_F + \left(1 - 16U_\times\right)\tfrac{\eta}{2} s_G + \left(1 - 4U_\times\right)\tfrac{\eta}{2} s_H \\
&\qquad + \left[1 - \tfrac{\eta}{2}\left(1 - 4U_\times\right)\right] s_{I_1} + \left[1 + 2U_\times - \tfrac{\eta}{2}\left(1 + \tfrac{2m_t^2}{\Delta_{\tilde{t}_i\tilde{t}_j}}\right)\right] s_{I_2} \\
&\qquad + m_t^2\left(\eta x_t^2 + 2\right) s_J + \tfrac{1}{2} s_{K_1} + \tfrac{1}{2}\left(\tfrac{\eta}{2} + x_t^2\right) s_{K_2} - s_{K_3}\bigg\},
\end{aligned}
\tag{D.2c}
$$

$$
\begin{aligned}
\Sigma_{AA}^{(2)\,\text{gen}} &= \frac{N_c c_\beta^2 h_t^4}{256\pi^4} s_A \\
&\quad + \sum_{\substack{i\,=\,1\\ j\,\neq\, i}}^{2} \frac{N_c c_\beta^2 h_t^4}{256\pi^4}\bigg\{ -\tfrac{3m_t^2\eta^2 + (1-12U_\times)Y_t^2}{\Delta_{\tilde{t}_i\tilde{t}_j}} s_D + \tfrac{m_t^2}{2}\left(\eta^2 - 4x_t^2 y_t^2\right) s_E - \tfrac{4m_t^2\eta^2 + (1-16U_\times)Y_t^2}{\Delta_{\tilde{t}_i\tilde{t}_j}} s_G \\
&\qquad + \tfrac{m_t^2\eta^2 + (1-4U_\times)Y_t^2}{\Delta_{\tilde{t}_i\tilde{t}_j}} s_H + \left[1 + \tfrac{m_t^2\eta^2}{\Delta_{\tilde{t}_i\tilde{t}_j}} + \left(1 - 4U_\times\right) y_t^2\right] s_{I_1} \\
&\qquad + \left(1 + y_t^2\right) s_{I_2} + \left(\tfrac{m_t^2\eta^2}{2} - 2U_\times Y_t^2\right) s_J + \tfrac{1}{2} s_{L_1} + \eta s_{L_2} - s_{L_3}\bigg\},
\end{aligned}
\tag{D.2d}
$$

$$
\begin{aligned}
\Sigma_{hA}^{(2)\,\text{gen}} &= \sum_{\substack{i\,=\,1\\ j\,\neq\, i}}^{2} \frac{N_c h_t^4}{256\pi^4}\frac{\Im\mathfrak{m}[X_t\mu^*]}{s_\beta c_\beta \Delta_{\tilde{t}_i\tilde{t}_j}}\bigg\{\left(1 - 12U_\times\right) s_D + 2m_t^2\left(1 + x_t^2\right) s_E - 2m_t^2 s_F + \left(1 - 16U_\times\right) s_G \\
&\qquad - \left(1 - 4U_\times\right)\left(s_H + s_{I_1}\right) - \left(1 + \tfrac{2m_t^2}{\Delta_{\tilde{t}_i\tilde{t}_j}}\right) s_{I_2} + 2m_t^2 x_t^2 s_J + \tfrac{1}{2} s_{K_2}\bigg\},
\end{aligned}
\tag{D.2e}
$$

$$
\begin{aligned}
\Sigma_{HA}^{(2)\,\text{gen}} &= \sum_{\substack{i\,=\,1\\ j\,\neq\, i}}^{2} \frac{N_c c_\beta h_t^4}{256\pi^4 s_\beta}\frac{\Im\mathfrak{m}[X_t\mu^*]}{s_\beta c_\beta \Delta_{\tilde{t}_i\tilde{t}_j}}\bigg\{ -\tfrac{6m_t^2\eta}{\Delta_{\tilde{t}_i\tilde{t}_j}} s_D + m_t^2\left(\eta - 2\right) s_E + 2m_t^2 s_F - \tfrac{8m_t^2\eta}{\Delta_{\tilde{t}_i\tilde{t}_j}} s_G \\
&\qquad + \tfrac{2m_t^2\eta}{\Delta_{\tilde{t}_i\tilde{t}_j}} s_H + \tfrac{2m_t^2\eta}{\Delta_{\tilde{t}_i\tilde{t}_j}} s_{I_1} + \tfrac{2m_t^2}{\Delta_{\tilde{t}_i\tilde{t}_j}} s_{I_2} + m_t^2\eta s_J + s_{L_2}\bigg\},
\end{aligned}
\tag{D.2f}
$$

$$
\begin{aligned}
\Sigma_{H^\pm H^\pm}^{(2)\,\text{gen}} &= \frac{N_c c_\beta^2 h_t^4}{256\pi^4}\Big\{s_A + \tfrac{\mu^2}{s_\beta^2 c_\beta^2}\tfrac{m_t^2}{\Delta_{\tilde{t}_i\tilde{b}_1}\Delta_{\tilde{t}_j\tilde{b}_1}} s_C\Big\} \\
&\quad + \sum_{\substack{i\,=\,1\\ j\,\neq\, i}}^{2} \frac{N_c c_\beta^2 h_t^4}{256\pi^4}\bigg\{\tfrac{\Delta_{\tilde{t}_i\tilde{t}_j}}{2\Delta_{\tilde{t}_i\tilde{b}_1}}\left[\left(y_t^2 + 1\right)\left(\tfrac{2m_t^2}{\Delta_{\tilde{t}_i\tilde{t}_j}} + 1 - U_-\right) - \tfrac{2\mu^2 m_t^2}{c_\beta^2 s_\beta^2 \Delta_{\tilde{t}_i\tilde{t}_j}^2}\right]\left(s_{I_1} + s_{I_2}\right) \\
&\qquad + \tfrac{m_t^2\mu^2\Delta_{\tilde{t}_i\tilde{t}_j}}{2s_\beta^2 c_\beta^2 \Delta_{\tilde{t}_i\tilde{b}_1}\Delta_{\tilde{t}_j\tilde{b}_1}} s_M + s_N + \tfrac{\Delta_{\tilde{t}_i\tilde{t}_j}}{\Delta_{\tilde{t}_i\tilde{b}_1}} s_O\bigg\}.
\end{aligned}
\tag{D.2g}
$$

$$
\begin{aligned}
s_A &= \mathrm{T}_{134}\Big(m_t^2, m_{\tilde{b}_1}^2, \mu^2\Big) - 3\mathrm{T}_{113}\big(m_t^2, m_t^2, \mu^2\big) - 2\mathrm{T}_{113}\big(m_t^2, m_t^2, m_t^2\big) + \mathrm{T}_{113}\Big(m_t^2, m_t^2, m_{\tilde{b}_1}^2\Big) \\
&\quad + \Big(m_t^2 - m_{\tilde{b}_1}^2 + \mu^2\Big)\,\mathrm{T}_{1134}\Big(m_t^2, m_t^2, m_{\tilde{b}_1}^2, \mu^2\Big) + \sum_{i=1}^{2} \mathrm{T}_{113}\Big(m_t^2, m_t^2, m_{\tilde{t}_i}^2\Big) \qquad \text{(D.3a)} \\
&\quad + c_\beta^2 s_A^H + s_\beta^2\, s_A^H\big|_{m_{H^\pm}\to 0,\ Y_t^2\to X_t^2,\ y_t^2\to x_t^2,\ \eta\to -2x_t^2}\ ,
\end{aligned}
$$

$$
\begin{aligned}
s_A^H &= 3\mathrm{T}_{113}\big(m_t^2, m_t^2, m_{H^\pm}^2\big) + \mathrm{T}_{134}\big(m_t^2, 0, m_{H^\pm}^2\big) + 2\mathrm{T}_{134}\big(m_t^2, m_t^2, m_{H^\pm}^2\big) \\
&\quad + \big(m_t^2 - m_{H^\pm}^2\big)\,\mathrm{T}_{1134}\big(m_t^2, m_t^2, 0, m_{H^\pm}^2\big) + 2\,\big(2m_t^2 - m_{H^\pm}^2\big)\,\mathrm{T}_{1134}\big(m_t^2, m_t^2, m_t^2, m_{H^\pm}^2\big), \qquad \text{(D.3b)}
\end{aligned}
$$

$$
\begin{aligned}
s_B &= \mathrm{T}_{1113}\Big(m_t^2, m_t^2, m_t^2, m_{\tilde{b}_1}^2\Big) - 3\mathrm{T}_{1113}\big(m_t^2, m_t^2, m_t^2, \mu^2\big) - 2\mathrm{T}_{1113}\big(m_t^2, m_t^2, m_t^2, m_t^2\big) \\
&\quad - \mathrm{T}_{1133}\big(m_t^2, m_t^2, m_t^2, m_t^2\big) + \mathrm{T}_{1134}\Big(m_t^2, m_t^2, m_{\tilde{b}_1}^2, \mu^2\Big) \\
&\quad + \Big(m_t^2 - m_{\tilde{b}_1}^2 + \mu^2\Big)\,\mathrm{T}_{11134}\Big(m_t^2, m_t^2, m_t^2, m_{\tilde{b}_1}^2, \mu^2\Big) \qquad \text{(D.4a)} \\
&\quad + \sum_{i=1}^{2}\Big[\Big(m_t^2 - m_{\tilde{t}_i}^2 + \mu^2\Big)\,\mathrm{T}_{11134}\Big(m_t^2, m_t^2, m_t^2, m_{\tilde{t}_i}^2, \mu^2\Big) + \mathrm{T}_{1113}\Big(m_t^2, m_t^2, m_t^2, m_{\tilde{t}_i}^2\Big)\Big] \\
&\quad + c_\beta^2 s_B^H + s_\beta^2\, s_B^H\big|_{m_{H^\pm}\to 0,\ Y_t^2\to X_t^2,\ y_t^2\to x_t^2,\ \eta\to -2x_t^2}\ ,
\end{aligned}
$$

$$
\begin{aligned}
s_B^H &= 3\mathrm{T}_{1113}\big(m_t^2, m_t^2, m_t^2, m_{H^\pm}^2\big) + \big(m_t^2 - m_{H^\pm}^2\big)\,\mathrm{T}_{11134}\big(m_t^2, m_t^2, m_t^2, 0, m_{H^\pm}^2\big) \\
&\quad + \mathrm{T}_{1134}\big(m_t^2, m_t^2, 0, m_{H^\pm}^2\big) + 4\mathrm{T}_{1134}\big(m_t^2, m_t^2, m_t^2, m_{H^\pm}^2\big) \qquad \text{(D.4b)} \\
&\quad + \big(2m_t^2 - m_{H^\pm}^2\big)\,\big(2\mathrm{T}_{11134}\big(m_t^2, m_t^2, m_t^2, m_t^2, m_{H^\pm}^2\big) + \mathrm{T}_{11334}\big(m_t^2, m_t^2, m_t^2, m_t^2, m_{H^\pm}^2\big)\big)\,,
\end{aligned}
$$

$$
\begin{aligned}
s_C &= -\mathrm{T}_{113}\Big(m_{\tilde{b}_1}^2, m_{\tilde{b}_1}^2, m_t^2\Big) - \mathrm{T}_{113}\Big(m_{\tilde{b}_1}^2, m_{\tilde{b}_1}^2, \mu^2\Big) + \mathrm{T}_{134}\Big(m_t^2, m_{\tilde{b}_1}^2, \mu^2\Big) \\
&\quad - \Big(m_t^2 - m_{\tilde{b}_1}^2 + \mu^2\Big)\,\mathrm{T}_{1134}\Big(m_{\tilde{b}_1}^2, m_{\tilde{b}_1}^2, m_t^2, \mu^2\Big) \\
&\quad + \tfrac{m_t^2}{\Delta_{\tilde{t}_i\tilde{b}_1}\Delta_{\tilde{t}_j\tilde{b}_1}}\Big[\mathrm{T}_{13}\Big(m_{\tilde{b}_1}^2, \mu^2\Big) - 4\mathrm{T}_{13}\Big(m_{\tilde{b}_1}^2, m_{\tilde{b}_1}^2\Big) - \Big(m_{\tilde{b}_1}^2 - \mu^2\Big)\,\mathrm{T}_{134}\Big(m_{\tilde{b}_1}^2, \mu^2, 0\Big)\Big] \\
&\quad + c_\beta^2\Big\{\mathrm{T}_{113}\Big(m_{\tilde{b}_1}^2, m_{\tilde{b}_1}^2, m_{H^\pm}^2\Big) - \tfrac{m_t^2}{\Delta_{\tilde{t}_i\tilde{b}_1}\Delta_{\tilde{t}_j\tilde{b}_1}}\Big[\mathrm{T}_{13}\Big(m_{\tilde{b}_1}^2, m_{H^\pm}^2\Big) + \mu^2\mathrm{T}_{134}\Big(m_{\tilde{b}_1}^2, m_{\tilde{b}_1}^2, m_{H^\pm}^2\Big)\Big]\Big\}, \qquad \text{(D.5a)}
\end{aligned}
$$

$$
s_D = \tfrac{U_-}{\Delta_{\tilde{t}_i\tilde{t}_j}}\Big[\mathrm{T}_{13}\Big(m_{\tilde{t}_i}^2, m_{\tilde{b}_1}^2\Big) - \mathrm{T}_{13}\Big(m_{\tilde{t}_i}^2, \mu^2\Big) + c_\beta^2\mathrm{T}_{13}\Big(m_{\tilde{t}_i}^2, m_{H^\pm}^2\Big)\Big]\,, \qquad \text{(D.6a)}
$$

$$
\begin{aligned}
s_E &= (1-U_-)\,\mathrm{T}_{1113}\Big(m_{\tilde{t}_i}^2, m_{\tilde{t}_i}^2, m_{\tilde{t}_i}^2, m_{\tilde{b}_1}^2\Big) - 2\,(8U_\times - 1)\,\mathrm{T}_{1113}\Big(m_{\tilde{t}_i}^2, m_{\tilde{t}_i}^2, m_{\tilde{t}_i}^2, m_{\tilde{t}_j}^2\Big) \\
&\quad - 2\,\Big(m_t^2 - m_{\tilde{t}_i}^2 + \mu^2\Big)\,\mathrm{T}_{11134}\Big(m_{\tilde{t}_i}^2, m_{\tilde{t}_i}^2, m_{\tilde{t}_i}^2, m_t^2, \mu^2\Big) + (U_- - 3)\,\mathrm{T}_{1113}\Big(m_{\tilde{t}_i}^2, m_{\tilde{t}_i}^2, m_{\tilde{t}_i}^2, \mu^2\Big) \\
&\quad + (1-U_-)\,\Big(m_{\tilde{t}_i}^2 - \mu^2\Big)\,\mathrm{T}_{11134}\Big(m_{\tilde{t}_i}^2, m_{\tilde{t}_i}^2, m_{\tilde{t}_i}^2, 0, \mu^2\Big) + 16U_\times\mathrm{T}_{1113}\Big(m_{\tilde{t}_i}^2, m_{\tilde{t}_i}^2, m_{\tilde{t}_i}^2, m_{\tilde{t}_i}^2\Big) \\
&\quad + 8U_\times\mathrm{T}_{1133}\Big(m_{\tilde{t}_i}^2, m_{\tilde{t}_i}^2, m_{\tilde{t}_i}^2, m_{\tilde{t}_i}^2\Big) - 2\mathrm{T}_{1113}\Big(m_{\tilde{t}_i}^2, m_{\tilde{t}_i}^2, m_{\tilde{t}_i}^2, m_t^2\Big) \\
&\quad + c_\beta^2 s_E^H + s_\beta^2\, s_E^H\big|_{m_{H^\pm}\to 0,\ Y_t^2\to X_t^2,\ y_t^2\to x_t^2,\ \eta\to -2x_t^2}\ , \qquad \text{(D.7a)}
\end{aligned}
$$

$$
\begin{aligned}
s_E^H &= 2m_t^2\,\big(1 + x_t^2y_t^2 - \eta\big)\,\Big[2\mathrm{T}_{11134}\Big(m_{\tilde{t}_i}^2, m_{\tilde{t}_i}^2, m_{\tilde{t}_i}^2, m_{\tilde{t}_i}^2, m_{H^\pm}^2\Big) + \mathrm{T}_{11334}\Big(m_{\tilde{t}_i}^2, m_{\tilde{t}_i}^2, m_{\tilde{t}_i}^2, m_{\tilde{t}_i}^2, m_{H^\pm}^2\Big)\Big] \\
&\quad + 2Y_t^2\,(1-2U_\times)\,\mathrm{T}_{11134}\Big(m_{\tilde{t}_i}^2, m_{\tilde{t}_i}^2, m_{\tilde{t}_i}^2, m_{\tilde{t}_j}^2, m_{H^\pm}^2\Big) + (3-U_-)\,\mathrm{T}_{1113}\Big(m_{\tilde{t}_i}^2, m_{\tilde{t}_i}^2, m_{\tilde{t}_i}^2, m_{H^\pm}^2\Big) \\
&\quad + \big(m_t^2\,(1 + U_- - 2\eta) + (1-U_-)\,Y_t^2\big)\,\mathrm{T}_{11134}\Big(m_{\tilde{t}_i}^2, m_{\tilde{t}_i}^2, m_{\tilde{t}_i}^2, m_{\tilde{b}_1}^2, m_{H^\pm}^2\Big), \qquad \text{(D.7b)}
\end{aligned}
$$

$$s_F = \left(m_t^2 - m_{\tilde{t}_i}^2 + \mu^2\right) \mathrm{T}_{11334}\left(m_{\tilde{t}_i}^2, m_{\tilde{t}_i}^2, m_t^2, m_t^2, \mu^2\right) + \mathrm{T}_{1133}\left(m_{\tilde{t}_i}^2, m_{\tilde{t}_i}^2, m_t^2, m_t^2\right), \tag{D.8a}$$

$$\begin{aligned} s_G = \tfrac{1-4U_\times}{\Delta_{\tilde{t}_i\tilde{t}_j}} \Big[&4\mathrm{T}_{13}\left(m_{\tilde{t}_i}^2, m_{\tilde{t}_i}^2\right) - 4\mathrm{T}_{13}\left(m_{\tilde{t}_i}^2, m_{\tilde{t}_j}^2\right) \\ &- c_\beta^2 Y_t^2 \mathrm{T}_{134}\left(m_{\tilde{t}_i}^2, m_{\tilde{t}_j}^2, m_{H^\pm}^2\right) - s_\beta^2 X_t^2 \mathrm{T}_{134}\left(m_{\tilde{t}_i}^2, m_{\tilde{t}_j}^2, 0\right)\Big], \end{aligned} \tag{D.9a}$$

$$s_H = -\mathrm{T}_{134}\left(m_{\tilde{t}_i}^2, m_t^2, \mu^2\right), \tag{D.10a}$$

$$\begin{aligned} s_{I_1} = &-\tfrac{1}{2}\left(1 - 3U_-\right) \mathrm{T}_{113}\left(m_{\tilde{t}_i}^2, m_{\tilde{t}_i}^2, m_{\tilde{b}_1}^2\right) + \left(m_t^2 - m_{\tilde{t}_j}^2 + \mu^2\right) \mathrm{T}_{1134}\left(m_{\tilde{t}_i}^2, m_{\tilde{t}_i}^2, m_t^2, \mu^2\right) \\ &- \left(9 - 40U_\times\right) \mathrm{T}_{113}\left(m_{\tilde{t}_i}^2, m_{\tilde{t}_i}^2, m_{\tilde{t}_j}^2\right) + \tfrac{3}{2}\left(1 - U_-\right) \mathrm{T}_{113}\left(m_{\tilde{t}_i}^2, m_{\tilde{t}_i}^2, \mu^2\right) \\ &+ 8\left(1 - 5U_\times\right) \mathrm{T}_{113}\left(m_{\tilde{t}_i}^2, m_{\tilde{t}_i}^2, m_{\tilde{t}_i}^2\right) + \mathrm{T}_{113}\left(m_{\tilde{t}_i}^2, m_{\tilde{t}_i}^2, m_t^2\right) \\ &+ c_\beta^2 s_{I_1}^H + s_\beta^2\ s_{I_1}^H\big|_{m_{H^\pm}\to 0,\ Y_t^2\to X_t^2,\ y_t^2\to x_t^2,\ \eta\to -2x_t^2}\ , \end{aligned} \tag{D.11a}$$

$$s_{I_1}^H = -Y_t^2\left(3 - 10U_\times\right) \mathrm{T}_{1134}\left(m_{\tilde{t}_i}^2, m_{\tilde{t}_i}^2, m_{\tilde{t}_j}^2, m_{H^\pm}^2\right) - \tfrac{3}{2}\left(1 - U_-\right) \mathrm{T}_{113}\left(m_{\tilde{t}_i}^2, m_{\tilde{t}_i}^2, m_{H^\pm}^2\right), \tag{D.11b}$$

$$\begin{aligned} s_{I_2} = U_- &\left[\mathrm{T}_{113}\left(m_{\tilde{t}_i}^2, m_{\tilde{t}_i}^2, \mu^2\right) - \mathrm{T}_{113}\left(m_{\tilde{t}_i}^2, m_{\tilde{t}_i}^2, m_{\tilde{b}_1}^2\right)\right] - \Delta_{\tilde{t}_i\tilde{t}_j} \mathrm{T}_{1134}\left(m_{\tilde{t}_i}^2, m_{\tilde{t}_i}^2, m_t^2, \mu^2\right) \\ &+ 8\left(1 - 4U_\times\right)\left[\mathrm{T}_{113}\left(m_{\tilde{t}_i}^2, m_{\tilde{t}_i}^2, m_{\tilde{t}_j}^2\right) - \mathrm{T}_{113}\left(m_{\tilde{t}_i}^2, m_{\tilde{t}_i}^2, m_{\tilde{t}_i}^2\right)\right] \\ &+ c_\beta^2 s_{I_2}^H + s_\beta^2\ s_{I_2}^H\big|_{m_{H^\pm}\to 0,\ Y_t^2\to X_t^2,\ y_t^2\to x_t^2,\ \eta\to -2x_t^2}\ , \end{aligned} \tag{D.12a}$$

$$s_{I_2}^H = 2Y_t^2\left(1 - 4U_\times\right) \mathrm{T}_{1134}\left(m_{\tilde{t}_i}^2, m_{\tilde{t}_i}^2, m_{\tilde{t}_j}^2, m_{H^\pm}^2\right) - U_- \mathrm{T}_{113}\left(m_{\tilde{t}_i}^2, m_{\tilde{t}_i}^2, m_{H^\pm}^2\right), \tag{D.12b}$$

$$s_J = -\left(1 - 8U_\times\right) \mathrm{T}_{1133}\left(m_{\tilde{t}_i}^2, m_{\tilde{t}_i}^2, m_{\tilde{t}_j}^2, m_{\tilde{t}_j}^2\right) - c_\beta^2 s_J^H - s_\beta^2\ s_J^H\big|_{m_{H^\pm}\to 0,\ Y_t^2\to X_t^2,\ y_t^2\to x_t^2,\ \eta\to -2x_t^2}\ , \tag{D.13a}$$

$$s_J^H = Y_t^2\left(1 - 2U_\times\right) \mathrm{T}_{11334}\left(m_{\tilde{t}_i}^2, m_{\tilde{t}_i}^2, m_{\tilde{t}_j}^2, m_{\tilde{t}_j}^2, m_{H^\pm}^2\right), \tag{D.13b}$$

$$\begin{aligned} s_{K_1} = &\left\{U_-\left[\left(x_t^2\left(2\tfrac{\mu^2 - m_{\tilde{t}_i}^2}{\Delta_{\tilde{t}_i\tilde{t}_j}} + 1\right)\left(1 - 12U_\times\right)\right) + 1 - 8U_\times\right] - x_t^2\left(1 - 4U_\times\right) - 1\right\} \mathrm{T}_{134}\left(m_{\tilde{t}_i}^2, \mu^2, 0\right) \\ &+ \left[-8U_\times\Delta_{\tilde{t}_i\tilde{t}_j} + 2m_t^2 + 2\left(\mu^2 - m_{\tilde{t}_i}^2\right)\right] \mathrm{T}_{1134}\left(m_t^2, m_t^2, m_{\tilde{t}_i}^2, \mu^2\right) \\ &- \Big\{\left(\mu^2 - m_{\tilde{t}_i}^2\right)\left[\left(1 - 4U_\times\right) + 1 - U_-\left(x_t^2\left(1 - 12U_\times\right) + 1 - 8U_\times\right)\right] \\ &\qquad + 4\left(1 - U_-\right) m_t^2\left(x_t^2 + 1\right)^2\Big\} \mathrm{T}_{1134}\left(m_{\tilde{t}_i}^2, m_{\tilde{t}_i}^2, 0, \mu^2\right) \\ &+ c_\beta^2 s_{K_1}^H + s_\beta^2\ s_{K_1}^H\big|_{m_{H^\pm}\to 0,\ Y_t^2\to X_t^2,\ y_t^2\to x_t^2,\ \eta\to -2x_t^2}\ , \end{aligned} \tag{D.14a}$$

$$\begin{aligned} s_{K_1}^H = &\left[-1 + \left(2\eta - U_-\right)\left(1 - 6U_\times\right)\left(1 - 4U_\times\right) - 2U_- x_t^2 y_t^2\left(1 - 12U_\times\right)\right] \mathrm{T}_{134}\left(m_{\tilde{t}_i}^2, m_{\tilde{b}_1}^2, m_{H^\pm}^2\right) \\ &+ 2\left\{-1 + \left[1 - 4U_\times\right]\left[\eta\left(1 - 6U_\times\right) - x_t^2 y_t^2\left(1 - 16U_\times\right)\right]\right\} \mathrm{T}_{134}\left(m_{\tilde{t}_i}^2, m_{\tilde{t}_i}^2, m_{H^\pm}^2\right) \\ &+ \Big\{\left(\eta - \tfrac{U_-}{2}\right)\left[\tfrac{2m_t^2}{\Delta_{\tilde{t}_i\tilde{t}_j}}\left(5 - 8U_\times\right) + 2U_\times\left(5 - 12U_\times\right)\right] + \left[1 - 4U_\times\right]\left[1 - U_\times - x_t^2 y_t^2\right] - \tfrac{5m_t^2}{\Delta_{\tilde{t}_i\tilde{t}_j}} \\ &\qquad + U_-\left[x_t^2 y_t^2\left(1 - 12U_\times\right) + y_t^2\left(1 - 8U_\times\right)\right] - 1 - y_t^2\Big\}\Delta_{\tilde{t}_i\tilde{t}_j} \mathrm{T}_{1134}\left(m_{\tilde{t}_i}^2, m_{\tilde{t}_i}^2, m_{\tilde{b}_1}^2, m_{H^\pm}^2\right) \\ &+ 4m_t^2\Big\{\eta\left[x_t^2\left(5 - 12U_\times\right) + 5 - 8U_\times\right] + x_t^2 y_t^2\left[-\left(5x_t^2\left(1 - 4U_\times\right) + 5 - 16U_\times\right)\right] \\ &\qquad - x_t^2\left[5 - 4U_\times\right] - 5\Big\} \mathrm{T}_{1134}\left(m_{\tilde{t}_i}^2, m_{\tilde{t}_i}^2, m_{\tilde{t}_i}^2, m_{H^\pm}^2\right), \end{aligned} \tag{D.14b}$$

$$
\begin{aligned}
s_{K_2} = 8 &\left\{\left(\mu^2 - m^2_{\tilde t_i}\right)\left(\frac{U_- m_t^2\left(x_t^2+\frac{1}{2}\right)}{\Delta_{\tilde t_i \tilde t_j}} + \frac{(1-U_-)(1-4U_\times)}{8}\right) - \frac{m_t^2\left(x_t^2+1\right)(1-U_-)}{2}\right\} \mathrm{T}_{1134}\left(m^2_{\tilde t_i}, m^2_{\tilde t_i}, \mu^2, 0\right) \\
&+ \left\{-U_-\left[(1-12U_\times)\left(2\frac{\mu^2-m^2_{\tilde t_i}}{\Delta_{\tilde t_i \tilde t_j}}+1\right) - \frac{4m_t^2}{\Delta_{\tilde t_i \tilde t_j}}\right] + 1 - 4U_\times\right\} \mathrm{T}_{134}\left(m^2_{\tilde t_i}, \mu^2, 0\right) \\
&+ 4m_t^2 \mathrm{T}_{1134}\left(m_t^2, m_t^2, m^2_{\tilde t_i}, \mu^2\right) + c_\beta^2 s^H_{K_2} + s^2_\beta\, s^H_{K_2}\big|_{m_{H^\pm}\to 0,\ Y_t^2 \to X_t^2,\ y_t^2\to x_t^2,\ \eta\to -2x_t^2}\ ,
\end{aligned} \tag{D.15a}
$$

$$
\begin{aligned}
s^H_{K_2} = &\left\{2\left[1-4U_\times\right]\left[1 + \frac{3m_t^2}{\Delta_{\tilde t_i \tilde t_j}}\left(2\eta - U_- m_t^2\right)\right] + 2U_- y_t^2\left[1-12U_\times\right]\right\} \mathrm{T}_{134}\left(m^2_{\tilde t_i}, m^2_{\tilde b_1}, m^2_{H^\pm}\right) \\
&+ 2\left(1-4U_\times\right)\left[1 + \frac{6\eta m_t^2}{\Delta_{\tilde t_i \tilde t_j}} + y_t^2\left(1-16U_\times\right)\right] \mathrm{T}_{134}\left(m^2_{\tilde t_i}, m^2_{\tilde t_i}, m^2_{H^\pm}\right) \\
&+ \left\{m_t^2\left[4x_t^2 + 7 - 4U_\times\right] + \left[\frac{4m_t^2}{\Delta_{\tilde t_i \tilde t_j}} - 3\left(1-4U_\times\right)\right]\left[2\eta m_t^2 + U_-\left(Y_t^2 - m_t^2\right)\right]\right. \\
&\quad \left. + Y_t^2\left[2U_- + 1 - 4U_\times\right]\right\} \mathrm{T}_{1134}\left(m^2_{\tilde t_i}, m^2_{\tilde t_i}, m^2_{\tilde b_1}, m^2_{H^\pm}\right) \\
&+ 4m_t^2\left[\frac{4\eta m_t^2}{\Delta_{\tilde t_i \tilde t_j}} + 2x_t^2 + 4 + \left(1-4U_\times\right)\left(1 - 3\eta + 2y_t^2 + 5x_t^2 y_t^2\right)\right] \mathrm{T}_{1134}\left(m^2_{\tilde t_i}, m^2_{\tilde t_i}, m^2_{\tilde t_i}, m^2_{H^\pm}\right),
\end{aligned} \tag{D.15b}
$$

$$
\begin{aligned}
s_{K_3} = \frac{c_\beta^2 \mu^2}{s_\beta^2 c_\beta^2} &\left\{2\left[\frac{m_t^2}{\Delta_{\tilde t_i \tilde t_j}} + U_\times\right]\left[\mathrm{T}_{1134}\left(m^2_{\tilde t_i}, m^2_{\tilde t_i}, m^2_{\tilde b_1}, m^2_{H^\pm}\right) + 2\mathrm{T}_{1134}\left(m^2_{\tilde t_i}, m^2_{\tilde t_i}, m^2_{\tilde t_i}, m^2_{H^\pm}\right)\right]\right. \\
&\left. + \frac{1-4U_\times}{\Delta_{\tilde t_i \tilde t_j}}\left[\mathrm{T}_{134}\left(m^2_{\tilde t_i}, m^2_{\tilde b_1}, m^2_{H^\pm}\right) + \mathrm{T}_{134}\left(m^2_{\tilde t_i}, m^2_{\tilde t_i}, m^2_{H^\pm}\right)\right]\right\},
\end{aligned} \tag{D.16a}
$$

$$
\begin{aligned}
s_{L_1} = &\left\{\frac{2U_-\left[Y_t^2 - 3\eta^2 m_t^2\right]\left[\mu^2 - m^2_{\tilde t_i}\right]}{\Delta^2_{\tilde t_i \tilde t_j}} + \frac{\eta m_t^2}{\Delta_{\tilde t_i \tilde t_j}}\left[\left(1-3U_-\right)\eta + 4U_-\right] - \left[1-U_-\right]\left[y_t^2+1\right]\right\} \mathrm{T}_{134}\left(m^2_{\tilde t_i}, \mu^2, 0\right) \\
&- \left\{\left[\mu^2 - m^2_{\tilde t_i}\right]\left[\frac{\eta m_t^2}{\Delta_{\tilde t_i \tilde t_j}}\left(\eta\left(1-3U_-\right) + 4U_-\right) - \left(1-U_-\right)\left(y_t^2+1\right)\right] + \left[\eta-2\right]^2\left[1-U_-\right] m_t^2\right\} \\
&\times \mathrm{T}_{1134}\left(m^2_{\tilde t_i}, m^2_{\tilde t_i}, \mu^2, 0\right) + 2\left[\mu^2 - m^2_{\tilde t_i} + \left(2\eta+1\right)m_t^2\right] \mathrm{T}_{1134}\left(m_t^2, m_t^2, m^2_{\tilde t_i}, \mu^2\right) \\
&+ c_\beta^2\, s^H_{L_1}\big|_{Y_t'^2\to Y_t^2,\ y_t'^2\to y_t^2,\ \eta'\to\eta} + s_\beta^2\, s^H_{L_1}\big|_{m_{H^\pm}\to 0,\ Y_t'^2\to X_t^2,\ y_t'^2\to x_t^2,\ \eta'\to -2x_t^2}\ ,
\end{aligned} \tag{D.17a}
$$

$$
\begin{aligned}
s^H_{L_1} = &\left\{\frac{4\eta^2 m_t^2}{\Delta_{\tilde t_i \tilde t_j}}\left(\frac{3m_t^2\eta'}{\Delta_{\tilde t_i \tilde t_j}} + 1\right) - U_-\left[2\frac{\left(m_t^2 - Y_t'^2\right)\left(3\eta^2 m_t^2 - Y_t^2\right)}{\Delta^2_{\tilde t_i \tilde t_j}} + \frac{4\eta m_t^2}{\Delta_{\tilde t_i \tilde t_j}} + 1\right]\right. \\
&\quad \left. - 2\eta'\left(\frac{2m_t^2 y_t^2}{\Delta_{\tilde t_i \tilde t_j}} + 1\right) - 2\eta\left(\frac{4m_t^2 y_t'^2}{\Delta_{\tilde t_i \tilde t_j}} - 1\right) - 4y_t'^2 - 1\right\} \mathrm{T}_{134}\left(m^2_{\tilde t_i}, m^2_{\tilde b_1}, m^2_{H^\pm}\right) \\
&+ 2\left\{\frac{2\eta^2 m_t^2}{\Delta_{\tilde t_i \tilde t_j}}\left(2U_\times\left(4x_t^2+3\right) - 2y_t'^2 - 1\right) + \frac{2m_t^2\eta' y_t^2}{\Delta_{\tilde t_i \tilde t_j}} + \left(y_t^2+1\right)y_t'^2 + 1\right. \\
&\quad \left. + \eta\left(\frac{4m_t^2 y_t'^2}{\Delta_{\tilde t_i \tilde t_j}} - 1\right) - x_t^2\left(4U_\times y_t^2 + 1\right)\right\} \mathrm{T}_{134}\left(m^2_{\tilde t_i}, m^2_{\tilde t_i}, m^2_{H^\pm}\right) \\
&+ \left\{m_t^2\left\{\eta^2\left[\left(1-3U_-\right)y_t'^2 - 2\right] + 8\left[\frac{\eta'\left(y_t^2+1\right)}{4} + \frac{\eta}{2} - y_t'^2 + \frac{1+U_-}{2}\left[\eta\left(y_t'^2 + \frac{1}{2}\right) - \frac{y_t^2}{4} - \frac{5}{4}\right]\right]\right\}\right. \\
&\quad \left. + \frac{\eta m_t^4\left[\eta + (3\eta-4)\left(U_- - 2\eta'\right)\right]}{\Delta_{\tilde t_i \tilde t_j}} - Y_t'^2\left(1-U_-\right)\left(y_t^2+1\right)\right\} \mathrm{T}_{1134}\left(m^2_{\tilde t_i}, m^2_{\tilde t_i}, m^2_{\tilde b_1}, m^2_{H^\pm}\right) \\
&+ 4m_t^2\left\{\eta^2\left[\frac{m_t^2}{\Delta_{\tilde t_i \tilde t_j}} - \left(1-5U_\times\right)y_t'^2 - 1\right] + \eta'\left[\frac{m_t^2\eta(4-3\eta)}{\Delta_{\tilde t_i \tilde t_j}} + y_t^2 + 1\right] + 4\eta\left[\left(1-2U_\times\right)y_t'^2 + 1\right]\right. \\
&\quad \left. - y_t'^2\left[x_t^2\left(y_t^2+1\right) + 4\right] - y_t^2 - 5\right\} \mathrm{T}_{1134}\left(m^2_{\tilde t_i}, m^2_{\tilde t_i}, m^2_{\tilde t_i}, m^2_{H^\pm}\right),
\end{aligned} \tag{D.17b}
$$

$$\begin{aligned}
s_{L_2} = {} & \left\{\tfrac{\eta m_t^2}{\Delta_{\tilde{t}_i\tilde{t}_j}}\left[6U_-\left(\tfrac{\mu^2-m_{\tilde{t}_i}^2}{\Delta_{\tilde{t}_i\tilde{t}_j}}+\tfrac{1}{2}\right)-1\right]-\tfrac{2U_-m_t^2}{\Delta_{\tilde{t}_i\tilde{t}_j}}\right\}\mathrm{T}_{134}\Big(m_{\tilde{t}_i}^2,\mu^2,0\Big)-2m_t^2\mathrm{T}_{1134}\Big(m_t^2,m_t^2,m_{\tilde{t}_i}^2,\mu^2\Big) \\
& + m_t^2\left\{\left[\eta\left(1-3U_-\right)+2U_-\right]\tfrac{\mu^2-m_{\tilde{t}_i}^2}{\Delta_{\tilde{t}_i\tilde{t}_j}}+\left(\eta-2\right)\left(1-U_-\right)\right\}\mathrm{T}_{1134}\Big(m_{\tilde{t}_i}^2,m_{\tilde{t}_i}^2,\mu^2,0\Big) \\
& + c_\beta^2\; s_{L_2}^H\big|_{Y_t'^2\to Y_t^2,\; y_t'^2\to y_t^2,\; \eta'\to\eta} + s_\beta^2\; s_{L_2}^H\big|_{m_{H^\pm}\to 0,\; Y_t'^2\to X_t^2,\; y_t'^2\to x_t^2,\; \eta'\to -2x_t^2}\;,
\end{aligned} \tag{D.18a}$$

$$\begin{aligned}
s_{L_2}^H = {} & m_t^2\left\{\tfrac{(3\eta-2)\left[m_t^2\left(2\eta'-U_-\right)+(1+U_-)Y_t'^2\right]-\eta\left(m_t^2+4Y_t'^2\right)}{\Delta_{\tilde{t}_i\tilde{t}_j}}-2\eta-U_--3\right\}\mathrm{T}_{1134}\Big(m_{\tilde{t}_i}^2,m_{\tilde{t}_i}^2,m_{\tilde{b}_1}^2,m_{H^\pm}^2\Big) \\
& + 4m_t^2\left\{\tfrac{(3\eta-2)m_t^2\eta'-\eta\left[m_t^2-(1-5U_\times)Y_t'^2\right]}{\Delta_{\tilde{t}_i\tilde{t}_j}}+\eta-2y_t'^2\left(1-2U_\times\right)-2\right\}\mathrm{T}_{1134}\Big(m_{\tilde{t}_i}^2,m_{\tilde{t}_i}^2,m_{\tilde{t}_i}^2,m_{H^\pm}^2\Big) \\
& + \tfrac{2m_t^2}{\Delta_{\tilde{t}_i\tilde{t}_j}}\left\{2y_t'^2+U_--\eta\left[\tfrac{6m_t^2\eta'}{\Delta_{\tilde{t}_i\tilde{t}_j}}-3U_-\tfrac{m_t^2-Y_t'^2}{\Delta_{\tilde{t}_i\tilde{t}_j}}+2\right]\right\}\mathrm{T}_{134}\Big(m_{\tilde{t}_i}^2,m_{\tilde{b}_1}^2,m_{H^\pm}^2\Big) \\
& + \tfrac{4m_t^2}{\Delta_{\tilde{t}_i\tilde{t}_j}}\left\{y_t'^2-\eta\left[\tfrac{3m_t^2\eta'}{\Delta_{\tilde{t}_i\tilde{t}_j}}+2\left(1-4U_\times\right)y_t'^2+1\right]\right\}\mathrm{T}_{134}\Big(m_{\tilde{t}_i}^2,m_{\tilde{t}_i}^2,m_{H^\pm}^2\Big),
\end{aligned} \tag{D.18b}$$

$$\begin{aligned}
s_{L_3} = {} & 2y_t^2U_\times\left(6U_-\left(\tfrac{\mu^2-m_{\tilde{t}_i}^2}{\Delta_{\tilde{t}_i\tilde{t}_j}}+\tfrac{1}{2}\right)-1\right)\mathrm{T}_{134}\Big(m_{\tilde{t}_i}^2,\mu^2,0\Big) \\
& + 2\left(\left(1-3U_-\right)y_t^2U_\times\left(\mu^2-m_{\tilde{t}_i}^2\right)-\left(1-U_-\right)\left(m_t^2-Y_t^2U_\times\right)\right)\mathrm{T}_{1134}\Big(m_{\tilde{t}_i}^2,m_{\tilde{t}_i}^2,\mu^2,0\Big) \\
& + c_\beta^2\; s_{L_3}^H\big|_{Y_t'^2\to Y_t^2,\; y_t'^2\to y_t^2,\; \eta'\to\eta} + s_\beta^2\; s_{L_3}^H\big|_{m_{H^\pm}\to 0,\; Y_t'^2\to X_t^2,\; y_t'^2\to x_t^2,\; \eta'\to -2x_t^2}\;,
\end{aligned} \tag{D.19a}$$

$$\begin{aligned}
s_{L_3}^H = {} & -4y_t^2U_\times\left\{\tfrac{6m_t^2\eta'}{\Delta_{\tilde{t}_i\tilde{t}_j}}-3U_-\tfrac{m_t^2-Y_t'^2}{\Delta_{\tilde{t}_i\tilde{t}_j}}+2\right\}\mathrm{T}_{134}\Big(m_{\tilde{t}_i}^2,m_{\tilde{b}_1}^2,m_{H^\pm}^2\Big) \\
& - 8y_t^2U_\times\left\{\tfrac{3m_t^2\eta'}{\Delta_{\tilde{t}_i\tilde{t}_j}}+2\left(1-4U_\times\right)y_t'^2+1\right\}\mathrm{T}_{134}\Big(m_{\tilde{t}_i}^2,m_{\tilde{t}_i}^2,m_{H^\pm}^2\Big) \\
& + 2m_t^2\left\{x_t^2y_t^2\left[\tfrac{6m_t^2\eta'-(1+3U_-)m_t^2-(1-3U_-)y_t'^2}{\Delta_{\tilde{t}_i\tilde{t}_j}}+2\right]-2y_t'-U_--1\right\}\mathrm{T}_{1134}\Big(m_{\tilde{t}_i}^2,m_{\tilde{t}_i}^2,m_{\tilde{b}_1}^2,m_{H^\pm}^2\Big) \\
& + 8m_t^2\left\{x_t^2y_t^2\left[\tfrac{3m_t^2\eta'-m_t^2+(1-5U_\times)Y_t'^2}{\Delta_{\tilde{t}_i\tilde{t}_j}}+1\right]-y_t'^2-1\right\}\mathrm{T}_{1134}\Big(m_{\tilde{t}_i}^2,m_{\tilde{t}_i}^2,m_{\tilde{t}_i}^2,m_{H^\pm}^2\Big),
\end{aligned} \tag{D.19b}$$

$$s_M = \tfrac{1-U_-}{\Delta_{\tilde{t}_i\tilde{t}_j}}\mathrm{T}_{113}\Big(m_{\tilde{b}_1}^2,m_{\tilde{b}_1}^2,m_{\tilde{t}_i}^2\Big)+c_\beta^2 s_M^H+s_\beta^2\; s_M^H\big|_{m_{H^\pm}\to 0,\; Y_t^2\to X_t^2,\; y_t^2\to x_t^2,\; \eta\to -2x_t^2}\;, \tag{D.20a}$$

$$s_M^H = \left(\tfrac{m_t^2}{\Delta_{\tilde{t}_i\tilde{t}_j}}\left(1+U_--2\eta\right)+\left(1-U_-\right)y_t^2\right)\mathrm{T}_{1134}\Big(m_{\tilde{b}_1}^2,m_{\tilde{b}_1}^2,m_{\tilde{t}_i}^2,m_{H^\pm}^2\Big). \tag{D.20b}$$

$$\begin{aligned}
s_N = {} & \tfrac{\Delta_{\tilde{t}_i\tilde{t}_j}}{2\Delta_{\tilde{t}_i\tilde{b}_1}}\left\{\tfrac{2\mu^2m_t^2}{c_\beta^2s_\beta^2\Delta_{\tilde{t}_i\tilde{t}_j}^2}+y_t^2\left(U_--1-\tfrac{2m_t^2}{\Delta_{\tilde{t}_i\tilde{t}_j}}\right)\right\}\mathrm{T}_{134}\Big(m_t^2,m_{\tilde{t}_i}^2,\mu^2\Big) \\
& + \left(m_t^2-m_{\tilde{t}_i}^2+\mu^2\right)\mathrm{T}_{1134}\Big(m_t^2,m_t^2,m_{\tilde{t}_i}^2,\mu^2\Big),
\end{aligned} \tag{D.21a}$$

$$\begin{aligned}
s_O = {} & \tfrac{1}{\Delta_{\tilde{t}_i\tilde{b}_1}}\Bigg\{y_t^2\left[-\tfrac{m_t^2}{\Delta_{\tilde{t}_i\tilde{t}_j}}\left(1-U_-\left(\tfrac{m_t^2}{\Delta_{\tilde{t}_i\tilde{t}_j}}+1\right)\right)+U_\times\left(\tfrac{4m_t^2}{\Delta_{\tilde{t}_i\tilde{t}_j}}-U_-+2\right)+\tfrac{U_--1}{2}\right] \\
& \qquad + \tfrac{\mu^2m_t^2}{c_\beta^2s_\beta^2\Delta_{\tilde{t}_i\tilde{t}_j}^2}\left[1-2U_\times-U_-\left(\tfrac{m_t^2}{\Delta_{\tilde{t}_i\tilde{t}_j}}+1\right)\right]\Bigg\}\mathrm{T}_{13}\Big(m_{\tilde{t}_i}^2,\mu^2\Big) \\
& + \tfrac{4}{\Delta_{\tilde{t}_i\tilde{b}_1}}\Bigg\{\left(1-4U_\times\right)\left[y_t^2\left(\tfrac{m_t^2}{\Delta_{\tilde{t}_i\tilde{t}_j}}\left(\tfrac{X_t^2-m_t^2}{\Delta_{\tilde{t}_i\tilde{t}_j}}+U_--1\right)+\tfrac{U_--1}{2}\right)\right. \\
& \qquad \left. + \tfrac{\mu^2m_t^2}{c_\beta^2s_\beta^2\Delta_{\tilde{t}_i\tilde{t}_j}^2}\left(\tfrac{m_t^2}{\Delta_{\tilde{t}_i\tilde{t}_j}}+1-U_-\right)\right]-\tfrac{2U_-U_\times\mu^2m_t^2}{c_\beta^2s_\beta^2\Delta_{\tilde{t}_i\tilde{t}_j}^2}\Bigg\}\mathrm{T}_{13}\Big(m_{\tilde{t}_i}^2,m_{\tilde{t}_i}^2\Big)
\end{aligned}$$

$$
\begin{aligned}
&+\frac{4m_t^4}{\Delta_{\tilde t_i\tilde b_1}\Delta^2_{\tilde t_j\tilde b_1}}\Bigg\{y_t^2\left(1-4U_\times\right)\left[\frac{m_t^2-X_t^2}{\Delta_{\tilde t_i\tilde t_j}}\left(\frac{m_t^2-X_t^2}{\Delta_{\tilde t_i\tilde t_j}}-2U_-\right)+1-4U_\times\right]\\
&\qquad+\frac{\mu^2}{c_\beta^2s_\beta^2\Delta_{\tilde t_i\tilde t_j}}\Bigg[2\left(1-x_t^2\frac{3m_t^2-X_t^2}{\Delta_{\tilde t_i\tilde t_j}}\right)\left(\frac{m_t^2\left(2x_t^2+U_-\right)}{\Delta_{\tilde t_i\tilde t_j}}-\frac{1}{2}\right)\\
&\qquad\qquad+\left(1-4U_\times\right)\frac{X_t^4-m_t^4}{\Delta^2_{\tilde t_i\tilde t_j}}+\frac{1}{8}\left(1-16U_\times\right)\Bigg]\Bigg\}\mathrm{T}_{13}\left(m^2_{\tilde t_i},m^2_{\tilde t_j}\right)\\
&+\frac{m_t^4}{\Delta_{\tilde t_i\tilde b_1}\Delta^2_{\tilde t_j\tilde b_1}}\Bigg\{\frac{\mu^2}{c_\beta^2s_\beta^2\Delta_{\tilde t_i\tilde t_j}}\left[\frac{m_t^2}{\Delta_{\tilde t_i\tilde t_j}}\left(\left(2x_t^2+U_-\right)\left(\frac{m_t^2-X_t^2}{\Delta_{\tilde t_i\tilde t_j}}-U_-\right)-1\right)+\frac{7}{2}\left(1-U_-\right)\right]\\
&\qquad-y_t^2\left[U_-\left(\frac{X_t^2-m_t^2}{\Delta_{\tilde t_i\tilde t_j}}\right)^2+2\left(1-4U_\times\right)\left(\frac{X_t^2-m_t^2}{\Delta_{\tilde t_i\tilde t_j}}+\frac{U_-}{2}\right)\right]\Bigg\}\mathrm{T}_{13}\left(m^2_{\tilde t_i},m^2_{\tilde b_1}\right)\\
&+\frac{\Delta_{\tilde t_i\tilde t_j}}{2\Delta_{\tilde t_i\tilde b_1}}\Bigg\{\frac{m^2_{\tilde t_i}-\mu^2}{\Delta_{\tilde t_i\tilde t_j}}\Bigg[y_t^2\left(1-4U_\times-U_-\left(1-\frac{2m_t^2}{\Delta_{\tilde t_i\tilde t_j}}\left(\frac{X_t^2-m_t^2}{\Delta_{\tilde t_i\tilde t_j}}+U_--1\right)\right)\right)\\
&\qquad+\frac{2\mu^2m_t^2}{c_\beta^2s_\beta^2\Delta^2_{\tilde t_i\tilde t_j}}\left(U_-\left(\frac{m_t^2}{\Delta_{\tilde t_i\tilde t_j}}+1\right)+2U_\times-1\right)\Bigg]\\
&\qquad+\left(y_t^2+1\right)\left[\left(U_--1\right)\left(\frac{m_t^2}{\Delta_{\tilde t_i\tilde t_j}}+1\right)^2+4U_\times\left(\frac{m_t^2}{\Delta_{\tilde t_i\tilde t_j}}+1\right)-\left(U_-+1\right)U_\times\right]\\
&\qquad-\frac{\mu^2m_t^2}{c_\beta^2s_\beta^2\Delta^2_{\tilde t_i\tilde t_j}}\left[\left(U_--1\right)\left(\frac{m_t^2}{\Delta_{\tilde t_i\tilde t_j}}+1\right)+2U_\times\right]\Bigg\}\mathrm{T}_{134}\left(m^2_{\tilde t_i},\mu^2,0\right)\\
&+\frac{\mu^2-m^2_{\tilde t_i}}{2}\left\{\frac{\mu^2m_t^2\left(U_--1\right)}{c_\beta^2s_\beta^2\Delta^2_{\tilde t_i\tilde t_j}}-\left(y_t^2+1\right)\left[\left(U_--1\right)\left(\frac{m_t^2}{\Delta_{\tilde t_i\tilde t_j}}+1\right)+2U_\times\right]\right\}\mathrm{T}_{1134}\left(m^2_{\tilde t_i},m^2_{\tilde t_i},\mu^2,0\right)\\
&+c_\beta^2\;s_O^H\Big|_{Y_t'^2\to Y_t^2,\;y_t'^2\to y_t^2,\;\mu'\to\mu}+s_\beta^2\;s_O^H\Big|_{m_{H^\pm}\to0,\;Y_t'^2\to X_t^2,\;y_t'^2\to x_t^2,\;\mu'\to0}\;,
\end{aligned}
\tag{D.22a}
$$

$$
\begin{aligned}
s_O^H=&\Bigg\{m_t^2\left[1-2U_\times-U_-\left(1+\frac{m_t^2}{\Delta_{\tilde t_i\tilde t_j}}\right)\right]\left(y_t^2-\frac{\mu^2}{c_\beta^2s_\beta^2\Delta_{\tilde t_i\tilde t_j}}\right)\\
&\quad+Y_t^2\left[2U_\times\left(-\frac{m_t^2}{\Delta_{\tilde t_i\tilde t_j}}+\frac{U_-}{2}-1\right)+\frac{1}{2}\left(1-U_-\right)\right]\Bigg\}\mathrm{T}_{13}\left(m^2_{\tilde t_i},m^2_{H^\pm}\right)\\
&-m_t^2\Bigg\{\frac{2m_t^2}{\Delta_{\tilde t_i\tilde t_j}}\Bigg[\frac{\mu^2}{c_\beta^2s_\beta^2\Delta_{\tilde t_i\tilde t_j}}\left(\frac{\mu'^2}{c_\beta^2s_\beta^2\Delta_{\tilde t_i\tilde t_j}}-\left(x_t^2+1\right)^2\right)+\frac{\mu'^2}{c_\beta^2s_\beta^2\Delta_{\tilde t_i\tilde t_j}}\left(x_t^4+x_t^2-1-\left(x_t^2+2\right)y_t^2\right)\\
&\qquad+\left(x_t^2+1\right)\left(y_t^2+1\right)\left(y_t'^2+1\right)\Bigg]\\
&\quad+\left(U_--1\right)\left(y_t^2+1\right)\left[\frac{\mu'^2}{c_\beta^2s_\beta^2\Delta_{\tilde t_i\tilde t_j}}-\left(x_t^2+1\right)\left(y_t'^2+1\right)\right]\Bigg\}\mathrm{T}_{1134}\left(m^2_{\tilde t_i},m^2_{\tilde t_i},m^2_{\tilde t_i},m^2_{H^\pm}\right)\\
&+\Delta_{\tilde t_i\tilde t_j}\Bigg\{\frac{m_t^4}{\Delta^2_{\tilde t_i\tilde t_j}}\Bigg[\frac{\mu^2}{c_\beta^2s_\beta^2\Delta_{\tilde t_i\tilde t_j}}\left(2x_t^2+1-\frac{\mu'^2}{c_\beta^2s_\beta^2\Delta_{\tilde t_i\tilde t_j}}\right)+\frac{\mu'^2}{c_\beta^2s_\beta^2\Delta_{\tilde t_i\tilde t_j}}\left(2y_t^2-x_t^2+1\right)\\
&\qquad-\left(y_t^2+1\right)\left(y_t'^2+2x_t^2+1\right)-\frac{U_--1}{2}\left(y_t^2+1-\frac{\mu^2}{c_\beta^2s_\beta^2\Delta_{\tilde t_i\tilde t_j}}\right)\Bigg]\\
&\quad+\frac{U_--1}{2}\left[U_\times\left(\frac{\mu'^2-\mu^2}{c_\beta^2s_\beta^2\Delta_{\tilde t_i\tilde t_j}}+y_t^2+1\right)-\frac{m_t^2}{\Delta_{\tilde t_i\tilde t_j}}\left(\frac{\mu'^2\left(1+2y_t^2\right)}{c_\beta^2s_\beta^2\Delta_{\tilde t_i\tilde t_j}}-2\left(y_t^2+1\right)y_t'^2\right)\right]\\
&\quad+\left(y_t^2+1\right)y_t'^2\left(\frac{U_--1}{2}+U_\times\right)\Bigg\}\mathrm{T}_{1134}\left(m^2_{\tilde t_i},m^2_{\tilde t_i},m^2_{\tilde b_1},m^2_{H^\pm}\right)
\end{aligned}
$$

$$
\begin{aligned}
&+\frac{\Delta_{\tilde{t}_i\tilde{t}_j}}{\Delta_{\tilde{t}_i\tilde{b}_1}}\Bigg\{\frac{U_--1}{2}\Bigg[\frac{\mu'^2-\mu^2}{c_\beta^2 s_\beta^2\Delta_{\tilde{t}_i\tilde{t}_j}}+y_t^2+y_t'^2\left(\frac{2m_t^2}{\Delta_{\tilde{t}_i\tilde{t}_j}}\left(1-2y_t^2\left(\frac{m_t^2}{\Delta_{\tilde{t}_i\tilde{t}_j}}+x_t^2+2U_\times\right)\right)+y_t^2+1\right)\\
&\qquad+\frac{2m_t^2}{\Delta_{\tilde{t}_i\tilde{t}_j}}\left(\frac{\mu'^2}{c_\beta^2 s_\beta^2\Delta_{\tilde{t}_i\tilde{t}_j}}\left(\left(-\frac{m_t^2}{\Delta_{\tilde{t}_i\tilde{t}_j}}+1-2U_\times\right)x_t^2+\frac{m_t^2\left(2x_t^2+3\right)y_t^2}{\Delta_{\tilde{t}_i\tilde{t}_j}}+1\right)\right.\\
&\qquad\qquad-\frac{\mu^2}{c_\beta^2 s_\beta^2\Delta_{\tilde{t}_i\tilde{t}_j}}\left(\frac{m_t^2}{\Delta_{\tilde{t}_i\tilde{t}_j}}\left(\frac{\mu'^2}{c_\beta^2 s_\beta^2\Delta_{\tilde{t}_i\tilde{t}_j}}-2x_t^2\left(x_t^2+1\right)\right)+x_t^2+2\right)\\
&\qquad\qquad\left.+y_t^2\left(1-x_t^2\left(\frac{2m_t^2}{\Delta_{\tilde{t}_i\tilde{t}_j}}+1\right)\right)+1\right)+1\Bigg]\\
&\quad+\frac{m_t^2}{\Delta_{\tilde{t}_i\tilde{t}_j}}\Bigg[\frac{2m_t^4}{\Delta_{\tilde{t}_i\tilde{t}_j}^2}\left(\frac{\mu'^2\left(x_t^2\left(1+2x_t^2\right)-2y_t^2\left(1+x_t^2\right)\right)}{c_\beta^2 s_\beta^2\Delta_{\tilde{t}_i\tilde{t}_j}}+\frac{\mu^2}{c_\beta^2 s_\beta^2\Delta_{\tilde{t}_i\tilde{t}_j}}\left(\frac{\mu'^2}{c_\beta^2 s_\beta^2\Delta_{\tilde{t}_i\tilde{t}_j}}-2x_t^2\left(x_t^2+1\right)\right)\right.\\
&\qquad\qquad\left.+y_t^2\left(2x_t^2y_t'^2+y_t'^2+x_t^2\right)\right)\\
&\qquad+\frac{m_t^2}{\Delta_{\tilde{t}_i\tilde{t}_j}}\left(\frac{\mu'^2\left(2x_t^4-1\right)}{c_\beta^2 s_\beta^2\Delta_{\tilde{t}_i\tilde{t}_j}}+\frac{\mu^2}{c_\beta^2 s_\beta^2\Delta_{\tilde{t}_i\tilde{t}_j}}\left(\frac{\mu'^2}{c_\beta^2 s_\beta^2\Delta_{\tilde{t}_i\tilde{t}_j}}-2x_t^2\left(x_t^2+1\right)+1\right)\right.\\
&\qquad\qquad\left.-y_t'^2-y_t^2\left(y_t'^2+2x_t^2\left(2x_t^2y_t'^2+y_t'^2+x_t^2\right)+1\right)-1\right)\\
&\qquad+x_t^2\left(\frac{\mu'^2-\mu^2}{c_\beta^2 s_\beta^2\Delta_{\tilde{t}_i\tilde{t}_j}}+y_t'^2+y_t'^2y_t^2+y_t^2+1\right)\Bigg]\Bigg\}\mathrm{T}_{134}\left(m_{\tilde{t}_i}^2,m_{\tilde{t}_i}^2,m_{H^\pm}^2\right)\\
&+\frac{m_t^4\Delta_{\tilde{t}_i\tilde{t}_j}}{\Delta_{\tilde{t}_i\tilde{b}_1}\Delta_{\tilde{t}_j\tilde{b}_1}^2}\Bigg\{\frac{\mu^2\left(1-U_--y_t'^2\right)}{c_\beta^2 s_\beta^2\Delta_{\tilde{t}_i\tilde{t}_j}}-x_t^4\left[\left(U_-y_t^2+1\right)y_t'^2+\frac{U_-+1}{2}+\left(1-2U_\times\right)\left(\frac{\mu'^2-\mu^2}{c_\beta^2 s_\beta^2\Delta_{\tilde{t}_i\tilde{t}_j}}+y_t^2\right)\right]\\
&\quad+\frac{\mu'^2\mu^2}{c_\beta^4 s_\beta^4\Delta_{\tilde{t}_i\tilde{t}_j}^2}\left[\frac{U_--1}{2}+U_-U_\times\right]-\left(1-6U_\times\right)\left[\frac{\mu'^2\left(1-2U_\times\right)+\mu^2}{c_\beta^2 s_\beta^2\Delta_{\tilde{t}_i\tilde{t}_j}}+y_t'^2+\frac{U_-+1}{2}\right]\\
&\quad+y_t^2\left[\frac{\mu'^2\left(1-8U_-U_\times\right)}{c_\beta^2 s_\beta^2\Delta_{\tilde{t}_i\tilde{t}_j}}-U_-\left(1-10U_\times\right)y_t'^2-2U_\times\right]\\
&\quad-x_t^2\left[\frac{\mu'^2\left(4U_\times y_t^2+U_-U_\times+1\right)}{c_\beta^2 s_\beta^2\Delta_{\tilde{t}_i\tilde{t}_j}}-\frac{2\mu^2}{c_\beta^2 s_\beta^2\Delta_{\tilde{t}_i\tilde{t}_j}}-4U_\times+2y_t'^2\left(y_t^2\left(1-5U_\times\right)+U_-\right)\right.\\
&\qquad\left.+\frac{U_-+1}{2}\left(\frac{\mu^2}{c_\beta^2 s_\beta^2\Delta_{\tilde{t}_i\tilde{t}_j}}+2\right)+U_-\left(2-5U_\times\right)\left(\frac{\mu'^2-\mu^2}{c_\beta^2 s_\beta^2\Delta_{\tilde{t}_i\tilde{t}_j}}+y_t^2\right)\right]\\
&\quad+\frac{m_t^2}{\Delta_{\tilde{t}_i\tilde{t}_j}}\left[-\frac{\mu'^2 4\left(1-6U_\times\right)y_t^2}{c_\beta^2 s_\beta^2\Delta_{\tilde{t}_i\tilde{t}_j}}-\frac{\mu^2}{2c_\beta^2 s_\beta^2\Delta_{\tilde{t}_i\tilde{t}_j}}\left(\frac{\mu'^2 12U_\times}{c_\beta^2 s_\beta^2\Delta_{\tilde{t}_i\tilde{t}_j}}+U_-\left(3-20U_\times\right)+1\right)\right.\\
&\qquad+U_-\left(-\frac{4U_\times\mu'^2}{c_\beta^2 s_\beta^2\Delta_{\tilde{t}_i\tilde{t}_j}}+\frac{2\mu'^2}{c_\beta^2 s_\beta^2\Delta_{\tilde{t}_i\tilde{t}_j}}+2y_t'^2-10U_\times y_t^2+3y_t^2+1\right)\\
&\qquad\left.+4\left(1-5U_\times\right)y_t'^2y_t^2-4U_\times+1\right]\\
&\quad+\frac{m_t^4}{\Delta_{\tilde{t}_i\tilde{t}_j}^2}\left[\frac{\mu'^2\left(8U_-y_t^2+2U_\times-1\right)}{c_\beta^2 s_\beta^2\Delta_{\tilde{t}_i\tilde{t}_j}}+\frac{\mu^2}{c_\beta^2 s_\beta^2\Delta_{\tilde{t}_i\tilde{t}_j}}\left(-\frac{3U_-\mu'^2}{c_\beta^2 s_\beta^2\Delta_{\tilde{t}_i\tilde{t}_j}}+3-10U_\times\right)\right.\\
&\qquad\left.-\left(3-10U_\times\right)y_t^2-\frac{U_-}{2}-y_t'^2\left(5U_-y_t^2+1\right)-\frac{1}{2}\right]\\
&\quad+\frac{m_t^6}{\Delta_{\tilde{t}_i\tilde{t}_j}^3}\left[\frac{2\mu'^2}{c_\beta^2 s_\beta^2\Delta_{\tilde{t}_i\tilde{t}_j}}\left(\frac{\mu^2}{c_\beta^2 s_\beta^2\Delta_{\tilde{t}_i\tilde{t}_j}}-2y_t^2\right)-\frac{U_-\mu^2}{c_\beta^2 s_\beta^2\Delta_{\tilde{t}_i\tilde{t}_j}}+y_t^2\left(2y_t'^2+U_-\right)\right]\\
&\quad+\left(1-10U_\times\right)\left(1-2U_\times\right)\left(\frac{\mu^2}{c_\beta^2 s_\beta^2\Delta_{\tilde{t}_i\tilde{t}_j}}-y_t^2\right)\Bigg\}\mathrm{T}_{134}\left(m_{\tilde{t}_i}^2,m_{\tilde{b}_1}^2,m_{H^\pm}^2\right)
\end{aligned}
$$

$$
\begin{aligned}
&+ \tfrac{m_t^4 \Delta_{\tilde{t}_i\tilde{t}_j}}{\Delta_{\tilde{t}_i\tilde{b}_1}\Delta^2_{\tilde{t}_j\tilde{b}_1}} \Bigg\{ \tfrac{\mu'^2}{c_\beta^2 s_\beta^2 \Delta_{\tilde{t}_i\tilde{t}_j}} \left(x_t^2 - y_t^2\right) \left[\tfrac{m_t^4\left(12x_t^4+1-4U_\times\right)}{\Delta^2_{\tilde{t}_i\tilde{t}_j}} + 2U_- U_\times \left(\tfrac{3m_t^2}{\Delta_{\tilde{t}_i\tilde{t}_j}} - x_t^2 \right) + 1 - 5U_\times \right] \\
&\qquad + \tfrac{\mu^2}{2c_\beta^2 s_\beta^2 \Delta_{\tilde{t}_i\tilde{t}_j}} \left[\tfrac{\mu'^2}{c_\beta^2 s_\beta^2 \Delta_{\tilde{t}_i\tilde{t}_j}} + \tfrac{m_t^2\left(4U_- y_t'^2 + 8U_\times^2 - 1\right)}{\Delta_{\tilde{t}_i\tilde{t}_j}} - 3x_t^2 \right. \\
&\qquad\qquad \left. - 2U_\times \left(-2x_t^2\left(U_- x_t^2 - 6U_\times + 2\right) + U_-\left(1 + 6U_\times\right)\right) \right] \\
&\qquad + \left(1 - 4U_\times\right) y_t'^2 y_t^2 \left[\frac{m_t^4}{\Delta^2_{\tilde{t}_i\tilde{t}_j}} + 2U_- \left(x_t^2 - \tfrac{m_t^2}{\Delta_{\tilde{t}_i\tilde{t}_j}} \right) + x_t^4 + 1 - 6U_\times \right] \Bigg\} \\
&\qquad \times \mathrm{T}_{134}\Big(m^2_{\tilde{t}_i}, m^2_{\tilde{t}_j}, m^2_{H^\pm}\Big)
\end{aligned}
\tag{D.22b}
$$

D.3. Genuine two-loop tadpoles

The explicit expressions for the genuine two-loop tadpoles of the Higgs bosons are given by

$$
\Upsilon_h^{(2)} = \frac{N_c s_\beta h_t^3 m_t}{128\sqrt{2}\pi^4} \Bigg\{ t_A + \sum_{\substack{i=1 \\ j\neq i}}^{2} \left[-x_t^2 t_B + \left(1 + x_t^2\right) t_C - x_t^2 t_{D_1} - t_{D_2} + t_{D_3} \right] \Bigg\}, \tag{D.23a}
$$

$$
\Upsilon_H^{(2)} = -\frac{N_c c_\beta h_t^3 m_t}{128\sqrt{2}\pi^4} \Bigg\{ t_A + \sum_{\substack{i=1 \\ j\neq i}}^{2} \left[\tfrac{\eta}{2} t_B + \left(1 - \tfrac{\eta}{2}\right) t_C + \tfrac{\eta}{2} t_{D_1} - t_{D_2} \right] \Bigg\}, \tag{D.23b}
$$

$$
\Upsilon_A^{(2)} = \sum_{\substack{i=1 \\ j\neq i}}^{2} \frac{N_c h_t^3 m_t}{128\sqrt{2}\pi^4 s_\beta} \frac{\Im\mathfrak{m}[X_t \mu^*]}{s_\beta c_\beta \Delta_{\tilde{t}_i\tilde{t}_j}} \Big\{ t_B - t_C + t_{D_1} \Big\}. \tag{D.23c}
$$

$$
t_A = s_A + \sum_{i=1}^{2} \left(m_t^2 - m^2_{\tilde{t}_i} + \mu^2\right) \mathrm{T}_{1134}\Big(m_t^2, m_t^2, m^2_{\tilde{t}_i}, \mu^2\Big), \tag{D.24a}
$$

$$
t_B = s_D + s_G + s_H, \tag{D.25a}
$$

$$
\begin{aligned}
t_C &= s_{I_1} + s_{I_2} + \tfrac{1}{2}\left(1 - U_-\right)\left(\mu^2 - m^2_{\tilde{t}_i}\right) \mathrm{T}_{1134}\Big(m^2_{\tilde{t}_i}, m^2_{\tilde{t}_i}, \mu^2, 0\Big) \\
&\quad + c_\beta^2 t_C^H + s_\beta^2\, t_C^H\big|_{m_{H^\pm}\to 0,\ Y_t^2 \to X_t^2,\ y_t^2 \to x_t^2,\ \eta \to -2x_t^2}\ ,
\end{aligned}
\tag{D.26a}
$$

$$
\begin{aligned}
t_C^H &= \left\{ m_t^2 \left(\eta - \tfrac{1+U_-}{2}\right) - \tfrac{1-U_-}{2} Y_t^2 \right\} \mathrm{T}_{1134}\Big(m^2_{\tilde{t}_i}, m^2_{\tilde{t}_i}, m^2_{\tilde{b}_1}, m^2_{H^\pm}\Big) \\
&\quad + 2m_t^2\left(\eta - x_t^2 y_t^2 - 1\right) \mathrm{T}_{1134}\Big(m^2_{\tilde{t}_i}, m^2_{\tilde{t}_i}, m^2_{\tilde{t}_i}, m^2_{H^\pm}\Big)\ ,
\end{aligned}
\tag{D.26b}
$$

$$
\begin{aligned}
t_{D_1} &= \left\{ \tfrac{1}{2} - U_- \left(\tfrac{\mu^2 - m^2_{\tilde{t}_i}}{\Delta_{\tilde{t}_i\tilde{t}_j}} + \tfrac{1}{2} \right) \right\} \mathrm{T}_{134}\Big(m^2_{\tilde{t}_i}, 0, \mu^2\Big) \\
&\quad + c_\beta^2 t_{D_1}^H + s_\beta^2\, t_{D_1}^H\big|_{m_{H^\pm}\to 0,\ Y_t^2 \to X_t^2,\ y_t^2 \to x_t^2,\ \eta \to -2x_t^2}\ ,
\end{aligned}
\tag{D.27a}
$$

$$
\begin{aligned}
t_{D_1}^H &= \left\{ \tfrac{2\eta m_t^2 + U_-\left(Y_t^2 - m_t^2\right)}{\Delta_{\tilde{t}_i\tilde{t}_j}} + 1 \right\} \mathrm{T}_{134}\Big(m^2_{\tilde{t}_i}, m^2_{\tilde{b}_1}, m^2_{H^\pm}\Big) \\
&\quad + \left\{ \tfrac{2\eta m_t^2 + Y_t^2\left(1 - 4U_\times\right)}{\Delta_{\tilde{t}_i\tilde{t}_j}} + 1 \right\} \mathrm{T}_{134}\Big(m^2_{\tilde{t}_i}, m^2_{\tilde{t}_i}, m^2_{H^\pm}\Big),
\end{aligned}
\tag{D.27b}
$$

$$t_{D_2} = \tfrac{1-U_-}{2}\mathrm{T}_{134}\Big(m_{\tilde{t}_i}^2, \mu^2, 0\Big) + c_\beta^2 t_{D_2}^H + s_\beta^2\ t_{D_2}^H\big|_{m_{H^\pm}\to 0,\ Y_t^2\to X_t^2,\ y_t^2\to x_t^2,\ \eta\to -2x_t^2}\ , \tag{D.28a}$$

$$t_{D_2}^H = \tfrac{2y_t^2+1+U_-}{2}\mathrm{T}_{134}\Big(m_{\tilde{t}_i}^2, m_{\tilde{b}_1}^2, m_{H^\pm}^2\Big) + \left(y_t^2+1\right)\mathrm{T}_{134}\Big(m_{\tilde{t}_i}^2, m_{\tilde{t}_i}^2, m_{H^\pm}^2\Big), \tag{D.28b}$$

$$t_{D_3} = c_\beta^2 \tfrac{\mu^2}{s_\beta^2 c_\beta^2 \Delta_{\tilde{t}_i\tilde{t}_j}}\Big[\mathrm{T}_{134}\Big(m_{\tilde{t}_i}^2, m_{\tilde{b}_1}^2, m_{H^\pm}^2\Big) + \mathrm{T}_{134}\Big(m_{\tilde{t}_i}^2, m_{\tilde{t}_i}^2, m_{H^\pm}^2\Big)\Big]. \tag{D.29a}$$

D.4. One-loop self-energies with counterterms

The one-loop self-energies with counterterm insertion are part of the full two-loop self-energies. They are given in the following:

$$\begin{aligned}
\Sigma_{hh}^{(2)\,\mathrm{ct}} &= \frac{N_c s_\beta^2 h_t^2}{16\pi^2}\left\{s_{A_1}^{\mathrm{ct}} + s_{A_2}^{\mathrm{ct}}\right\} \\
&+ \sum_{\substack{i=1\\ j\neq i}}^{2} \frac{N_c s_\beta^2 h_t^2}{16\pi^2}\Bigg\{\left(1+x_t^2\right)s_{A_3}^{\mathrm{ct}} + \left(1+x_t^2\right)^2 s_{A_4}^{\mathrm{ct}} + x_t^2\left(1-4U_\times\right)s_{A_5}^{\mathrm{ct}} - 2x_t^4 s_{B_1}^{\mathrm{ct}} \\
&\qquad + x_t^2 s_{B_2}^{\mathrm{ct}} + x_t^2\left(1-4U_\times\right)s_{D_1}^{\mathrm{ct}} + x_t^2\left(1+x_t^2\right)s_{D_2}^{\mathrm{ct}}\Bigg\},
\end{aligned} \tag{D.30a}$$

$$\begin{aligned}
\Sigma_{hH}^{(2)\,\mathrm{ct}} &= -\frac{N_c s_\beta c_\beta h_t^2}{16\pi^2}\left\{s_{A_1}^{\mathrm{ct}} + s_{A_2}^{\mathrm{ct}}\right\} \\
&- \sum_{\substack{i=1\\ j\neq i}}^{2} \frac{N_c s_\beta c_\beta h_t^2}{16\pi^2}\Bigg\{\left(1-\tfrac{\eta}{4}+\tfrac{x_t^2}{2}\right)s_{A_3}^{\mathrm{ct}} - \left(\tfrac{\eta}{2}-1\right)\left(1+x_t^2\right)s_{A_4}^{\mathrm{ct}} - \tfrac{\eta}{2}\left(1-4U_\times\right)s_{A_5}^{\mathrm{ct}} \\
&\qquad + \eta x_t^2 s_{B_1}^{\mathrm{ct}} + \left(\tfrac{x_t^2}{2}-\tfrac{\eta}{4}\right)s_{B_2}^{\mathrm{ct}} + \tfrac{\Im\mathrm{m}[X_t\mu^*]}{s_\beta c_\beta \Delta_{\tilde{t}_i\tilde{t}_j}}\left(x_t^2 s_{B_3}^{\mathrm{ct}} - s_{B_4}^{\mathrm{ct}}\right) \\
&\qquad - \left(\tfrac{\eta}{2}+x_t^2\right)\left[\left(1-4U_\times\right)s_{C_1}^{\mathrm{ct}} + \left(1+x_t^2\right)s_{C_2}^{\mathrm{ct}}\right] + x_t^2 s_{D_2}^{\mathrm{ct}} \\
&\qquad + \left(\tfrac{x_t^2}{2}-\tfrac{\eta}{4}\right)\left[\left(1-4U_\times\right)s_{D_1}^{\mathrm{ct}} + x_t^2 s_{D_2}^{\mathrm{ct}}\right] + \left(\tfrac{\eta^2}{4}-x_t^2 y_t^2\right)s_{D_3}^{\mathrm{ct}}\Bigg\},
\end{aligned} \tag{D.30b}$$

$$\begin{aligned}
\Sigma_{HH}^{(2)\,\mathrm{ct}} &= \frac{N_c c_\beta^2 h_t^2}{16\pi^2}\left\{s_{A_1}^{\mathrm{ct}} + s_{A_2}^{\mathrm{ct}}\right\} \\
&+ \sum_{\substack{i=1\\ j\neq i}}^{2} \frac{N_c c_\beta^2 h_t^2}{16\pi^2}\Bigg\{-\left(\tfrac{\eta}{2}-1\right)s_{A_3}^{\mathrm{ct}} + \left(\tfrac{\eta}{2}-1\right)^2 s_{A_4}^{\mathrm{ct}} - \tfrac{m_t^2\eta^2-Y_t^2}{\Delta_{\tilde{t}_i\tilde{t}_j}}s_{A_5}^{\mathrm{ct}} \\
&\qquad - \tfrac{\eta^2}{2}s_{B_1}^{\mathrm{ct}} - \tfrac{\eta}{2}s_{B_2}^{\mathrm{ct}} - \tfrac{\Im\mathrm{m}[X_t\mu^*]}{s_\beta c_\beta \Delta_{\tilde{t}_i\tilde{t}_j}}\left(\eta s_{B_3}^{\mathrm{ct}} + 2s_{B_4}^{\mathrm{ct}}\right) \\
&\qquad + \left[\eta\left(1-4U_\times\right) - 2\tfrac{m_t^2\eta^2-Y_t^2}{\Delta_{\tilde{t}_i\tilde{t}_j}}\right]s_{C_1}^{\mathrm{ct}} + \left(\tfrac{\eta}{2}-1\right)\left(\eta+2x_t^2\right)s_{C_2}^{\mathrm{ct}} \\
&\qquad + \tfrac{\eta}{2}\left(1-4U_\times\right)s_{D_1}^{\mathrm{ct}} - \left(\tfrac{\eta}{2}-1\right)x_t^2 s_{D_2}^{\mathrm{ct}} + \left(\tfrac{\eta^2}{2}-2x_t^2 y_t^2\right)s_{D_3}^{\mathrm{ct}}\Bigg\},
\end{aligned} \tag{D.30c}$$

$$\begin{aligned}
\Sigma_{AA}^{(2)\,\mathrm{ct}} &= \frac{N_c c_\beta^2 h_t^2}{16\pi^2}s_{A_1}^{\mathrm{ct}} \\
&+ \sum_{\substack{i=1\\ j\neq i}}^{2} \frac{N_c c_\beta^2 h_t^2}{16\pi^2}\Bigg\{-\left(\tfrac{\eta^2}{4}-x_t^2 y_t^2\right)s_{A_4}^{\mathrm{ct}} + \tfrac{m_t^2\eta^2+(1-4U_\times)Y_t^2}{\Delta_{\tilde{t}_i\tilde{t}_j}}s_{A_5}^{\mathrm{ct}} + \left(\tfrac{\eta^2}{2}-2x_t^2 y_t^2\right)s_{B_1}^{\mathrm{ct}} \\
&\qquad + \tfrac{\Im\mathrm{m}[X_t\mu^*]}{s_\beta c_\beta \Delta_{\tilde{t}_i\tilde{t}_j}}\eta s_{B_3}^{\mathrm{ct}} + 2\left(\tfrac{\eta}{2}+\tfrac{m_t^2\eta^2+(1-4U_\times)Y_t^2}{\Delta_{\tilde{t}_i\tilde{t}_j}}\right)s_{C_1}^{\mathrm{ct}} - \left(\tfrac{\eta^2}{2}-2x_t^2 y_t^2\right)s_{C_2}^{\mathrm{ct}} \\
&\qquad - \tfrac{\eta}{2}s_{D_1}^{\mathrm{ct}} + \left(\tfrac{\eta^2}{2}-2x_t^2 y_t^2\right)\left[\left(1-4U_\times\right)s_{D_3}^{\mathrm{ct}} + x_t^2 s_{D_4}^{\mathrm{ct}}\right]\Bigg\},
\end{aligned} \tag{D.30d}$$

$$
\begin{aligned}
\Sigma_{hA}^{(2)\,\mathrm{ct}} = \sum_{\substack{i\,=\,1\\ j\,\neq\, i}}^{2} \frac{N_c s_\beta c_\beta h_t^2}{16\pi^2} \frac{\mathfrak{Im}[X_t\mu^*]}{s_\beta c_\beta \Delta_{\tilde{t}_i\tilde{t}_j}} \Big\{ & -\tfrac{1}{2} s_{A_3}^{\mathrm{ct}} - \left(1+x_t^2\right) s_{A_4}^{\mathrm{ct}} - \left(1-4U_\times\right) s_{A_5}^{\mathrm{ct}} \\
& + 2x_t^2 s_{B_1}^{\mathrm{ct}} - \tfrac{1}{2} s_{B_2}^{\mathrm{ct}} - \tfrac{s_\beta c_\beta \Delta_{\tilde{t}_i\tilde{t}_j}}{\mathfrak{Im}[X_t\mu^*]} \tfrac{\eta}{2} \left(x_t^2 s_{B_3}^{\mathrm{ct}} - s_{B_4}^{\mathrm{ct}}\right) \\
& - \left(1-4U_\times\right)\left(s_{C_1}^{\mathrm{ct}} + \tfrac{1}{2} s_{D_1}^{\mathrm{ct}}\right) - \left(1+x_t^2\right)\left(s_{C_2}^{\mathrm{ct}} - x_t^2 s_{D_4}^{\mathrm{ct}}\right) \\
& - \tfrac{x_t^2}{2} s_{D_2}^{\mathrm{ct}} + \left[\tfrac{\eta}{2} + x_t^2\left(1-4U_\times\right)\right] s_{D_3}^{\mathrm{ct}} \Big\},
\end{aligned}
\tag{D.30e}
$$

$$
\begin{aligned}
\Sigma_{HA}^{(2)\,\mathrm{ct}} = \sum_{\substack{i\,=\,1\\ j\,\neq\, i}}^{2} \frac{N_c c_\beta^2 h_t^2}{16\pi^2} \frac{\mathfrak{Im}[X_t\mu^*]}{s_\beta c_\beta \Delta_{\tilde{t}_i\tilde{t}_j}} \Big\{ & \tfrac{1}{2} s_{A_3}^{\mathrm{ct}} - \left(\tfrac{\eta}{2} - 1\right) s_{A_4}^{\mathrm{ct}} + \tfrac{2m_t^2\eta}{\Delta_{\tilde{t}_i\tilde{t}_j}} s_{A_5}^{\mathrm{ct}} + \tfrac{\eta}{2} s_{B_1}^{\mathrm{ct}} \\
& + \tfrac{1}{2} s_{B_2}^{\mathrm{ct}} - \tfrac{s_\beta c_\beta \Delta_{\tilde{t}_i\tilde{t}_j}}{\mathfrak{Im}[X_t\mu^*]} \left[\left(\tfrac{\eta^2}{2} - x_t^2 y_t^2\right) s_{B_3}^{\mathrm{ct}} + \tfrac{\eta}{2} s_{B_4}^{\mathrm{ct}}\right] \\
& + \tfrac{4m_t^2}{\Delta_{\tilde{t}_i\tilde{t}_j}} \left(\eta + x_t^2\right) s_{C_1}^{\mathrm{ct}} - \left(\eta + x_t^2 - 1\right) s_{C_2}^{\mathrm{ct}} \\
& - \tfrac{2m_t^2}{\Delta_{\tilde{t}_i\tilde{t}_j}} x_t^2 \left(s_{D_1}^{\mathrm{ct}} + \eta s_{D_3}^{\mathrm{ct}}\right) + \tfrac{x_t^2}{2} s_{D_2}^{\mathrm{ct}} + \left(\tfrac{\eta}{2} - 1\right) x_t^2 s_{D_4}^{\mathrm{ct}} \Big\},
\end{aligned}
\tag{D.30f}
$$

$$
\begin{aligned}
\Sigma_{H^\pm H^\pm}^{(2)\,\mathrm{ct}} = {} & \frac{N_c c_\beta^2 h_t^2}{16\pi^2} \Big\{ s_E^{\mathrm{ct}} - s_{F_1}^{\mathrm{ct}} - s_{F_2}^{\mathrm{ct}} \Big\} \\
& + \sum_{\substack{i\,=\,1\\ j\,\neq\, i}}^{2} \frac{N_c c_\beta^2 h_t^2}{16\pi^2} \Big\{ s_G^{\mathrm{ct}} + s_H^{\mathrm{ct}} + \tfrac{m_t^2\left(\eta - |\mathbf{U}_{\tilde{t}\,1i}|^2\right) - Y_t^2 |\mathbf{U}_{\tilde{t}\,1j}|^2}{\Delta_{\tilde{t}_i\tilde{b}_1}} s_I^{\mathrm{ct}} + s_J^{\mathrm{ct}} + s_K^{\mathrm{ct}} + s_{L_1}^{\mathrm{ct}} + s_{L_2}^{\mathrm{ct}} \\
& \qquad + s_{M_1}^{\mathrm{ct}} + s_{M_2}^{\mathrm{ct}} \Big\}.
\end{aligned}
\tag{D.30g}
$$

$$
\begin{aligned}
s_{A_1}^{\mathrm{ct}} = {} & 2\left[\tfrac{\delta^{(1)}h_t}{h_t} + \tfrac{\delta^{(1)}Z_{\mathcal{H}_2}}{2}\right]\left[-2A_0\!\left(m_t^2\right) + \sum_{i\,=\,1}^{2} A_0\!\left(m_{\tilde{t}_i}^2\right)\right] \\
& - 4m_t^2 \tfrac{\delta^{(1)}m_t}{m_t} B_0\!\left(0, m_t^2, m_t^2\right) + \sum_{i\,=\,1}^{2} \delta^{(1)} m_{\tilde{t}_i\tilde{t}_i}^2 B_0\!\left(0, m_{\tilde{t}_i}^2, m_{\tilde{t}_i}^2\right),
\end{aligned}
\tag{D.31a}
$$

$$
s_{A_2}^{\mathrm{ct}} = -8m_t^2\left[\tfrac{\delta^{(1)}m_t}{m_t} + \tfrac{\delta^{(1)}h_t}{h_t} + \tfrac{\delta^{(1)}Z_{\mathcal{H}_2}}{2}\right] B_0\!\left(0, m_t^2, m_t^2\right) - 16m_t^4 \tfrac{\delta^{(1)}m_t}{m_t} C_0\!\left(0,0,0,m_t^2,m_t^2,m_t^2\right),
\tag{D.31b}
$$

$$
s_{A_3}^{\mathrm{ct}} = 4m_t^2 \tfrac{\delta^{(1)}m_t}{m_t} B_0\!\left(0, m_{\tilde{t}_i}^2, m_{\tilde{t}_i}^2\right),
\tag{D.31c}
$$

$$
s_{A_4}^{\mathrm{ct}} = 4m_t^2 \left\{\left[\tfrac{\delta^{(1)}h_t}{h_t} + \tfrac{\delta^{(1)}Z_{\mathcal{H}_2}}{2}\right] B_0\!\left(0, m_{\tilde{t}_i}^2, m_{\tilde{t}_i}^2\right) + \delta^{(1)} m_{\tilde{t}_i\tilde{t}_i}^2 C_0\!\left(0,0,0,m_{\tilde{t}_i}^2, m_{\tilde{t}_i}^2, m_{\tilde{t}_i}^2\right)\right\},
\tag{D.31d}
$$

$$
s_{A_5}^{\mathrm{ct}} = 2\left[\tfrac{\delta^{(1)}h_t}{h_t} + \tfrac{\delta^{(1)}Z_{\mathcal{H}_2}}{2}\right] A_0\!\left(m_{\tilde{t}_i}^2\right) - \delta^{(1)} m_{\tilde{t}_i\tilde{t}_i}^2 \left[B_0\!\left(0, m_{\tilde{t}_i}^2, m_{\tilde{t}_j}^2\right) - B_0\!\left(0, m_{\tilde{t}_i}^2, m_{\tilde{t}_i}^2\right)\right],
\tag{D.31e}
$$

$$
s_{B_1}^{\mathrm{ct}} = \tfrac{4\left(|\mathbf{U}_{\tilde{t}\,11}|^2 - |\mathbf{U}_{\tilde{t}\,12}|^2\right)|\mathbf{U}_{\tilde{t}\,12}|^2}{X_t^2} \mathfrak{Re}\left[\tfrac{\delta^{(1)} m_{\tilde{t}_1\tilde{t}_2}^2 \mathbf{U}_{\tilde{t}\,22}\mathbf{U}_{\tilde{t}\,11}^*}{m_t X_t}\right]\left[A_0\!\left(m_{\tilde{t}_i}^2\right) - \tfrac{\Delta_{\tilde{t}_i\tilde{t}_j}}{2} B_0\!\left(0, m_{\tilde{t}_i}^2, m_{\tilde{t}_i}^2\right)\right],
\tag{D.32a}
$$

$$
s_{B_2}^{\mathrm{ct}} = \tfrac{4\left(|\mathbf{U}_{\tilde{t}\,11}|^2 - |\mathbf{U}_{\tilde{t}\,12}|^2\right)|\mathbf{U}_{\tilde{t}\,12}|^2}{X_t^2} \mathfrak{Re}\left[\tfrac{\delta^{(1)} m_{\tilde{t}_1\tilde{t}_2}^2 \mathbf{U}_{\tilde{t}\,22}\mathbf{U}_{\tilde{t}\,11}^*}{m_t X_t}\right] \Delta_{\tilde{t}_i\tilde{t}_j} B_0\!\left(0, m_{\tilde{t}_i}^2, m_{\tilde{t}_i}^2\right),
\tag{D.32b}
$$

$$
s_{B_3}^{\mathrm{ct}} = \tfrac{4|\mathbf{U}_{\tilde{t}\,12}|^2}{X_t^2} \mathfrak{Im}\left[\tfrac{\delta^{(1)} m_{\tilde{t}_1\tilde{t}_2}^2 \mathbf{U}_{\tilde{t}\,22}\mathbf{U}_{\tilde{t}\,11}^*}{m_t X_t}\right]\left[A_0\!\left(m_{\tilde{t}_i}^2\right) - \tfrac{\Delta_{\tilde{t}_i\tilde{t}_j}}{2} B_0\!\left(0, m_{\tilde{t}_i}^2, m_{\tilde{t}_i}^2\right)\right],
\tag{D.32c}
$$

$$
s_{B_4}^{\mathrm{ct}} = \tfrac{2|\mathbf{U}_{\tilde{t}\,12}|^2}{X_t^2} \mathfrak{Im}\left[\tfrac{\delta^{(1)} m_{\tilde{t}_1\tilde{t}_2}^2 \mathbf{U}_{\tilde{t}\,22}\mathbf{U}_{\tilde{t}\,11}^*}{m_t X_t}\right] \Delta_{\tilde{t}_i\tilde{t}_j} B_0\!\left(0, m_{\tilde{t}_i}^2, m_{\tilde{t}_i}^2\right),
\tag{D.32d}
$$

$$
s_{C_1}^{\mathrm{ct}} = \left[\tfrac{\delta^{(1)}\mu}{\mu} - \tfrac{\delta^{(1)}t_\beta}{t_\beta}\right] A_0\!\left(m_{\tilde{t}_i}^2\right),
\tag{D.33a}
$$

$$s^{\rm ct}_{C_2} = 2m_t^2\left[\frac{\delta^{(1)}\mu}{\mu} - \frac{\delta^{(1)}t_\beta}{t_\beta}\right]B_0\Big(0, m^2_{\tilde{t}_i}, m^2_{\tilde{t}_i}\Big), \tag{D.33b}$$

$$s^{\rm ct}_{D_1} = \frac{\delta^{(1)}x_t^2}{x_t^2}A_0\Big(m^2_{\tilde{t}_i}\Big), \tag{D.34a}$$

$$s^{\rm ct}_{D_2} = 2m_t^2\frac{\delta^{(1)}x_t^2}{x_t^2}B_0\Big(0, m^2_{\tilde{t}_i}, m^2_{\tilde{t}_i}\Big), \tag{D.34b}$$

$$s^{\rm ct}_{D_3} = \frac{s_\beta c_\beta \Delta_{\tilde{t}_i\tilde{t}_j}\delta^{(1)}\phi_X}{\Im\mathfrak{m}[X_t\mu^*]}A_0\Big(m^2_{\tilde{t}_i}\Big), \tag{D.34c}$$

$$s^{\rm ct}_{D_4} = 2m_t^2\frac{s_\beta c_\beta \Delta_{\tilde{t}_i\tilde{t}_j}\delta^{(1)}\phi_X}{\Im\mathfrak{m}[X_t\mu^*]}B_0\Big(0, m^2_{\tilde{t}_i}, m^2_{\tilde{t}_i}\Big), \tag{D.34d}$$

$$\begin{aligned} s^{\rm ct}_{E} &= 2\left[\frac{\delta^{(1)}h_t}{h_t} + \frac{\delta^{(1)}Z_{\mathcal{H}_2}}{2}\right]\left[A_0\Big(m^2_{\tilde{b}_1}\Big) - 2A_0\big(m_t^2\big) + \sum_{\substack{i=1\\ j\neq i}}^{2}|\mathbf{U}_{\tilde{t}\,1j}|^2 A_0\Big(m^2_{\tilde{t}_i}\Big)\right] \\ &\quad - 4m_t^2\frac{\delta^{(1)}m_t}{m_t}B_0\big(0, m_t^2, m_t^2\big) + \delta^{(1)}m^2_{\tilde{b}_1\tilde{b}_1}\left(1 - \frac{\eta m_t^2\Delta_{\tilde{t}_1\tilde{t}_2}}{\Delta_{\tilde{t}_1\tilde{b}_1}\Delta_{\tilde{t}_2\tilde{b}_1}}\right)B_0\Big(0, m^2_{\tilde{b}_1}, m^2_{\tilde{b}_1}\Big), \end{aligned} \tag{D.35a}$$

$$s^{\rm ct}_{F_1} = \frac{\Delta^2_{\tilde{t}_1\tilde{t}_2}\left[2x_t^2\big(m_t^2 - Y_t^2\big) + \Delta_{\tilde{t}_1\tilde{t}_2}\eta\big(|\mathbf{U}_{\tilde{t}\,11}|^2 - |\mathbf{U}_{\tilde{t}\,12}|^2\big)\right]}{\Delta_{\tilde{t}_1\tilde{b}_1}\Delta_{\tilde{t}_2\tilde{b}_1}}\frac{|\mathbf{U}_{\tilde{t}\,12}|^2}{X_t^2}\Re\mathfrak{e}\left[\frac{\delta^{(1)}m^2_{\tilde{t}_1\tilde{t}_2}\mathbf{U}_{\tilde{t}\,22}\mathbf{U}^*_{\tilde{t}\,11}}{m_t X_t}\right]A_0\Big(m^2_{\tilde{b}_1}\Big), \tag{D.36a}$$

$$s^{\rm ct}_{F_2} = \frac{\Delta^2_{\tilde{t}_1\tilde{t}_2}}{\Delta_{\tilde{t}_1\tilde{b}_1}\Delta_{\tilde{t}_2\tilde{b}_1}}\frac{2\Im\mathfrak{m}[X_t\mu^*]}{c_\beta s_\beta}\frac{|\mathbf{U}_{\tilde{t}\,12}|^2}{X_t^2}\Im\mathfrak{m}\left[\frac{\delta^{(1)}m^2_{\tilde{t}_1\tilde{t}_2}\mathbf{U}_{\tilde{t}\,22}\mathbf{U}^*_{\tilde{t}\,11}}{m_t X_t}\right]A_0\Big(m^2_{\tilde{b}_1}\Big), \tag{D.36b}$$

$$s^{\rm ct}_{G} = -\frac{|\mathbf{U}_{\tilde{t}\,1i}|^2\Big(m_t^2\Delta_{\tilde{t}_j\tilde{b}_1} + Y_t^2\Delta_{\tilde{t}_i\tilde{b}_1}\Big)}{\Delta_{\tilde{t}_i\tilde{b}_1}\Delta_{\tilde{t}_j\tilde{b}_1}}\delta^{(1)}m^2_{\tilde{b}_1\tilde{b}_1}B_0\Big(0, m^2_{\tilde{b}_1}, m^2_{\tilde{b}_1}\Big), \tag{D.37a}$$

$$s^{\rm ct}_{H} = \left[|\mathbf{U}_{\tilde{t}\,1j}|^2\left(\frac{Y_t^2}{\Delta_{\tilde{t}_i\tilde{b}_1}} + 1\right) + \frac{m_t^2\big(|\mathbf{U}_{\tilde{t}\,1i}|^2 - \eta\big)}{\Delta_{\tilde{t}_i\tilde{b}_1}}\right]\delta^{(1)}m^2_{\tilde{t}_i\tilde{t}_i}B_0\Big(0, m^2_{\tilde{t}_i}, m^2_{\tilde{t}_i}\Big), \tag{D.38a}$$

$$s^{\rm ct}_{I} = 2\left[\frac{\delta^{(1)}h_t}{h_t} + \frac{\delta^{(1)}Z_{\mathcal{H}_2}}{2} + \frac{\delta^{(1)}m^2_{\tilde{b}_1\tilde{b}_1} - \delta^{(1)}m^2_{\tilde{t}_i\tilde{t}_i}}{2\Delta_{\tilde{t}_i\tilde{b}_1}}\right]\left[A_0\Big(m^2_{\tilde{b}_1}\Big) - A_0\Big(m^2_{\tilde{t}_i}\Big)\right], \tag{D.39a}$$

$$s^{\rm ct}_{J} = \frac{\eta - 2|\mathbf{U}_{\tilde{t}\,1i}|^2}{\Delta_{\tilde{t}_i\tilde{b}_1}}m_t^2\frac{\delta^{(1)}m_t}{m_t}\left[A_0\Big(m^2_{\tilde{b}_1}\Big) - A_0\Big(m^2_{\tilde{t}_i}\Big)\right], \tag{D.40a}$$

$$s^{\rm ct}_{K} = \frac{m_t^2\big(\eta + 2x_t^2\big) - \Delta_{\tilde{t}_i\tilde{t}_j}|\mathbf{U}_{\tilde{t}\,1j}|^2\big(\eta + 2y_t^2\big)}{\Delta_{\tilde{t}_i\tilde{b}_1}}\left[\frac{\delta^{(1)}\mu}{\mu} - \frac{\delta^{(1)}t_\beta}{t_\beta}\right]\left[A_0\Big(m^2_{\tilde{b}_1}\Big) - A_0\Big(m^2_{\tilde{t}_i}\Big)\right], \tag{D.41a}$$

$$s^{\rm ct}_{L_1} = -\frac{2m_t^2x_t^2 - \Delta_{\tilde{t}_i\tilde{t}_j}\eta|\mathbf{U}_{\tilde{t}\,1j}|^2}{2\Delta_{\tilde{t}_i\tilde{b}_1}}\frac{\delta^{(1)}x_t^2}{x_t^2}\left[A_0\Big(m^2_{\tilde{b}_1}\Big) - A_0\Big(m^2_{\tilde{t}_i}\Big)\right], \tag{D.42a}$$

$$s^{\rm ct}_{L_2} = \frac{2\Im\mathfrak{m}[X_t\mu^*]}{c_\beta s_\beta}\frac{|\mathbf{U}_{\tilde{t}\,1j}|^2}{\Delta_{\tilde{t}_i\tilde{b}_1}}\delta^{(1)}\phi_X\left[A_0\Big(m^2_{\tilde{b}_1}\Big) - A_0\Big(m^2_{\tilde{t}_i}\Big)\right], \tag{D.42b}$$

$$s^{\rm ct}_{M_1} = \left\{2|\mathbf{U}_{\tilde{t}\,1j}|^2 - \frac{\Delta_{\tilde{t}_i\tilde{t}_j}\left[2x_t^2\big(m_t^2 - Y_t^2\big) + \Delta_{\tilde{t}_i\tilde{t}_j}\eta U_-\right]}{\Delta_{\tilde{t}_i\tilde{b}_1}}\frac{|\mathbf{U}_{\tilde{t}\,1j}|^2}{X_t^2}\right\}\Re\mathfrak{e}\left[\frac{\delta^{(1)}m^2_{\tilde{t}_i\tilde{t}_j}\mathbf{U}_{\tilde{t}\,2j}\mathbf{U}^*_{\tilde{t}\,1i}}{m_t X_t}\right]A_0\Big(m^2_{\tilde{t}_i}\Big), \tag{D.43a}$$

$$s^{\rm ct}_{M_2} = -\frac{\Delta_{\tilde{t}_i\tilde{t}_j}}{\Delta_{\tilde{t}_i\tilde{b}_1}}\frac{2\Im\mathfrak{m}[X_t\mu^*]}{c_\beta s_\beta}\frac{|\mathbf{U}_{\tilde{t}\,1j}|^2}{X_t^2}\Im\mathfrak{m}\left[\frac{\delta^{(1)}m^2_{\tilde{t}_i\tilde{t}_j}\mathbf{U}_{\tilde{t}\,2j}\mathbf{U}^*_{\tilde{t}\,1i}}{m_t X_t}\right]A_0\Big(m^2_{\tilde{t}_i}\Big). \tag{D.43b}$$

D.5. One-loop tadpoles with counterterms

The one-loop tadpoles with counterterm insertion are part of the two-loop tadpoles of the Higgs bosons. They are given by

$$\Upsilon_h^{(2)\,\rm ct} = \frac{N_c s_\beta h_t m_t}{8\sqrt{2}\pi^4}\left\{t^{\rm ct}_{A_1} + \sum_{\substack{i=1\\ j\neq i}}^{2}\left[\big(1 + x_t^2\big)\,t^{\rm ct}_{A_2} + x_t^2 t^{\rm ct}_{B_1} + \frac{x_t^2}{2}t^{\rm ct}_{D_1}\right]\right\}, \tag{D.44a}$$

$$\Upsilon_H^{(2)\,\mathrm{ct}} = \frac{N_c c_\beta h_t m_t}{8\sqrt{2}\pi^4}\Bigg\{-t_{A_1}^{\mathrm{ct}} + \sum_{\substack{i=1\\ j\neq i}}^{2}\bigg[\left(\tfrac{\eta}{2}-1\right)t_{A_2}^{\mathrm{ct}} + \tfrac{\eta}{2}t_{B_1}^{\mathrm{ct}} + \tfrac{\mathfrak{Im}[X_t\mu^*]}{s_\beta c_\beta \Delta_{\tilde{t}_i\tilde{t}_j}}t_{B_2}^{\mathrm{ct}} + \left(\tfrac{\eta}{2}+x_t^2\right)t_C^{\mathrm{ct}} - \tfrac{x_t^2}{2}t_{D_1}^{\mathrm{ct}}\bigg]\Bigg\}, \tag{D.44b}$$

$$\Upsilon_A^{(2)\,\mathrm{ct}} = -\sum_{\substack{i=1\\ j\neq i}}^{2}\frac{N_c c_\beta h_t m_t}{8\sqrt{2}\pi^4}\frac{\mathfrak{Im}[X_t\mu^*]}{s_\beta c_\beta \Delta_{\tilde{t}_i\tilde{t}_j}}\Big\{t_{A_2}^{\mathrm{ct}} + t_{B_1}^{\mathrm{ct}} - \tfrac{s_\beta c_\beta\Delta_{\tilde{t}_i\tilde{t}_j}}{\mathfrak{Im}[X_t\mu^*]}\tfrac{\eta}{2}t_{B_2}^{\mathrm{ct}} + t_C^{\mathrm{ct}} - x_t^2 t_{D_2}^{\mathrm{ct}}\Big\}. \tag{D.44c}$$

$$t_{A_1}^{\mathrm{ct}} = -2\left[\tfrac{\delta^{(1)}h_t}{h_t} + \tfrac{\delta^{(1)}Z_{\mathcal{H}_2}}{2}\right]A_0\big(m_t^2\big) - \tfrac{\delta^{(1)}m_t}{m_t}\left(2A_0\big(m_t^2\big) + 4m_t^2 B_0\big(0,m_t^2,m_t^2\big) - \sum_{i=1}^{2}A_0\Big(m_{\tilde{t}_i}^2\Big)\right), \tag{D.45a}$$

$$t_{A_2}^{\mathrm{ct}} = \left[\tfrac{\delta^{(1)}h_t}{h_t} + \tfrac{\delta^{(1)}Z_{\mathcal{H}_2}}{2}\right]A_0\Big(m_{\tilde{t}_i}^2\Big) + \delta^{(1)}m_{\tilde{t}_i\tilde{t}_i}^2 B_0\Big(0,m_{\tilde{t}_i}^2,m_{\tilde{t}_i}^2\Big), \tag{D.45b}$$

$$t_{B_1}^{\mathrm{ct}} = \tfrac{\left(|\mathbf{U}_{\tilde{t}\,11}|^2 - |\mathbf{U}_{\tilde{t}\,12}|^2\right)|\mathbf{U}_{\tilde{t}\,12}|^2\Delta_{\tilde{t}_i\tilde{t}_j}}{m_t^2 x_t^2}\mathfrak{Re}\left[\tfrac{\delta^{(1)}m_{\tilde{t}_1\tilde{t}_2}^2\mathbf{U}_{\tilde{t}\,22}\mathbf{U}_{\tilde{t}\,11}^*}{m_t X_t}\right]A_0\Big(m_{\tilde{t}_i}^2\Big), \tag{D.46a}$$

$$t_{B_2}^{\mathrm{ct}} = \tfrac{|\mathbf{U}_{\tilde{t}\,12}|^2\Delta_{\tilde{t}_i\tilde{t}_j}}{m_t^2 x_t^2}\mathfrak{Im}\left[\tfrac{\delta^{(1)}m_{\tilde{t}_1\tilde{t}_2}^2\mathbf{U}_{\tilde{t}\,22}\mathbf{U}_{\tilde{t}\,11}^*}{m_t X_t}\right]A_0\Big(m_{\tilde{t}_i}^2\Big), \tag{D.46b}$$

$$t_C^{\mathrm{ct}} = s_{C_1}^{\mathrm{ct}}, \tag{D.47a}$$

$$t_{D_1}^{\mathrm{ct}} = s_{D_1}^{\mathrm{ct}}, \tag{D.48a}$$

$$t_{D_2}^{\mathrm{ct}} = s_{D_3}^{\mathrm{ct}}. \tag{D.48b}$$

D.6. Renormalization constants for subrenormalization

The required renormalization constants are explicitly expressed in the following:

$$\delta^{(1)}T_h = \frac{3s_\beta h_t}{8\sqrt{2}\pi^2}\Bigg\{-\sum_{i=1}^{2}\left(m_t + \mathfrak{Re}\left[X_t\mathbf{U}_{\tilde{t}\,i1}\mathbf{U}_{\tilde{t}\,i2}^*\right]\right)A_0\Big(m_{\tilde{t}_i}^2\Big) + 2m_t A_0\big(m_t^2\big)\Bigg\}, \tag{D.49a}$$

$$\delta^{(1)}T_H = \frac{3c_\beta h_t}{8\sqrt{2}\pi^2}\Bigg\{\sum_{i=1}^{2}\left(m_t + \mathfrak{Re}\left[Y_t\mathbf{U}_{\tilde{t}\,i1}\mathbf{U}_{\tilde{t}\,i2}^*\right]\right)A_0\Big(m_{\tilde{t}_i}^2\Big) - 2m_t A_0\big(m_t^2\big)\Bigg\}, \tag{D.49b}$$

$$\delta^{(1)}T_A = -\frac{3c_\beta h_t}{8\sqrt{2}\pi^2}\sum_{i=1}^{2}\mathfrak{Im}\left[Y_t\mathbf{U}_{\tilde{t}\,i1}\mathbf{U}_{\tilde{t}\,i2}^*\right]A_0\Big(m_{\tilde{t}_i}^2\Big), \tag{D.49c}$$

$$\begin{aligned}\delta^{(1)}m_{H^\pm}^2 = \frac{3c_\beta^2 h_t^2}{16\pi^2}\Bigg\{&\sum_{i=1}^{2}\left[|\mathbf{U}_{\tilde{t}\,i2}|^2 A_0\Big(m_{\tilde{t}_i}^2\Big) + |m_t\mathbf{U}_{\tilde{t}\,i1}^* + Y_t\mathbf{U}_{\tilde{t}\,i2}^*|^2\mathfrak{Re}\Big[B_0\Big(0,m_{\tilde{t}_i}^2,m_{\tilde{b}_1}^2\Big)\Big]\right]\\ &- 2m_t^2\mathfrak{Re}\left[B_0\big(0,0,m_t^2\big)\right] + A_0\Big(m_{\tilde{b}_1}^2\Big)\Bigg\},\end{aligned} \tag{D.50a}$$

$$\delta^{(1)}Z_{\mathcal{H}_1} = 0, \tag{D.51a}$$

$$\delta^{(1)}Z_{\mathcal{H}_2} = -\frac{3h_t^2}{16\pi^2\epsilon}, \tag{D.51b}$$

$$\begin{aligned}\frac{\delta^{(1)}M_W^2}{M_W^2} = \frac{3s_\beta^2}{16\pi^2}\frac{h_t^2}{m_t^2}\Bigg\{&2\left(2\mathfrak{Re}\left[B_{00}\big(0,0,m_t^2\big)\right] - m_t^2\mathfrak{Re}\left[B_0\big(0,0,m_t^2\big)\right]\right) + A_0\Big(m_{\tilde{b}_1}^2\Big)\\ &+ \sum_{i=1}^{2}|\mathbf{U}_{\tilde{t}\,i1}|^2\left(A_0\Big(m_{\tilde{t}_i}^2\Big) - 4\mathfrak{Re}\Big[B_{00}\Big(0,m_{\tilde{b}_1}^2,m_{\tilde{t}_i}^2\Big)\Big]\right)\Bigg\},\end{aligned} \tag{D.52a}$$

$$\begin{aligned}\frac{\delta^{(1)}M_Z^2}{M_Z^2} &= \frac{3s_\beta^2}{16\pi^2}\frac{h_t^2}{m_t^2}\bigg\{-m_t^2\Re\mathfrak{e}\big[B_0\big(0,m_t^2,m_t^2\big)\big] + \sum_{i=1}^{2}|\mathbf{U}_{\tilde{t}\,i1}|^2|\mathbf{U}_{\tilde{t}\,i2}|^2 A_0\Big(m_{\tilde{t}_i}^2\Big)\\ &\qquad - 4\Re\mathfrak{e}\Big[B_{00}\Big(0,m_{\tilde{t}_1}^2,m_{\tilde{t}_2}^2\Big)\Big]|\mathbf{U}_{\tilde{t}\,11}|^2|\mathbf{U}_{\tilde{t}\,12}|^2\bigg\},\end{aligned} \tag{D.52b}$$

$$\begin{aligned}\frac{\delta^{(1)}m_t}{m_t} &= \frac{h_t^2}{32\pi^2}\bigg\{-\Re\mathfrak{e}\Big[B_1\Big(m_t^2,\mu^2,m_{\tilde{t}_1}^2\Big) + B_1\Big(m_t^2,\mu^2,m_{\tilde{t}_2}^2\Big) + B_1\Big(m_t^2,\mu^2,m_{\tilde{b}_1}^2\Big)\Big]\\ &\qquad + c_\beta^2\frac{\delta^{(1)}m_t^H}{m_t} + s_\beta^2\,\frac{\delta^{(1)}m_t^H}{m_t}\bigg|_{m_{H^\pm}\to 0}\bigg\},\end{aligned} \tag{D.53a}$$

$$\frac{\delta^{(1)}m_t^H}{m_t} = \Re\mathfrak{e}\big[B_0\big(m_t^2,m_{H^\pm}^2,m_t^2\big) + B_1\big(m_t^2,m_{H^\pm}^2,m_t^2\big) - B_1\big(m_t^2,0,m_{H^\pm}^2\big) + B_1\big(m_t^2,m_t^2,m_{H^\pm}^2\big)\big], \tag{D.53b}$$

$$\begin{aligned}\delta^{(1)}m_{\tilde{t}_i\tilde{t}_i}^2 &= \frac{h_t^2}{16\pi^2}\bigg\{-2m_{\tilde{t}_i}^2\,\Re\mathfrak{e}\Big[B_1\Big(m_{\tilde{t}_i}^2,m_t^2,\mu^2\Big)\Big] + 8U_\times A_0\Big(m_{\tilde{t}_i}^2\Big) + (1-8U_\times)\,A_0\Big(m_{\tilde{t}_j}^2\Big)\\ &\qquad - 2\left(|\mathbf{U}_{\tilde{t}\,1j}|^2+1\right)A_0\big(\mu^2\big) + |\mathbf{U}_{\tilde{t}\,1j}|^2 A_0\Big(m_{\tilde{b}_1}^2\Big)\\ &\qquad - 2m_t^2\Re\mathfrak{e}\Big[B_0\Big(m_{\tilde{t}_i}^2,m_t^2,\mu^2\Big)\Big] - 2m_{\tilde{t}_i}^2|\mathbf{U}_{\tilde{t}\,1j}|^2\Re\mathfrak{e}\Big[B_1\Big(m_{\tilde{t}_i}^2,0,\mu^2\Big)\Big]\\ &\qquad + c_\beta^2\delta^{(1)}m_{\tilde{t}_i\tilde{t}_i}^{2H} + s_\beta^2\,\delta^{(1)}m_{\tilde{t}_i\tilde{t}_i}^{2H}\Big|_{m_{H^\pm}\to 0,\ Y_t^2\to X_t^2,\ y_t^2\to x_t^2,\ \eta\to -2x_t^2}\bigg\}, \qquad j\neq i,\end{aligned} \tag{D.54a}$$

$$\begin{aligned}\delta^{(1)}m_{\tilde{t}_i\tilde{t}_i}^{2H} &= Y_t^2\,(1-2U_\times)\,\Re\mathfrak{e}\Big[B_0\Big(m_{\tilde{t}_i}^2,m_{H^\pm}^2,m_{\tilde{t}_j}^2\Big)\Big] - 2m_t^2\,\big(\eta - x_t^2y_t^2 - 1\big)\,\Re\mathfrak{e}\Big[B_0\Big(m_{\tilde{t}_i}^2,m_{H^\pm}^2,m_{\tilde{t}_i}^2\Big)\Big]\\ &\quad + \big(m_t^2|\mathbf{U}_{\tilde{t}\,1i}|^2 + Y_t^2|\mathbf{U}_{\tilde{t}\,1j}|^2 - \eta m_t^2\big)\,\Re\mathfrak{e}\Big[B_0\Big(m_{\tilde{t}_i}^2,m_{H^\pm}^2,m_{\tilde{b}_1}^2\Big)\Big] + \big(|\mathbf{U}_{\tilde{t}\,1j}|^2+1\big)\,A_0\big(m_{H^\pm}^2\big),\end{aligned} \tag{D.54b}$$

$$\begin{aligned}\delta^{(1)}m_{\tilde{t}_1\tilde{t}_2}^2 &= \frac{h_t^2\mathbf{U}_{\tilde{t}\,11}\mathbf{U}_{\tilde{t}\,22}^*|\mathbf{U}_{\tilde{t}\,12}|^2\Delta_{\tilde{t}_1\tilde{t}_2}}{16\pi^2 m_t X_t^*}\bigg\{\sum_{i=1}^{2}\Big[4U_- A_0\Big(m_{\tilde{t}_i}^2\Big) - m_{\tilde{t}_i}^2\,\Re\mathfrak{e}\Big[B_1\Big(m_{\tilde{t}_i}^2,0,\mu^2\Big)\Big]\Big]\\ &\qquad - 2A_0\big(\mu^2\big) + A_0\Big(m_{\tilde{b}_1}^2\Big)\\ &\qquad - \frac{i\,c_\beta^2\Im\mathfrak{m}[X_t\mu^*]\Delta_{\tilde{t}_1\tilde{t}_2}}{2c_\beta s_\beta X_t^2}\sum_{i,j=1}^{2}\bigg\{\Re\mathfrak{e}\Big[B_0\Big(m_{\tilde{t}_i}^2,m_{H^\pm}^2,m_{\tilde{t}_j}^2\Big)\Big]\\ &\qquad\qquad + \Re\mathfrak{e}\Big[B_0\Big(m_{\tilde{t}_i}^2,m_{H^\pm}^2,m_{\tilde{b}_1}^2\Big)\Big]\bigg\}\\ &\qquad + c_\beta^2\delta^{(1)}m_{\tilde{t}_1\tilde{t}_2}^{2H} + s_\beta^2\,\delta^{(1)}m_{\tilde{t}_1\tilde{t}_2}^{2H}\Big|_{m_{H^\pm}\to 0,\ y_t^2\to x_t^2,\ \eta\to -2x_t^2}\bigg\},\end{aligned} \tag{D.55a}$$

$$\begin{aligned}\delta^{(1)}m_{\tilde{t}_1\tilde{t}_2}^{2H} &= A_0\big(m_{H^\pm}^2\big) - \frac{\Delta_{\tilde{t}_1\tilde{t}_2}^2}{2X_t^2}\sum_{\substack{i=1\\ j\neq i}}^{2}\Big[\tfrac{\eta U_-}{2} - x_t^2y_t^2 + U_\times\Big]\,\Re\mathfrak{e}\Big[B_0\Big(m_{\tilde{t}_i}^2,m_{H^\pm}^2,m_{\tilde{b}_1}^2\Big)\Big]\\ &\quad - \frac{\Delta_{\tilde{t}_1\tilde{t}_2}^2}{2X_t^2}\sum_{\substack{i=1\\ j\neq i}}^{2}U_-\,\big[\tfrac{\eta}{2} - x_t^2y_t^2\big]\,\Re\mathfrak{e}\Big[B_0\Big(m_{\tilde{t}_i}^2,m_{H^\pm}^2,m_{\tilde{t}_i}^2\Big) + B_0\Big(m_{\tilde{t}_j}^2,m_{H^\pm}^2,m_{\tilde{t}_i}^2\Big)\Big],\end{aligned} \tag{D.55b}$$

$$\delta^{(1)}m_{\tilde{t}_2\tilde{t}_1}^2 = \Big(\delta^{(1)}m_{\tilde{t}_1\tilde{t}_2}^2\Big)^*, \tag{D.56a}$$

$$\frac{\delta^{(1)}\mu}{\mu} = -\frac{3h_t^2}{32\pi^2}\bigg\{\Re\mathfrak{e}\Big[B_1\Big(\mu^2,m_t^2,m_{\tilde{b}_1}^2\Big)\Big] + \sum_{i=1}^{2}|\mathbf{U}_{\tilde{t}\,i2}|^2\Re\mathfrak{e}\Big[B_1\Big(\mu^2,0,m_{\tilde{t}_i}^2\Big)\Big]\bigg\}. \tag{D.57a}$$

List of Symbols

Common symbols

δ_{ij}	Kronecker's delta
$\boldsymbol{e}$	Euler's constant
$\epsilon_{\alpha\beta}$	Levi–Civita symbol
e	elementary-charge constant
γ_{E}	Euler–Mascheroni constant
$\boldsymbol{i}$	imaginary unit
$\mathfrak{Im}[x]$	the imaginary part of x
$\mathbf{1}$	identity matrix
N_{c}	number of colors; $N_{\mathrm{c}} = 3$
$\mathcal{O}(x)$	indicates the terms of the order of x
$\mathbf{0}$	zero matrix
$\mathfrak{Re}[x]$	the real part of x
s_x, c_x, t_x	the sine, cosine and tangent of x respectively
h_t	the top-Yukawa coupling
CP	charge–parity operator
g_Y	gauge coupling of the hypercharge
g_{s}	gauge coupling of the strong interaction
g_{w}	gauge coupling of the weak interaction
$\mathcal{L}$	Lagrangian density
m_f	fermion mass with fermion index f
M_W	W boson mass
M_Z	Z boson mass
$U(1)_Y$	unitary group of degree one as symmetry group of the hypercharge
$SU(2)_{\mathrm{L}}$	special unitary group of degree two as symmetry group of the left-handed weak interaction
$\overset{SU}{\odot}$	$SU(2)_{\mathrm{L}}$ product
$SU(3)_{\mathrm{c}}$	special unitary group of degree three as symmetry group of the strong interaction

v_1, v_2	vacuum expectation values of the Higgs-boson doublets
t_β	the tangent of beta; the ratio v_2/v_1
$\mathcal{W}$	superpotential
s_w, c_w	sine and cosine of the Weinberg angle θ_w

Chapter 2: Supersymmetry

γ^5	chirality matrix
γ^μ	Dirac gamma matrices
σ^i	Pauli matrices, $i \in \{1, 2, 3\}$
g	gauge coupling
$g^{\mu\nu}$	metric tensor
$\sigma^{\mu\nu}$, $\bar{\sigma}^{\mu\nu}$	spin matrices
θ_A, $\bar{\theta}_{\dot{A}}$	Grassmann two-spinor space elements
∂^A, $\bar{\partial}^{\dot{A}}$	derivatives with respect to θ_A or $\bar{\theta}_{\dot{A}}$
x^μ	Minkowski spacetime element
∂^μ	derivative with respect to x_μ
m^2_{ij}, a_i, b_{ij}, c_{ijk}, M_λ	coefficients of soft supersymmetry-breaking terms
D^A, $\bar{D}^{\dot{A}}$	chiral covariant derivatives
f^{abc}	fine-structure constants of a group
F	general superfield
f, M, N, D, $A^{A\dot{B}}$, ξ^A, ζ^A, $\bar{\chi}^{\dot{A}}$, $\bar{\lambda}^{\dot{A}}$	components of a general superfield
Φ	chiral superfield
A, F, ξ	components of a chiral superfield
T	infinitesimal supersymmetry transformation
V	vector superfield
Λ	chiral gauge superfield
W^A, $\bar{W}^{\dot{A}}$	super-gauge field strength
G^a	generators of a group
$J^{\mu\nu}$	angular momentum operator
P^μ	energy–momentum operator
Q	fermionic generator; supersymmetry generator
W^μ	Pauli–Lubański vector
R	generator of the R-symmetry

Chapter 3: The Minimal Supersymmetric Standard Model

$\tilde{f}$	if not stated otherwise $\tilde{f} \in \{\tilde{u}, \tilde{d}, \tilde{e}, \tilde{c}, \tilde{s}, \tilde{\mu}, \tilde{t}, \tilde{b}, \tilde{\tau}\}$
f	if not stated otherwise $f \in \{u, d, e, c, s, \mu, t, b, \tau\}$
i, j	if not stated otherwise $i, j \in \{1, 2, 3\}$; generation and/or color indices
$\theta, \bar{\theta}$	Grassmann variables
$A_{f,ij}$	trilinear soft supersymmetry-breaking parameter matrix with generation indices i, j and fermion-type index $f \in \{u, d, e\}$
$\left(m^2_{\tilde{f}_\mathrm{L}}\right)_{ij}$	bilinear soft supersymmetry-breaking parameters with generation indices i, j and sfermion index $\tilde{f} \in \{\tilde{q}, \tilde{l}\}$
$\left(m^2_{\tilde{f}_\mathrm{R}}\right)_{ij}$	bilinear soft supersymmetry-breaking parameters with generation indices i, j and sfermion index $\tilde{f} \in \{\tilde{u}, \tilde{d}, \tilde{e}\}$
$\tilde{m}_1^2, \tilde{m}_2^2, b_{\mathcal{H}_1\mathcal{H}_2}$	soft supersymmetry-breaking parameters for the Higgs bosons
$M_1, M_2, \tilde{m}_{\tilde{g}}$	soft supersymmetry-breaking parameters for the gauginos
$\tilde{B}$	bino, superpartner of B^μ
B^μ	interaction particle of the hypercharge
$\tilde{d}_{i,\mathrm{R}}$	superpartner of $d_{i,\mathrm{R}}$
D_i^C	down-type charge conjugated superfield in generation i
$d_{i,\mathrm{L},j}$	left-handed down-type particle in generation i with color j
$d_{i,\mathrm{R},j}$	right-handed down-type particle in generation i with color j
$\tilde{e}_{i,\mathrm{R}}$	superpartner of $e_{i,\mathrm{R}}$
E_i^C	electron-type charge conjugated superfield in generation i
$e_{i,\mathrm{L}}$	left-handed electron-type particle in generation i
$e_{i,\mathrm{R}}$	right-handed electron-type particle in generation i
$\tilde{G}$	gluinos, superpartners of G^μ
G^μ	interaction particles of the strong charge
$\mathcal{H}_1, \mathcal{H}_2$	bosonic parts of the Higgs-superfield $SU(2)_\mathrm{L}$ doublets
$\tilde{\mathcal{H}}_1, \tilde{\mathcal{H}}_2$	fermionic parts of the Higgs-superfield $SU(2)_\mathrm{L}$ doublets
$H, G, G^\pm$	the Higgs and Goldstone bosons of the Standard Model
H_1, H_2	Higgs-superfield $SU(2)_\mathrm{L}$ doublets
ϕ_1, χ_1, ϕ_1^-	components of $\mathcal{H}_1$
ϕ_2, χ_2, ϕ_2^+	components of $\mathcal{H}_2$
$\tilde{h}_1^0, \tilde{h}_1^-$	components of $\tilde{\mathcal{H}}_1$
$\tilde{h}_2^0, \tilde{h}_2^+$	components of $\tilde{\mathcal{H}}_2$
$\lambda_A, \lambda_Z, \lambda_W^\pm$	gauginos after electroweak symmetry breaking
$\tilde{l}_{i,\mathrm{L}}$	superpartner $SU(2)_\mathrm{L}$ doublet of $l_{i,\mathrm{L}}$

$l_{i,\mathrm{L}}$	left-handed $SU(2)_\mathrm{L}$ doublet of leptons in generation i
L_i	lepton-superfield $SU(2)_\mathrm{L}$ doublet in generation i
$\nu_{i,\mathrm{L}}$	left-handed neutrino in generation i
$\tilde{q}_{i,\mathrm{L}}$	superpartner $SU(2)_\mathrm{L}$ doublet of $q_{i,\mathrm{L}}$
$q_{i,\mathrm{L},j}$	left-handed $SU(2)_\mathrm{L}$ doublet of quarks in generation i with color j
Q_i	quark-superfield $SU(2)_\mathrm{L}$ doublet in generation i
$\tilde{u}_{i,\mathrm{R}}$	superpartner of $u_{i,\mathrm{R}}$
U_i^C	up-type charge conjugated superfield in generation i
$u_{i,\mathrm{L},j}$	left-handed up-type particle in generation i with color j
$u_{i,\mathrm{R},j}$	right-handed up-type particle in generation i with color j
$\tilde{W}$	winos, superpartners of W^μ
W^μ	interaction particles of the weak charge
$\tilde{\chi}^\pm$, $\tilde{\chi}^0$	charginos and neutralinos
$\hat{Y}$, τ, λ	gauge-group generators
$\mathbf{h}_f$, $h_{f,ij}$	Yukawa-coupling matrices and matrix elements with generation indices i, j and fermion-type index $f \in \{u, d, e\}$
μ	coefficient of the bilinear Higgs term in the superpotential
A_f	$A_{f,ij}$ for minimal flavor violation
$m_{\tilde{f}_{1/2}}$	sfermion mass eigenvalues with sfermion index $\tilde{f}$
κ_f	equal to t_β for down-type and electron-type fermion index f; equal to $1/t_\beta$ for up-type fermion index f
$\mathbf{N}$, $\mathbf{U}$, $\mathbf{V}$	gaugino and higgsino mixing matrices
$\mathbf{X}$, $\mathbf{Y}$	chargino and neutralino interaction matrices
$m_{\tilde{\chi}^\pm}$, $m_{\tilde{\chi}^0}$	masses of the charginos and neutralinos
$X_{\tilde{\chi}^\pm}$	the combination $M_2\,\mu - 2\,M_W^2\,c_\beta\,s_\beta$
X_f	the combination $A_f^* - \mu\kappa_f$
Q_f	electrical charge of the fermion f
ω_Y, ω_w^a, ω_s^b	gauge-group functions
T_f^3	third component of the isospin of the fermion f
$\mathbf{U}_{\tilde{f}}$	sfermion mixing matrix with sfermion index $\tilde{f}$

Chapter 4: Higher-order calculations

ϵ' . . . . infinitesimal deviation from the real axis to obtain causal Feynman propagators

m_i . . . . propagator masses

p_i . . . . incoming momenta

q_i . . . . loop momenta

Φ^{cyc} . . . . a purely finite part of T_{134}

A_0 . . . . one-point one-loop integral

B_i . . . . two-point one-loop integrals

C_i . . . . three-point one-loop integrals

$\tilde{F}_i$, F_i . . . . integrals of i loop oder in 4 and D dimensions respectively

$\tilde{f}_i$, f_i . . . . integrand of i loop oder in 4 and D dimensions respectively

k_i . . . . kinematic invariants composed of p and q_i in two-point two-loop integrals

$\mathrm{T}_{a_1 \ldots a_n}$ . . . . . . two-point two-loop integrals, $a_i \in \{1, 2, 3, 4, 5\}$

Chapter 5: Renormalization

$\beta(g)$ . . . . the beta function of g

$\delta^{(i)}$ . . . . indicator for a renormalization constant of loop level i

γ_i . . . . the anomalous dimension of ψ_i

$\Gamma_{\psi_1,\ldots,\psi_n}$ . . . . . . bare one-particle-irreducible n-point Green's function

$\hat{\Gamma}_{\psi_1,\ldots,\psi_n}$ . . . . . . renormalized one-particle-irreducible n-point Green's function

ψ . . . . quantum field

g . . . . coupling parameter; trilinear or quadruple field coefficient

g_{B}, ψ_{B} . . . . . . parameter and field of the Lagrangian that do not depend on μ_{D}

m . . . . mass parameter; bilinear field coefficient

Z . . . . multiplicative renormalization constant

Chapter 6: Higgs bosons in the MSSM

$\hat{}$	indicator for a renormalized quantity
α, β_n, β_c	tree-level mixing angles between interaction and mass eigenstates of the Higgs and Goldstone bosons
$\beta^{(k)}(t_\beta)$	beta function of t_β at kth loop order
$\Delta^{(k)}$	indicator for the kth order counterterm that is composed of genuine kth order and products of lower-order counterterms
$\gamma_1^{(k)}$, $\gamma_2^{(k)}$	anomalous dimensions of the Higgs doublets of kth loop order
$\mathbf{\Sigma}$	matrix of self-energies
$\mathbf{D}_x$	(2×2) rotation matrix with angle x
$\mathbf{M}_{ij}$	mass matrices; bilinear coefficient of fields i, j
$\Sigma_{ij}^{(k)}$	self-energy diagrams of kth loop level for fields i, j
$\Upsilon_i^{(k)}$	tadpole diagrams of kth loop level for field i
ξ_i, ξ_i'	gauge-fixing parameters of an R_ξ gauge fixing
ζ	relative complex phase between the two Higgs $SU(2)_\mathrm{L}$ doublets
ζ'	complex phase of m_{12}^2
F_i	gauge-fixing functions with $i \in \{A, Z, W\}$
m_1^2, m_2^2, m_{12}^2	soft supersymmetry-breaking parameters of the Higgs sector; correlated with $\tilde{m}_1^2$, $\tilde{m}_2^2$, $b_{\mathcal{H}_1\mathcal{H}_2}$ and μ
$m_{h_1^\pm}$, $m_{h_2^\pm}$	loop-corrected charged Higgs-boson masses
m_{h_1}, m_{h_2}, m_{h_3}	loop-corrected neutral Higgs-boson masses
T_i	tadpole; linear coefficient of field i
V_H	Higgs potential
m_h, m_H, m_A, m_G, $m_{H^\pm}$, $m_{G^\pm}$	tree-level masses of the neutral and charged Higgs and Goldstone bosons respectively
h, H, A, G, $H^\pm$, $G^\pm$	Higgs and Goldstone bosons of the MSSM

Chapter 7: Two-loop top-Yukawa-coupling corrections

$\Delta^{(k)}r$	finite shifts of r at kth loop order
Φ, Φ^0, Φ^-	placeholders for the neutral and charged tree-level Higgs- and Goldstone-boson mass eigenstates respectively
c, C	couplings of Higgs bosons, higgsinos, tops, bottoms, stops and sbottoms to each other in the top-Yukawa approximation
G_F	the Fermi constant
$\tilde{\mathfrak{Re}}[x]$	applies $\mathfrak{Re}$ only on the loop functions inside of x

Chapter 8: Numerical investigation of the top-Yukawa corrections

ϕ_μ	the phase of the complex MSSM parameter μ
ϕ_{A_t}	the phase of the complex MSSM parameter A_t
m_h^{low}	the scenario with a low value for the lightest Higgs-boson mass
m_h^{max}	the scenario with a maximal value for the lightest Higgs-boson mass, $X_t = 2\, m_{\tilde{t}}$
$m_h^{\text{mod},\pm}$	the scenario with a moderate value for the lightest Higgs-boson mass, $X_t = \pm 1.5\, m_{\tilde{t}}$
$m_{\tilde{t}}$	the universal soft-breaking stop mass $m_{\tilde{t}} \equiv m_{\tilde{t}_\text{L}} = m_{\tilde{t}_\text{R}}$
X_t	the quantity $A_t^* - \mu/t_\beta$ of the stop sector

List of Figures

List of Tables

Bibliography

Chapter 1: Introduction

[Aad+12] G. Aad et al., *Observation of a new particle in the search for the Standard Model Higgs boson with the ATLAS detector at the LHC*, Phys.Lett. **B716** (2012), pp. 1–29, DOI: `10.1016/j.physletb.2012.08.020`, arXiv: `1207.7214` (cit. on pp. 1, 2, 115).

[Aad+14] G. Aad et al., *Measurement of the Higgs boson mass from the $H \to \gamma\gamma$ and $H \to ZZ^* \to 4\ell$ channels with the ATLAS detector using 25 fb^{-1} of pp collision data* (2014), arXiv: `1406.3827` (cit. on pp. 2, 115, 117).

[Aal+08] T. Aaltonen et al., *Forward-Backward Asymmetry in Top Quark Production in $p\bar{p}$ Collisions at $\sqrt{s} = 1.96$ TeV*, Phys.Rev.Lett. **101** (2008), p. 202001, DOI: `10.1103/PhysRevLett.101.202001`, arXiv: `0806.2472` (cit. on p. 1).

[Aba+08] V. M. Abazov et al., *First measurement of the forward-backward charge asymmetry in top quark pair production*, Phys.Rev.Lett. **100** (2008), p. 142002, DOI: `10.1103/PhysRevLett.100.142002`, arXiv: `0712.0851` (cit. on p. 1).

[All+04] B. C. Allanach et al., *Precise determination of the neutral Higgs boson masses in the MSSM*, JHEP **0409** (2004), p. 044, DOI: `10.1088/1126-6708/2004/09/044`, arXiv: `hep-ph/0406166` (cit. on p. 2).

[Ben+06] G. W. Bennett et al., *Final Report of the Muon E821 Anomalous Magnetic Moment Measurement at BNL*, Phys.Rev. **D73** (2006), p. 072003, DOI: `10.1103/PhysRevD.73.072003`, arXiv: `hep-ex/0602035` (cit. on p. 1).

[Bri+02] A. Brignole et al., *On the $\mathcal{O}(\alpha_t^2)$ two loop corrections to the neutral Higgs boson masses in the MSSM*, Nucl.Phys. **B631** (2002), pp. 195–218, DOI: `10.1016/S0550-3213(02)00184-0`, arXiv: `hep-ph/0112177` (cit. on pp. 2–4, 79, 97).

[Car+00] M. S. Carena et al., *Renormalization group improved effective potential for the MSSM Higgs sector with explicit CP violation*, Nucl.Phys. **B586** (2000), pp. 92–140, DOI: 10.1016/S0550-3213(00)00358-8, arXiv: hep-ph/0003180 (cit. on p. 2).

[Cas+95] J. A. Casas et al., *The Lightest Higgs boson mass in the minimal supersymmetric standard model*, Nucl.Phys. **B436** (1995), pp. 3–29, DOI: 10.1016/0550-3213(94)00508-C, arXiv: hep-ph/9407389; M. S. Carena et al., *Analytical expressions for radiatively corrected Higgs masses and couplings in the MSSM*, Phys.Lett. **B355** (1995), pp. 209–221, DOI: 10.1016/0370-2693(95)00694-G, arXiv: hep-ph/9504316, (cit. on p. 2).

[Cha+12a] S. Chatrchyan et al., *Observation of a new boson at a mass of 125 GeV with the CMS experiment at the LHC*, Phys.Lett. **B716** (2012), pp. 30–61, DOI: 10.1016/j.physletb.2012.08.021, arXiv: 1207.7235 (cit. on pp. 1, 2, 115).

[Cha+14] S. Chatrchyan et al., *Measurement of the properties of a Higgs boson in the four-lepton final state*, Phys.Rev. **D89** (2014), p. 092007, DOI: 10.1103/PhysRevD.89.092007, arXiv: 1312.5353 (cit. on pp. 2, 115, 117).

[Deg+03] G. Degrassi et al., *Towards high precision predictions for the MSSM Higgs sector*, Eur.Phys.J. **C28** (2003), pp. 133–143, DOI: 10.1140/epjc/s2003-01152-2, arXiv: hep-ph/0212020 (cit. on pp. 2, 3, 99).

[Dem99] D. A. Demir, *Effects of the supersymmetric phases on the neutral Higgs sector*, Phys.Rev. **D60** (1999), p. 055006, DOI: 10.1103/PhysRevD.60.055006, arXiv: hep-ph/9901389; S. Y. Choi, M. Drees, and J. Lee, *Loop corrections to the neutral Higgs boson sector of the MSSM with explicit CP violation*, Phys.Lett. **B481** (2000), pp. 57–66, DOI: 10.1016/S0370-2693(00)00421-4, arXiv: hep-ph/0002287; T. Ibrahim and P. Nath, *Corrections to the Higgs boson masses and mixings from chargino, W and charged Higgs exchange loops and large CP phases*, Phys.Rev. **D63** (2001), p. 035009, DOI: 10.1103/PhysRevD.63.035009, arXiv: hep-ph/0008237; T. Ibrahim and P. Nath, *Neutralino exchange corrections to the Higgs boson mixings with explicit CP violation*, Phys.Rev. **D66** (2002), p. 015005, DOI: 10.1103/PhysRevD.66.015005, arXiv: hep-ph/0204092, (cit. on p. 2).

[Fra+07] M. Frank et al., *The Higgs boson masses and mixings of the complex MSSM in the Feynman-diagrammatic approach*, Journal of High Energy Physics **JHEP02** (2007), DOI: 10.1088/1126-6708/2007/02/047 (cit. on pp. 3, 35, 55).

[Gla61] S. L. Glashow, *Partial-symmetries of weak interactions*, Nuclear Physics **22** (1961), pp. 579–588, DOI: 10.1016/0029-5582(61)90469-2 (cit. on pp. 1, 15).

[GM08] M. C. Gonzalez-Garcia and M. Maltoni, *Phenomenology with Massive Neutrinos*, Phys.Rept. **460** (2008), pp. 1–129, DOI: 10.1016/j.physrep.2007.12.004, arXiv: 0704.1800 (cit. on p. 1).

[GM13] B. Grinstein and C. W. Murphy, *Bottom-Quark Forward-Backward Asymmetry in the Standard Model and Beyond*, Phys.Rev.Lett. **111** (2013), p. 062003, DOI: 10.1103/PhysRevLett.111.062003, arXiv: 1302.6995 (cit. on p. 1).

[Gol61] J. Goldstone, *Field theories with Superconductor solutions*, Nuovo Cimento **19** (1961), pp. 154–164, DOI: 10.1007/BF02812722 (cit. on pp. 2, 16).

[GSW62] J. Goldstone, A. Salam, and S. Weinberg, *Broken Symmetries*, Physical Review **127** (1962), pp. 965–970, DOI: 10.1103/PhysRev.127.965 (cit. on pp. 2, 16).

[Hah+09] T. Hahn et al., *FeynHiggs: A program for the calculation of MSSM Higgs-boson observables - Version 2.6.5*, Comput.Phys.Commun. **180** (2009), pp. 1426–1427, DOI: 10.1016/j.cpc.2009.02.014 (cit. on pp. 3, 101).

[Hei+05] S. Heinemeyer et al., *High-precision predictions for the MSSM Higgs sector at $\mathcal{O}(\alpha_b\alpha_s)$*, Eur.Phys.J. **C39** (2005), pp. 465–481, DOI: 10.1140/epjc/s2005-02112-6, arXiv: hep-ph/0411114 (cit. on p. 2).

[Hei+07] S. Heinemeyer et al., *The Higgs sector of the complex MSSM at two-loop order: QCD contributions*, Phys.Lett. **B652** (2007), pp. 300–309, DOI: 10.1016/j.physletb.2007.07.030, arXiv: 0705.0746 (cit. on pp. 2, 3, 65, 82).

[HHW00c] S. Heinemeyer, W. Hollik, and G. Weiglein, *FeynHiggs: A Program for the calculation of the masses of the neutral CP even Higgs bosons in the MSSM*, Comput.Phys.Commun. **124** (2000), pp. 76–89, DOI: 10.1016/S0010-4655(99)00364-1, arXiv: hep-ph/9812320 (cit. on p. 3).

[HHW06] S. Heinemeyer, W. Hollik, and G. Weiglein, *Electroweak precision observables in the minimal supersymmetric standard model*, Phys.Rept. **425** (2006), pp. 265–368, DOI: 10.1016/j.physrep.2005.12.002, arXiv: hep-ph/0412214 (cit. on p. 2).

[HHW98] S. Heinemeyer, W. Hollik, and G. Weiglein, *QCD corrections to the masses of the neutral CP-even Higgs bosons in the MSSM*, Phys.Rev. **D58** (1998), p. 091701, DOI: 10.1103/PhysRevD.58.091701, arXiv: hep-ph/9803277; S. Heinemeyer, W. Hollik, and G. Weiglein, *Precise prediction for the mass of the lightest Higgs boson in the MSSM*, Phys.Lett. **B440** (1998), pp. 296–304, DOI: 10.1016/S0370-2693(98)01116-2, arXiv: hep-ph/9807423, (cit. on p. 2).

[HHW99a] S. Heinemeyer, W. Hollik, and G. Weiglein, *The Mass of the lightest MSSM Higgs boson: A Compact analytical expression at the two loop level*, Phys.Lett. **B455** (1999), pp. 179–191, DOI: 10.1016/S0370-2693(99)00417-7, arXiv: hep-ph/9903404; M. S. Carena et al., *Reconciling the two loop diagrammatic and effective field theory computations of the mass of the lightest CP-even Higgs boson in the MSSM*, Nucl.Phys. **B580** (2000), pp. 29–57, DOI: 10.1016/S0550-3213(00)00212-1, arXiv: hep-ph/0001002, (cit. on p. 2).

[HHW99b] S. Heinemeyer, W. Hollik, and G. Weiglein, *The Masses of the neutral CP-even Higgs bosons in the MSSM: Accurate analysis at the two loop level*, Eur.Phys.J. **C9** (1999), pp. 343–366, DOI: 10.1007/s100529900006, arXiv: hep-ph/9812472 (cit. on pp. 2, 3).

[HK85] H. E. Haber and G. L. Kane, *The Search for Supersymmetry: Probing Physics Beyond the Standard Model*, Phys.Rept. **117** (1985), pp. 75–263, DOI: 10.1016/0370-1573(85)90051-1 (cit. on pp. 1, 16).

[HP14a] W. Hollik and S. Paßehr, *Two-loop top-Yukawa-coupling corrections to the Higgs boson masses in the complex MSSM*, Phys.Lett. **B733** (2014), pp. 144–150, DOI: 10.1016/j.physletb.2014.04.026, arXiv: 1401.8275 (cit. on p. 3).

[HP14b] W. Hollik and S. Paßehr, *Full results of the two-loop top-Yukawa-coupling corrections to the Higgs boson masses in the complex MSSM*, preparation (2014) (cit. on p. 3).

[JN09] F. Jegerlehner and A. Nyffeler, *The Muon $g-2$*, Phys.Rept. **477** (2009), pp. 1–110, DOI: `10.1016/j.physrep.2009.04.003`, arXiv: `0902.3360` (cit. on p. 1).

[Lan13] G. Landsberg, *Higgs Bosons in the Standard Model and Beyond* (2013), arXiv: `1310.5705 [hep-ex]`; F. Cerutti, *Properties of the new boson* (2013), (cit. on p. 2).

[LEP+04] LEP et al., *A Combination of preliminary electroweak measurements and constraints on the standard model* (2004), arXiv: `hep-ex/0412015` (cit. on p. 1).

[Mar02] S. P. Martin, *Two loop effective potential for a general renormalizable theory and softly broken supersymmetry*, Phys.Rev. **D65** (2002), p. 116003, DOI: `10.1103/PhysRevD.65.116003`, arXiv: `hep-ph/0111209`; S. P. Martin, *Two loop effective potential for the minimal supersymmetric standard model*, Phys.Rev. **D66** (2002), p. 096001, DOI: `10.1103/PhysRevD.66.096001`, arXiv: `hep-ph/0206136`; S. P. Martin, *Complete two loop effective potential approximation to the lightest Higgs scalar boson mass in supersymmetry*, Phys.Rev. **D67** (2003), p. 095012, DOI: `10.1103/PhysRevD.67.095012`, arXiv: `hep-ph/0211366`; S. P. Martin, *Evaluation of two loop selfenergy basis integrals using differential equations*, Phys.Rev. **D68** (2003), p. 075002, DOI: `10.1103/PhysRevD.68.075002`, arXiv: `hep-ph/0307101`; S. P. Martin, *Two loop scalar self energies in a general renormalizable theory at leading order in gauge couplings*, Phys.Rev. **D70** (2004), p. 016005, DOI: `10.1103/PhysRevD.70.016005`, arXiv: `hep-ph/0312092`; S. P. Martin, *Strong and Yukawa two-loop contributions to Higgs scalar boson self-energies and pole masses in supersymmetry*, Phys.Rev. **D71** (2005), p. 016012, DOI: `10.1103/PhysRevD.71.016012`, arXiv: `hep-ph/0405022`; S. P. Martin, *Two-loop scalar self-energies and pole masses in a general renormalizable theory with massless gauge bosons*, Phys.Rev. **D71** (2005), p. 116004, DOI: `10.1103/PhysRevD.71.116004`, arXiv: `hep-ph/0502168`; S. P. Martin and D. G. Robertson, *TSIL: A Program for the calculation of two-loop self-energy integrals*, Comput.Phys.Commun. **174** (2006), pp. 133–151, DOI: 10.1016/j.cpc.2005.08.005, arXiv: hep-ph/0501132, (cit. on p. 2).

[Mil+12] J. P. Miller et al., *Muon $(g-2)$: Experiment and Theory*, Ann.Rev.Nucl.Part.Sci. **62** (2012), pp. 237–264, DOI: 10.1146/annurev-nucl-031312-120340 (cit. on p. 1).

[Nam60] Y. Nambu, *Quasi-Particles and Gauge Invariance in the Theory of Superconductivity*, Physical Review **117** (1960), pp. 648–663, DOI: 10.1103/PhysRev.117.648 (cit. on pp. 2, 16).

[Pec12] B. D. Pecjak, *The top-quark forward-backward asymmetry in the standard model*, Nuovo Cim. **C035N3** (2012), pp. 147–152, DOI: 10.1393/ncc/i2012-11237-2 (cit. on p. 1).

[Pil98] A. Pilaftsis, *CP odd tadpole renormalization of Higgs scalar–pseudoscalar mixing*, Phys.Rev. **D58** (1998), p. 096010, DOI: 10.1103/PhysRevD.58.096010, arXiv: hep-ph/9803297 (cit. on p. 2).

[Pon57] B. Pontecorvo, *Mesonium and anti-mesonium*, Sov.Phys.JETP **6** (1957), p. 429 (cit. on p. 1).

[Pon68] B. Pontecorvo, *Neutrino Experiments and the Problem of Conservation of Leptonic Charge*, Sov.Phys.JETP **26** (1968), pp. 984–988 (cit. on p. 1).

[PR03] P. J. E. Peebles and Bharat Ratra, *The Cosmological constant and dark energy*, Rev.Mod.Phys. **75** (2003), pp. 559–606, DOI: 10.1103/RevModPhys.75.559, arXiv: astro-ph/0207347 (cit. on p. 1).

[PW99] A. Pilaftsis and C. E. M. Wagner, *Higgs bosons in the minimal supersymmetric standard model with explicit CP violation*, Nucl.Phys. **B553** (1999), pp. 3–42, DOI: 10.1016/S0550-3213(99)00261-8, arXiv: hep-ph/9902371 (cit. on p. 2).

[Sal68] A. Salam, *Weak and electromagnetic interactions*, Elementary Particle Theory: Relativistic Groups and Analyticity (Nobel Symposium No. 8) (1968), ed. by N. Svartholm, pp. 367–377 (cit. on pp. 1, 15).

[t H76a] G. 't Hooft, *Computation of the Quantum Effects Due to a Four-Dimensional Pseudoparticle*, Phys.Rev. **D14** (1976), pp. 3432–3450, DOI: 10.1103/PhysRevD.18.2199.3,10.1103/PhysRevD.14.3432 (cit. on p. 1).

[t H76b] G. 't Hooft, *Symmetry Breaking Through Bell-Jackiw Anomalies*, Phys.Rev.Lett. **37** (1976), pp. 8–11, DOI: `10.1103/PhysRevLett.37.8` (cit. on p. 1).

[Tri87] V. Trimble, *Existence and Nature of Dark Matter in the Universe*, Ann.Rev.Astron.Astrophys. **25** (1987), pp. 425–472, DOI: `10.1146/annurev.aa.25.090187.002233` (cit. on p. 1).

[Wei67] S. Weinberg, *A Model of Leptons*, Physical Review Letters **19** (1967), pp. 1264–1266, DOI: `10.1103/PhysRevLett.19.1264` (cit. on pp. 1, 15).

[Wei75] S. Weinberg, *The $U(1)$ Problem*, Phys.Rev. **D11** (1975), pp. 3583–3593, DOI: `10.1103/PhysRevD.11.3583` (cit. on p. 1).

[Zha99] R. Zhang, *Two loop effective potential calculation of the lightest CP even Higgs boson mass in the MSSM*, Phys.Lett. **B447** (1999), pp. 89–97, DOI: `10.1016/S0370-2693(98)01575-5`, arXiv: `hep-ph/9808299`; J. R. Espinosa and R. Zhang, *MSSM lightest CP even Higgs boson mass to $\mathcal{O}(\alpha_s\alpha_t)$: The Effective potential approach*, JHEP **0003** (2000), p. 026, DOI: `10.1088/1126-6708/2000/03/026`, arXiv: `hep-ph/9912236`; J. R. Espinosa and I. Navarro, *Radiative corrections to the Higgs boson mass for a hierarchical stop spectrum*, Nucl.Phys. **B615** (2001), pp. 82–116, DOI: `10.1016/S0550-3213(01)00429-1`, arXiv: `hep-ph/0104047`; G. Degrassi, P. Slavich, and F. Zwirner, *On the neutral Higgs boson masses in the MSSM for arbitrary stop mixing*, Nucl.Phys. **B611** (2001), pp. 403–422, DOI: `10.1016/S0550-3213(01)00343-1`, arXiv: `hep-ph/0105096`; R. Hempfling and A. H. Hoang, *Two loop radiative corrections to the upper limit of the lightest Higgs boson mass in the minimal supersymmetric model*, Phys.Lett. **B331** (1994), pp. 99–106, DOI: `10.1016/0370-2693(94)90948-2`, arXiv: `hep-ph/9401219`; A. Brignole et al., *On the two loop sbottom corrections to the neutral Higgs boson masses in the MSSM*, Nucl.Phys. **B643** (2002), pp. 79–92, DOI: `10.1016/S0550-3213(02)00748-4`, arXiv: `hep-ph/0206101`; A. Dedes, G. Degrassi, and P. Slavich, *On the two loop Yukawa corrections to the MSSM Higgs boson masses at large* $\tan(\beta)$, Nucl.Phys. **B672** (2003), pp. 144–162, DOI: `10.1016/j.nuclphysb.2003.08.033`, arXiv: `hep-ph/0305127`, (cit. on p. 2).

[Zwi33] F. Zwicky, *Die Rotverschiebung von extragalaktischen Nebeln*, Helv.Phys.Acta **6** (1933), pp. 110–127 (cit. on p. 1).

[Zwi37] F. Zwicky, *On the Masses of Nebulae and of Clusters of Nebulae*, Astrophys.J. **86** (1937), pp. 217–246, DOI: 10.1086/143864 (cit. on p. 1).

Chapter 2: Supersymmetry

[Bar+05] R. Barbier et al., *R-parity violating supersymmetry*, Phys.Rept. **420** (2005), pp. 1–202, DOI: 10.1016/j.physrep.2005.08.006, arXiv: hep-ph/0406039 (cit. on p. 12).

[CM67] S. Coleman and J. Mandula, *All Possible Symmetries of the S-Matrix*, Physical Review **159** (1967), pp. 1251–1256, DOI: 10.1103/PhysRev.159.1251 (cit. on p. 6).

[Col88] S. Coleman, *Aspects of Symmetry*, Cambridge University Press, 1988 (cit. on p. 12).

[DGR04] M. Drees, R. Godbole, and P. Roy, *Theory and Phenomenology of Sparticles*, World Scientific Publishing Company, 2004 (cit. on pp. 6, 8, 9, 13).

[Fay75] P. Fayet, *Supergauge Invariant Extension of the Higgs Mechanism and a Model for the electron and Its Neutrino*, Nucl.Phys. **B90** (1975), pp. 104–124, DOI: 10.1016/0550-3213(75)90636-7 (cit. on p. 7).

[Fay76] P. Fayet, *Higgs Model and Supersymmetry*, Nuovo Cim. **A31** (1976), p. 626, DOI: 10.1007/BF02734654 (cit. on p. 13).

[Fay77] P. Fayet, *Mixing Between Gravitational and Weak Interactions Through the Massive Gravitino*, Phys.Lett. **B70** (1977), p. 461, DOI: 10.1016/0370-2693(77)90414-2 (cit. on p. 11).

[FI74] P. Fayet and J. Iliopoulos, *Spontaneously Broken Supergauge Symmetries and Goldstone Spinors*, Phys.Lett. **B51** (1974), pp. 461–464, DOI: 10.1016/0370-2693(74)90310-4 (cit. on p. 13).

[FW83] G. R. Farrar and S. Weinberg, *Supersymmetry at ordinary energies. II. R invariance, Goldstone bosons, and gauge-fermion masses*, Physical Review D **27** (1983), pp. 2732–2746, DOI: 10.1103/PhysRevD.27.2732 (cit. on p. 11).

[GG82] L. Girardello and M. T. Grisaru, *Soft breaking of supersymmetry*, Nuclear Physics B **194** (1982), pp. 65–76, DOI: 10.1016/0550-3213(82)90512-0 (cit. on p. 13).

[GL71] Y. A. Golfand and E. P. Likhtman, *Extension of the Algebra of Poincare Group Generators and Violation of p Invariance*, JETP Lett. **13** (1971), pp. 323–326 (cit. on p. 5).

[HŁS75] R. Haag, J. T. Łopuszański, and M. Sohnius, *All Possible Generators of Supersymmetries of the S-Matrix*, Nuclear Physics B **88** (1975), p. 257, DOI: `10.1016/0550-3213(75)90279-5` (cit. on pp. 5, 6).

[KL04] P. Kumar and D. Lykken, *Visible sector supersymmetry breaking revisited*, Journal of High Energy Physics **7** (2004), DOI: `10.1088/1126-6708/2004/07/001` (cit. on p. 13).

[MW87] H. J. W. Müller-Kirsten and A. Wiedemann, *Supersymmetry: An Introduction With Conceptual and Calculational Details*, World Scientific Publishing Company, 1987 (cit. on p. 6).

[Nil84] H. P. Nilles, *Supersymmetry, supergravity and particle physics*, Physics Reports **110** (1984), pp. 1–162, DOI: `10.1016/0370-1573(84)90008-5` (cit. on p. 13).

[ORa75] L. O'Raifeartaigh, *Spontaneous Symmetry Breaking for Chiral Scalar Superfields*, Nucl.Phys. **B96** (1975), p. 331, DOI: `10.1016/0550-3213(75)90585-4` (cit. on p. 13).

[Ram71] P. Ramond, *Dual Theory for Free Fermions*, Phys.Rev. **D3** (1971), pp. 2415–2418, DOI: `10.1103/PhysRevD.3.2415`; A. Neveu and J. H. Schwarz, *Factorizable dual model of pions*, Nucl.Phys. **B31** (1971), pp. 86–112, DOI: `10.1016/0550-3213(71)90448-2`; J.-L. Gervais and B. Sakita, *Field Theory Interpretation of Supergauges in Dual Models*, Nucl.Phys. **B34** (1971), pp. 632–639, DOI: `10.1016/0550-3213(71)90351-8`, (cit. on p. 5).

[Soh85] M. Sohnius, *Introducing Supersymmetry*, Physics Reports **128** (1985), pp. 39–204, DOI: `10.1016/0370-1573(85)90023-7` (cit. on pp. 6, 7).

[SS74] A. Salam and J. A. Strathdee, *Supergauge Transformations*, Nucl.Phys. **B76** (1974), pp. 477–482, DOI: `10.1016/0550-3213(74)90537-9` (cit. on p. 5).

[VA73] D. V. Volkov and V. P. Akulov, *Is the Neutrino a Goldstone Particle?*, Phys.Lett. **B46** (1973), pp. 109–110, DOI: `10.1016/0370-2693(73)90490-5` (cit. on p. 5).

[Wei82] S. Weinberg, *Supersymmetry at Ordinary Energies. 1. Masses and Conservation Laws*, Phys.Rev. **D26** (1982), p. 287, DOI: `10.1103/PhysRevD.26.287` (cit. on p. 12).

[WZ74a] J. Wess and B. Zumino,
A Lagrangian Model Invariant Under Supergauge Transformations,
Phys.Lett. **B49** (1974), p. 52, DOI: `10.1016/0370-2693(74)90578-4`;
J. Iliopoulos and B. Zumino,
Broken Supergauge Symmetry and Renormalization,
Nucl.Phys. **B76** (1974), p. 310,
DOI: `10.1016/0550-3213(74)90388-5`;
S. Ferrara, J. Iliopoulos, and B. Zumino,
Supergauge Invariance and the Gell-Mann–Low Eigenvalue,
Nucl.Phys. **B77** (1974), p. 413,
DOI: `10.1016/0550-3213(74)90372-1`; B. Zumino,
Supersymmetry and the Vacuum, Nucl.Phys. **B89** (1975), p. 535,
DOI: `10.1016/0550-3213(75)90194-7`;
M. T. Grisaru, W. Siegel, and M. Rocek,
Improved Methods for Supergraphs, Nucl.Phys. **B159** (1979), p. 429,
DOI: `10.1016/0550-3213(79)90344-4`, (cit. on p. 13).

[WZ74b] J. Wess and B. Zumino,
Supergauge Invariant Extension of Quantum Electrodynamics,
Nuclear Physics B **78** (1974), pp. 1–13,
DOI: `10.1016/0550-3213(74)90112-6` (cit. on pp. 5, 10).

[WZ74c] J. Wess and B. Zumino,
Supergauge Transformations in Four-Dimensions,
Nucl.Phys. **B70** (1974), pp. 39–50,
DOI: `10.1016/0550-3213(74)90355-1` (cit. on p. 5).

Chapter 3: The Minimal Supersymmetric Standard Model

[BDJ01] M. Böhm, A. Denner, and H. Joos,
Gauge Theories of the Strong and Electroweak Interaction, 3. Auflage,
Teubner, 2001 (cit. on p. 15).

[Ber+12] J. Beringer et al., *Review of Particle Physics (RPP)*,
Phys.Rev. **D86** (2012), p. 010001, DOI: `10.1103/PhysRevD.86.010001`
(cit. on p. 16).

[BJN13] J. Bulava, K. Jansen, and A. Nagy, *Constraining a fourth generation of quarks: non-perturbative Higgs boson mass bounds*,
Phys.Lett. **B723** (2013), pp. 95–99,
DOI: `10.1016/j.physletb.2013.04.041` (cit. on p. 16).

[BS59] N. N. Bogoliubov and D. V. Shirkov,
Introduction to the Theory of Quantized Fields, Volume 3,
Interscience Publishers, 1959 (cit. on p. 15).

[Cab63] Nicola Cabibbo, *Unitary Symmetry and Leptonic Decays*, Phys.Rev.Lett. **10** (1963), pp. 531–533, DOI: 10.1103/PhysRevLett.10.531 (cit. on p. 19).

[Dec+89] D. Decamp et al., *Determination of the Number of Light Neutrino Species*, Phys.Lett. **B231** (1989), p. 519, DOI: 10.1016/0370-2693(89)90704-1 (cit. on p. 16).

[EB64] F. Englert and R. Brout, *Broken Symmetry and the Mass of Gauge Vector Mesons*, Physical Review Letters **13** (1964), pp. 321–323, DOI: 10.1103/PhysRevLett.13.321 (cit. on p. 15).

[Gel62] M. Gell-Mann, *Symmetries of Baryons and Mesons*, Physical Review **125** (1962), pp. 1067–1084 (cit. on p. 15).

[GHK64] G. S. Guralnik, C. R. Hagen, and T. W. B. Kibble, *Global Conservation Laws and Massless Particles*, Physical Review Letters **13** (1964), pp. 585–587, DOI: 10.1103/PhysRevLett.13.585 (cit. on p. 15).

[Gla61] S. L. Glashow, *Partial-symmetries of weak interactions*, Nuclear Physics **22** (1961), pp. 579–588, DOI: 10.1016/0029-5582(61)90469-2 (cit. on pp. 1, 15).

[Gol61] J. Goldstone, *Field theories with Superconductor solutions*, Nuovo Cimento **19** (1961), pp. 154–164, DOI: 10.1007/BF02812722 (cit. on pp. 2, 16).

[GSW62] J. Goldstone, A. Salam, and S. Weinberg, *Broken Symmetries*, Physical Review **127** (1962), pp. 965–970, DOI: 10.1103/PhysRev.127.965 (cit. on pp. 2, 16).

[Hig64] P. W. Higgs, *Broken Symmetries and the Masses of Gauge Bosons*, **13** (1964), pp. 508–509, DOI: 10.1103/PhysRevLett.13.508 (cit. on p. 15).

[HK85] H. E. Haber and G. L. Kane, *The Search for Supersymmetry: Probing Physics Beyond the Standard Model*, Phys.Rept. **117** (1985), pp. 75–263, DOI: 10.1016/0370-1573(85)90051-1 (cit. on pp. 1, 16).

[KM73] Makoto Kobayashi and Toshihide Maskawa, *CP Violation in the Renormalizable Theory of Weak Interaction*, Prog.Theor.Phys. **49** (1973), pp. 652–657, DOI: 10.1143/PTP.49.652 (cit. on p. 19).

[Len13] Alexander Lenz, *Constraints on a fourth generation of fermions from Higgs Boson searches*, Adv.High Energy Phys. **2013** (2013), p. 910275, DOI: 10.1155/2013/910275 (cit. on p. 16).

[LY56] T. D. Lee and C. N. Yang, *Question of Parity Conservation in Weak Interactions*, Physical Review **104** (1956), pp. 254–258, DOI: 10.1103/PhysRev.104.254 (cit. on p. 15).

[Nam60] Y. Nambu, *Quasi-Particles and Gauge Invariance in the Theory of Superconductivity*, Physical Review **117** (1960), pp. 648–663, DOI: 10.1103/PhysRev.117.648 (cit. on pp. 2, 16).

[Sal68] A. Salam, *Weak and electromagnetic interactions*, Elementary Particle Theory: Relativistic Groups and Analyticity (Nobel Symposium No. 8) (1968), ed. by N. Svartholm, pp. 367–377 (cit. on pp. 1, 15).

[Tak27] T. Takagi, Japanese J. Math. **1** (1927), p. 83 (cit. on p. 21).

[Wei67] S. Weinberg, *A Model of Leptons*, Physical Review Letters **19** (1967), pp. 1264–1266, DOI: 10.1103/PhysRevLett.19.1264 (cit. on pp. 1, 15).

[Wu+57] C. S. Wu et al., *Experimental Test of Parity Conservation in Beta Decay*, Physical Review **105** (1957), pp. 1413–1415, DOI: 10.1103/PhysRev.105.1413 (cit. on p. 15).

[YM54] C. N. Yang and R. Mills, *Conservation of Isotopic Spin and Isotopic Gauge Invariance*, Physical Review **96** (1954), pp. 191–195, DOI: 10.1103/PhysRev.96.191 (cit. on p. 15).

[Yuk35] H. Yukawa, *On the interaction of elementary particles*, Proc.Phys.Math.Soc.Jap. **17** (1935), pp. 48–57 (cit. on p. 16).

Chapter 4: Higher-order calculations

[Ash72] J. F. Ashmore, *A Method of Gauge Invariant Regularization*, Lett.Nuovo Cim. **4** (1972), pp. 289–290, DOI: 10.1007/BF02824407 (cit. on p. 23).

[BCH13] S. Borowka, J. Carter, and G. Heinrich, *Numerical Evaluation of Multi-Loop Integrals for Arbitrary Kinematics with SecDec 2.0*, Comput.Phys.Commun. **184** (2013), pp. 396–408, DOI: 10.1016/j.cpc.2012.09.020, arXiv: 1204.4152 (cit. on p. 26).

[BG72] C. G. Bollini and J. J. Giambiagi, *Lowest order divergent graphs in ν-dimensional space*, Phys.Lett. **B40** (1972), pp. 566–568, DOI: 10.1016/0370-2693(72)90483-2 (cit. on p. 23).

[BW08] C. Bogner and S. Weinzierl, *Resolution of singularities for multi-loop integrals*, Comput.Phys.Commun. **178** (2008), pp. 596–610, DOI: `10.1016/j.cpc.2007.11.012`, arXiv: `0709.4092` (cit. on p. 26).

[CJN80] D. M. Capper, D. R. T. Jones, and P. van Nieuwenhuizen, *Regularization by Dimensional Reduction of Supersymmetric and Nonsupersymmetric Gauge Theories*, Nucl.Phys. **B167** (1980), p. 479, DOI: `10.1016/0550-3213(80)90244-8` (cit. on p. 23).

[CM72] G. M. Cicuta and E. Montaldi, *Analytic renormalization via continuous space dimension*, Lett.Nuovo Cim. **4** (1972), pp. 329–332, DOI: `10.1007/BF02756527` (cit. on p. 23).

[EG73] H. Epstein and V. Glaser, *The Role of locality in perturbation theory*, Annales Poincare Phys.Theor. **A19** (1973), pp. 211–295 (cit. on p. 24).

[Fre12] A. Freitas, *Numerical evaluation of multi-loop integrals using subtraction terms*, JHEP **1207** (2012), p. 132, DOI: `10.1007/JHEP07(2012)132,10.1007/JHEP09(2012)129`, arXiv: `1205.3515` (cit. on p. 26).

[Glu+11] J. Gluza et al., *Numerical Evaluation of Tensor Feynman Integrals in Euclidean Kinematics*, Eur.Phys.J. **C71** (2011), p. 1516, DOI: `10.1140/epjc/s10052-010-1516-y`, arXiv: `1010.1667` (cit. on p. 26).

[PV49] W. Pauli and F. Villars, *On the Invariant regularization in relativistic quantum theory*, Rev.Mod.Phys. **21** (1949), pp. 434–444, DOI: `10.1103/RevModPhys.21.434` (cit. on p. 24).

[PV79] G. Passarino and M. Veltman, *One-loop corrections for e^+e^- annihilation into $\mu^+\mu^-$ in the Weinberg model*, Nuclear Physics B **160** (1979), pp. 151–207, DOI: `10.1016/0550-3213(79)90234-7` (cit. on pp. 24, 125).

[Sie79] W. Siegel, *Supersymmetric dimensional regularization via dimensional reduction*, Physics Letters B **84** (1979), pp. 193–196, DOI: `10.1016/0370-2693(79)90282-X` (cit. on p. 23).

[Smi13] A. V. Smirnov, *FIESTA 3: cluster-parallelizable multiloop numerical calculations in physical regions* (2013), arXiv: `1312.3186` (cit. on p. 26).

[SV12] D. Stöckinger and P. Varšo, *FeynArts model file for MSSM transition counterterms from DREG to DRED*, Comput.Phys.Commun. **183** (2012), pp. 422–430, DOI: `10.1016/j.cpc.2011.10.010`, arXiv: `1109.6484` (cit. on p. 24).

[tV72] G. 't Hooft and M. J. G. Veltman, *Regularization and renormalization of gauge fields*, Nuclear Physics B **44** (1972), pp. 189–213, DOI: 10.1016/0550-3213(72)90279-9 (cit. on p. 23).

[tV79] G. 't Hooft and M. J. G. Veltman, *Scalar One Loop Integrals*, Nucl.Phys. **B153** (1979), pp. 365–401, DOI: 10.1016/0550-3213(79)90605-9 (cit. on p. 24).

[UF08] T. Ueda and J. Fujimoto, *New implementation of the sector decomposition on FORM*, PoS **ACAT08** (2008), p. 120, arXiv: 0902.2656 (cit. on p. 26).

[Var10] P. Varšo, *Supersymmetrie restaurierende Counterterme in Einschleifenordnung*, Diplomarbeit, Technische Universität Dresden, 2010 (cit. on p. 24).

[Wei09] S. Weinzierl, *Introduction to Feynman Integrals* (2009), arXiv: 1005.1855[hep-ph] (cit. on p. 23).

[WSB94b] G. Weiglein, R. Scharf, and M. Böhm, *Reduction of general two-loop self-energies to standard scalar integrals*, Nuclear Physics B **416** (1994), pp. 606–642, DOI: 10.1016/0550-3213(94)90325-5 (cit. on pp. 26, 127).

Chapter 5: Renormalization

[Aok+80] K. I. Aoki et al., *One Loop Corrections to Neutrino e Scattering in Weinberg-Salam Theory: Neutral Current Processes*, Prog.Theor.Phys. **64** (1980), p. 707, DOI: 10.1143/PTP.64.707; K. I. Aoki et al., *Electroweak Radiative Corrections to High-Energy Neutrino e Scatterings*, Prog.Theor.Phys. **65** (1981), p. 1001, DOI: 10.1143/PTP.65.1001; K. I. Aoki et al., *Electroweak Theory. Framework of On-Shell Renormalization and Study of Higher Order Effects*, Prog.Theor.Phys.Suppl. **73** (1982), pp. 1–225, DOI: 10.1143/PTPS.73.1, (cit. on p. 30).

[BP55] N. N. Bogolyubov and O. S. Parasyuk, *A theory of multiplication of causative singular functions*, Doklady Akademii Nauk SSSR **100** (1955), pp. 25–28 (cit. on p. 29).

[BSH86] M. Bohm, H. Spiesberger, and W. Hollik, *On the One Loop Renormalization of the Electroweak Standard Model and Its Application to Leptonic Processes*, Fortsch.Phys. **34** (1986), pp. 687–751, DOI: 10.1002/prop.19860341102 (cit. on p. 30).

[Hep66] K. Hepp,
Proof of the Bogolyubov-Parasyuk theorem on renormalization,
Commun.Math.Phys. **2** (1966), pp. 301–326,
DOI: 10.1007/BF01773358 (cit. on p. 29).

[Hol+02] W. Hollik et al.,
Renormalization of the minimal supersymmetric standard model,
Nucl.Phys. **B639** (2002), pp. 3–65,
DOI: 10.1016/S0550-3213(02)00538-2, arXiv: hep-ph/0204350
(cit. on pp. 30, 45, 63).

[PQ77] R. D. Peccei and H. R. Quinn,
CP Conservation in the Presence of Instantons,
Phys.Rev.Lett. **38** (1977), pp. 1440–1443,
DOI: 10.1103/PhysRevLett.38.1440; R. D. Peccei and H. R. Quinn,
Constraints Imposed by CP Conservation in the Presence of Instantons, Phys.Rev. **D16** (1977), pp. 1791–1797,
DOI: 10.1103/PhysRevD.16.1791, (cit. on pp. 33, 37).

[Zim69] W. Zimmermann, *Convergence of Bogolyubov's method of renormalization in momentum space*,
Commun.Math.Phys. **15** (1969), pp. 208–234,
DOI: 10.1007/BF01645676 (cit. on p. 29).

Chapter 6: Higgs bosons in the MSSM

[BBS08] N. Baro, F. Boudjema, and A. Semenov,
Automatised full one-loop renormalisation of the MSSM. I. The Higgs sector, the issue of $\tan(\beta)$ *and gauge invariance*,
Phys.Rev. **D78** (2008), p. 115003,
DOI: 10.1103/PhysRevD.78.115003, arXiv: 0807.4668
(cit. on pp. 45, 55, 63).

[Bri92] A. Brignole, *Radiative corrections to the supersymmetric neutral Higgs boson masses*, Phys.Lett. **B281** (1992), pp. 284–294,
DOI: 10.1016/0370-2693(92)91142-V (cit. on p. 50).

[CH03] M. S. Carena and H. E. Haber,
Higgs boson theory and phenomenology,
Prog.Part.Nucl.Phys. **50** (2003), pp. 63–152,
DOI: 10.1016/S0146-6410(02)00177-1, arXiv: hep-ph/0208209
(cit. on p. 43).

[CPR92] P. H. Chankowski, S. Pokorski, and J. Rosiek, *One loop corrections to the supersymmetric Higgs boson couplings and LEP phenomenology*, Phys.Lett. **B286** (1992), pp. 307–314, DOI: 10.1016/0370-2693(92)91780-D; P. H. Chankowski, S. Pokorski, and J. Rosiek, *Complete on-shell renormalization scheme for the minimal supersymmetric Higgs sector*, Nucl.Phys. **B423** (1994), pp. 437–496, DOI: 10.1016/0550-3213(94)90141-4, arXiv: hep-ph/9303309, (cit. on p. 55).

[Dab95] A. Dabelstein, *The One loop renormalization of the MSSM Higgs sector and its application to the neutral scalar Higgs masses*, Z.Phys. **C67** (1995), pp. 495–512, DOI: 10.1007/BF01624592, arXiv: hep-ph/9409375; A. Dabelstein, *Fermionic decays of neutral MSSM Higgs bosons at the one loop level*, Nucl.Phys. **B456** (1995), pp. 25–56, DOI: 10.1016/0550-3213(95)00523-2, arXiv: hep-ph/9503443, (cit. on p. 55).

[Den93] A. Denner, *Techniques for calculation of electroweak radiative corrections at the one loop level and results for W physics at LEP-*200, Fortsch.Phys. **41** (1993), pp. 307–420, DOI: 10.1002/prop.2190410402, arXiv: 0709.1075 (cit. on p. 59).

[Fra+02] M. Frank et al., *FeynHiggs1.2: Hybrid MS-bar / on-shell renormalization for the CP even Higgs boson sector in the MSSM* (2002), arXiv: hep-ph/0202166 (cit. on p. 50).

[Fra+07] M. Frank et al., *The Higgs boson masses and mixings of the complex MSSM in the Feynman-diagrammatic approach*, Journal of High Energy Physics **JHEP02** (2007), DOI: 10.1088/1126-6708/2007/02/047 (cit. on pp. 3, 35, 55).

[FS02] A. Freitas and D. Stöckinger, *Gauge dependence and renormalization of tan beta in the MSSM*, Phys.Rev. **D66** (2002), p. 095014, DOI: 10.1103/PhysRevD.66.095014, arXiv: hep-ph/0205281 (cit. on pp. 50, 55).

[Hol+02] W. Hollik et al., *Renormalization of the minimal supersymmetric standard model*, Nucl.Phys. **B639** (2002), pp. 3–65, DOI: 10.1016/S0550-3213(02)00538-2, arXiv: hep-ph/0204350 (cit. on pp. 30, 45, 63).

[PQ77] R. D. Peccei and H. R. Quinn, *CP Conservation in the Presence of Instantons*, Phys.Rev.Lett. **38** (1977), pp. 1440–1443, DOI: 10.1103/PhysRevLett.38.1440; R. D. Peccei and H. R. Quinn, *Constraints Imposed by CP Conservation in the Presence of Instantons*, Phys.Rev. **D16** (1977), pp. 1791–1797, DOI: 10.1103/PhysRevD.16.1791, (cit. on pp. 33, 37).

[Spe13] M. Sperling, *Renormierung von Vakuumerwartungswerten in spontan gebrochenen Eichtheorien*, Diplomarbeit, Technische Universität Dresden, 2013 (cit. on p. 61).

[SSV13] M. Sperling, D. Stöckinger, and A. Voigt, *Renormalization of vacuum expectation values in spontaneously broken gauge theories*, JHEP **1307** (2013), p. 132, DOI: 10.1007/JHEP07(2013)132, arXiv: 1305.1548 (cit. on pp. 43, 55, 61).

[SSV14] M. Sperling, D. Stöckinger, and A. Voigt, *Renormalization of vacuum expectation values in spontaneously broken gauge theories: Two-loop results*, JHEP **1401** (2014), p. 068, DOI: 10.1007/JHEP01(2014)068, arXiv: 1310.7629 (cit. on pp. 60, 74).

[WRW11] K. E. Williams, H. Rzehak, and G. Weiglein, *Higher order corrections to Higgs boson decays in the MSSM with complex parameters*, Eur.Phys.J. **C71** (2011), p. 1669, DOI: 10.1140/epjc/s10052-011-1669-3, arXiv: 1103.1335 (cit. on pp. 45, 63).

Chapter 7: Two-loop top-Yukawa-coupling corrections

[BB09] N. Baro and F. Boudjema, *Automatised full one-loop renormalisation of the MSSM II: The chargino-neutralino sector, the sfermion sector and some applications*, Phys.Rev. **D80** (2009), p. 076010, DOI: 10.1103/PhysRevD.80.076010, arXiv: 0906.1665 (cit. on p. 78).

[BBS08] N. Baro, F. Boudjema, and A. Semenov, *Automatised full one-loop renormalisation of the MSSM. I. The Higgs sector, the issue of* $\tan(\beta)$ *and gauge invariance*, Phys.Rev. **D78** (2008), p. 115003, DOI: 10.1103/PhysRevD.78.115003, arXiv: 0807.4668 (cit. on pp. 45, 55, 63).

[Bha+12] A. Bharucha et al., *Neutralino Decays in the Complex MSSM at One-Loop: a Comparison of On-Shell Renormalization Schemes*, Phys.Rev. **D86** (2012), p. 075023, DOI: 10.1103/PhysRevD.86.075023, arXiv: 1208.4106 (cit. on p. 78).

[Bri+02] A. Brignole et al., *On the $\mathcal{O}(\alpha_t^2)$ two loop corrections to the neutral Higgs boson masses in the MSSM*, Nucl.Phys. **B631** (2002), pp. 195–218, DOI: `10.1016/S0550-3213(02)00184-0`, arXiv: `hep-ph/0112177` (cit. on pp. 2–4, 79, 97).

[Cha+12b] A. Chatterjee et al., *On the On-Shell Renormalization of the Chargino and Neutralino Masses in the MSSM*, Phys.Rev. **D85** (2012), p. 075013, DOI: `10.1103/PhysRevD.85.075013`, arXiv: `1107.5218` (cit. on p. 78).

[CPR94] D. J. Castano, E. J. Piard, and P. Ramond, *Renormalization group study of the Standard Model and its extensions. 2. The Minimal supersymmetric Standard Model*, Phys.Rev. **D49** (1994), pp. 4882–4901, DOI: `10.1103/PhysRevD.49.4882`, arXiv: `hep-ph/9308335` (cit. on p. 74).

[Fri+13] T. Fritzsche et al., *The Implementation of the Renormalized Complex MSSM in FeynArts and FormCalc* (2013), arXiv: `1309.1692` (cit. on pp. 63, 66).

[Hah01] T. Hahn, *Generating Feynman diagrams and amplitudes with FeynArts 3*, Comput.Phys.Commun. **140** (2001), pp. 418–431, DOI: `10.1016/S0010-4655(01)00290-9`, arXiv: `hep-ph/0012260` (cit. on p. 63).

[Hei+07] S. Heinemeyer et al., *The Higgs sector of the complex MSSM at two-loop order: QCD contributions*, Phys.Lett. **B652** (2007), pp. 300–309, DOI: `10.1016/j.physletb.2007.07.030`, arXiv: `0705.0746` (cit. on pp. 2, 3, 65, 82).

[HL08] T. Hahn and P. Lang, *FeynEdit: A Tool for drawing Feynman diagrams*, Comput.Phys.Commun. **179** (2008), pp. 931–935, DOI: `10.1016/j.cpc.2008.08.005`, arXiv: `0711.1345` (cit. on p. 64).

[Hol+02] W. Hollik et al., *Renormalization of the minimal supersymmetric standard model*, Nucl.Phys. **B639** (2002), pp. 3–65, DOI: `10.1016/S0550-3213(02)00538-2`, arXiv: `hep-ph/0204350` (cit. on pp. 30, 45, 63).

[HP99] T. Hahn and M. Perez-Victoria, *Automatized one loop calculations in four-dimensions and D-dimensions*, Comput.Phys.Commun. **118** (1999), pp. 153–165, DOI: `10.1016/S0010-4655(98)00173-8`, arXiv: `hep-ph/9807565` (cit. on p. 64).

[SSV14] M. Sperling, D. Stöckinger, and A. Voigt, *Renormalization of vacuum expectation values in spontaneously broken gauge theories: Two-loop results*, JHEP **1401** (2014), p. 068, DOI: 10.1007/JHEP01(2014)068, arXiv: 1310.7629 (cit. on pp. 60, 74).

[WRW11] K. E. Williams, H. Rzehak, and G. Weiglein, *Higher order corrections to Higgs boson decays in the MSSM with complex parameters*, Eur.Phys.J. **C71** (2011), p. 1669, DOI: 10.1140/epjc/s10052-011-1669-3, arXiv: 1103.1335 (cit. on pp. 45, 63).

[WSB94a] G. Weiglein, R. Scharf, and M. Bohm, *Reduction of general two loop selfenergies to standard scalar integrals*, Nucl.Phys. **B416** (1994), pp. 606–644, DOI: 10.1016/0550-3213(94)90325-5, arXiv: hep-ph/9310358 (cit. on p. 64).

Chapter 8: Numerical investigation of the top-Yukawa corrections

[Ben+12] R. Benbrik et al., *Confronting the MSSM and the NMSSM with the Discovery of a Signal in the two Photon Channel at the LHC*, Eur.Phys.J. **C72** (2012), p. 2171, DOI: 10.1140/epjc/s10052-012-2171-2, arXiv: 1207.1096; P. Bechtle et al., *MSSM Interpretations of the LHC Discovery: Light or Heavy Higgs?*, Eur.Phys.J. **C73** (2013), p. 2354, DOI: 10.1140/epjc/s10052-013-2354-5, arXiv: 1211.1955, (cit. on p. 98).

[BFS12] A. Bottino, N. Fornengo, and S. Scopel, *Phenomenology of light neutralinos in view of recent results at the CERN Large Hadron Collider*, Phys.Rev. **D85** (2012), p. 095013, DOI: 10.1103/PhysRevD.85.095013, arXiv: 1112.5666; M. Drees, *A Supersymmetric Explanation of the Excess of Higgs–Like Events at the LHC and at LEP*, Phys.Rev. **D86** (2012), p. 115018, DOI: 10.1103/PhysRevD.86.115018, arXiv: 1210.6507, (cit. on p. 98).

[BGK99] M. Brhlik, Gerald W. J. Good, and G. L. Kane, *Electric dipole moments do not require the CP violating phases of supersymmetry to be small*, Phys.Rev. **D59** (1999), p. 115004, DOI: 10.1103/PhysRevD.59.115004, arXiv: hep-ph/9810457 (cit. on p. 108).

[Brh+99] M. Brhlik et al., *A Resolution to the supersymmetric CP problem with large soft phases via D-branes*, Phys.Rev.Lett. **83** (1999), pp. 2124–2127, DOI: `10.1103/PhysRevLett.83.2124`, arXiv: `hep-ph/9905215` (cit. on p. 108).

[Bri+02] A. Brignole et al., *On the $\mathcal{O}(\alpha_t^2)$ two loop corrections to the neutral Higgs boson masses in the MSSM*, Nucl.Phys. **B631** (2002), pp. 195–218, DOI: `10.1016/S0550-3213(02)00184-0`, arXiv: `hep-ph/0112177` (cit. on pp. 2–4, 79, 97).

[Car+03] M. S. Carena et al., *Suggestions for benchmark scenarios for MSSM Higgs boson searches at hadron colliders*, Eur.Phys.J. **C26** (2003), pp. 601–607, DOI: `10.1140/epjc/s2002-01084-3`, arXiv: `hep-ph/0202167` (cit. on p. 96).

[Car+13] M. S. Carena et al., *MSSM Higgs Boson Searches at the LHC: Benchmark Scenarios after the Discovery of a Higgs-like Particle*, Eur. Phys. J. **C73** (2013), p. 2552, DOI: `10.1140/epjc/s10052-013-2552-1`, arXiv: `1302.7033` (cit. on pp. 96, 99, 100).

[col13a] CMS collaboration, *Higgs to $\tau\,\tau$ (MSSM)* (2013) (cit. on p. 99).

[col13b] The ATLAS collaboration, *Search for charged Higgs bosons in the τ+jets final state with pp collision data recorded at $\sqrt{s} = 8$ TeV with the ATLAS experiment* (2013) (cit. on p. 99).

[Deg+03] G. Degrassi et al., *Towards high precision predictions for the MSSM Higgs sector*, Eur.Phys.J. **C28** (2003), pp. 133–143, DOI: `10.1140/epjc/s2003-01152-2`, arXiv: `hep-ph/0212020` (cit. on pp. 2, 3, 99).

[DM13] A. Djouadi and G. Moreau, *The couplings of the Higgs boson and its CP properties from fits of the signal strengths and their ratios at the $7+8$ TeV LHC*, Eur.Phys.J. **C73** (2013), p. 2512, DOI: `10.1140/epjc/s10052-013-2512-9`, arXiv: `1303.6591` (cit. on p. 107).

[FO96] T. Falk and K. A. Olive, *Electric dipole moment constraints on phases in the constrained MSSM*, Phys.Lett. **B375** (1996), pp. 196–202, DOI: `10.1016/0370-2693(96)00249-3`, arXiv: `hep-ph/9602299`; T. Falk and K. A. Olive, *More on electric dipole moment constraints on phases in the constrained MSSM*, Phys.Lett. **B439** (1998), pp. 71–80, DOI: `10.1016/S0370-2693(98)01022-3`, arXiv: `hep-ph/9806236`;

T. Ibrahim and P. Nath,
The Chromoelectric and purely gluonic operator contributions to the neutron electric dipole moment in $N = 1$ supergravity,
Phys.Lett. **B418** (1998), pp. 98–106,
DOI: 10.1016/S0370-2693(97)01482-2, arXiv: hep-ph/9707409;
T. Ibrahim and P. Nath, *The Neutron and the electron electric dipole moment in $N = 1$ supergravity unification*,
Phys.Rev. **D57** (1998), pp. 478–488,
DOI: 10.1103/PhysRevD.58.019901,10.1103/PhysRevD.60.079903,
10.1103/PhysRevD.60.119901,10.1103/PhysRevD.57.478,
arXiv: hep-ph/9708456; T. Ibrahim and P. Nath,
The Neutron and the lepton EDMs in MSSM, large CP violating phases, and the cancellation mechanism,
Phys.Rev. **D58** (1998), p. 111301,
DOI: 10.1103/PhysRevD.60.099902,10.1103/PhysRevD.58.111301,
arXiv: hep-ph/9807501; T. Ibrahim and P. Nath,
Large CP phases and the cancellation mechanism in EDMs in SUSY, string and brane models, Phys.Rev. **D61** (2000), p. 093004,
DOI: 10.1103/PhysRevD.61.093004, arXiv: hep-ph/9910553;
E. Accomando, R. L. Arnowitt, and B. Dutta, *Grand unification scale CP violating phases and the electric dipole moment*,
Phys.Rev. **D61** (2000), p. 115003,
DOI: 10.1103/PhysRevD.61.115003, arXiv: hep-ph/9907446;
A. Bartl et al., *Electron and neutron electric dipole moments in the constrained MSSM*, Phys.Rev. **D60** (1999), p. 073003,
DOI: 10.1103/PhysRevD.60.073003, arXiv: hep-ph/9903402;
V. D. Barger et al., *CP violating phases in SUSY, electric dipole moments, and linear colliders*, Phys.Rev. **D64** (2001), p. 056007,
DOI: 10.1103/PhysRevD.64.056007, arXiv: hep-ph/0101106,
(cit. on p. 104).

[Fra+13] M. Frank et al., *Charged Higgs Boson Mass of the MSSM in the Feynman Diagrammatic Approach*,
Phys.Rev. **D88**.5 (2013), p. 055013,
DOI: 10.1103/PhysRevD.88.055013, arXiv: 1306.1156
(cit. on pp. 102, 113).

[Hah+07] T. Hahn et al.,
Higgs Masses and More in the Complex MSSM with FeynHiggs
(2007), pp. 442–449, arXiv: 0710.4891 (cit. on p. 101).

[Hah+09] T. Hahn et al., *FeynHiggs: A program for the calculation of MSSM Higgs-boson observables - Version 2.6.5*,
Comput.Phys.Commun. **180** (2009), pp. 1426–1427,
DOI: 10.1016/j.cpc.2009.02.014 (cit. on pp. 3, 101).

[Hah+14] T. Hahn et al., *High-precision predictions for the light CP-even Higgs Boson Mass of the MSSM*, Phys.Rev.Lett. **112** (2014), p. 141801, DOI: `10.1103/PhysRevLett.112.141801`, arXiv: `1312.4937` (cit. on p. 96).

[Hei+01] S. Heinemeyer et al., *Neutral MSSM Higgs boson production at e^+e^- colliders in the Feynman diagrammatic approach*, Eur.Phys.J. **C19** (2001), pp. 535–546, DOI: `10.1007/s100520100631`, arXiv: `hep-ph/0102081` (cit. on p. 94).

[HHW00a] S. Heinemeyer, W. Hollik, and G. Weiglein, *Constraints on* $\tan(\beta)$ *in the MSSM from the upper bound on the mass of the lightest Higgs boson*, JHEP **0006** (2000), p. 009, DOI: `10.1088/1126-6708/2000/06/009`, arXiv: `hep-ph/9909540` (cit. on p. 96).

[HHW00b] S. Heinemeyer, W. Hollik, and G. Weiglein, *Decay widths of the neutral CP even MSSM Higgs bosons in the Feynman diagrammatic approach*, Eur.Phys.J. **C16** (2000), pp. 139–153, DOI: `10.1007/s100520050010`, arXiv: `hep-ph/0003022` (cit. on p. 94).

[HSW12] S. Heinemeyer, O. Stål, and G. Weiglein, *Interpreting the LHC Higgs Search Results in the MSSM*, Phys.Lett. **B710** (2012), pp. 201–206, DOI: `10.1016/j.physletb.2012.02.084`, arXiv: `1112.3026` (cit. on p. 98).

[MS97] A. Masiero and L. Silvestrini, *CP violation in low-energy SUSY* (1997), arXiv: `hep-ph/9709242` (cit. on p. 108).

[Sch+06] S. Schael et al., *Search for neutral MSSM Higgs bosons at LEP*, Eur.Phys.J. **C47** (2006), pp. 547–587, DOI: `10.1140/epjc/s2006-02569-7`, arXiv: `hep-ex/0602042` (cit. on p. 96).

Appendices

[Aad+12] G. Aad et al., *Observation of a new particle in the search for the Standard Model Higgs boson with the ATLAS detector at the LHC*, Phys.Lett. **B716** (2012), pp. 1–29, DOI: `10.1016/j.physletb.2012.08.020`, arXiv: `1207.7214` (cit. on pp. 1, 2, 115).

[Aad+14] G. Aad et al., *Measurement of the Higgs boson mass from the $H \to \gamma\gamma$ and $H \to ZZ^* \to 4\ell$ channels with the ATLAS detector using* 25 *fb*$^{-1}$ *of* pp *collision data* (2014), arXiv: `1406.3827` (cit. on pp. 2, 115, 117).

[Ber66] F. Berezin, *The Method of Second Quantization*, Academic Press (1966) (cit. on p. 120).

[BT94] F. A. Berends and J. B. Tausk, *On the numerical evaluation of scalar two loop selfenergy diagrams*, Nucl.Phys. **B421** (1994), pp. 456–470, DOI: `10.1016/0550-3213(94)90336-0` (cit. on p. 127).

[Cha+12a] S. Chatrchyan et al., *Observation of a new boson at a mass of 125 GeV with the CMS experiment at the LHC*, Phys.Lett. **B716** (2012), pp. 30–61, DOI: `10.1016/j.physletb.2012.08.021`, arXiv: `1207.7235` (cit. on pp. 1, 2, 115).

[Cha+14] S. Chatrchyan et al., *Measurement of the properties of a Higgs boson in the four-lepton final state*, Phys.Rev. **D89** (2014), p. 092007, DOI: `10.1103/PhysRevD.89.092007`, arXiv: `1312.5353` (cit. on pp. 2, 115, 117).

[PV79] G. Passarino and M. Veltman, *One-loop corrections for e^+e^- annihilation into $\mu^+\mu^-$ in the Weinberg model*, Nuclear Physics B **160** (1979), pp. 151–207, DOI: `10.1016/0550-3213(79)90234-7` (cit. on pp. 24, 125).

[Wei+95] G. Weiglein et al., *Computer algebraic calculation of two loop selfenergies in the electroweak standard model*, La Londe-les-Maures 1992, New computing techniques in physics research II (1995), pp. 617–623 (cit. on p. 127).

[WSB94b] G. Weiglein, R. Scharf, and M. Böhm, *Reduction of general two-loop self-energies to standard scalar integrals*, Nuclear Physics B **416** (1994), pp. 606–642, DOI: `10.1016/0550-3213(94)90325-5` (cit. on pp. 26, 127).

Acknowledgments

I am very grateful for many friends and colleagues.

My doctoral adviser Prof. Wolfgang Hollik always had a sympathetic ear when I had difficulties in understanding the various physical problems which were arising during my studies. He also helped me to attend summer schools, conferences and workshops, and as one of the directors he is responsible for the pleasant environment at the Max Planck Institute for Physics in Munich. Another related subject is the organization of the local international Max Planck research school by Frank Steffen. The block courses, workshops and seminars were enriching the atmosphere not only in an academic way.

Thomas Hahn answered my one thousand and one questions related to the code of the program `FeynHiggs` without ever losing his nerves. Also his expertise in technical questions and his administrative work behind the scenes were worth a mint. Pietro Slavich helped me to understand his contributions to `FeynHiggs` thus making a comparison with my result possible.

Sven Heinemeyer and Heidi Rzehak helped me to understand the physics of the Higgs potential and its renormalization. They sacrificed time to reply to each of my emails or direct questions without exception. Furthermore, Christian Schappacher was involved in fixing the problems that occured in the used model file.

Stefano di Vita gave me the crucial hint to get rid of my divergences. I profit a lot by his experience in higher-order calculations.

Peter Drechsel, Luminita Mihaila, Dominik Stöckinger and Alexander Voigt introduced me to the topic of the renormalization group. Many discussions resulted in the present depiction of the renormalization of t_β.

The members of my working group at the Max Planck Institute for Physics, especially Sophia Borowka, Stephan Hessenberger, Jonas Lindert, Cyril Pietsch and Hendrik Vogel, helped me to find the answers to several small problems.

Special thanks for proof-reading this thesis to Stefano di Vita, Stephan Hessenberger, Cyril Pietsch and Shangyu Sun.

Thank you all for your valuable support and candid share of knowledge.

How could I have focussed on this thesis if there would not have been a balance outside of physics?

Grazie Alessandro, le escursioni in montagna sono sempre state rilassanti, sia in estate che in inverno. Mi hai insegnato il modo di vita italiano e tuoi pasta è la migliore!

Gràcies Ana, per contagiar-me el teu somriure i l'alegria per la vida.

Gracias Javier, gracias a ti las noches del viernes fueron siempre especiales.

Danke Marlene und Sebastian, eure hervorragenden Künste im Kochen und Backen haben für Gaumenschmaus und viele gesellige Abende gesorgt und mich außerdem zum Nachahmen animiert.

這些神秘的旅程，到境外之境，入域外之域，揭無人知曉之物。
為此，尚右，謝謝你。

これまで励ましてくれてありがとう。
あなたがあなたの大志を楽しみながら実現していくのを見て、
私にとってすごくよい例となってくれています。
健、本当にありがとう。

Furthermore, thanks to the PhD representatives for organizing barbecues. Also many thanks to the football team of the institute for challenging matches.

Thanks to the administrative staff of the Max Planck Institute for Physics for their technical assistance.

Thanks to all the people, who are not mentioned here, but who made my life more pleasant.

Ganz besonderer Dank gilt meinen Eltern und meinem Bruder, die mich immer unterstützt und mir mit Rat und Tat zur Seite gestanden haben, wenn es darum ging, Probleme jenseits der Physik zu lösen.